UNIVERSITY OF Southampton

Faculty of Medicine

Clinical and Experimental Sciences

Not just skin deep: circulating lipids in a “localised” disease and their role in angiogenesis

by

Jemma Alanna Jane Paterson

Thesis for the degree of Doctor of Philosophy

April 2020

UNIVERSITY OF SOUTHAMPTON

ABSTRACT

Psoriasis affects on average approximately 3% of the world's population and varies widely in severity. It is thought to be an autoimmune disease as immune cells invade the dermis and epidermis resulting in hyperproliferation of keratinocytes, however no autoantigen has been found despite extensive studies. There is no cure for psoriasis however there are a number of treatments which often have side effects and are not always particularly effective. Psoriasis patients are known to have dyslipidaemia, an abnormal amount of lipids in the blood, and this predisposes them to other diseases such as cardiovascular disease and diabetes. This thesis investigates Low Density Lipoprotein (LDL) and its oxidised product oxLDL as LDL is known to be problematic in other diseases. Previous work has shown that oxidised LDL affected angiogenesis in a concentration dependent manner with lower concentrations (5μg/ml) showing a stimulatory effect and high concentrations (100μg/ml) having an inhibitory effect. This previous work has hinted that oxLDL signals through another bioactive lipid, Sphingosine-1-phosphate (S1P), and therefore the effect of S1P on migration and angiogenesis has so far been the focus of this research. S1P has previously been linked to other diseases such as cancer and atherosclerosis and due to its link with these diseases, it is therefore possible that S1P is also involved in psoriasis, potentially by protecting proliferating keratinocytes from apoptosis. It was found that like oxLDL, S1P has an inhibitory effect on both migration and angiogenesis at high concentrations (10μM), however no stimulatory effect at lower concentrations (1μM-1nM) was seen. The effect of S1P on intracellular signalling has also been studied, with results showing that S1P has concentration dependent effects on both the levels of ERK phosphorylation and increases in calcium flux. Various inhibitors have also been utilised to better understand the mechanism through which S1P exerts its effects. The inhibitors had no effect at blocking S1P directed migration, however the use of inhibitors that block the S1P receptors have shown variation in the levels of phosphorylated ERK suggesting that it is the addition of the exogenous S1P that causes this phosphorylation. This research will provide further insight into the underlying molecular mechanisms leading to the development of psoriasis which may one day lead to additional treatment to those already in place and improve the quality of life for these patients.

Table of Contents

List of Tables

List of Figures

DECLARATION OF AUTHORSHIP

I, ... [please print name]

declare that this thesis and the work presented in it are my own and has been generated by me as the result of my own original research.

[title of thesis] .....

.....

I confirm that:

1. This work was done wholly or mainly while in candidature for a research degree at this University;
2. Where any part of this thesis has previously been submitted for a degree or any other qualification at this University or any other institution, this has been clearly stated;
3. Where I have consulted the published work of others, this is always clearly attributed;
4. Where I have quoted from the work of others, the source is always given. With the exception of such quotations, this thesis is entirely my own work;
5. I have acknowledged all main sources of help;
6. Where the thesis is based on work done by myself jointly with others, I have made clear exactly what was done by others and what I have contributed myself;
7. [Delete as appropriate] None of this work has been published before submission [or] ~~Parts of this work have been published as~~: [please list references below]:

Signed: .....

Date: .....

Acknowledgements

I wish to thank my supervisors Dr Tim Millar and Dr Alan Hunt for their support. I also wish to thank the midwives at the Princess Anne hospital for collecting the placentas and umbilical cords for this study.

Definitions and Abbreviations

ApoM- Apolipoprotein M

AUC- Area under curve

BMI- Body Mass Index

CETP- Cholesteryl ester transfer protein

DNPH- 2,4-Dinitrophenylhydrazine

DTT- Dithiothreitol

ECM- Extracellular matrix

ECL- Enhanced chemiluminescence

EDTA- Ethylenediaminetetraacetic acid

eNOS- Endothelial nitric oxide synthase

ER- Endoplasmic reticulum

ERK- Extracellular Signal-regulated Kinase

FACS- Fluorescence-activated cell sorting

FDA- Food and Drug Administration

FGF- Fibroblast growth factor

GIRK- G-protein–coupled inwardly rectifying potassium channels

GPCR- G protein-coupled receptor

GSIS- Glucose-stimulated insulin secretion

HBSS- Hanks balanced salt solution

HCl- Hydrochloric acid

HDL- High density lipoprotein

HMG CoA- 3-hydroxy-3-methylglutaryl CoA

HMG-CoA reductase - 3-hydroxy-3-methylglutaryl CoA reductase

HRP- Horseradish peroxidase

ICAM1- Intercellular Adhesion Molecule 1

IDL- Intermediate-density lipoprotein

IL-17- Interleukin 17

IFNγ- Interferon γ

IFPA- International Federation of Psoriasis Associations

JAK- Janus activated kinase

JNK- Jun N-terminal kinase

LDL- Low density lipoprotein

Lp(a)- Lipoprotein(a)

MAPK- Mitogen-activated protein kinases

MDA- Malonaldehyde bis(dimethyl acetal)

MI- Myocardial infarction

MS- Multiple sclerosis

NF- κB- Nuclear factor κB

oxLDL- oxidised Low density lipoprotein

PAI-1- Plasminogen activator inhibitor 1

PASI- Psoriasis area and severity index

PBMC- Peripheral blood mononuclear cell

PBS- Phosphate Buffered Saline

PCSK9- Proprotein convertase-subtilisin/kexin type 9

PDGF- Platelet-derived growth factor

PECAM-1- Platelet/endothelial cell adhesion molecule 1

PUVA- Psoralen photochemotherapy

PVDF- Polyvinylidene difluoride

S1P- Sphingosine-1-phosphate

S1PL- S1P Lyase

S1PR1-5- Sphingosine-1-phosphate receptor 1-5

SREBPs- Sterol regulatory element binding proteins

SKI-I- Sphingosine kinase II

Spns2- Spinster 2

STAT- Signal transducer and activator of transcription

TBA- Thiobarbituric acid

TBARS- Thiobarbituric acid reactive substances

TCA- Trichloroacetic acid

Th-17- T-helper 17

TNFα- Tumour Necrosis Factor α

UVB- Ultra-violet B

VCAM1- Vascular cell adhesion molecule 1

VEGF- Vascular endothelial growth factor

vLDL- Very low-density lipoproteins

VSMC- Vascular smooth muscle cells

vWF- Von Willebrand factor

WHO- World Health Organisation

Chapter 1: Introduction

1.1 Normal skin composition and function

The skin is a vital organ that acts as a barrier and first line of defence, giving protection from harmful pathogens and environmental insults while helping to retain water. It is the largest organ in the body and has two major anatomical regions known as the dermis and the epidermis, separated by the basement membrane as shown in Figure 1. The dermis is primarily composed of connective tissue and forms the extracellular matrix that provides support for the epidermis and is composed of fibroblasts and collagen as well as immune cells such as macrophages and mast cells (Quan et al., 2015). The dermis also has an extensive blood supply which is important for maintaining homeostasis including thermoregulation, immune surveillance and water regulation; all of which are vital functions of the skin (McGrath et al., 2004).

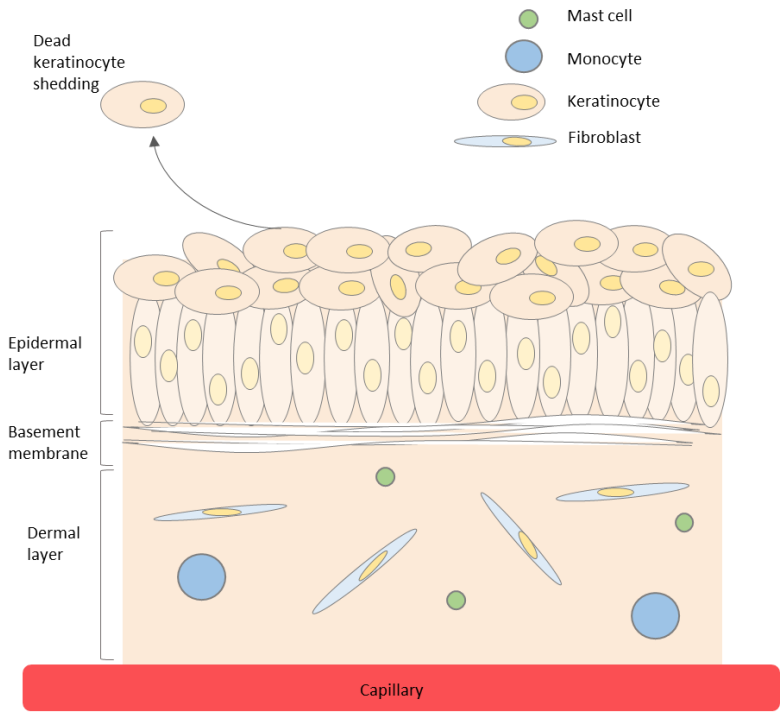

Figure 1 Diagram of healthy skin, showing the dermal and epidermal layers.
The dermis is composed of connective tissue, mast cells and macrophages. The epidermis mainly contains keratinocytes; those that are actively dividing are found towards the basement membrane and those that are older are pushed up towards the surface of the epidermis, become cornified and die to form a protective layer and are eventually shed and replaced. Information for diagram from (Lowes et al., 2007).

The epidermis can be further divided into several distinct layers with the majority of structural cells being keratinocytes (90%) but also containing Langerhans cells, melanocytes and fibroblasts. The layer of keratinocytes at the junction of the dermis and epidermis are known as basal cells and form the Stratum basale; these are the least differentiated form of keratinocytes. Upon division, some cells will stay in this layer as stem cells while others will migrate towards the surface of the epidermis, moving through the Stratum spinosum, Stratum granulosum and Stratum lucidum. During this migration the cells become more differentiated until they die and form the outermost layer of the epidermis, the Stratum corneum, before eventually being shed (Eckert and Rorke, 1989). Due to this continual turnover and migration of keratinocytes, the epidermis is in effect completely replaced every 39 days (Weinstein et al., 1984).

1.2 General background to Psoriasis

Psoriasis was classified in 2016 by the World Health Organisation (WHO) as a "serious global problem", along with the statement that "psoriasis has a serious negative effect on patients' quality of life". The International Federation of Psoriasis Associations (IFPA) has reported that nearly 3% of the World's population lives with psoriasis, with the prevalence in developed countries being between 1.5% and 5% (IFPA, 2017).

1.2.1 Epidemiology

Psoriasis is a hyperproliferative disease and can appear at any age, however, it is most likely to appear at around 25 years in women and slightly later at 28 years in males (Lonnberg et al., 2016). Interestingly there seems to be a hereditary link, with 60-90% of patients having a family history of the disease. Genome-wide association studies have identified 24 loci linked to a person's susceptibility of developing the disease and a mutation in these appears to cause an earlier onset, with a more severe form of psoriasis developing (Oka et al., 2012).

1.2.2 Cause of psoriasis

Psoriasis is a chronic systemic disease mediated by both innate and adaptive immune systems and includes the vasculature (Menter A et al., 2011). It is characterised by the excessive growth and build-up of dead keratinocytes, inflammation of the affected area caused by neutrophils and T cells invading the tissue and the formation of scales on the skin (see Figure 2), compared to normal or unaffected skin where dead keratinocytes are shed from the surface due to a continual turnover of cells.

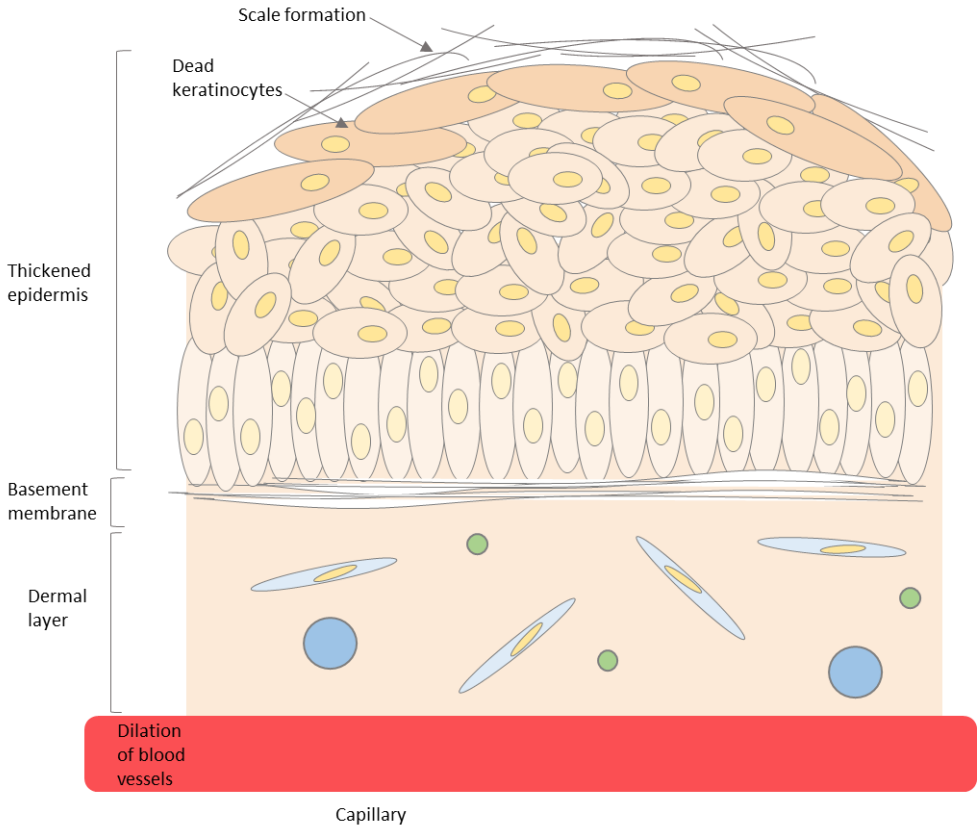

Figure 2 Diagram of plaque formation on psoriasis
Psoriasis is characterised by hyperproliferation of the keratinocytes leading to a thickened epidermis. Dead keratinocytes also retain their nuclei and fail to be shed, exaggerating this effect. The affected area becomes inflamed, with immune cells invading the skin. Scales also begin to form on the surface of the skin which becomes dry and itchy. Information for diagram from (Lowes et al., 2007).

It is possible that psoriasis is an autoimmune disease, however no autoantigen to date has been found to support this theory (Anand et al., 2017). There are convincing arguments for both sides of this debate, with some studies reporting a correlation of psoriasis with other autoimmune diseases (Wielosz et al., 2008) and other groups arguing that the lack of specific antibody and B-cell activation, along with the lack of genetic risk factors suggests that it may not be an autoimmune disease (Fry et al., 2015). Those in the latter group suggest instead that it is the resident bacteria in the skin, with *Streptococcus sp*. having been found to be the most common genus involved, that can cause the development of psoriasis (Fry et al., 2013). Whether psoriasis proves to be an autoimmune disease remains to be seen, however the involvement of the immune system is now well established.

The vasculature is also known to be involved in the development of psoriasis, with existing capillaries around the plaques becoming dilated and contorted and new vessels being formed. Angiogenesis, or the formation of new blood vessels, is a vital part of embryonic development and continues to remain important throughout life. This complex process involves both the migration and differentiation of the endothelium in order to form new capillary networks and is tightly regulated by numerous stimuli (Bielenberg and Zetter, 2015).

Angiogenesis occurs through a number of stages that begins with pro-angiogenic factors, such as vascular-endothelial growth factor (VEGF) and fibroblast growth factor (FGF), being released by cells short of oxygen or nutrients such as the hyperproliferating keratinocytes in psoriasis plaques. The endothelium remodels in response to these signals, and new tubes are formed to accommodate the increased demand for oxygen and nutrients. As psoriasis is known to include the vasculature, angiogenesis is believed to be important for both the development and progression of the disease, as without it, the plaques would not be able to grow.

1.2.3 Types of psoriasis

There are seven types of psoriasis, the most common of which is psoriasis vulgaris or plaque psoriasis (see Figure 3). Psoriasis vulgaris occurs in roughly 80% of patients and causes the red, inflamed skin covered in plaques that is most commonly associated with the appearance of the disease. This type can appear anywhere on the body, however it is most commonly localised to the elbows and knees (Langley et al., 2005).

Figure 3 Example images of plaque psoriasis
Example images showing plaque psoriasis. Plaque psoriasis can occur anywhere on the body (left) and is characterised by plaques (right) formed by excessive growth and build-up of dead keratinocytes. Images taken from Burden and Kirby (2016).

After plaque psoriasis, guttate psoriasis is the second most common type seen in children, accounting for 9-29% of cases in a study conducted in the US (Tollefson et al., 2010). Guttate psoriasis presents as small (2-10mm) red dots, typically localised to the torso and thighs and can be triggered by stress and bacterial infection (namely *Streptococcus*) (Smith, 2016).

Flexural (Inverse) Psoriasis is a rarer form of psoriasis accounting for only 3-7% of all cases. It is characterised by smooth, red patches, lacking the scales and plaques seen in psoriasis vulgaris. Typically, flexural psoriasis occurs around the genitals and armpits where conditions are generally warmer and more moist and where the constant friction leads to maceration; hence no scale formation. Due to the sensitive nature of the location, this type is often difficult to treat as topical medication can permeate deeper than in other areas of skin. This, combined with the added possibility of sexually transmitted diseases or fungal infection, can result in a resistance to the treatment developing (Guglielmetti et al., 2012).

Pustular psoriasis is a rare form of psoriasis that appears as pustules on the skin filled with puss and can be triggered by systemic drugs, infections and stress. These pustules can be restricted to a single area or cover the majority of the body; this is known as generalised pustular psoriasis and can be life threatening (Armstrong et al., 2016). Treatments available for generalised pustular psoriasis are limited. However, recently Interleukin-17 Receptor A inhibitors such as Brodalumab and Secukinumab have shown promising results (Yamasaki et al., 2017) and (Armstrong et al., 2016).

Erythrodermic psoriasis is the rarest (1% of cases) and most serious type of psoriasis, which affects the majority of the body. Two types of erythrodermic psoriasis have been documented, the first arising from psoriasis vulgaris which has gradually worsened to result in the plaques becoming joined. The second type results from an uncontrolled psoriasis that has become aggravated by any of a number of factors, including systemic drugs, infection or stopping a corticosteroid treatment (Langley et al., 2005). Current treatments have unsatisfactory results and therefore erythrodermic psoriasis is very difficult to control, with the patient often having to be hospitalised (Lee et al., 2015b).

There is often nail involvement in all types of psoriasis, with one study suggesting that over a lifetime this could even be as high as in 90% of cases (Jiaravuthisan et al., 2007). Nail psoriasis has a significant negative impact on the quality of life of the patient due to the psychosocial impact and can lead to reduced physical capability. There are two main features of nail psoriasis: involvement of the nail matrix causing pitting of the nail and nail bed involvement resulting in the formation of “oil spots” (Radtke et al., 2013). The pitting arises from abnormal nail growth and is seen in roughly 68% of cases, while the discolouration of the nail is due to parakeratosis (build-up of keratinocytes) in the nail bed. Similarly to other types of psoriasis, the treatment options for nail psoriasis are limited, possibly due to the fact that most research and recent developments have been focused on the skin and the involvement of the nails has largely been overlooked (Jiaravuthisan et al., 2007).

The final form of psoriasis is psoriatic arthritis, which occurs when a patient with psoriasis develops an inflammatory arthritis. This development occurs roughly 10 years after the psoriasis diagnosis (Gladman et al., 2005) and is estimated to have a 30% incidence rate (Mease et al., 2013). Some studies have suggested a link between psoriatic arthritis and nail psoriasis, with the type and severity of the nail psoriasis correlating to the chance of arthritic development. For example, it has been found that patients with onychodystrophy (breakdown of the nail) have an increased chance of developing psoriatic arthritis at a later stage (Dalbeth et al., 2012).

1.2.4 Cytokine involvement in psoriasis

Cytokines have also been found to be linked to the development of psoriasis, with tumour necrosis factor α (TNFα) and interferon γ (IFNγ) having been identified as major contributors to the disease. Both these cytokines are able to stimulate endothelial cells and keratinocytes leading to the activation of downstream inflammatory pathways resulting in the recruitment of immune cells which is important for the progression of psoriasis (Johnson-Huang et al., 2012). For example, IFNγ is believed to be involved early on in the disease due to the activation of Janus activated kinases 1 and 2 (JAK1 and 2) which in turn can activate Signal transducer and activator of transcription 1 (STAT1) (Ramana et al., 2002). This leads to the activation of other factors involved in cell growth and the regulation of genes found to be expressed in the skin lesions of patients with psoriasis. One group has even suggested that IFNγ could be used as a possible prognostic biomarker due to their observation of a positive correlation between IFNγ levels and the psoriasis area and severity index (PASI) scores (Abdallah et al., 2009).

TNFα is involved in the maturation and antigen presentation of dendritic cells as well as being vital for infiltration of T-cells into skin lesions (Goldminz et al., 2013). In this case, TNFα brings about its response through the activation of the transcription factor nuclear factor κB (NF- κB), the activated levels of which are increased in psoriasis (Lizzul et al., 2005). NF- κB has a variety of downstream effects such as cellular proliferation and differentiation as well as exerting control over apoptosis. In psoriasis these processes are altered, with increased proliferation of keratinocytes leading to the thickening of the epidermal layer while reduced apoptotic signals and increased survival signals prevent the cells from dying and subsequently being shed. This contributes to the build-up of the characteristic plaques (Weinstein et al., 1985). For this reason, many of the drugs used to alleviate the symptoms of psoriasis are TNFα inhibitors and therefore indirectly target the NF-κB pathway (Rozenblit and Lebwohl, 2009).

1.2.5 Current treatments

There is no cure for psoriasis; however, there are a number of treatments available such as immunosuppression, emollients or topical agents and Ultra-violet B (UVB) phototherapy. These treatments vary in their effectiveness and ongoing research is aimed at improving this as well as reducing the side effects some of these treatments can cause.

Psoriasis patients are scored using the psoriasis area and severity index (PASI) which gives each patient a score based on the severity of the plaques and the extent of coverage. This score can be used to assist the clinician in deciding the best course of treatment for each individual patient (Smith et al., 2009).

The use of UV phototherapy to treat psoriasis is a more traditional approach and has been in use for over 90 years. Currently, narrowband-UVB is the most common type of phototherapy used, however, psoralen photochemotherapy (PUVA) is mainly used on patients with chronic psoriasis vulgaris as it has shown a greater clearing capability and remission time than that of narrowband-UVB on patients with higher PASI scores (Mehta and Lim, 2016) and (Tanew et al., 1999).

The use of emollients is an important part of psoriasis treatment as they help to reduce pruritus and scaling. They form a protective film over the skin and therefore help prevent water loss, giving the skin a chance to rehydrate, while moisturising factors help to accelerate this process. There is also some evidence to suggest that the use of emollients help topical steroids permeate the skin further and therefore improves their efficacy (Jacobi et al., 2015) and (Fluhr et al., 2008).

New drugs can be developed to target specific molecules and immune agents as more is understood about the immunology of psoriasis. Among the most common immunosuppressive drugs available are TNF antagonists and interleukin inhibitors, which are becoming more common in treatment regimens and examples of which are shown in Table 1.

Table 1 Examples of drugs available for the treatment of psoriasis

Drug category	Example of drugs	Mechanism of action	Source
TNF antagonists	Infliximab	chimeric monoclonal antibody	(Goedkoop et al., 2004)
	Adalimumab	human IgG1 monoclonal antibody	(Gordon et al., 2006)
	Etanercept	recombinant fusion protein	(Leonardi et al., 2003)
IL-12/IL-23 inhibitors	Ustekinumab	human IgG1κ monoclonal antibody	(Meng et al., 2014)
IL-17 inhibitors	Secukinumab	human interleukin-17A monoclonal antibody	(Langley et al., 2014)
Phosphodiesterase inhibitors	Apremilast	phosphodiesterase-4 inhibitor	(Edwards et al., 2016)
Janus kinase inhibitors	Tofacitinib	Competitive inhibitor of ATP in binding site of JAK1&JAK3	(Papp et al., 2015)

With the exception of the TNF antagonists, the majority of these drugs were primarily developed to treat psoriasis vulgaris as this is the most common form of psoriasis. They are however, also prescribed as treatment for the other types of psoriasis and can be just as effective against these as psoriasis vulgaris; for example, Apremilast is widely used to treat psoriatic arthritis (Edwards et al., 2016).

1.2.6 Diseases associated with psoriasis

Patients with psoriasis often develop other diseases concomitantly and therefore treatment for these may need to be included with the treatment for psoriasis. Many psoriasis patients have an increased Body Mass Index (BMI) and hyperlipidaemia, leading to the so-called metabolic syndrome associated with psoriasis. Some of the main conditions associated with psoriasis are therefore cardiovascular disease (mainly myocardial infarction (MI) and atherosclerosis), hypertension, obesity and diabetes (Augustin et al., 2017). The development of these diseases may be due to the more sedentary habits of psoriasis patients, which in turn are most likely due to the psychosocial effects of the disease and therefore a tendency to lead a more reclusive lifestyle (Alsufyani et al., 2010).

The increased risk of cardiovascular disease, particularly MI, correlates with an increased severity of psoriasis and some studies suggest a similarity between the plaques seen in psoriasis and atherosclerotic plaques (Balta et al., 2014). This may be due to a number of factors such as stress and lifestyle as mentioned previously, however there is also an argument that the increased involvement of the immune system, leading to increased inflammation, predisposes patients to developing further health issues (Gelfand et al., 2006).

There have been a number of studies demonstrating the link between psoriasis and obesity; however, it is still unclear which condition predisposes to which (Neimann et al., 2006). While it is now generally accepted that there is indeed a relationship between the two, the order is still being debated and studies are ongoing (Herron et al., 2005) and (Setty et al., 2007).

Interestingly, the incidence of some skin disorders in patients with psoriasis is significantly decreased. For example, one study found that psoriasis patients are three times less likely to develop contact dermatitis and 25 times less likely to develop atopic dermatitis compared to patients without psoriasis (Henseler and Christophers, 1995). A recent study looking into the malignancy rates in patients with psoriasis has revealed that those patients treated with a biological agent (such as a TNF inhibitor) have a higher rate of cutaneous squamous cell carcinoma. It was also reported that overall, the rate of developing non-melanoma skin cancer was increased by 42% in patients that had received a systemic biological treatment compared to those who had not (Asgari et al., 2017). A review of the literature found that there was no significant increased risk of patients developing skin cancer when receiving UVB phototherapy alone, however when UVB is combined with PUVA there have been some reports of an increase in basal cell carcinomas. There is some argument that as this treatment is normally reserved for the more severe cases of psoriasis, that there are underlying factors that need to be considered. One of the main factors that could potentially result in this increased risk is that there is prolonged stimulation of inflammatory factors

along with hyperproliferation of cells that alone could lead to the development of cancer (Lee et al., 2005) and (Chiesa Fuxench et al., 2016).

Not only do patients with psoriasis therefore have to live with the impact of the disease, many of them also have to live with additional conditions and the impacts these bring. Thus, more research is needed into not only treatments for psoriasis but also into the underlying biological mechanisms that lead to the development of the disease.

1.3 Cholesterol and lipoproteins

The levels of cholesterol and lipoproteins in the blood have now been firmly established to be linked to the risk of heart disease and atherosclerosis. It is therefore thought that they may also be implicated in a number of other diseases, including psoriasis, and that their circulating levels may tie in to the development of these diseases.

1.3.1 Cholesterol

Cholesterol is a sterol (steroid alcohol) and is grouped with lipids such as triglycerides and phospholipids despite the lack of a fatty acid group. Along with other members of the lipid group, cholesterol makes up a vital part of cellular membranes by providing structural integrity, allowing cells to maintain their shape without the need for a cell wall, while retaining enough fluidity to allow the cell to change shape and move. Cholesterol found within the body has either been ingested in the diet or has been made *de novo* in the liver through a number of complex steps. For simplicity, these steps can be split into three main stages. In the first stage, isopentenyl pyrophosphate is synthesised from acetyl CoA, with the irreversible conversion of 3-hydroxy-3-methylglutaryl CoA (HMG CoA) to mevalonate by 3-hydroxy-3-methylglutaryl CoA reductase (HMG-CoA reductase) being the rate limiting step in cholesterol synthesis. The second stage is the formation of squalene from six molecules of isopentenyl pyrophosphate and in the third stage, squalene becomes tetracyclic and cholesterol is formed from this product (Berg JM, 2015).

As well as being a component of cell membranes, cholesterol is also a precursor for a number of important molecules including hormones such as progesterones and glucocorticoids, as well as other molecules such as vitamin D. Cholesterol is therefore vital for maintaining a healthy functioning body, however too much can lead to serious health issues such as cardio vascular disease.

1.3.2 Role of lipoproteins

Lipoproteins play a vital role in metabolism as they are responsible for transporting lipids throughout the body. They are made up of a combination of lipid and protein, hence the name, which allows non-polar, insoluble lipids such as cholesterol to move through the polar environment of the blood. The structure of lipoproteins is able to facilitate this transport as hydrophobic lipids are contained within the central core of the particle, while on the outside surface, various proteins and the hydrophilic heads of phospholipids provide a membrane and barrier between the lipid and plasma (Feingold and Grunfeld, 2015).

There are a wide number of proteins that can form part of these complexes, however apolipoproteins are the most commonly thought of as being associated with lipoproteins. Other proteins that have been found to associate with the lipoprotein complex include those liked with inflammation and wound healing. In fact it has now been found that there are more proteins associated with other functions than apolipoproteins in lipoprotein complexes (Vaisar et al., 2007) and (von Zychlinski et al., 2011).

For example, 18 apolipoproteins have been found associated with high density lipoprotein (HDL) compared to 71 other lipoprotein-associated proteins, with the likelihood being that the functionality will change depending on the associated proteins. It is however believed that these other proteins have a much more transient presence which has led to further studies investigating the roles they may play in healthy and diseased states and their potential link to the development of cardio vascular disease. It has also been hypothesised that the exact make up of lipoproteins could prove to be a valuable prognostic and diagnostic biomarker (von Zychlinski and Kleffmann, 2015).

As alluded to earlier, there are more lipoprotein complexes that can be grouped in order of size, apolipoprotein content and the lipids they transport. In total there are seven classes of lipoproteins, ranging from 5-1200nm in diameter, that together provide transport for cholesterol, phospholipids and triglycerides. Chylomicrons are the largest of the lipoproteins, followed by chylomicron remnants, very low-density lipoproteins (vLDL), lipoprotein(a) (Lp(a)), intermediate-density lipoprotein (IDL) and low density lipoprotein (LDL), with HDL being the smallest and most dense (Feingold and Grunfeld, 2015). These can be further split into pro and anti-atherogenic.

1.3.2.1 Pro-atherogenic lipoproteins

Chylomicrons are typically between 75-1200nm and therefore have the lowest density of all the lipoproteins at less than 0.93g/ml. They are generated in the intestine from absorbed dietary lipids through a number of complex steps, starting with the formation of the pre-chylomicron in the endoplasmic reticulum of enterocytes and ending with the release of the mature chylomicron from the Golgi (Mansbach and Siddiqi, 2010). Chylomicrons transport triglycerides from the intestine to adipose tissue and cholesterol to the liver and, as mentioned above, they vary widely in size. Their size is dependent on how much dietary fat has been ingested, with meals high in fat leading to the formation of the largest chylomicrons in order to deal with the increased load of triglycerides. Like all lipoproteins, they contain a number of different apolipoproteins including Apo B-48, Apo C, Apo E, Apo A-I, A-II and A-IV (Feingold and Grunfeld, 2015). Apo B-48 provides the main structure to the core of the chylomicron (all chylomicrons contain at least one of these molecules) while the addition of Apo A1 is needed to form the mature lipoprotein (Mansbach and Siddiqi, 2010).

Once chylomicrons reach their target tissue, the triglycerides are hydrolysed through the action of lipoprotein lipase. This allows the delivery of fatty acids to the adipose tissue or muscle and the now depleted chylomicron becomes a chylomicron remnant. These remnants have a higher density (0.930- 1.006g/ml) than the mature chylomicron as they are between 30 and 80nm and they also contain a higher percentage of cholesterol ester which is carried to the liver. Only the shortened Apo B-48 and Apo E apolipoproteins are associated with the chylomicron remnant, with Apo E being important for the rapid clearance of the remnants by the liver. Apo E is recognised and bound by receptors on hepatocytes where hepatic lipase hydrolyses the lipoprotein phospholipids into small particles that the hepatocytes are able to clear (Crawford and Borensztajn, 1999) and (Cooper, 1997).

Very low-density lipoproteins (vLDL) are another type of lipoproteins which are generated in the liver. These lipoproteins can also vary in size (30-80nm) depending on the amount of triglyceride carried and therefore their density can also vary from 0.930- 1.006g/ml. There are a number of apolipoproteins found associated with vLDL, these are Apo B-100, C-I, C-II, C-III, and E. Much like Apo B-48 in the chylomicron, Apo B-100 provides the main structural core of this lipoprotein with each vLDL particle containing one Apo B-100 protein (Feingold and Grunfeld, 2015). vLDL can also be hydrolysed by lipoprotein lipase in the bloodstream to generate vLDL remnants and IDL, from which LDL is derived. The current mechanism and understanding of LDL generation will be discussed in detail in the next section.

Intermediate-density lipoproteins (IDL) are formed when vLDL is hydrolysed. These particles are therefore smaller than vLDL (around 25-35nm compared to 30-80nm) and are more dense (1.006-

1.019g/ml), containing a higher percentage of cholesterol and reduced amount of triglycerides. Similarly to other lipoproteins, IDL also contains Apo B-100, along with Apo E and Apo C.

LDL (and its oxidised form) is one of the main focuses of this report and will therefore be discussed further in the following section. LDL is approximately 18-25nm in size and has a density of 1.019-1.063g/ml. Unlike the other lipoproteins, LDL only contains one Apo B-100 protein, with no others having been found to be associated. These lipoproteins are enriched with cholesterol and are responsible for the majority of cholesterol found in the circulation, leading to it being known colloquially as “bad cholesterol”.

Lipoprotein(a) is a further class of lipoprotein, however it varies significantly both structurally and metabolically from the others. So far not much is known about its function, although it appears to be made up of an LDL-like particle containing an Apo B-100 protein through which an apolipoprotein(a) molecule is bound via a disulphide bridge. These lipoproteins are formed in the liver and are around 30nm in size meaning they have the highest density (1.055- 1.085g/ml) of all the pro- atherogenic lipoproteins (Maranhao et al., 2014).

1.3.2.2 Anti-atherogenic lipoproteins

HDL is the only anti-atherogenic lipoprotein as it transports cholesterol back to the liver from the peripheral tissues, leading to it becoming known in lay terms as the “good cholesterol”. HDL is the smallest (5-12nm) and most dense (1.063- 1.210g/ml) of all the lipoproteins and unlike the others, it does not contain an Apo B apolipoprotein. Instead it contains Apo A-I, A-II, A-IV, C-I, C-II, C-III, and E. In this case, Apo A-I provides the main structural component for the core of HDL and each HDL complex can contain multiple Apo A-I proteins. Due to this wide variety of apolipoproteins that can be associated with HDL, it is a very heterogeneous particle and therefore the HDL class of lipoproteins can be further divided. This is achieved by using a number of techniques that separate the complexes not only by the apolipoproteins present but also by size and density (Feingold and Grunfeld, 2015).

1.4 Low density lipoprotein

The link between the levels of HDL/LDL-cholesterol in the blood and diseases such as atherosclerosis has now been well established, with increased levels of LDL leading to an increased risk of cardiovascular disease. Previous work has also shown that LDL is involved in regulating the migration and angiogenesis of endothelial cells and therefore LDL and its oxidised form, oxLDL, are a major focus of this report.

1.4.1 Formation and function of LDL

LDL is just one class of lipoprotein and is responsible for the majority of cholesterol found in circulation. For this reason, there has been a lot of interest into how LDL is formed and regulated and this process will briefly be described here.

LDL is formed via a two-step sequential process involving the generation of an intermediary lipoprotein, see Figure 4. Once vLDL has been released from the liver and has entered the circulation, lipoprotein lipase and hepatic lipase are able to remove triglycerides that will be used either immediately for energy or stored. At this stage, before the subsequent transfer of cholesterol, the depleted vLDL complex becomes known as IDL. Another protein, the cholesteryl ester transfer protein (CETP), then further removes triglycerides and phospholipids from the IDL particle and transfers them to HDL, while at the same time, cholesterol esters are removed from HDL and transferred to the newly formed LDL particle. The c-terminal end of the Apo B-100 apolipoprotein present in LDL is then able to bind to the LDL receptor allowing LDL to be removed from the circulation via the LDL receptor pathway (von Zychlinski and Kleffmann, 2015) and (Brown and Goldstein, 1987). Unsurprisingly, CETP inhibitors have been developed as a way to treat the growing incidence of cardiovascular disease as by blocking the transfer of cholesterol from HDL to LDL, they can simultaneously increase the levels of HDL-cholesterol returning to the liver and decrease the levels of LDL-cholesterol depositing cholesterol in the peripheral tissues (Klerkx et al., 2006).

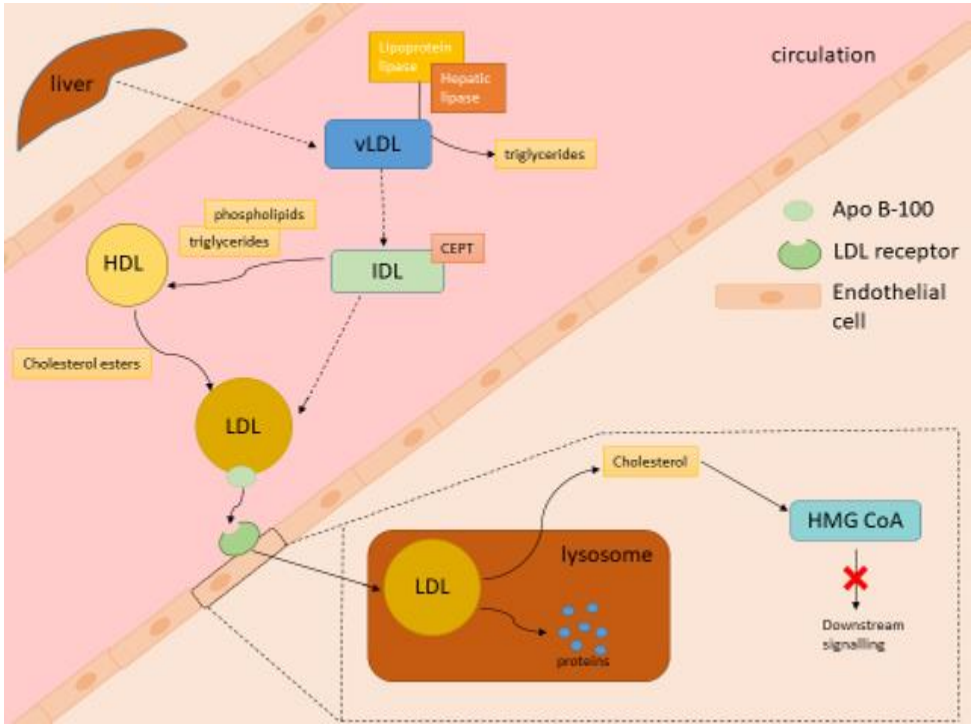

Figure 4 Formation of LDL and subsequent removal from circulation
LDL is formed from vLDL through a two-step sequential process involving the removal of triglycerides, phospholipids and cholesterol. Once formed, LDL is cleared through the action of the LDL receptor, with Apolipoprotein B-100 being vital for the uptake of LDL into the cells and subsequent degradation in the lysosome.

The LDL receptor pathway is the mechanism in which LDL leaves the blood and enters the tissue. LDL binds to the receptor and is endocytosed, ending up in a lysosome where the protein is degraded and the cholesterol released, enabling it to repress 3-hydroxy-3-methylglutaryl coenzyme A (HMG CoA) reductase which is the rate limiting step in cholesterol synthesis. These receptors are therefore one of the key ways in which the plasma concentration of LDL is regulated, as both the production and clearance rate of LDL is governed by the abundance of receptors. It therefore follows that an increase in receptors leads to a decrease in circulating LDL due to a higher clearance rate, with the reverse also being true. The liver is highly enriched in these receptors and it is estimated that around 70% of the total LDL is removed in this way, with the remaining 30% being taken up by the peripheral tissues. As the abundance of receptors plays such an important role in the regulation of lipoproteins, they themselves must be subjected to strict regulation. This is achieved through a feedback loop, with a decrease in cholesterol in the liver leading to an increase in the levels of transcription of the LDL receptors through the action of sterol regulatory element binding proteins (SREBPs). Once the receptors are on the cell surface, they can also be endocytosed and degraded in the lysosome by the binding of proprotein convertase-subtilisin/kexin type 9 (PCSK9), providing another layer of regulation to assist in the fine tuning of plasma LDL concentration (Goldstein and Brown, 2009).

1.4.2 Oxidised LDL (oxLDL)

Like many other lipids and proteins, LDL can be modified in various ways including becoming oxidised.

The oxidised form of LDL (oxLDL) emerged as a marker of cardiovascular disease around 30 years ago, however it is still unclear exactly what role it plays with arguments for it being both pro and anti-atherogenic being put forward. It should also be noted that other lipoproteins (such as vLDL and even HDL) can undergo this modification, again leading to alterations in their respective atherogenic properties. It is understood that oxLDL is generated through a number of non-enzymatic changes to the Apo B portion of LDL while in the circulation, although oxidative changes to the lipid have also been noted. This oxidation causes a noticeable structural change to the lipoprotein, leading macrophages to recognise it as being damaged and actively scavenge the oxidised LDL in order to remove and degrade it (Fong et al., 1987).

Scavenger receptors (particularly type A) and Cluster of Differentiation 36 (CD36) (also known as fatty acid translocase) are the main receptors on the macrophage that recognised oxLDL and facilitate its endocytosis via a lipid raft dependent mechanism. Recent work has shown that of these two receptors, CD36 is the one linked to the pathogenic effect of oxLDL in the development of atherosclerosis. When there is a high concentration of oxLDL in the blood, the macrophages essentially become “full” of lipid and become what is known as a foam cell. These are the cells that are directly involved in the development of atherosclerosis as they form the basis of the actual plaque build-up in the arteries (Yu et al., 2013).

Macrophages are not the only cells able to internalise oxLDL; endothelial cells have also been found to be able to clear oxLDL. This is achieved through a different set of receptors as the scavenger receptors are not present on endothelial cells, or at least not present in a large enough quantity to allow rapid uptake of oxLDL. Instead, LOX-1 was found to be the receptor responsible for binding oxLDL and facilitating its endocytosis. This interaction of LOX-1 with oxLDL also leads to the activation of the endothelial cell which can cause damage as a result of the pathways that are activated. For example, once internalised, oxLDL is able to activate the MAPK p42/44 pathway that leads to the ultimate expression of genes involved in cell adhesion, including monocyte adhesion to the endothelium and apoptosis (Li and Mehta, 2005).

It is thought that this is a vital step in the initial plaque formation in atherosclerosis, as the recruitment and binding to the endothelium of the monocytes is a pre-requisite step for eventual foam cell generation (Kita et al., 2006).

1.4.3 OxLDL and disease

The role of oxLDL in the development of cardiovascular disease, and particularly atherosclerosis, has now been well established, however the circulating levels of oxLDL can also be attributed to the development and progression of other, non-coronary diseases. OxLDL plays a major role in the deposition of lipids in the arteries leading to the formation of the characteristic plaques seen in atherosclerosis. It has now also been established that as well as increasing inflammatory signals in the local environment, oxLDL can also influence every aspect of atherosclerosis development. This includes early atherogenesis, that can lead to both coronary and peripheral arterial disease, hypertension caused by the blood vessels becoming smaller due to plaque build-up, right through to the development of much more serious ischaemic cerebral infarction and acute coronary syndromes such as myocardial infarction and angina (Trpkovic et al., 2015).

Oxidised LDL has also been linked to the metabolic syndrome (characterised by dislipidemia and hypertension, often as a result of obesity) and type 2 diabetes (Holvoet et al., 2004). This is to be expected, as both an increased BMI and an increase in circulating LDL-cholesterol are well-known risk factors for the development of both of these diseases. A study by Rosen et al. (2001) discovered that for type 2 diabetes, it was the levels of oxLDL and not LDL that had the greatest prognostic value, potentially due to the link with oxidative stress and inflammation.

In another study, the relationship between obesity, diabetes and oxLDL was examined. This was a much more comprehensive study and included looking at the differences between races as it is known that the incidence of obesity varies depending on ethnicity. It was confirmed that the circulating levels of oxLDL is indeed linked to both type 2 diabetes and obesity (measured using BMI and body fat percentage) across ethnicities. Additionally, it was noted that oxLDL was only associated with levels of fasting glucose in the white population. Further investigation also highlighted a positive link between oxLDL and insulin resistance, with the authors postulating that this could be due to the decrease in adiponectin observed as it is a measure of a person's sensitivity to insulin (Njajou et al., 2009).

1.4.4 OxLDL in psoriasis

Obesity and diabetes are linked with psoriasis and therefore it would be reasonable to suggest that oxLDL may also play a role in some stage of its development. Some autoimmune diseases have already been linked with increased levels of oxLDL such as systemic lupus erythematosus and systemic sclerosis.

It has been found that psoriasis patients have oxLDL present in their skin lesions, whereas in healthy individuals, and indeed in the healthy areas of psoriasis patient's skin, oxLDL cannot be detected. This is most likely as a result of the action of proteolytic enzymes or myeloperoxidase released by leukocytes which produce reactive oxygen species that oxidise lipids and proteins (Coimbra et al., 2010). It has been reported that levels of oxLDL in the plaques are reduced after a standard treatment (12 weeks) of phototherapy but still do not return to healthy baseline levels. This suggests that it would be beneficial to monitor the levels of oxLDL in patients as it could prove to be a useful biomarker, however, it is yet to be approved as a prognostic marker for psoriasis (Kaur et al., 2017). Patients with psoriatic arthritis have also been found to have the highest concentration of ApoB as well as LDL/HDL ratios, with the oxidative state correlating with the ApoB levels as well as the total cholesterol concentration (Pietrzak et al., 2019).

As mentioned previously, LOX-1 is an oxLDL receptor and as well as being expressed in endothelial cells, it is also found in the epidermis. Mice fed a high cholesterol diet have been found to have an increased expression of LOX-1, with oxLDL signalling through this receptor leading to increased keratinocyte activity and accentuated effect of TNF-α within the epidermis (Shih et al., 2018). LOX-1 may therefore become a novel target to treat psoriasis in the future.

1.5 Sphingosine-1-phosphate

Previous work has demonstrated that oxLDL is able to regulate both angiogenesis and endothelial migration and it is believed that oxLDL may signal through sphingosine-1-phosphate (S1P) to exert its effect on the endothelium. Sphingosine-1-phosphate (S1P) is a bioactive lipid that was found to be involved in the regulation of cell growth by Zhang et al. (1991). Since then S1P has also been observed to be involved in many other vital cellular processes such as migration, angiogenesis and overall survival. For this reason, S1P signalling is crucial during embryogenesis and development, but as these processes are also part of homeostatic mechanisms, changes to S1P regulation may point to its involvement in disease (Mendelson et al., 2013).

1.5.1 Metabolism and export of S1P

Sphingosine is a highly regulated membrane lipid involved in membrane trafficking (Lima et al., 2017) and apoptosis among other functions (Woodcock, 2006). Sphingosine-1-phosphate is a metabolite of sphingosine, formed by the deacetylation of ceramide by ceramidase. Ceramide makes up the backbone of the majority of mammalian sphingolipids and can be synthesised either through the action of sphingomyelinase on sphingomyelin or de novo through a number of steps that occur at the endoplasmic reticulum. There are two isoforms of the sphingosine kinase (SKI and SKII) that phosphorylate sphingosine, generating S1P, a process that can be reversed by the action of S1P phosphatase. S1P can also be cleaved by S1P lyase (S1PL), an irreversible step that results in the formation of phosphoethanolamine and hexadecenal, see Figure 5 (Le Stunff et al., 2004). These can be further metabolised to form phosphatidylethanolamine and other glycerophospholipids, which make up a major part of mammalian cellular membranes (Hishikawa et al., 2014).

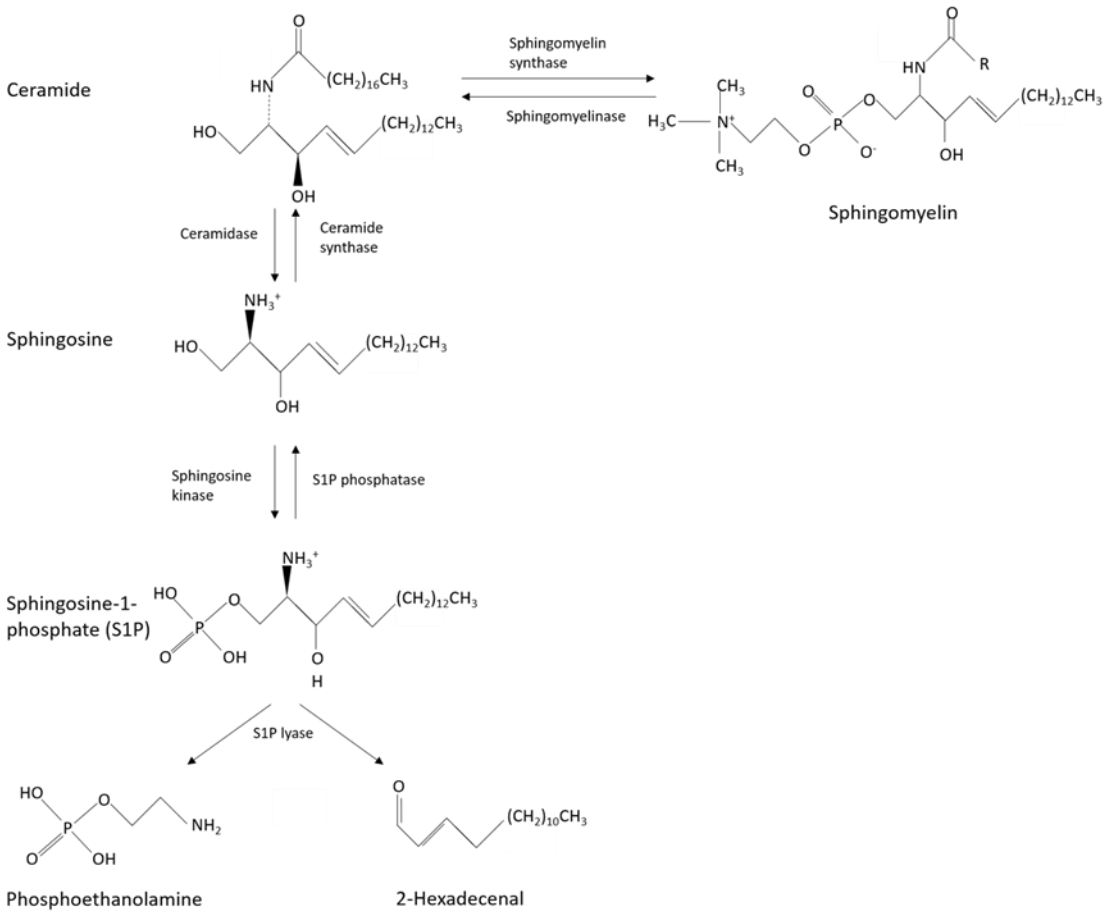

Figure 5 Formation of Sphingosine-1-phosphate

Sphingosine-1-phosphate is generated through a number of reversible steps from ceramide, which arises from sphingomyelin. The R group in sphingomyelin represents a hydrocarbon chain that can be of varying lengths. Ceramide is metabolised to sphingosine, which is then phosphorylated by sphingosine kinase to produce S1P. S1P lyase converts S1P into phosphoethanolamine and hexadecenal, which can be metabolised further to phosphatidylethanolamine and glycerophospholipids, both major components of cellular membranes (Le Stunff et al., 2004).

Due to the reversibility of the steps leading to S1P synthesis, there is a delicate balance in place that is adjusted to accommodate cellular and extracellular demands on the cell. S1P is involved in the migration, growth and survival of the cell, as mentioned previously, whereas ceramide and sphingosine are known to be pro-apoptotic and inhibit cell growth. S1P levels are kept low in the cell whereas sphingosine and ceramide levels are higher as they are relatively inactive and act as a store, ready to supply the cell with S1P on demand (Edsall et al., 1998). S1P is also found pooled in red blood cells ready to provide an immediate supply when required. Therefore the actions of the various enzymes involved in this pathway ultimately determine cell survival (Spiegel and Milstien, 2002).

1.5.2 S1P transport and receptors

Once S1P has been synthesised it is exported from the red blood cells through ATP-binding cassette transporters (ABC transporters) or Spinster 2 (Spns2) (Donoviel et al., 2015). The ABC family of transporters has been found to export S1P from a number of cell types including red blood cells (through ABCA7) (Olivera et al., 2013), astrocytes (through ABCA1) (Nagahashi et al., 2014) and endothelial cells (through ABCA1 and ABCC1) (Lee et al., 2007). Endothelial cells also rely on Spns2, part of the major facilitator superfamily, to transport S1P out of the cell and thereby maintaining the S1P gradient (Nagahashi et al., 2014). Spns2 is a homolog of two of hearts, which was originally discovered in zebrafish as the cause of cardia bifida, a condition that could be recovered by adding S1P (Osborne et al., 2008). Spns2 is also able to transport analogues of S1P, such as FTY720 (Fingolimod), a drug recently approved by the US Food and Drug Administration (FDA) to treat multiple sclerosis (Hisano et al., 2011) and (Patmanathan et al., 2017).

Originally Sphingosine-1-phosphate was thought to be an intracellular second messenger but has since been found to be a ligand for G protein-coupled receptors (GPCRs). There are now known to be five GPCRs that S1P can bind to and activate, designated $S1PR_{1-5}$ (see Figure 6). $S1PR_{1-3}$ are widely expressed, including in endothelial cells, with $S1PR_4$ being found in immune cells and lymphoid tissues and $S1PR_5$ being expressed in the brain, spleen and in natural killer cells (Dillmann et al., 2015), (Zhang et al., 2013) and (Chun et al., 2010).

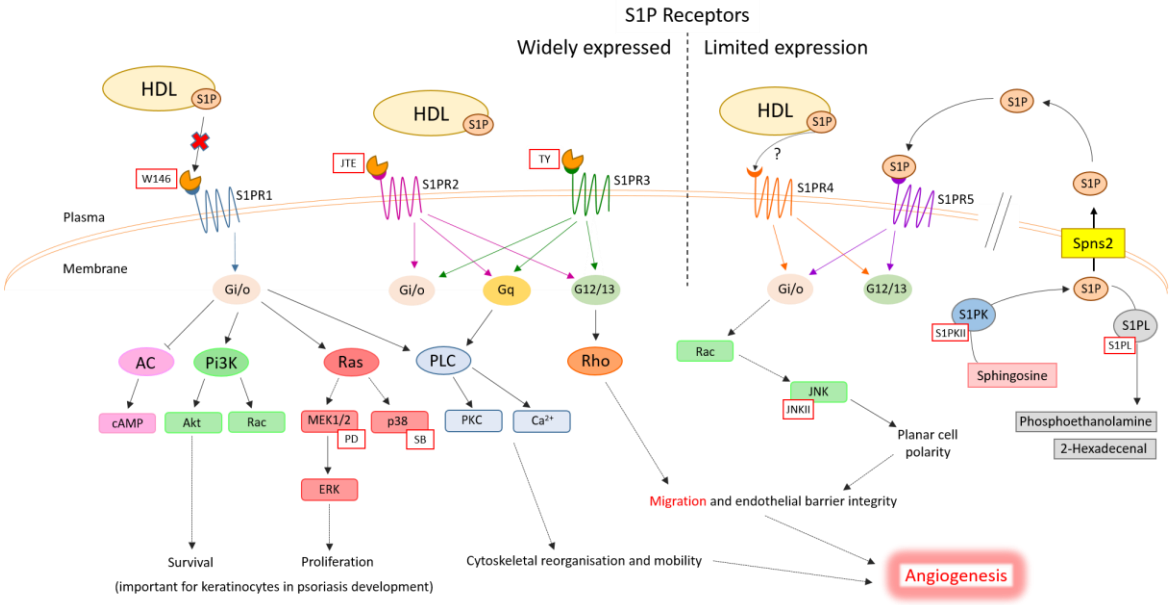

Figure 6 The S1P Receptors and some of the pathways they activate
In endothelial cells, S1P is exported through Spinster 2 where it either binds to HDL in the plasma or acts in an autocrine fashion by flipping onto the outer membrane. It can then bind to 5 different GPCRs and thereby activate a range of intracellular pathways, although the mechanism behind the dissociation of S1P from HDL and its subsequent binding to the receptor is still unclear. Receptor activation leads to vital biological responses such as migration, angiogenesis, survival and proliferation, all of which are also important processes in the development of psoriasis. Red boxes indicate various inhibitors for different stages of the pathways that have been utilised in this thesis. Information for diagram taken from (Brinkmann, 2007).

It is now known that S1P does not travel freely in the blood and is instead either found pooled in red blood cells or bound to albumin or Apolipoprotein M (ApoM) in high density lipoprotein (HDL). This helps to explain how the plasma and serum concentration of S1P can be roughly 200nM and 500nM respectively (Yatomi et al., 1997), while the dissociation constant for the S1P receptors is between 2-30nM (Okajima, 2002), as the concentration of free S1P able to bind to the receptor is much less than the total S1P. Recent work looking at the dissociation constant of S1P from apoM-HDL, apoM-LDL and human serum albumin has yielded values of 21nM, 2.4nM and 22µM respectively. During this study it was also found that S1P had a roughly 10 times stronger affinity for apoM-LDL than apoM-HDL, presumably because S1P bound to LDL is targeted to be cleared whereas S1P bound to HDL needs to become available to bind to the S1P receptors, although it is not clear if S1P first needs to become disassociated from HDL or whether HDL assists in receptor binding (Fleming et al., 2016b). S1P is also found within cells and this intracellular store is able to respond to extracellular stimuli to bring about a variety of actions. It is thought that the cellular location of S1P production will influence its intracellular targets, for example when it is synthesised at the endoplasmic reticulum (ER) the resultant effect is an increase in intracellular calcium, with

studies suggesting that the thapsigargin-sensitive calcium channels are activated, however as yet, no specific targets have been identified (Mattie et al., 1994) and (Strub et al., 2010).

1.5.3 Fingolimod

As mentioned previously, Fingolimod (FTY720) is an analogue of S1P currently being used to treat highly active relapsing multiple sclerosis (MS). Fingolimod is an immunomodulating drug which, in MS, works by preventing the egress of lymphocytes (mainly T cells) from the lymph nodes by inhibiting the S1P receptor 1 (Baer et al., 2018). Once phosphorylated by sphingosine kinase, Fingolimod becomes active and is therefore able to bind to four of the five S1P receptors (1 & 3-5), resulting in their down-regulation and subsequently preventing the binding and downstream signalling of S1P.

S1P has a wide range of biological effects and as the receptors are ubiquitously expressed, there are a number of potential side effects associated with continual treatment with this competitive agonist. At the onset of treatment, patients need to be monitored for several hours to ensure they don't develop bradycardia (a slow heart rate) as if left untreated this can develop into a cardiac arrest and can be fatal. Atrial myocytes are rich in S1P receptors that, once activated, are responsible for activating G-protein–coupled inwardly rectifying potassium (GIRK) channels which govern the action potential and pacemaker functions of the heart i.e. how often the heart contracts and beats. Once these GIRK channels are activated, there is a period of hyperpolarisation which prevents the cells from being excited and generating a further action potential, hence the bradycardia seen upon Fingolimod activation of the S1P receptors (Camm et al., 2014).

Another potential side effect of Fingolimod is a reduction in endothelial barrier integrity leading to leaky blood vessels; the most common presentation of this is macular oedema. S1P plays a vital role in the permeability of blood vessels by altering the junctions between cells as well as between the cell and the extracellular matrix. S1PR1 activation leads to tighter intracellular junctions whereas S1PR2&3 lead to an increase in permeability. As the primary target of Fingolimod is S1PR1, shown by the binding affinity (0.2nM compared to 5nM for S1PR3), it therefore follows that when the S1PR1 receptor is downregulated through the binding of Fingolimod, S1P is free to bind S1PR2 or 3 leading to the fluid build-up seen in the macular (Lee et al., 2009).

1.5.4 S1P and disease

The role of S1P in multiple sclerosis was briefly touched upon in the previous section and the role of S1P in other diseases will be further discussed here. As highlighted in Figure 6, S1P can activate many different pathways which have a wide range of biological effects. It is therefore logical that S1P is involved in a number of diseases, ranging from atherosclerosis to diabetes to cancer.

1.5.4.1 Atherosclerosis

The role of S1P in atherosclerosis has been extensively studied and, due to its complex signalling nature, has been found to have both pro- and anti-atherosclerotic effects. For example, all three S1P receptors found in endothelial cells have potentially protective and detrimental effects on vascular health depending on which downstream pathway is activated. Some of these dual effects are highlighted in Table 2 below and will be discussed further in this section (Kurano and Yatomi, 2018). It has also been proposed that the plaques seen in atherosclerosis are similar to those in psoriasis and therefore it is possible that S1P plays a role in the development of both these diseases.

Table 2 Pro- and anti-atherosclerotic effects of the S1P receptors

Receptor	Anti-atherosclerotic	Pro-atherosclerotic	*In vivo* overall effect
S1PR1	Phosphorylation of eNOS	Chemotaxis of lymphocytes	Anti-atherosclerotic
	↓ICAM1/VCAM1		
S1PR2	↓ migration VSMC	Chemotaxis of macrophages	Pro- atherosclerotic
		↑ PAI-1	
S1PR3	Phosphorylation of eNOS	Chemotaxis of macrophages	Most likely anti-atherosclerotic
	Anti-apoptotic		

Activation of the S1PR1 receptor can lead to the phosphorylation of endothelial nitric oxide synthase (eNOS) and the reduction of Intercellular adhesion molecule 1 (ICAM1) and vascular cell adhesion molecule 1 (VCAM1) expression on endothelial cells. Both of these processes are anti-atherosclerotic as the phosphorylation of eNOS causes vasodilation of the blood vessels, resulting in tighter intracellular junctions and an inhibition of endothelial contraction (Argraves et al., 2008). ICAM1 and VCAM1 endothelial expression are vital in the early stages of atherosclerosis and therefore reducing their expression levels prevents blood cells from attaching to the endothelial layer, in turn preventing the formation of the atherosclerotic plaques (Kimura et al., 2006). Conversely, S1PR1 is involved in the egress of lymphocytes from the lymph nodes (as discussed previously) and subsequently activation of this receptor also has pro-atherosclerotic effects due to the promotion of inflammation.

Similarly, S1PR2 also has a dual functionality in the development of atherosclerosis. S1P signalling through S1PR2 has been found to prevent the migration and proliferation of vascular smooth muscle cells (VSMC), both of which are important steps in the formation of atherosclerotic lesions (Tamama et al., 2005). Activation of S1PR2 inhibits platelet-derived growth factor (PDGF) and therefore interrupts the migration of VSMC by promoting actin filament disassembly. S1P mimics the downstream signalling of the PDGF receptor, however this results in a prolonged and greater increase in calcium flux than seen by PDGF receptor activation, resulting in an increase in cyclic AMP and consequent signalling. This in turn causes an inhibition of actin filament assembly and nucleation and ultimately prevents cellular migration by disrupting the carefully controlled cytoskeleton dynamics and formation of lamellipodia at the leading edge of the cell (Bornfeldt et al., 1995). S1PR2 has also been found to be pro-atherosclerotic due to its involvement in the recruitment of macrophages and therefore plays a role in inflammation. Potentially more problematic in the development of atherosclerosis is the association of S1PR2 with the increase of endothelial plasminogen activator inhibitor 1 (PAI-1). It has now been established that elevated levels of PAI-1 are linked with cardiovascular disease, with a number of important steps in the development of atherosclerotic plaques being attributed to high plasma levels. PAI-1 plays an important role in thrombosis which, combined with the deposition of lipids, is one of the first steps in the formation of vascular lesions. PAI-1 is also able to signal through the LDL receptor, resulting in the migration of VSMC. Interestingly, oxLDL is able to stimulate PAI-1 production in both endothelial cells and VSMC, further fuelling the negative health effects of both signalling molecules (Baluta and Vintila, 2015).

S1PR3 signalling has similar effects on atherosclerosis as S1PR1 stimulation. Both receptors can lead to the phosphorylation of eNOS thereby activating this enzyme which results in the relaxation of the blood vessel and tighter intracellular junctions and both play a role in the recruitment of inflammatory cells. S1PR1&3 have also been reported to promote survival through the Phosphoinositide 3-kinases (PI3K) and Akt pathway, protecting the cardiomyocytes from apoptosis and the heart from ischemia (Kurano and Yatomi, 2018).

The dual nature of S1P observed in the pathogenesis of atherosclerosis has led to multiple animal studies to further investigate the involvement of S1P *in vivo*. This has led to the identification of whether each receptor is more pro- or anti-atherosclerotic in a living model. It has been well established in animal studies that an S1PR1 knockout is embryonic lethal and therefore these studies have had to make use of inhibitors against this receptor instead. Overall it has been found that S1PR1 has mainly anti-atherosclerotic properties *in vivo*, with one study finding that an agonist against S1PR1 protected a LDL receptor knockout model from developing atherosclerosis (Liu et al., 2000). Similar results have also been found for S1PR3, suggesting that this receptor most likely also

functions in an anti-atherosclerotic manner. For example, knockout mice were found to be largely resistant to the known beneficial effects of S1P bound HDL, while another study showed that macrophage recruitment and smooth muscle cell modification was also increased in this knockout strain (Theilmeier et al., 2006) and (Keul et al., 2011).

In contrast to findings for S1PR1 and 3, S1PR2 has been found to promote the development of atherosclerosis, with knockout mice showing decreased levels of foam cells in atherosclerotic plaques. This suggests that S1PR2 plays a role in not only attracting macrophages and other inflammatory mediators to the plaques but also plays a role in retaining them and regulating their cytokine secretion, further assisting in the development of atherosclerosis (Skoura et al., 2011).

Further studies that are currently being carried out include using an inhibitor against sphingosine kinase to look at the effects of varying circulating levels of S1P as well as the overexpression of ApoM and the potential differential role S1P plays when bound to HDL versus albumin (Kurano and Yatomi, 2018). These findings will enhance the current knowledge of the role of S1P in atherosclerosis and potentially lead to new targets to treat this aspect of cardiovascular disease.

1.5.4.2 Diabetes and obesity

As discussed in the previous section, S1P is involved in the development of atherosclerotic plaques and this section will explore its role in diabetes and obesity. These conditions are often concurrent with psoriasis due to the dislipidemia observed within this patient group and are often associated with the metabolic syndrome as described previously. The formation of atherosclerotic plaques is also accelerated in diabetes. S1P is involved in the development of both these diseases and provides a common link between them and psoriasis, as well as being associated with the outcome of the metabolic syndrome (Donnelly and Davis, 2000).

This section will focus on the role of S1P in type 2 diabetes (or adult onset) which accounts for 90% of all diabetic cases and is a result of insulin resistance rather than a failure to produce insulin as is the case in type 1 diabetes. Obesity and Type 2 diabetes are intimately linked due to their similarities regarding altered lipid metabolism and associated signalling, with a high BMI being one of the main risk factors for type 2 diabetes onset (Chatterjee et al., 2017).

With regard to diabetes, it has been found that there is a multifaceted interplay between S1P and insulin with S1P promoting the survival of pancreatic β-cells and protecting them against TNF-α-induced apoptosis. In contrast, S1P is also elevated in lipotoxic environments and under these conditions attenuates the growth and pro-survival signals of insulin via S1PR2, resulting in detrimental downstream signalling through the JNK pathway and simultaneous inhibition of the Akt pathway (Japtok et al., 2015). It has also been found that glucose is able to specifically stimulate the production of intracellular S1P in mouse β-cells, with the levels of other sphingolipids remaining unaffected. As S1P is involved in insulin release in response to glucose, glucose-stimulated insulin secretion (GSIS) was in turn also increased in line with the rising S1P levels. This has been confirmed by studies showing that the inhibition of sphingosine kinase leads to a decrease in GSIS while inhibition of the S1P phosphatase resulted in greater GSIS (Cantrell Stanford et al., 2012). To further support the role of S1P in diabetes, Fingolimod has been found to return blood glucose levels to normal by increasing insulin levels, without changing the sensitivity, and therefore preventing the development of type 2 diabetes in diabetic mouse models (Moon et al., 2013a).

Sphingosine kinases themselves have also been found to be important in diabetes and in some of the associated pathologies. In both obesity and diabetes it has been found that activation of the sphingosine kinases enhances hepatic insulin signalling, with decreased levels being detected in high fat diet fed mice (Ng et al., 2017). With ongoing studies into the impact of the sphingosine kinases on disease, differences between the two isoforms have now become apparent. For example, the overexpression of sphingosine kinase 1 reduces triacylglycerol production in the liver, however this does not affect glucose metabolism and therefore suggests that isoform 1 does not

play a key role in insulin production and signalling (Kowalski et al., 2015). In contrast, sphingosine kinase 2 has been found to be heavily involved in glucose metabolism and is the main isoform in the liver. Studies using diabetic mice have shown that overexpression of this isoform leads to an increase in hepatic S1P levels and subsequently improved glucose and lipid metabolism through the activation of the Akt pathway. Sphingosine kinase 2 therefore has an active role in the prevention of insulin resistance and therefore the development of type 2 diabetes (Lee et al., 2015a).

It has been found that circulating levels of S1P are elevated in obese people (like in psoriasis patients) and correlated with BMI, waist circumference and percentage of body fat (Donnelly and Davis, 2000). It has also been discovered that S1P adjusts energy homeostasis via the S1PR1 receptor and the STAT3 pathway in rats (Silva et al., 2014). Studies using injected S1P found that the melanocortin and STAT3 pathways were activated and resulted in an overall decreased intake of food and a greater energy use. This has been corroborated by other studies which have found that there is a discrepancy in the S1P (via S1PR1) and STAT3 signalling pathways in obesity models and that this can be modulated pharmacologically (Silva et al., 2014).

S1P regulates adipogenesis and lipolysis to reduce the levels of stored fat through several different pathways. For example, in pre-adipocytes S1P downregulates markers of differentiation in a dose dependent manner resulting in reduced lipid build-up. S1P also downregulates both Jun N-terminal kinase (JNK) and p38 MAPK to regulate adipogenesis while Fingolimod has been found to increase lipolysis. This suggests that S1P is able to control the balance between lipid storage and expenditure and therefore potentially may represent a therapeutic target for obesity (Chen et al., 2016).

The role of S1P in inflammation is now widely accepted and inflammation is also known to be involved in obesity. Studies looking at the levels of S1P and inflammatory markers in healthy and obese adolescent humans found a correlation between S1P and TNF-α, with mice studies supporting these findings. Mouse studies also revealed an overall increase in S1P in obese mice which promoted adipocyte expression of TNF-α as well as interleukin (IL)-6 and monocyte chemoattractant protein-1 (Majumdar and Mastrandrea, 2012) and (Samad et al., 2006). Interestingly, further studies altering sphingosine kinase signalling found that in diet-induced obesity mice models, adipocyte expression of interleukin 10 and adiponectin were increased while IL-6, TNF-α and macrophage recruitment was decreased (Wang et al., 2014). S1P therefore plays a complex role in obesity and has the potential to not only regulate the balance between the deposition and release of lipids in adipocytes but also to mediate associated inflammatory factors.

1.5.4.3 Cancer

As discussed in previous sections, S1P is involved in a wide range of physiological functions such as cell survival, proliferation, migration, angiogenesis and inflammation. It is well known that all these processes are involved in the development of cancer and therefore it should come as no surprise that S1P plays a role in tumour growth and survival. One of the main reasons S1P is involved in cancer progression is due to the influence it exerts on the tumour microenvironment.

Most components of the S1P signalling pathway have been found to play a part in cancer and appear to result in increasing S1P levels surrounding the tumour. For example, many cancer cells overexpress sphingosine kinases resulting in inter and extracellular signalling leading to alterations in gene expression as well as regulating the tumour microenvironment (Alvarez et al., 2010). Sphingosine kinase 1 has been found to be involved in the metastasis of melanoma by generating S1P which is released from the melanoma cells and results in the differentiation of fibroblasts. These become myofibroblasts and sphingosine kinase 1 again produces S1P, resulting in the S1PR3 dependent metastasis of melanoma (Albinet et al., 2014).

The S1P transporters are also involved in the microenvironment regulation and control the levels of S1P in the extracellular space. The MCF-7 breast cancer cell line has been found to export S1P through an ABC transporter in response to estradiol (Takabe et al., 2010) while Spns2 regulates the levels of S1P in the surrounding lymph nodes and subsequently controls the trafficking of immune cells (Nagahashi et al., 2013). Importantly, it has been found that breast cancer tissue has a much higher concentration of S1P than healthy tissue, suggesting that the S1P present in the immediate tumour microenvironment has been produced and exported by the cancer cells themselves (Nagahashi et al., 2016).

In contrast to the over expression of the sphingosine kinases, both S1P phosphatase and lyase have been found to be downregulated in cancer cells and therefore a decrease in apoptotic signals. For example, phosphatase levels have been found to be significantly lower in gastric cancer cells compared to healthy tissue and this reduced level has been associated with both lymph and distant metastasis (Gao et al., 2015). Similarly, both the levels and the activity of S1P lyase were found to be reduced in human colon cancer and mouse studies have confirmed this decrease in intestinal cancer models (Oskouian et al., 2006).

As the extracellular S1P concentration increases, so too does the S1P receptor activation leading to an increase in cellular functions such as angiogenesis which ensures the tumour has enough oxygen and nutrients. Migration, proliferation and survival of the cancer cells is also favoured by increased S1P signalling while inflammatory mediators are able to stimulate S1P production in the

surrounding non-cancerous cells ensuring continual signalling. It is also possible that S1P released from cells in nearby lymph and blood vessels acts as a chemoattractant allowing the cancerous cells to migrate towards the more nutrient-rich environment (Nakajima et al., 2017).

Due to the complex nature of S1P signalling, there are a number of potential targeted therapeutic options that could be developed. For instance, Fingolimod has been shown to lower the levels of S1P and in animals with inflammation has been found to suppress tumour progression. Studies have also shown that downregulating S1PR1 inhibits angiogenesis and therefore prevents the growth of the tumour by limiting nutrient availability (Chae et al., 2004). It is therefore possible that by modulating the S1P signalling pathway, novel cancer treatments may be found.

1.5.5 S1P in psoriasis

S1P is known to be involved in the development and progression of a number of diseases, including psoriasis, and a brief discussion of the current knowledge in this field will be presented in this section.

Previous research has shown that the lipid composition in psoriasis patients is altered compared to healthy individuals, with lipids such as LDL and triglycerides being elevated while HDL levels are significantly lower (Ma et al., 2014). This has prompted investigation into sphingolipids due to their structural role in the skin and the complex signalling pathways their derivatives are involved in. S1P is amongst one of the most physiologically active and is known to play an important role in a number of processes such as cell migration and angiogenesis (Mendelson et al., 2013). These processes are also highly involved in the development of psoriasis and therefore S1P has become the focus of several studies.

A recent study measuring the circulating levels of sphingolipids in patients with psoriasis showed that the levels of ceramides were significantly decreased in these patients, with the authors hypothesising that this may be linked to the lower levels observed in the skin lesions which have previously been reported (Mysliwiec et al., 2017). The reduced levels of ceramides has been found to help perpetuate the development of psoriasis due to reduced apoptosis and an increase in hyperproliferation of keratinocytes resulting in new plaque formation (Lew et al., 2006). A correlation between the PASI score and the level of ceramide reduction has also been established (Cho et al., 2004).

The study by Mysliwiec et al. (2017) also showed that the S1P serum concentration is significantly increased in patients with psoriasis, suggesting that ceramide is being converted into S1P at an increased rate. Currently the activity of ceramidase has not been reported to be increased in psoriasis however a positive link between ceramidase activity in the plaques and the clinical severity has been demonstrated (Moon et al., 2013b).

A separate investigation used analogues of ceramide which are unable to be converted to S1P in order to assess the effect of S1P in a mouse model of psoriasis. This study found that both calprotectin and the Toll-like receptor 4 calprotectin receptor production was decreased which is interesting because it has been noted that in most models of psoriasis calprotectin is upregulated as well as in human psoriasis. Calprotectin protects against oxidative stress by reactive oxygen species and this reduction therefore lead to reduced immune infiltrate and subsequently prevented the thickening of the epidermis. Overall the study concluded that by re-establishing the skin barrier using stable versions of ceramide, anti-angiogenic IL-12 was upregulated while IL-22 (which

promotes an inflammatory response) was downregulated, highlighting the wide array of effects S1P has in psoriasis (Arbiser et al., 2017).

There are a variety of potential ways to modulate S1P activity in psoriasis patients and a number of research groups are currently investigating these. For instance, numerous S1P receptor modulators are in development however ponesimod (targeting S1PR1) is the only one so far to be tested in psoriasis. Ponesimod prevents the egress of lymphocytes from the lymph nodes and results from a Phase II study showed that PASI scores decreased over the 16 week trial in response to ponesimod, with maintenance therapy continuing to improve the score up to week 28 (Krause et al., 2018). This is most likely due to the reduction in the recruitment of T cells to the plaques and therefore attenuation of the inflammatory stimulation seen in psoriasis.

Another S1PR1 modulator, Syl930, is currently in Phase I trials for rheumatoid arthritis and its effect on mouse models of psoriasis is currently being established. So far it appears as though it may be a promising treatment, with results showing an inhibition of proliferation in basal cells of the epithelium and reduction in the overall pathological damage to the skin (Ji et al., 2018).

A recent study has been published and has shown the effect of S1P produced specifically by the sphingosine kinase 2 isoform in psoriasis. It is reported that inhibiting S1P production through this kinase reduces suppressor of cytokine signalling 1 (SOCS1) levels which has a vital role in suppressing the negative effect of IFN-γ on the STAT3 pathway necessary for the differentiation of $CD4^+$ T cells to T-helper (Th) 17 cells. The increase in circulating levels of S1P may therefore assist in this process by elevating levels of SOCS1 and therefore Th17 cells. This is important because Th17 cells are one of the main drivers of psoriasis due to their production of IL-17, IL-22 and IL-9 which are important for maintaining the inflammatory state of keratinocytes and mediating the overall inflammatory response (Shin et al., 2019).

For these reasons the role of S1P is being studied further, with the aim of increasing the current understanding of the underlying mechanisms involved that lead to the development of psoriasis.

1.6 Hypothesis and Aims

It is hypothesised that the concentration and proportions of lipids are important factors that play a role in mediating both systemic and localised disease.

It is hypothesised that oxLDL signals through S1P to bring about its effects on migration and angiogenesis.
It is therefore also hypothesised that by reducing the activity or levels of S1P or interfering with the potential mechanism of oxLDL activation via S1P, that a therapeutic target may be discovered for the aberrant effects seen in psoriasis and cardiovascular disease.

Specific aims of this project will be:

- to characterise isolated cells and check cell viability under all used conditions using FACS
- to investigate the role of S1P, TNF and various inhibitors of the S1P pathway, as well as the MS drug Fingolimod, in migration and angiogenesis using isolated HUVEC
- to study any cellular changes (phosphorylated ERK expression and Ca^{2+} flux) that are brought about by the regulation of cellular lipids (namely S1P) or addition of inhibitors of the S1P pathway
- to discover how oxLDL exerts its effects on angiogenesis, potentially via S1P

This will aid further understanding of psoriasis development and allow the identification of the roles lipids play during plaque formation.

Chapter 2: Materials and Methods

In order to investigate the aims and hypothesis set out previously, a number of different methods had to be used. The following table provides a brief overview of the main experimental approaches used along with any associated methods and the reason for their use.

Table 3 List of Experimental approaches used

Experimental Approaches		
Method	**Reason for Use**	**Associated methods**
HUVEC Isolation	Harvesting of cells	washing/feeding cells, splitting cells
FACS	Characterisation/viability of cells	S1PR1 expression
Scratch assays	To study migration	
Cell spreading	To measure the circularity of cells	
Angiogenesis assays	To study angiogenesis	
Western blots	Intracellular signalling (pERK)	lysing cells, SDS-PAGE
Calcium flux	Intracellular signalling (Ca2+)	

The methods outlined in Table 3 will be discussed in detail in this chapter and will include the composition of any buffers or reagents used as well as the exact procedure followed.

2.1 HUVEC Isolation Procedure

2.1.1 Materials

Endothelial cell growth media

Endothelial cells were isolated and grown in media consisting of 4.75g M199 powder and 1.1g sodium bicarbonate that was dissolved in 500ml ddH_2O. 50ml human serum per 250ml media was added in a tissue culture hood and filter sterilised (0.22μm filter) to form media with final 20% human serum. 2.5ml Pen/strep/glutamine (1% v/v final solution) was added to each 250ml bottle to reduce bacterial contamination and as a source of energy respectively and the media stored at 4^0C.

Cord Buffer

Enzyme extraction of endothelial cells was carried out in Cord Buffer - 16.36g NaCl, 0.59g KCl, 3.97g D-glucose, 0.4 ml of 1M monobasic sodium phosphate ($NaH_2PO_4.H_20$) and 1.6ml of 1M dibasic sodium phosphate ($Na_2HPO_4.7H_20$). The volume was brought to 2 litres with ddH_2O and pH to 7.2 before being filter sterilised (0.22μm filter) into 500 ml bottles and stored at 4^0C.

Collagenase (0.1% w/v final concentration)

Worthington collagenase type I enzyme (~250U/mg) was used to remove endothelial cells from the umbilical vein. 0.05g of dry collagenase was re-suspended in 50 mL of warmed cord buffer and filter sterilised through a 0.22μm filter.

Gelatin (0.2% w/v final concentration)

Isolated endothelial cells were plated onto gelatin coated tissue culture plastic. 0.5g of gelatin was added to 250ml of water, which was then warmed with stirring to 55^{o}C before being filter sterilized through a 0.22μm filter and stored at 4^{0}C. Tissue culture plastic was routinely coated with gelatin for 30min at room temperature before removal by aspiration and addition of cells.

2.1.2 Equipment

Cords (collected from maternity ward)
Nitrile gloves (non-sterile)
Barrier gown
Protective apron
Diaper absorbent pad
Cannula (one for each cord)
Cord clamps
2x 500ml beaker
Haemostats
Scissors
4x4 non-sterile gauze
Syringes (one for each cord and one for collagenase)
0.22μm Syringe filter
30ml Universal tube
50ml conical centrifuge tubes (one for each cord, plus one for cord buffer and one for collagenase)
T75/T25 tissue culture flasks
5% (v/v) biocleanse
Centrifuge

2.1.3 Method

All the necessary materials for the procedure were gathered and the cord buffer and media warmed to 37°C in a water bath. T75 flasks were gelatinised prior to the isolation procedure and for at least 30min before addition of cells.

Cords, collected from the maternity ward with ethical approval (07/H0502/83), were removed from the placenta by cutting with scissors as close to the placenta margin as possible. Cords were cleaned with 4x4ply gauze to remove any excess blood or blood clots. The cords were also checked at this point for puncture holes caused during blood gas analysis as part of the birthing process or cord blood isolation prior to collection.

The umbilical cord consists of one vein and two arteries. The vein was identified as a relatively large opening vessel with thin walls due to the reduced layer of smooth muscle compared to the arteries and the cannula inserted. A cord clamp was then used to hold the cannula in place, see Figure 7. This was repeated for all the cords.

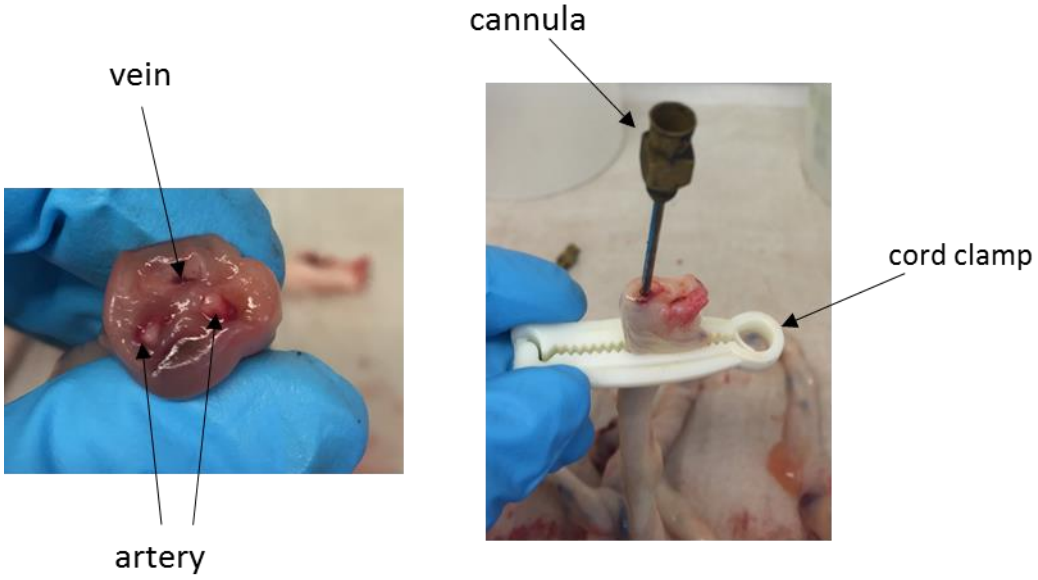

Figure 7 Anatomy of the umbilical cord
The vein and two arteries are highlighted, and the setup of the cannula and the cord clamp are shown for reference.

The cord buffer was removed from the water bath and a syringe filled to approximately 20ml volume. The syringe was then attached to the cannula and the cord placed into a plastic beaker. The buffer was carefully pushed through the cord to remove blood with visible clots being massaged to loosen them. Any obvious puncture holes were clamped with a pair of haemostats to prevent

leakage of cord buffer or the cord discarded if it was excessively damaged. This was repeated twice until the fluid exiting the vein was relatively clear of red cells. The open end of the cord was then clamped.

0.1% (w/v) collagenase solution was added to each cord with a volume between 10 – 25mL dependent on the length of the cord. The pressure and volume applied was sufficient to inflate the cord without causing the collagenase solution to leak back into the syringe. The cord was placed into a clean 500mL plastic beaker and submerged in warm cord buffer. The cord was left to incubate for 10 minutes and the beaker gently swirled periodically.

Following incubation, the cord was removed from the beaker and slowly massaged to dislodge the cells. The collagenase was removed using the syringe and added to 3mL of full media in a 50mL conical centrifuge tube to deactivate the collagenase enzyme. The syringe was then filled to approximately 20ml with fresh cord buffer and the vein washed to remove any remaining cells while repeating the massage. The buffer was removed and added to the same centrifuge tube. This was repeated for each cord. Cell suspensions were pelleted by centrifugation at 430g for 5 minutes at room temperature.

The supernatant was removed by vacuum aspiration being careful not to dislodge the pellet. The cells were re-suspended in their own volume by flicking the base of the centrifuge tube.

Cells were then re-suspended in an appropriate amount of media (10 mL of media for a T75 flask, 5mL if using T25 flasks) and cells from each cord plated separately in to a T75 flask or split into three T25 flasks. The cells were then incubated at 37°C in 5% CO_2 balanced air in a humidified incubator and allowed to adhere to the surface of the flask. Cells were routinely washed after 24h with Ca^{2+} Mg^{2+} free Hanks balanced salt solution (HBSS) and fed with fresh media every 48h until confluent or until used. The time taken from isolation to use in experiments was routinely five to seven days depending on the efficiency and number of cells isolated.

2.2 Washing and feeding procedure

2.2.1 Materials

Flask of cells to be washed

Media- see 2.1.1

Microscope

HBSS (Ca^{2+} Mg^{2+} free) prepared according to package directions, pH to 7.2 and filter sterilized.

2.2.2 Method

The flasks of cells to be washed were removed from the incubator and the media aspirated. In a tissue culture hood, the cells were then washed with 10ml HBSS (Ca^{2+} Mg^{2+} free) and observed using a phase contrast microscope to determine if the isolation had been a success. The HBSS was removed and 10ml media was then added before the cells were returned to the incubator.

2.3 Splitting Cells

2.3.1 Materials

Confluent flask of cells (either T25 or T75)

Media- see 2.1.1

Trypsin EDTA (0.05%)

15ml conical centrifuge tubes

Centrifuge

Haemocytometer

Microscope

2.3.2 Method

0.2% (w/v) gelatin was added to the tissue culture plastic and left for at least half an hour at room temperature. A flask of cells was removed from the incubator and the media aspirated. 4mL of 0.05% trypsin EDTA at 4°C was added to enzymatically dislodge cells and the side of the flask was tapped to speed up the process. A microscope was used to check that all the cells had detached. The cell suspension was then removed and added to a 15ml conical centrifuge tube containing 4ml media and centrifuged at 430g for 5 minutes. The supernatant was aspirated and the pellet re-suspended initially in its own volume and then in 1mL full media. The cells were counted using a haemocytometer and the media needed to achieve the desired dilution of cells calculated. The gelatin was then aspirated from the plastic and the cells seeded before being placed in the incubator and left for 24 hours or until use, typically before 72 hours.

Seeding density:

24 well plate- 100,000 cells per well in 0.7ml media

12 well plate- 200,000 cells per well in 1ml media

96 well plate- 20,000 cells per well in 200µl media

Angiogenesis assay- 500,000 cells per ml needed

2.4 Delipidised HUVEC media

Delipidised media was made by adding human serum to a bijou tube containing fumed silica to give a final silica concentration of 20mg/mL and mixing well by shaking. The mixture was then placed on a blood roller over night at room temperature. The next morning the serum/silica mix was transferred to a conical centrifuge tube, being careful to pipette to the bottom of the tube, and centrifuged at 2000g for 15 minutes with no break at room temperature. The supernatant was removed and placed in a clean conical centrifuge tube, again being careful to pipette to the bottom of the tube, and the centrifugation step repeated. The supernatant was removed and added to M199 media (made up in proportion to how much serum was being delipidised) before being filter sterilised and Pen/strep/glutamine (1% solution) added (Ferraz et al., 2004).

2.5 Oxidation of LDL and Albumin

2.5.1 Oxidation Protocol

Low density lipoprotein (LDL) and albumin were oxidised using copper sulphate ($CuSO_4$). LDL was made up to a concentration of 1mg/ml in PBS while copper sulphate was made up to 20µM in PBS. Albumin (from bovine serum albumin) was also oxidised at this time and was made up to a concentration of 10% (w/v), again in PBS. In a sterile 35mm dish, equal volumes of either LDL or albumin were combined with the copper sulphate solution to give final concentrations of 0.5mg/ml, 5% (w/v) and 10 µM respectively. The solutions were mixed gently, being careful to avoid bubbles, before being incubated at 37^0C for 18 hours. The oxidation was subsequently stopped by adding 0.5M ethylenediaminetetraacetic acid (EDTA) at a final concentration of 1mM.

At this point an aliquot (300µl) was taken of the oxidised LDL and albumin in order to perform either a TBARS assay to test for oxidation of LDL (see 2.5.2) or a protein carbonyl assay to test for albumin oxidations (see 2.5.3).

The oxidised samples were then dialysed to remove the $CuSO_4$ and EDTA. The dialysis tubing (with a molecular weight cut off of 12,000) was first soaked in 0.5M EDTA and then rinsed thoroughly in distilled water before being knotted at one end, the sample loaded and then knotted at the free end. The samples were dialysed against 3 changes of PBS (1L) at 4^0C over 24 hours, after which the samples were filtered sterilised through a 0.22µm filter before being used (Scoccia et al., 2001).

2.5.2 Thiobarbituric acid reactive substances (TBARS) Assay

Malonaldehyde bis(dimethyl acetal) (MDA) was used as the standard for this assay and was prepared to a final concentration of 500µM by adding 4.17µl MDA to 1ml ethanol and adding 49ml water. In order to precipitate the proteins, 600µl ice cold 10% (w/v) trichloroacetic acid (TCA) was added to 300µl of MDA, the aliquots of oxLDL and albumin from the end of stage 2.5.1 and LDL (made up to 0.5mg/ml). The samples were incubated on ice for 15 minutes before being centrifuged at 4000g for 15 minutes at room temperature. 0.67% (w/v) thiobarbituric acid (TBA) was made by adding 1ml DMSO to 67mg TBA and adding 9ml water. 400µl of the supernatant from each sample was then placed in a new Eppendorf tube and an equal volume of TBA added. Finally, the samples were boiled for 10 minutes in a water bath.

200µl of the samples were loaded onto a 96 well plate in triplicate. 200µl of known concentration of MDA was also loaded in triplicate and a doubling dilution made in order to provide a standard curve. The plate was placed in a spectrophotometer and absorbance measured at a wavelength of

532nm and the TBARS for each sample calculated in Prism from the MDA absorbance (Scoccia et al., 2001).

2.5.3 Protein carbonyl detection

In order to detect protein carbonyls present on the oxidised albumin sample, the following solutions had to be prepared. Firstly, 2.5M hydrochloric acid (HCl) was made by adding 24.5ml concentrated HCl slowly to 60ml water. Once cooled the volume was adjusted to 100ml. 10mM 2,4-dinitrophenylhydrazine (DNPH) was prepared by dissolving 0.02g in 10ml 2.5M HCl and was stored in the dark until needed. 50% (w/v) TCA was made by dissolving 5g TCA in 10ml water and ethanol/ethyl acetate (1:1) was made by combining equal volumes and mixing well. This solution was stored in the fridge as it is needed cold for the assay. Finally, 6M guanidine-hydrochloride was prepared by dissolving 5.732g in 10ml water.

The oxidised samples of albumin were diluted to a concentration of 1mg/ml and 250µl pipetted into two 1.5ml Eppendorf tubes. To the first tube (+DNPH), 250µl 10mM DNPH was added while 250µl HCl was added to the second tube (-DNPH). Both solutions were vortexed and then incubated in the dark at room temperature for 15 minutes, vortexing every 5 minutes. 125µl 50% (w/v) TCA was then added to each tube. The samples were vortexed and incubated at -20^0C for at least 15 minutes before being centrifuged at 9000g for 15 minutes at 4^0C. The supernatant was removed, being careful not to disturb the pellet, and the pellet washed three times with ice cold ethanol/ethyl acetate. Between each wash, the samples were centrifuged at 9000g for 2 minutes and the supernatant discarded after each wash. The protein pellets were re-dissolved in 1ml 6M guanidine-hydrochloride and mixed well. The absorbance of the solutions was then measured at 370nm using a spectrophotometer, with 6M guanidine-hydrochloride being used to zero the spectrophotometer.

The carbonyl concentration is calculated using the extinction coefficient of DNPH at 370nm which is 22,000M/cm. Therefore, the carbonyl concentration (moles/L) = the absorbance at 370nm/ 22,000. This can be converted into nmol/ml by multiplying by $1x10^6$. For example, if an absorbance of 0.038 was detected at 370nm, then (0.038/22,000) x $1x10^6$ = 2.7nmol/ml.

2.6 Characterisation of cells

2.6.1 Cell viability staining

24 well plates were used to assess the effect of the various compounds on the viability of the cells. Each compound (at the concentrations used in the assays) was added to the cells 24 hours prior to being stained and analysed by FACS. The exception to this is the control dead cells which had 0.7ml 100% ethanol added 10 minutes before the staining process.

The media from each well (or ethanol from the control dead well) was pipetted into a FACS tube and 300µl trypsin added to lift the cells from the plastic in order to transfer them to the FACS tubes containing the corresponding media. Each tube was centrifuged for 5 minutes at 430g and during this time the live/dead stain was made up to 1:1000 in PBS. The supernatant was aspirated from each tube and the cells re-suspended in their own volume. 100µl dye was added to each tube and mixed well, for the unstained control 100µl PBS was added instead of the dye. The tubes were then incubated on ice and in the dark for 45 minutes, during which time 1% (w/v) BSA in PBS was prepared. 1ml 1% (w/v) PBSA was used to wash the cells before being centrifuged at 400g for 5 minutes. The supernatant was aspirated and the cells re-suspended in 300µl 1% (w/v) BSA in PBS and kept on ice until being analysed by FACS.

2.6.2 HUVEC surface staining

The cells were prepared for characterisation in the same way as for the cell viability staining, with the antibodies, or the corresponding isotype control, against specific cell markers added. A full list of antibodies used is shown in Table 4.

Table 4 Antibody panel used for FACS

Marker	Fluorophore	Ex/Em (nm)	Clone	Concentration	Host/ Isotype	Supplier
Live/dead	APC-Cy7	633/780	N/A	1:1000	N/A	Life technologies
Live/dead	Aqua	367/526	N/A	1:1000	N/A	Life technologies
CD363 (S1PR1)	eFluor® 660	640/668	SW4GYPP	0.5µg/test	Mouse/IgG1, kappa	eBioscience
CD31 (PECAM)	APC	640/660	WM59	0.5µg/test	Mouse/IgG1, kappa	eBioscience
CD105 (Endoglin)	PE	496/578	SN6	1µg/test	Mouse/IgG1, kappa	eBioscience

The expression of S1PR1 after stimulation with S1P, Fingolimod, oxLDL and LDL was also studied. Here cells were stimulated for 30 minutes with the aforementioned compounds before the media was aspirated and 300µl accutase added to lift the cells. Accutase was used instead of trypsin for this assay as trypsin could cleave off the receptor and therefore reduce the expression level. The cells were added to FACS tubes containing 300µl media and centrifuged for 5 minutes at 400g. The supernatant was aspirated and the cells re-suspended in their own volume before being fixed in 200µl 4% (v/v) paraformaldehyde. The cells were incubated at room temperature for 10 minutes before being washed in 2ml PBS and the centrifugation step repeated. Again, the supernatant was removed and the cells re-suspended in 100µl 1% (w/v) BSA in PBS. 5µl of either the antibody or isotype was then added and the cells incubated on ice and in the dark for 45 minutes. The cells were then washed in 2ml PBS and the centrifugation step repeated. The supernatant was aspirated and the cells re-suspended in 200µl 1% (w/v) BSA in PBS and kept on ice until being analysed by FACS.

2.6.3 PBMC and neutrophil isolation

6% (w/v) Dextran: 15g Dextran (100,000 MW), 2.25g NaCl, 250ml ddH_2O
Blocking buffer: 1% (w/v) BSA and 5% (v/v) human serum in PBS
FACS buffer: 1% (w/v) BSA in PBS

30ml Blood was collected from healthy volunteers in EDTA tubes with ethical approval (07/H0504/93) and poured into a 50ml falcon tube. Half the total blood volume (15ml) of 6% (w/v) Dextran was added and the tube gently inverted a number of times before being left in the hood for 60-90 minutes to allow the blood to separate (the lid of the tube was left off to prevent bubbles forming). The top layer containing the white blood cells was removed using a stripette and placed in a new 50ml conical centrifuge tube before being centrifuged at 264g for 12 minutes with no brake. During this time 0.2% and 1.6% (v/v) NaCl in ddH_2O was prepared. Once the supernatant had been aspirated and the cells resuspended, 25ml of 0.2% (v/v) NaCl was added for precisely 19 seconds while inverting the tube in order to cause hypotonic lysis of the red cells. On the 19 second mark, 25 ml 1.6% (v/v) NaCl was added to the tube to generate an isotonic solution and the cell suspension centrifuged at 380g for 5 minutes with a low brake (setting 1) and the supernatant aspirated.

Depending on whether whole blood (minus the red blood cells) or separated peripheral blood mononuclear cells (PBMCs) and neutrophils were required dictated the following steps. If whole blood was required then the cells were re-suspended in 10ml HBSS+1% (w/v) BSA before being counted and stained.

If, however it was necessary to separate the neutrophils and PBMCs the following steps were taken:

Once the supernatant was aspirated the cells were re-suspended in 5ml HBSS before being transferred to a 15ml falcon tube. A Pasteur pipette was used to underlay 5ml Lymphoprep (being careful to avoid bubbles) and the tube centrifuged at 380g for 30 minutes with no brake. The PBMCs form a layer on top of the gradient and this was collected and the rest of the supernatant discarded. For the neutrophils (the pellet), 5ml of blocking buffer was added and the cells counted ready for staining. For the PBMCs, 15ml HBSS was added to wash the cells before being centrifuged at 380g for 5 minutes. The supernatant was aspirated and the cells re-suspended in 2.5ml blocking buffer before being counted.

2.6.4 PBMC and neutrophil staining

Cells were added to FACS tubes (either 50µl of neutrophils and PBMCs or 100µl RBC-depleted whole blood) and an equal volume of 100% ethanol added to the control dead cell sample. Live/dead stain (made up in HBSS) was added at a final concentration of 1:1000 to each tube along with 5µl antibody and isotype control and incubated on ice for 45 minutes in the dark. Cells were then washed with HBSS (roughly 3ml), centrifuged at 400g for 5 minutes and re-suspended in 200µl FACS buffer. Cells were kept on ice until being analysed by FACS.

2.7 Scratch Assay

2.7.1 Materials

Media- see 2.1.1

Microscope (Olympus) with camera attachment

24-well plate of cells

Ca^{2+} Mg^{2+} free HBSS

2.7.2 Method

Cells were harvested from a confluent T75 flask as described and the cells seeded at 100,000 cells per well into a 24-well plate and returned to the incubator for 24 hours (see 2.3).

The middle of the monolayer of cells was gently scratched with a 200µl pipette tip, keeping the tip perpendicular to the bottom of the well to ensure an even scratch. The plate was then turned and a further line scratched at 90 degrees to the first, creating a cross. This was repeated for each well. The media was aspirated and the cells washed with Ca^{2+} Mg^{2+} free HBSS. The HBSS was then aspirated and 0.7ml media added containing various components of interest e.g. drugs to inhibit migration. Each well was imaged immediately following the scratch (time 0) and after 24 and 48 hours.

2.7.3 S1P and inhibitors used for scratch assay

The effect of a large number of compounds were used to assess their effect on migration. These are listed below with the concentration (or range of concentrations) that was used. The solvent and final solvent concentrations are also shown, these were low enough to not be cytotoxic to the cells and therefore would not affect the results of the assays.

Table 5 Concentration of compounds used

Compound	Concentration used	Solvent	Highest solvent concentration in assay
S1P	10µM-1nM	NaOH (0.3M)	300mM
Fingolimod	10µM-1nM	DMSO	0.1%
TNFα	10nM-1pM	ddH_2O	n/a
W146	1µM	DMSO	0.1%
JTE	1µM	DMSO	0.1%
TY	10µM	DMSO	0.1%
SKII	10µM	DMSO	0.1%
S1PL	1mM	ddH_2O	n/a
PD	10µM	DMSO	0.1%
SB	10µM	DMSO	0.1%
JNKII	10µM	DMSO	0.1%
oxLDL/LDL	5 & 100µg/ml	PBS	n/a
Lipid supplement	1:100 & 1:1000	Media	n/a
Albumin/ox-albumin	1% (w/v)	PBS	n/a

The log_{10} range of S1P (10µM-1nM) concentrations was used to create a concentration gradient that mimicked physiological levels of S1P. From these assays, a concentration of 1µM was used for other assays as a standard stimulus and 10µM was used as a standard inhibitor.
Fingolimod, an analogue of sphingosine, was also used at equivalent concentrations.

TNFα was used in a range from 10nM-1pM to create a concentration gradient known to have a stimulatory effect on migration.

S1P receptor 1-3 antagonists were used at W146- 1µM, JTE- 1µM and TY- 10µM respectively as this was equivalent to 100x the IC50 or Ki as reported in the literature. The sphingosine kinase inhibitor (SKII) was used at 10µM while the lyase inhibitor was used at 1mM.
The MEK, p38 and SAPK/JNK inhibitors (PD, SB and JNKII respectively) were used at 10µM.

oxLDL and LDL were used at both 100µg/ml and 5µg/ml as these concentrations have previously been shown to be inhibitory and stimulatory respectively. A lipid supplement was also used at 1:100 and 1:1000 as per manufacturers instructions.

Albumin and oxidised albumin were used at 1% (w/v). S1P bound to albumin and oxidised albumin was also used (10µM S1P was added to 10% (w/v) albumin or 5% (w/v) ox-albumin and incubated for 1 hour at 37^0C before being dialysed against 3 changes of PBS over 24 hours). This method was

adapted from (Ruiz et al., 2017a) where they added an excess of S1P to ApoM for 30 minutes at room temperature.

2.8 Cell spreading

Dilutions of oxLDL and LDL were prepared at concentrations of 200µg/ml, 20µg/ml and 2µg/ml and dilutions of S1P and Fingolimod were prepared at concentrations of 20µM and 2µM in order to generate final concentrations of 100µg/ml, 10µg/ml and 1µg/ml and 10µM and 1µM respectively. Cells were then harvested from a confluent T75 flask as described (see 2.3) and added at a concentration of 80,000 cells per ml in a 1:1 ratio to each dilution. The cells in the dilutions were then seeded onto a gelatin coated 24-well plate generating a final concentration of 40,000 cells per well. Each well was then imaged using a microscope after 4 and 24 hours at 10x magnification. Fiji was used to analyse each image to find the circularity of the cells; a measure of cell spreading.

2.9 Angiogenesis assay

2.9.1 Materials

Confluent T25 flask

Trypsin EDTA (0.05%)

Media

Geltrex

Angiogenesis slide (15 well)

Microscope (Olympus) with camera attachment

2.9.2 Method

Geltrex forms a hydrogel at elevated temperatures but is liquid at 4°C. A gel matrix was formed from the Geltrex by allowing it initially to thaw from -80°C on ice overnight in a fridge at 4°C. 10µl Geltrex liquid was then dispensed to each inner well on the angiogenesis slide (being careful to prevent bubbles) and the slide incubated at 37°C for 45 minutes (see Figure 8). During this time, the stimuli were prepared and a T25 flask of cells split (see 2.3). Cells were then added to the stimulus dilutions in a 1:1 ratio to generate the final cell density and stimulus concentrations. For the control, cells were mixed with media instead of a stimulus. After the incubation period, 50µl of the cell and stimulus mix was added to each well, being careful not to make any bubbles. The slide was then placed back in the incubator and an image of each well taken after 2, 4, 6, 8 and 24 hours.

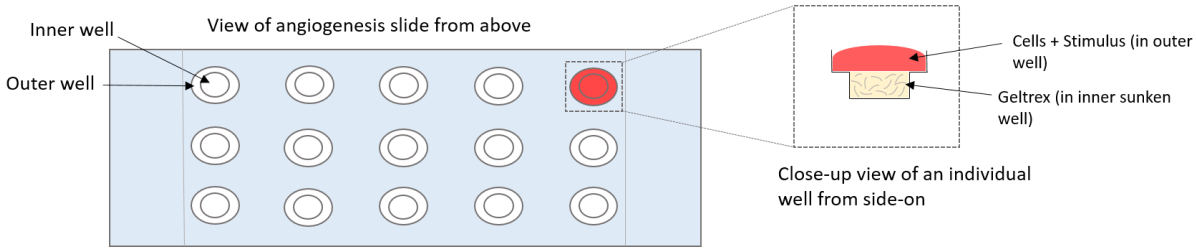

Figure 8 Angiogenesis slide
A diagram of the angiogenesis slide used as viewed from above and the set-up of the two wells is shown. A close-up example of the inner, sunken well containing Geltrex and the outer well containing the cells and any stimulus/inhibitor used is also shown.

The angiogenesis images were then analysed in batch using the Angiogenesis Analyser plugin in Fiji and the graphs generated in Prism.

2.10 Lysing cells

2.10.1 Materials

12 well plate of cells (see 2.3)

Drugs to be added to cells

2x Laemlli's+dithiothreitol (DTT)- 2.42g Trizma base in 20ml ddH_2O. 1.6g SDS, 14mg Bromothymol blue and 8ml glycerol were added and the pH adjusted to 6.8 with HCl. The final volume was brought to 40ml with ddH_2O and the solution stored at room temperature.

2.10.2 Method

All drugs to be used were prepared before a 12 well plate of cells was removed from the incubator. The drugs were then added to the cells and incubated at 37^0C for either 10 minutes or 1 hour before the media was aspirated and 50µl Laemmli +DTT added to each well. The cells were lysed and the resultant protein solution was collected in 1.5mL microcentrifuge tubes for immediate use or stored at -20^0C for future use.

2.11 Western blots

Western blots (or immunoblotting) are a common method used to look at protein expression within a sample and provide qualitative and semi-quantitative information about the target protein. In order to achieve this, three main steps are carried out to firstly separate the proteins in a sample based on their size, followed by transferring the proteins to a membrane and finally detecting the protein of interest. Sample preparation is also an important stage and ensures that the proteins are denatured through the use of SDS. This also adds an overall negative charge to the proteins to allow the proteins to move towards a positive charge through gel electrophoresis. The disulphide bonds present in the proteins also need to be reduced and prevented from reforming (achieved using 2-mercaptoethanol or Dithiothreitol) to ensure that the protein is completely unfolded and therefore migrates in accordance with its molecular weight. Once the proteins have been transferred to a membrane, the membrane is blocked to prevent unspecific binding and the target protein is detected by an antibody. A secondary antibody with a reporter such as horseradish peroxidase (HRP) is then added and detected using enhanced chemiluminescence (ECL), resulting in a light signal which is detected using x-ray film. Therefore the more protein in the sample, the greater the signal and band on the film.

2.11.1 Materials

Molecular weight ladder

Samples

Butanol

1.5M Tris pH 8.8 (Resolving Buffer) - 181.5g Trizma base in 500ml ddH_2O. pH to 8.8 with HCl, bring to 1L with ddH_2O and store at 4^0C.

1.0M Tris pH 6.8 (Stacking Buffer) - 121g Trizma Base in 120ml ddH_2O. pH to 6.8 with HCl, bring to 1L with ddH_2O and store at 4^0C.

5x Running buffer- 12.15g Tris Base, 72.0g Glycine, 5.0g SDS. Bring to 500ml with ddH_2O

Transfer buffer- 250ml 1x running buffer, 50ml methanol

Acrylamide

10% (w/v) SDS

TEMED

10x PBS- 80.06 g NaCl, 2.01 g KCl, 21.71 g Na_2HPO_4 and 2.00 g KH_2PO_4 were added to 1L ddH2O

Skimmed non-fat milk powder

Tween 20

Primary antibody- either for total-ERK or phospho-ERK, both rabbit monoclonal antibodies.

Secondary antibody Donkey - α-rabbit HRP conjugated

ECL reagents

Stripping buffer

Conical centrifuge tube

Glass plates

Casting gates

Casting stand

Comb

Gel tank and power pack

Semi-dry transfer system

PVDF membrane

Whatman® filter paper

Stripping buffer

2.11.2 Methods

2.11.2.1 Gel preparation, loading and running

10% resolving gels were prepared and cast using a BioRad miniProtean system, see Table **6** for volumes for two gels. Once the resolving gel had polymerised, a 5% stacking gel was formed using a 10 well comb. To each well 30µL of sample was added which had been previously boiled at 100°C for 10 minutes suspended in a water bath. The proteins were separated based on molecular size by the addition of an electric charge across the gel in an electrophoretic buffer. These proteins were separated for two hours or until the tracking dye in the molecular weight marker containing pre-stained proteins had run off the bottom of the gel.

Table 6 Ingredients for two SDS-PAGE gels

Resolving Gel (10%)		**Stacking Gel (5%)**	
ddH2O	8.025ml	ddH2O	7.35ml
1.5M Tris	5.375ml	1M Tris	1.25ml
Acrylamide 30% (v/v) (37.5:1)	7.5ml	Acrylamide 30% (v/v) (37.5:1)	1.3ml
10% (w/v) SDS	50µl	10% (w/v) SDS	100µl
TEMED	52.5µl	TEMED	10µl
10% (w/v) APS	79.5µl	10% (w/v) APS	50µl

2.11.2.2 Transferring

Polyvinylidene difluoride (PVDF) membrane was cut to size and equilibrated in methanol. Transfer buffer was prepared and the Whatman paper and membranes equilibrated in transfer buffer. Gels were removed from the glass plates and a gel sandwich made, with Whatman paper on the bottom followed by the membrane, gel and finally more Whatman paper. Care was taken to prevent bubbles forming between the gel and the membrane. The gel sandwich was then transferred to the semi-dry transfer apparatus and proteins transferred at 300mA for one and a half hours.

2.11.2.3 Blocking and Primary antibody

Once the transfer of protein was complete, the membrane was blocked for an hour on a roller under 5mL 3% (w/v) skimmed milk in 0.05% (v/v) PBST. This was to prevent non-specific binding of antibody as part of the detection system. A 1:750 dilution of primary antibody was added to 10ml 0.05% (v/v) PBST and added to membranes. The membranes were incubated overnight at room temperature with mixing on a roller.

2.11.2.4 Secondary antibody and developing

The primary antibody was recovered the following morning and stored at -20^{0}C to be used up to two more times. The membrane was washed 3x 5 minutes in 0.05% (v/v) PBST and placed under the secondary antibody which was conjugated to horse radish peroxidase (HRP) in 3% (w/v) skimmed milk PBST (6.7µL in 10ml) and incubated on a rocker for one hour. After this time, the antibody was removed and the membrane washed 3x 5 minutes 0.05% (v/v) PBST. Detection was via enhanced luminol chemiluminescence (ECL). 1mL of each ECL reagent (luminol and stabilised benzyl peroxide solution) was added to the membrane and incubated for 2 minutes. The excess ECL was removed and the membrane placed between acetate sheets, ensuring all air bubbles were removed, before being placed in a light safe X-ray cassette.

The cassette was taken to a dark room and the light generated by the HRP conjugated secondary antibody luminol peroxidase reaction was detected using light sensitive X-ray film. Each film was initially exposed to membrane for 3 minutes. The film was then submerged in developer for 1 minute with agitation, rinsed in water then submerged in fixer solution until the photographic emulsion had been removed followed by a final rinse in water. The films were allowed to drip dry. Timed exposures of varying lengths were employed to determine the optimal signal to noise ratio e.g. from 30 seconds, 10 minutes to 1 hour.

2.11.2.5 Stripping and Re-probing

Membranes can be re-probed to allow detection of additional separated proteins by stripping the initial antibody pair from the protein using a stripping buffer. 1mL stripping buffer (Millipore) and 9ml 0.05% (v/v) PBST were added to the membrane and incubated on a rocker at room temperature for 30 minutes. The membrane was then washed once with 0.05% (v/v) PBST for 5 minutes before being re-blocked for 30 minutes in 10mL 3% (w/v) skimmed milk PBST. The primary antibody was added and the membrane incubated and developed as described in 2.11.2.3 and 2.11.2.4.

2.12 Calcium flux

Calcium flux under various conditions was measured using Fluo-4.

2µM of Fluo-4 was prepared in 1% (w/v) HBSA and kept in the dark.

Media was aspirated from a 96 well plate and 100µL Fluo-4 (2µM) added to each well and incubated for 30 minutes. During this time a compound plate was made up containing ten-fold dilution series of histamine (100µM-1nM), S1P and Fingolimod (both 10µM-100pM) and placed in the analyser to warm to 37°C. Cells were washed with 100µl 1% (w/v) HBSA and left for 30 minutes before the HBSA was aspirated and 50µL fresh 1% (w/v) HBSA added. The plate was then placed in the analyser to warm up while the programme was being set (see below) and the calcium flux measured.

Machine settings:

Fluo-4

Wavelength – number= 1: excitation= 494nm and emission= 530nm with an auto cut off at 515nm.

Timing interval= 1.7 seconds with a run time of 120 seconds

Compound transfer – initial volume= 50µL with 1 transfer of 50µL at rate 2

2.13 Statistics

Various statistical tests were used to determine the significance of the results obtained. Firstly one-way analysis of variance (ANOVA) tests were performed to generate a p-value, followed by Dunnett's or Tukey's multiple comparisons test to determine which results were significantly different from the rest. One sample t tests were also used to discover which values were significantly different from a hypothetical value which was a representation of the control. All statistics were performed using Prism with *=$p<0.05$, **=$p<0.01$, ***=$p<0.001$ and ****=$p<0.0001$.

Chapter 3: Characterisation of endothelial cells and Intracellular signalling

3.1 Characterisation of endothelial cells

3.1.1 Introduction

The endothelial cells used in all assays were obtained from human umbilical cords, as described in the methods section 2.1. During this process it is possible to isolate other unwanted cell types, such as smooth muscle cells. Collagenase digestion of the basement membrane can liberate these cell types if incubation periods are prolonged or the enzymatic activity of the collagenase used is too high leading to over digestion and contamination of the culture. It was therefore necessary to characterise the cells isolated in order to show that they were endothelial in nature. This was achieved using flow cytometry, a technique that can interrogate multiple cellular parameters in mixed populations rapidly and simultaneously on a cell by cell basis often referred to as Fluorescence Activated Cell Sorting (FACS).

Flow cytometry is a method used to analyse the size and shape of cells in suspension, as well as the expression of cell surface and intracellular markers, metabolic activity, cell cycle state and viability as well as other cellular parameters. Single cells are passed through a laser beam within a hydrodynamically focused stream of fluid. The light is then scattered at various angles of reflection and detected in photo multiplier tubes (PMTs). Light that has a low scattering ~10 degrees from incident, known as forward scatter (FSC), gives the parameter of relative cell size. Light scattered at greater angles, ~90 degrees from incident, known as side scatter (SSC), measures the granularity and internal complexity of the cell. The scattered light can also induce fluorescence in fluorophore probes attached to cells and this can be detected via PMTs dependent on specific fluorescence emission wavelengths. In this way, multiple parameters based on the excitation and emission wavelengths of the laser and fluorophore used can be interrogated in each cell of a population. Certain types of flow cytometers are able to sort cells into distinct populations depending on their characteristics e.g. size or fluorescence labelling (Ormerod, 2015). In this case, Fluorescence-activated cell sorting (FACS) was used and the basic set up is shown below in Figure 9.

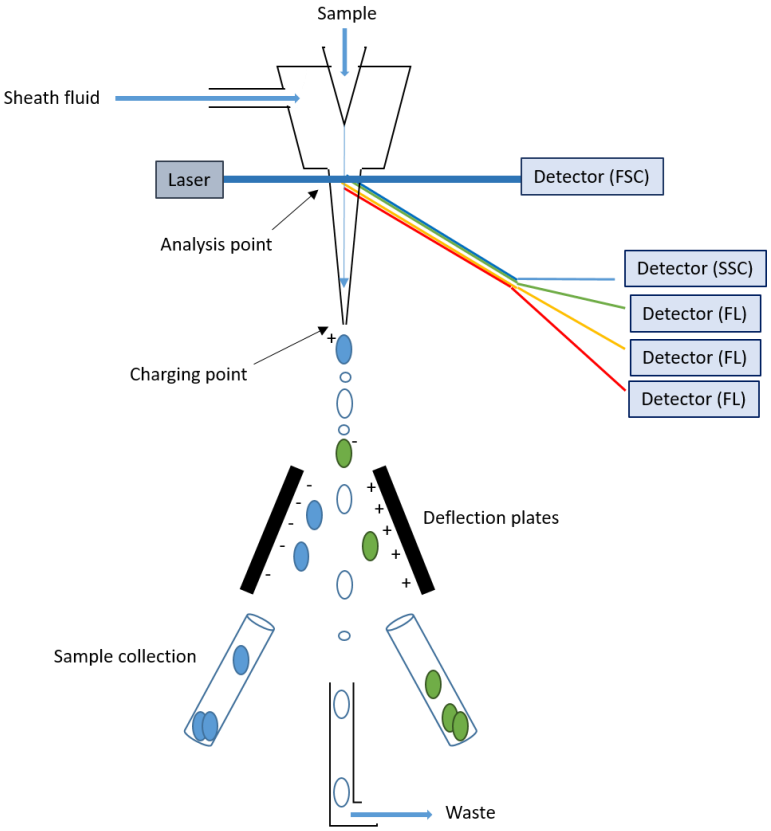

Figure 9 Basic set up of fluorescence-activated cell sorting
The sample is loaded into the chamber and is mixed with the sheath fluid where it becomes a single cell suspension. The cells cross a laser and their forward (FSC) and side scatter (SSC) and fluorescence (FL) is measured. The stream then breaks into even droplets and becomes charged depending on a pre-determined set of criteria e.g. the fluorescence of the cell within the droplet. As the charged particles travel through the deflection plates, the droplets become separated and are collected in the collection tubes. Any droplet that has not had a charge applied will continue to travel straight and is collected in the waste. Figure adapted from Ormerod (2015).

As well as characterising the cells obtained during the isolation procedure and checking their viability in response to various compounds, the expression level of S1PR1 was also investigated. As discussed in depth in the Introduction (1.5.2), S1P can bind to five receptors, three of which (S1PR1-3) are present on endothelial cells. Once activated by S1P, the receptors are removed from the cell surface and either recycled back to the surface or degraded. It was decided to look at the change in expression levels of S1PR1 in response to the addition of S1P and other compounds such as Fingolimod. Fingolimod is an S1P agonist that prevents the egress of lymphocytes from the lymph nodes by downregulating the S1P receptors (mainly S1PR1), therefore it was expected that a change in surface expression level would be seen (Baer et al., 2018). The effect of oxLDL on S1P receptor expression was also investigated as this may provide an indication that oxLDL and S1P share a signalling pathway as this is essentially an assay of S1P dependent activation.

3.1.2 Hypothesis and Aims

It is hypothesised that the cells isolated from the umbilical cords are endothelial in origin. It is also hypothesised that they express the S1P receptor 1 and that expression levels change in response to the addition of exogenous S1P.

Specific aims of this section are:

- to characterise isolated cells
- to check the cell viability under all used conditions using FACS
- to investigate HUVEC S1PR1 expression levels in response to various compounds e.g. S1P and Fingolimod
- to investigate PBMC S1PR1 expression levels

3.1.3 Method

In order to characterise the cells and check their viability, the cells were labelled with a number of antibodies which are listed in Table 4 in Methods section 2.6.2. A live/dead stain was used to ensure that the various conditions and compounds the cells were exposed to did not result in an increase in cell death. This dye works by binding to free amines on the surface of live cells which results in a weak fluorescence signal. Once the cell membrane has been compromised, as is the case with dead and dying cells, the stain has access to a greater number of free amines, both on the surface of the cell and intracellularly. It therefore follows that a greater fluorescence signal is generated and allows the separation of live and dead cells as there is also a clear shift in the forward and side scatter of dead and dying cells (Perfetto et al., 2010).

In order to investigate the effect of S1P, Fingolimod, oxLDL and LDL on S1PR1 expression, it was necessary to fix the cells in 4% (v/v) paraformaldehyde to ensure that the receptor expression represented the specific time point due to the dynamic nature of endocytosis and re-expression. A number of studies have been carried out in lymphocytes and other cell types to investigate the effect of fixing cells on the forward and side scatter. For the most part it is accepted that fixing cells does not significantly affect either the forward or the side scatter, providing the fixative is washed off and the cells are stored in a suitable buffer until analysed (Stewart et al., 2007). This guidance was followed and cells were stored for a maximum of 24 hours before being analysed by FACS, therefore it is believed that the fixation of HUVEC will have had a minimal effect on the forward and side scatter that was obtained. These cells were also not permeabilised as no detergent was used in the fixation process.

Once the cells had been analysed by FACS, the data was analysed using FlowJo software. Firstly, for each experimental setup an unstained control was used to identify the cells of interest and gate the population of HUVEC to exclude any debris that might be present. Expert advice on the gating of HUVEC and PBMCs was sought from the lab manager who runs the flow cytometry facility. This gate was then applied to all other samples from within the same assay. New gates were drawn each time an experiment was performed due to slight changes in cytometer setup including small variations in laser power. Once the population of HUVEC was established, the recorded events within this population could further be gated into positive and negative depending on which stain and cell parameter was being used. Representative images are used in this chapter, with each condition being carried out on at least three separate occasions.

3.1.4 Results

3.1.4.1 Characterisation and cell surface staining

The characterisation of endothelial cells was necessary as all the non-immune cells used for this study were primary cells obtained from human umbilical cords and an estimate of the purity of cultures used was required. The isolated cells were characterised by using fluorescently labelled antibodies against CD31/PECAM-1 (platelet/endothelial cell adhesion molecule 1) and CD105/ endoglin which are known to be expressed on endothelial cells and in combination, highlight the endothelium specifically. Figure 10 shows the results of staining with the CD31 antibody using the APC-A laser.

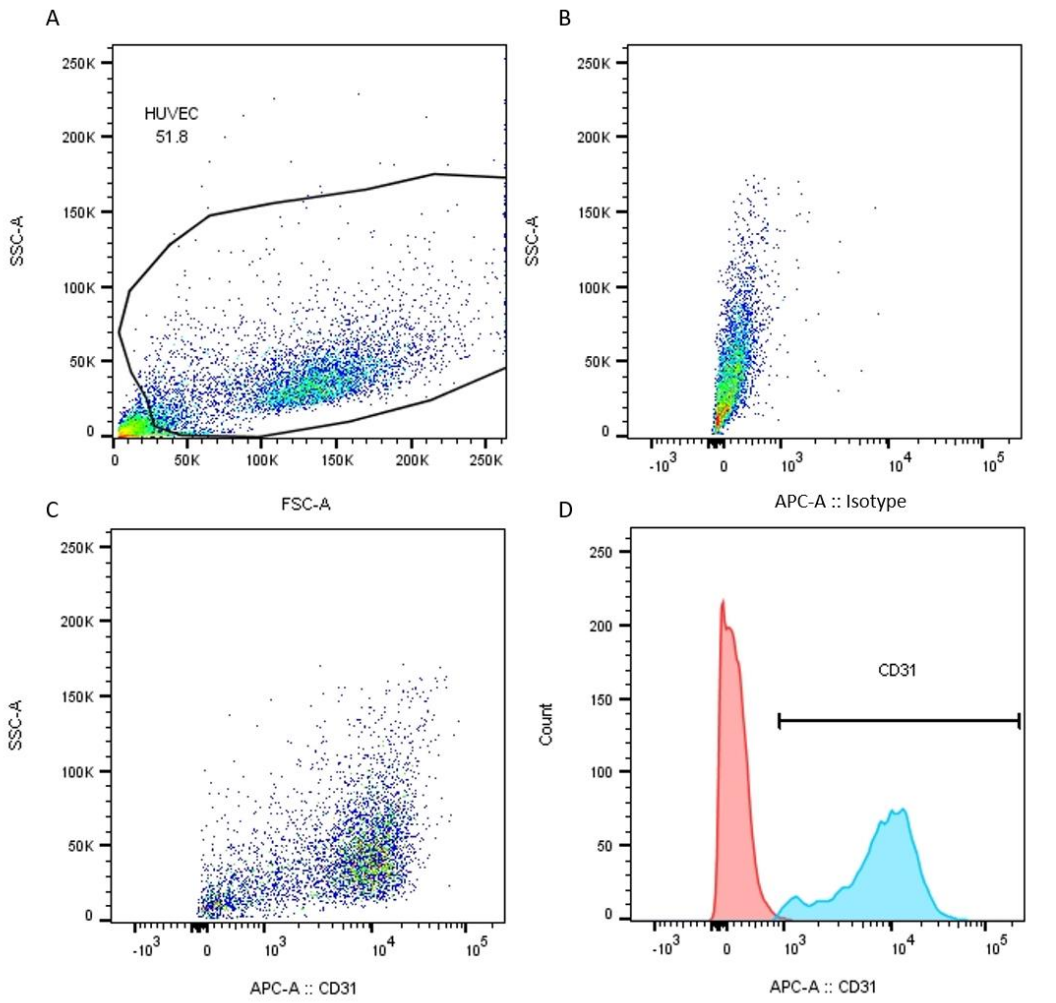

Figure 10 showing the difference between the isotype and the CD31 antibody
A- The total number of events recorded and the 10,000 gated events showing the HUVEC cells. **B**- The gated cells showing background autofluorescence in the presence of the isotype. **C**- The gated cells showing a positive signal in the presence of the CD31 antibody. **D**- Overlaid histogram highlighting the peak separation between the isotype (red) and CD31 antibody (blue) stained cells. Plots shown are representative of three independent experiments.

Figure 10 shows that there is a right shift in the population to higher fluorescence levels when stained with CD31 antibody compared to isotype controls suggesting positive expression of this endothelial marker. The whole population is also shown to be expressing this marker as there is a clear right shift in the fluorescence. This was then repeated with an antibody directed against CD105 and is shown below in Figure 11.

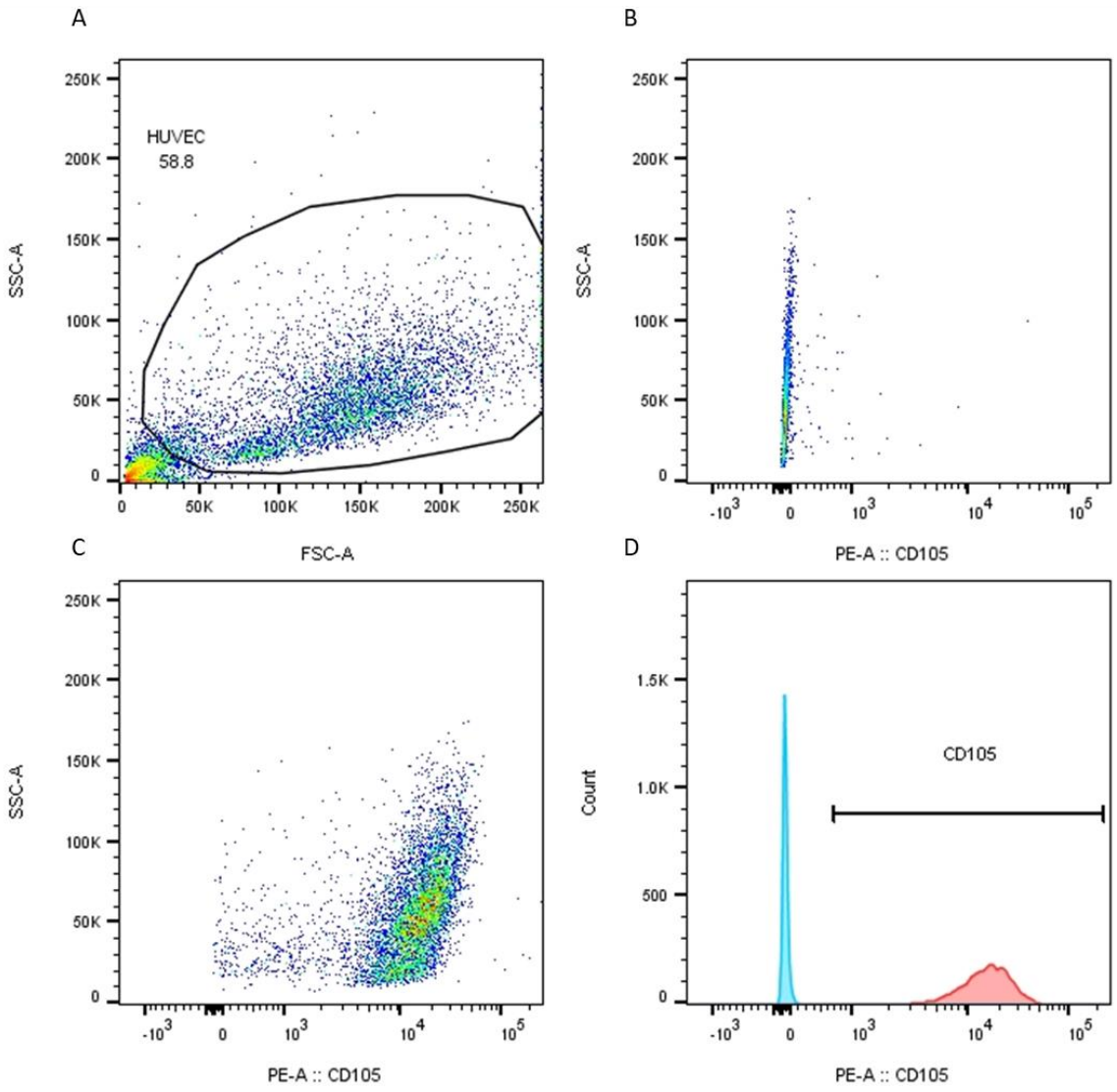

Figure 11 showing the difference between the isotype and the CD105 antibody
A- The total number of events recorded and the gated HUVEC cells. **B**- The gated cells showing no signal in the presence of the isotype. **C**- The gated cells showing a positive signal in the presence of the CD105 antibody. **D**- Overlapped histogram highlighting the peak separation between the isotype (blue) and CD105 antibody (red). Plots shown are representative of three independent experiments.

Figure 11 shows that the gated cells are positive for CD105 and therefore, taken together with the positive result for CD31 expression, it can be concluded that the cells isolated from the human umbilical cords are indeed endothelial in origin.

3.1.4.2 Cell viability

As well as characterising the endothelial cells, it was also important to check that the cells were viable following treatment with the various compounds that were to be used in the functional assays. This ensured that any changes seen in the functional cellular responses in assays was due to the treatment and not because of an effect on viability or increased cell death. This was achieved by using an APC-Cy7 live/dead stain that shows dead cells as having a relatively higher fluorescence because of the retention of the dye by surface and internal amines due to a loss of membrane integrity in dead and dying cells. Plots of untreated 'live' and 100% ethanol treated 'dead' cells are shown below in Figure 12.

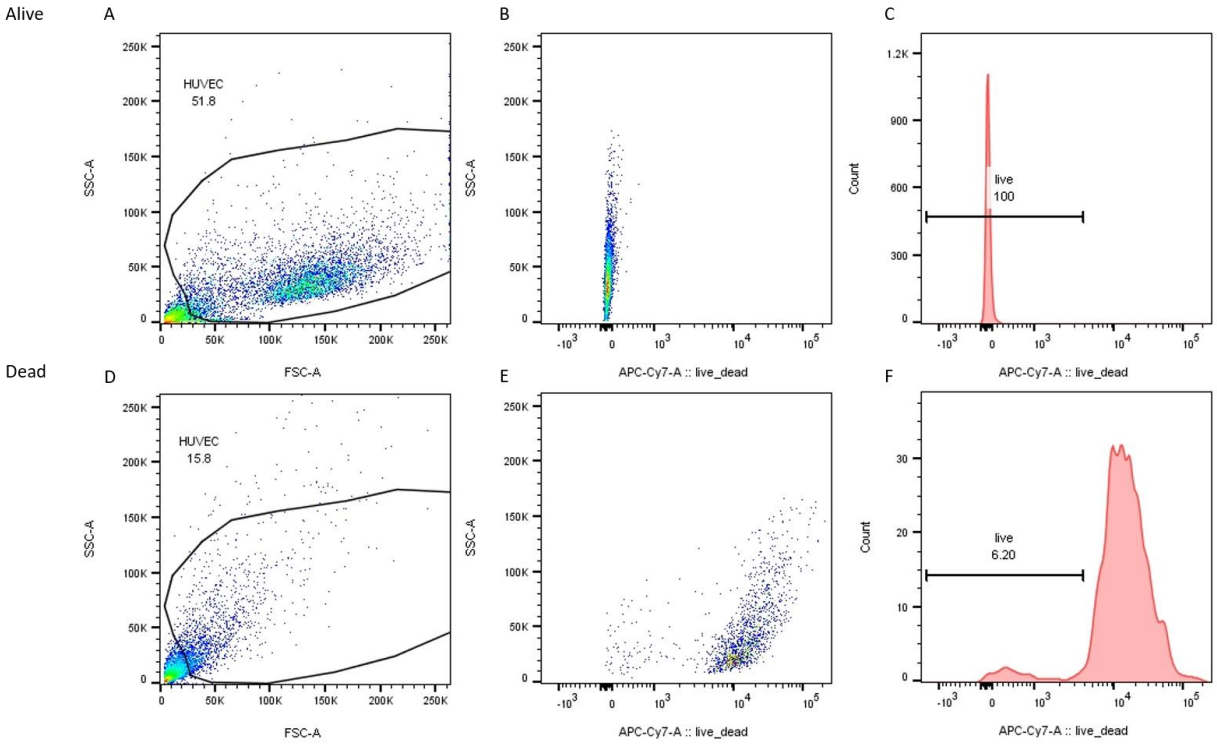

Figure 12 FACS plots of live and dead cells

The top row of plots shows the untreated 'live' control cells and the bottom row shows 100% ethanol treated 'dead' cells following incubation with the live/dead stain. **A** and **D** show the total number of events recorded and the gate from the control (**A**) which was applied to all samples. **B** and **E** show the signal from staining with the live/dead stain while **C** and **F** show this result as a histogram, with the gate for the live cells established from the dead control (**F**). Plots shown are representative of three independent experiments.

Figure 12 highlights the large difference in fluorescence between live and dead cells and therefore shows that the stain used can clearly separate the two populations. The gate for HUVEC was established from the unstained control cells and was applied to all other samples while the live gate was taken from the ethanol treated cells and applied to those cells which were included in the first HUVEC gate. This result also allows future comparisons of the proportion of dead cells to be made between the various compounds and conditions the assays employ and the control population of

HUVEC. Of note is the effect of ethanol on the forward and side scatter parameters of the HUVEC populations compared to non-treated cells.

3.1.4.2.1 Compounds in full media

The viability of the cells in response to the compounds used was firstly assessed in full media. Cells were incubated with the compound(s) for 24 hours before being stained for live/dead analysis by FACS as the majority of the assays used required cell stimulation for this length of time.

All concentrations of S1P used (10μM-1nM) were analysed with APC-Cy7 live/dead stain as described previously and the results are shown below in Figure 13.

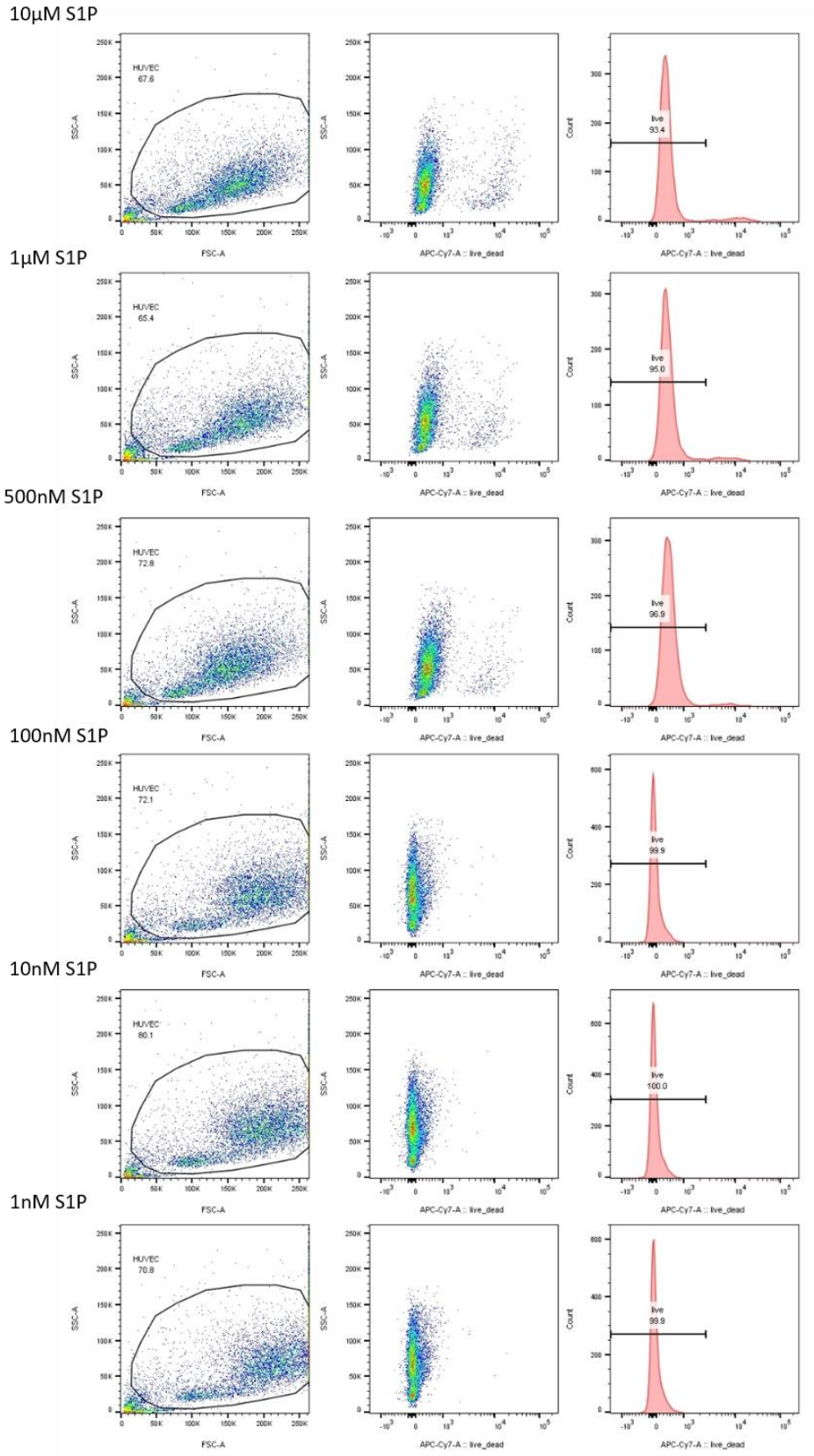

Figure 13 Live/dead FACS plots of S1P in normal media

The left panels show the total number of events that were recorded for each S1P concentration and the gate from the control that was applied to each sample. The middle panels show the events within the gate and whether they were positive for the live/dead stain. The right panels show a histogram of these events determined by the gate from the dead control. Plots shown are representative of three independent experiments.

Figure 13 shows that the addition of 10µM S1P to the cells results in a slight increase of dead cells but that the vast majority (>90%) are still alive. As the concentration of S1P decreases, the amount of cell death also decreases, with 100nM-1nM showing all cells are alive.

The viability of the cells in the presence of the S1P antagonist Fingolimod was also checked as described above and the results shown below in Figure 14.

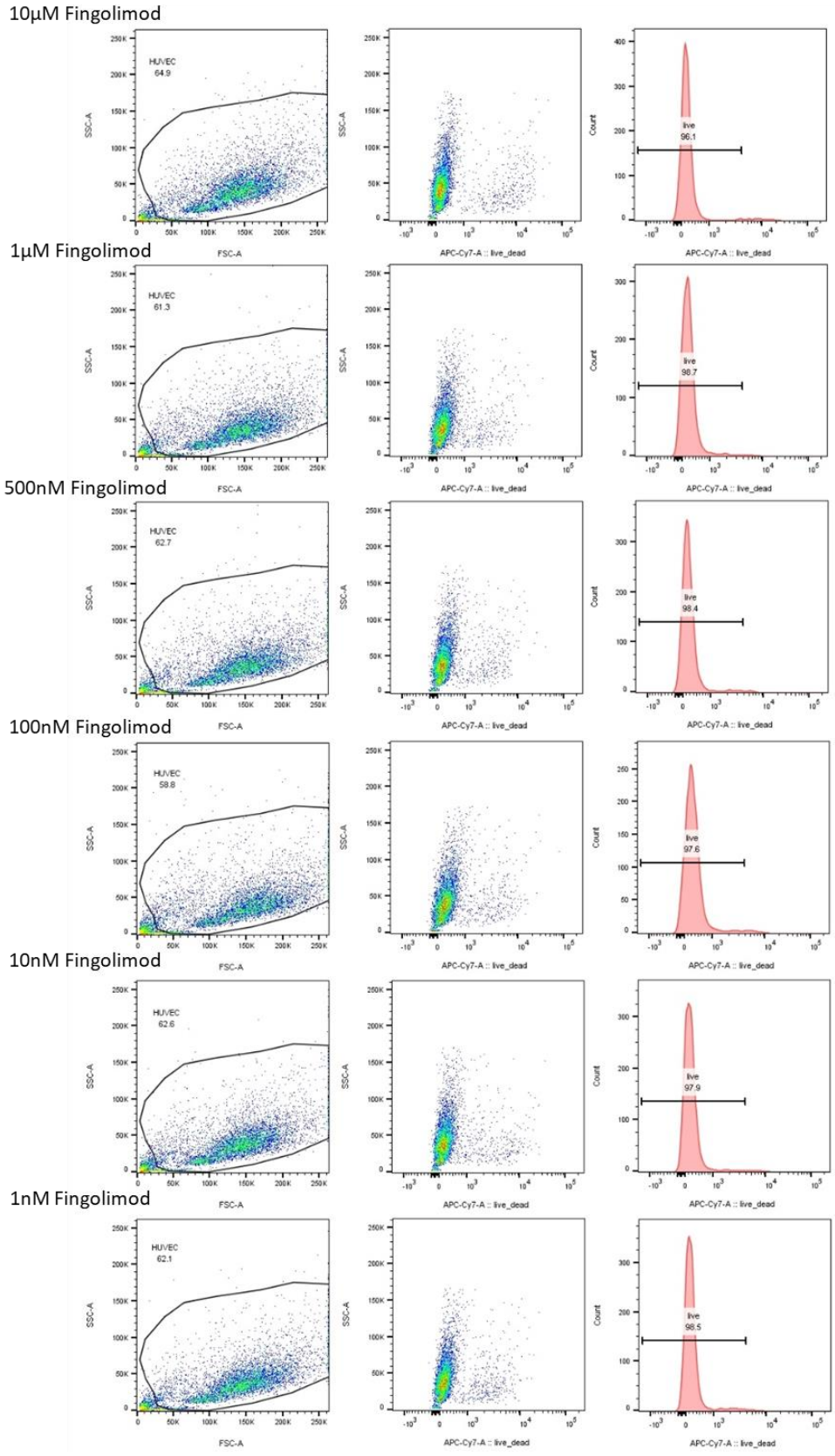

Figure 14 Live/dead FACS plots of Fingolimod in normal media

The left panels show the total number of events that were recorded for each Fingolimod concentration and the gate from the control that was applied to each sample. The middle panels show the events within the gate and whether they were positive for the live/dead stain. The right panels show a histogram of these events determined by the gate from the dead control. Plots shown are representative of three independent experiments.

Figure 14 shows that the addition of Fingolimod to HUVEC for 24 hours, at any of the concentrations used, does not result in an increase in cell death over the time exposure used for subsequent assays.

The following graph (Figure 15) shows the percentage viability of HUVEC from three separate assays when exposed to S1P and Fingolimod for 24 hours.

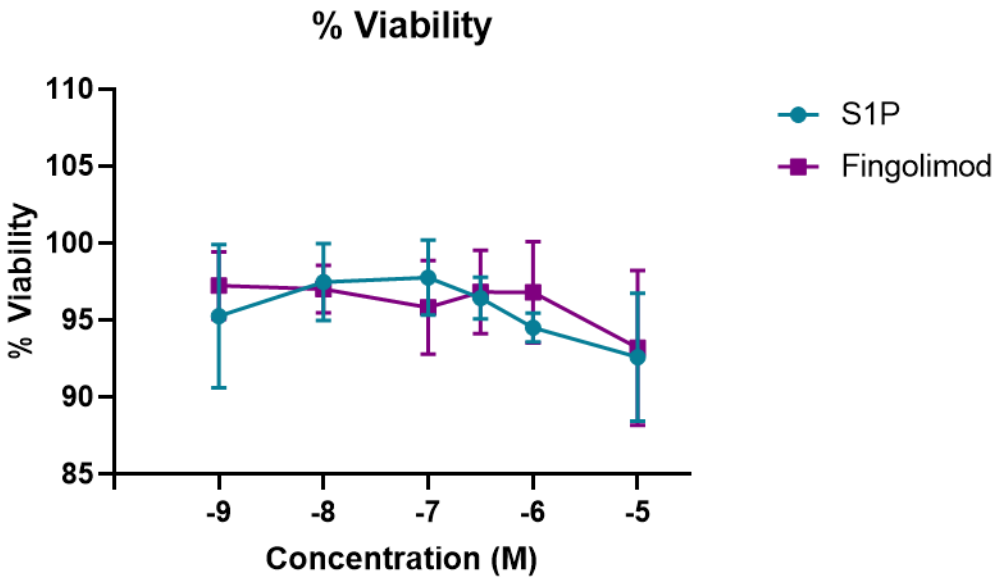

Figure 15 Percentage viability of HUVEC exposed to S1P and Fingolimod
The effect of varying concentrations of S1P and Fingolimod did not result in a decrease in cell viability. Error bars show the mean viability +/- the standard deviation, data is from 3 independent experiments, with 10,000 events recorded in each.

Figure 15 shows that even at high concentrations, S1P and Fingolimod do not result in a significant increase in cell death. Therefore, any inhibitory results obtained in future assays will not be as a result of cell death.

Oxidised LDL was also used to stimulate the cells for 24 hours and the viability of those cells was assessed. LDL was also included as a control, so any effect of the oxidative modification could also be determined and the results are shown in Figure 16 below.

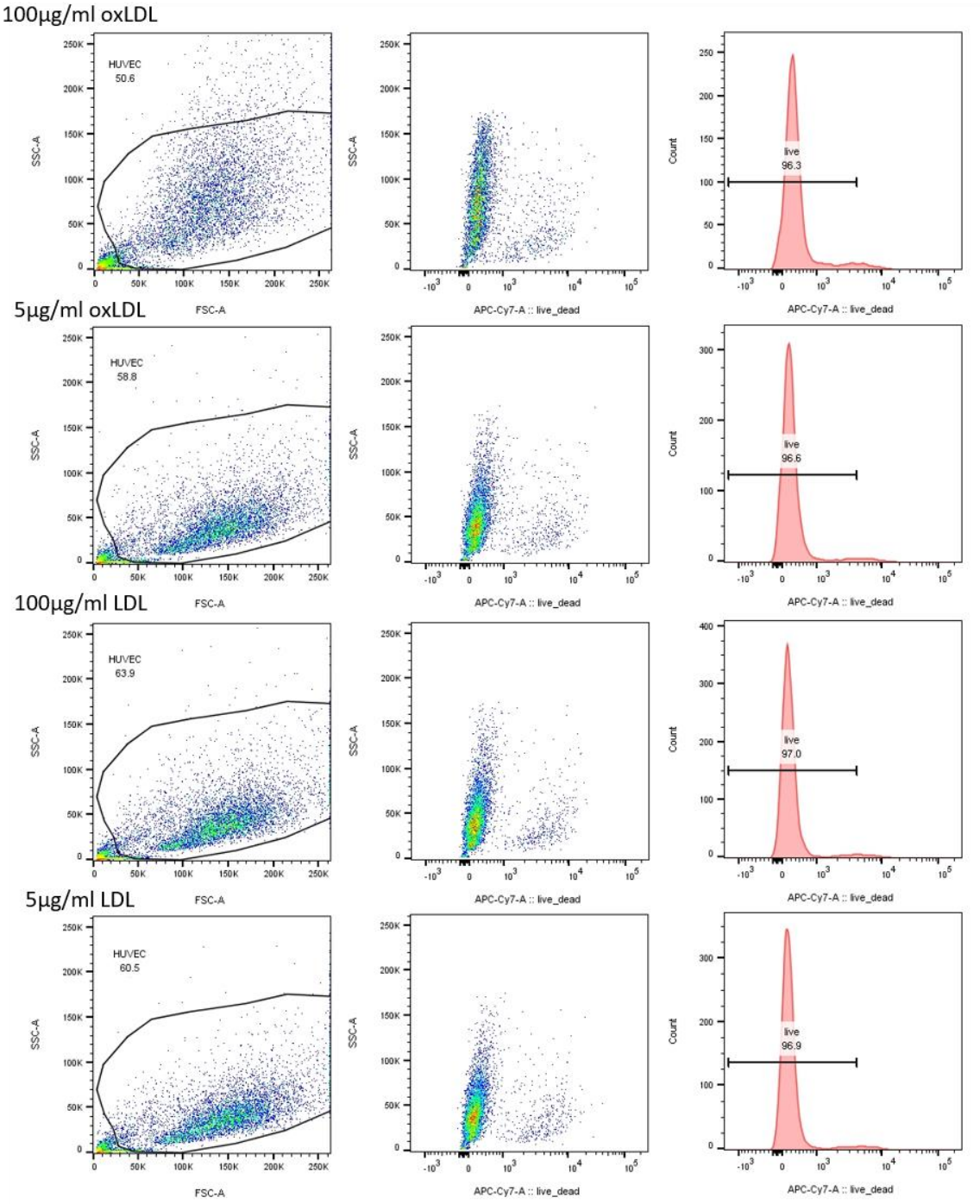

Figure 16 Live/dead FACS plots of oxLDL/LDL in normal media

The left panel shows the total number of events that were recorded for each condition and the gate from the control that was applied to each sample. The middle panel shows the events within the gate and whether they were positive for the live/dead stain. The third panel shows a histogram of these events determined by the gate from the dead control. Plots shown are representative of three independent experiments.

Figure 16 shows that the addition of oxLDL does result in a slight increase in cell death, however cell viability is still greater than 95% for all lipid concentrations and would not be expected to interfere with the results of future assays. It was also noted that 100µg/mL oxLDL caused a large spread in the SSC, whereas no difference was seen with the same concentration of LDL. oxLDL therefore has no effect on cell viability however it does cause a morphological change and this is highlighted in Figure 17.

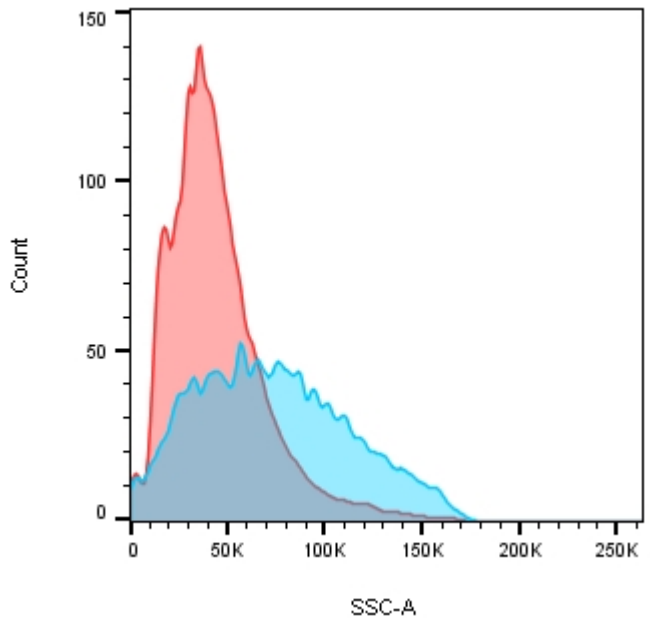

Figure 17 Difference in side scatter between oxLDL and LDL
100µg/ml LDL (red) has a much narrower range of SSC than 100µg/ml oxLDL (blue). Histograms show the side scatter of the gated HUVEC population as determined from the control. Histograms shown are representative of three independent experiments.

Figure 17 shows the histograms of the side scatter of 100µg/ml oxLDL and LDL overlaid and confirms the increase in SSC seen in Figure 16 after the addition of 100µg/ml oxLDL. The mean fluorescent intensity (MFI) of the side scatter was also plotted to highlight the difference between oxLDL and LDL. This is shown below in Figure 18.

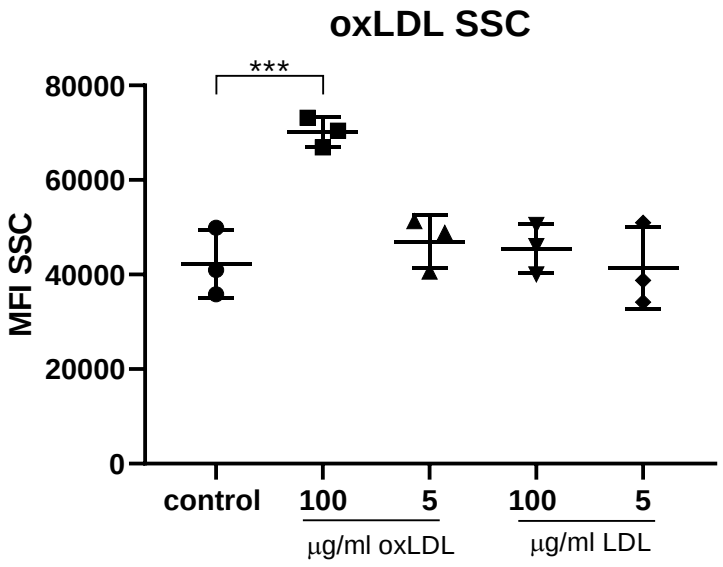

Figure 18 Comparison of SSC MFI between oxLDL and LDL
The mean fluorescent intensity of the two concentrations of oxLDL and LDL were calculated in FlowJo and plotted to highlight the differences in side scatter. The error bars represent the mean fluorescent intensity of the side scatter +/- SD, n= 3.

Figure 18 shows a clear difference between the side scatter of the two oxLDL concentrations, with 5μg/ml oxLDL showing the same level of side scatter as that of LDL and the control and 100μg/ml showing a nearly two-fold increase in MFI. One way ANOVA gave a p value of 0.0011 and multiple comparison testing showed that the SSC of 100μg/ml oxLDL was statistically different to the control, with a p value of 0.0009. This concentration was also statistically different ($p<0.01$) to 5μg/ml oxLDL and to both concentrations of LDL.

The effect of albumin and ox-albumin on the viability of HUVEC was also investigated and the results are shown below in Figure 19.

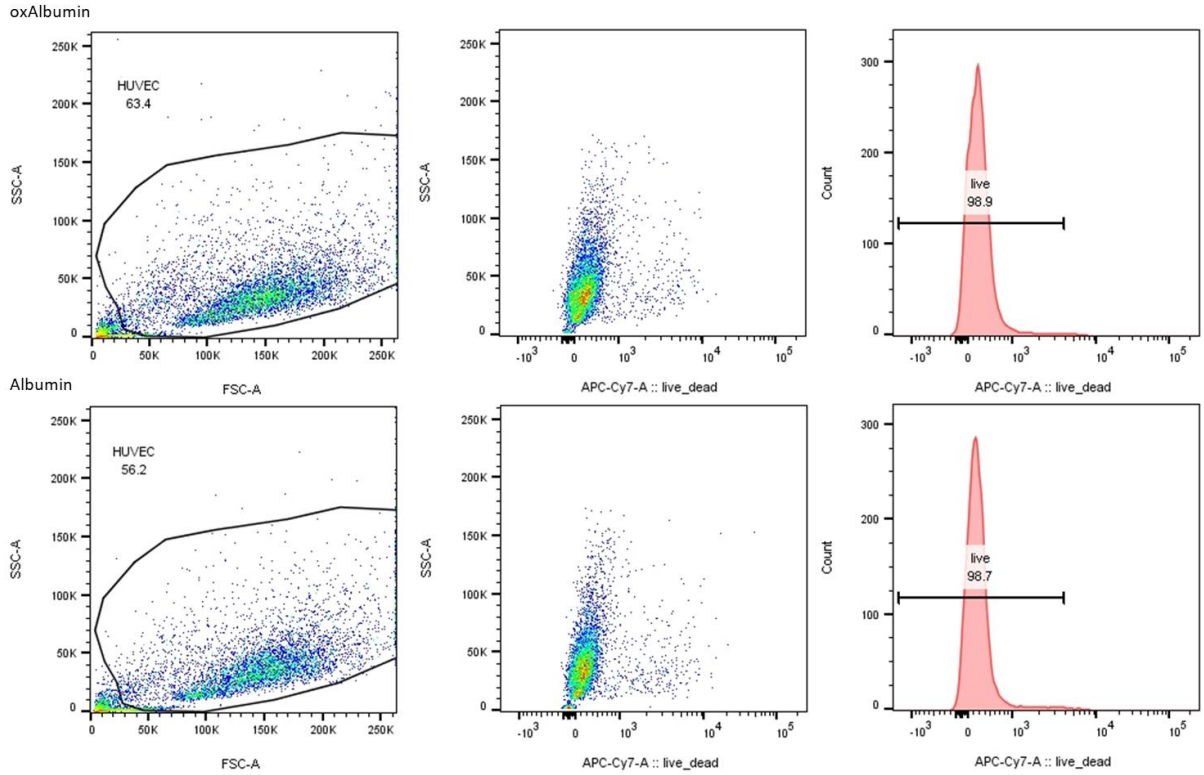

Figure 19 Live/dead FACS plots of ox-albumin and albumin in normal media
The left panel shows the total number of events that were recorded for each condition and the gate from the control that was applied to each sample. The middle panel shows the events within the gate and whether they were positive for the live/dead stain. The third panel shows a histogram of these events determined by the gate from the dead control. Plots shown are representative of three independent experiments.

No difference was seen in the viability of cells exposed to albumin or the oxidised form, with nearly a 100% survival rate achieved under both conditions.

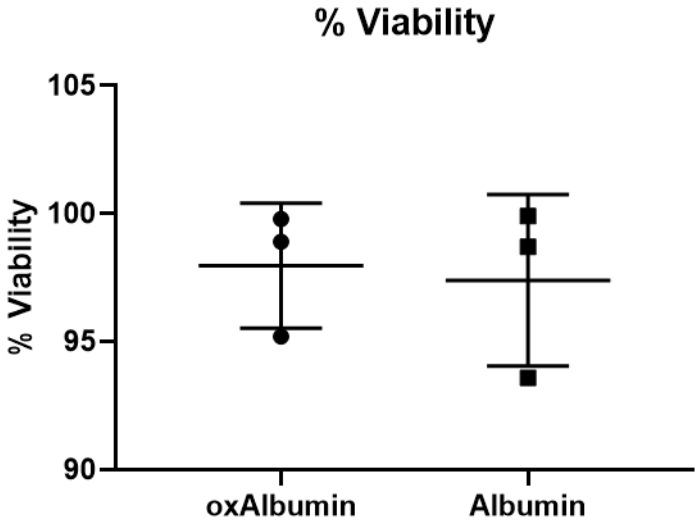

Figure 20 Percentage viability of HUVEC exposed to ox-albumin and albumin
The effect of ox-albumin and albumin did not result in a decrease in cell viability. Error bars show the mean viability +/- the standard deviation, data is from 3 independent experiments, with 10,000 events recoded in each.

Figure 20 shows the viability of HUVEC exposed to either ox-albumin or albumin for 24 hours. There is no significant difference between the oxidised form and albumin and neither have a significant effect on cell viability as determined by comparing the mean to a hypothetical value of 100% using a one sample t-test.

As it was noticed that the addition of oxLDL to HUVEC resulted in an increase in SSC, the effect of ox-albumin on side scatter was also investigated to see if it was possible to compare oxidative stresses caused by these two compounds.

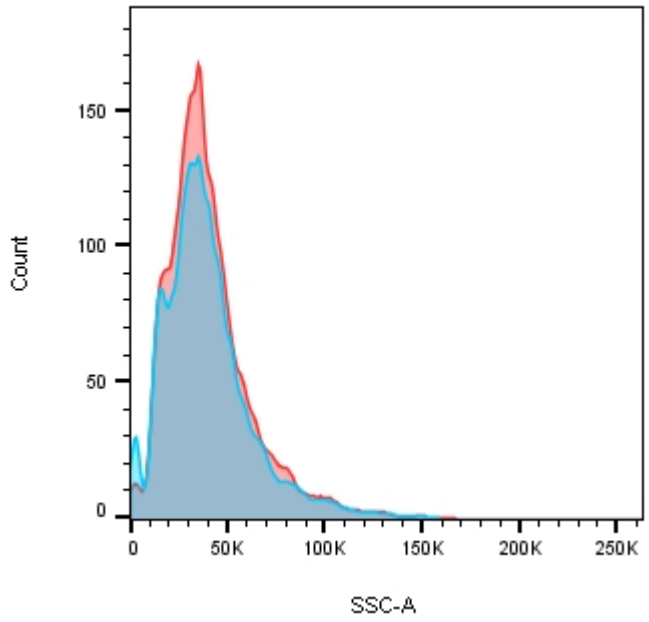

Figure 21 Difference in side scatter between albumin and ox-albumin
There is no difference between the side scatter of ox-albumin (red) and albumin (blue). Histograms show the side scatter of the gated HUVEC population as determined from the control and are representative of three independent experiments.

Figure 21 shows that in contrast to oxLDL, there is no difference in side scatter between albumin and ox-albumin.

3.1.4.2.2 Compounds in delipidised media

This project aims to investigate the effect of lipids on the endothelium and therefore serum based culture conditions add serum lipids that may complicate the assays. Assays were therefore carried out using a delipidised media to determine the effects of various compounds in a reduced lipid environment. It was therefore necessary to ensure that the cells were able to survive under these conditions in combination with the treatments.

A different colour of live/dead stain (Aqua) was used for these assays and therefore Figure 22 has been included to show that this stain is an equivalent method to differentiate between live and dead cells. The effect of the reduced lipid media and the basic M199 media on cell viability is also included in Figure 22 for comparison to the control. The M199 media was included as both albumin and oxidised albumin were added to this media as well as the delipidised media in the subsequent functional assays.

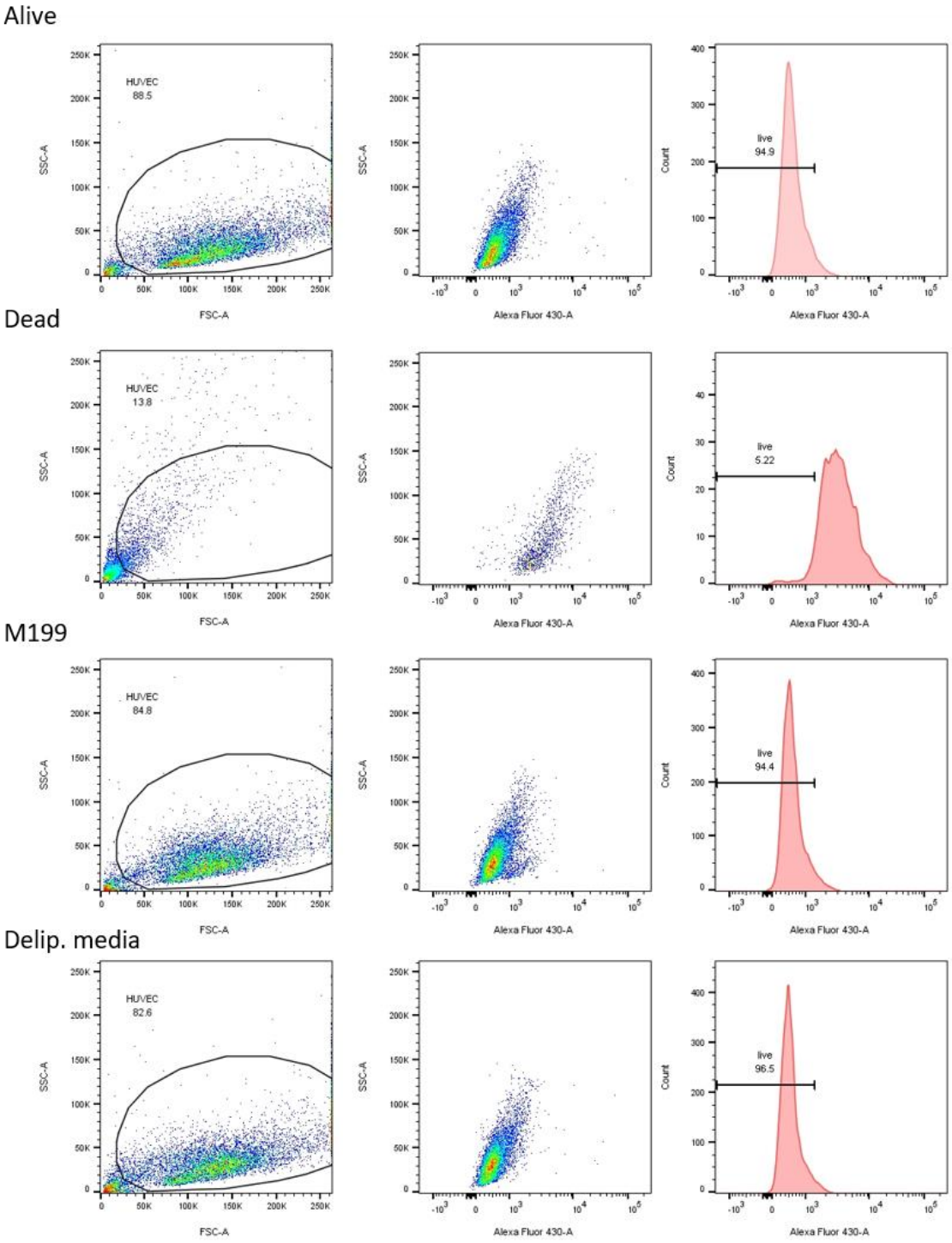

Figure 22 Aqua live/dead staining of HUVEC

The live cells are the unstained control in full media, the dead cells were killed with 100% ethanol. The plots on the left show the total number of events recorded and the gate from the control which was applied to all samples. The middle plots show the signal as a result of staining with the Aqua live/dead stain. The rightmost plots show this result as a histogram, with the gate for the live/dead cells established from the dead control and applied to all samples. Plots shown are representative of three independent experiments.

The unstained control cells were gated as previously described and the gate applied to the rest of the samples. It can be seen that cultures in either the basic M199 media without human serum or the delipidised media did not increase the number of dead cells, with the cell viability of both medias comparable to that of the full lipid control.

A lipid supplement that contains a defined lipid profile was also tested by adding it to the delipidised serum containing media to determine if this had an effect on the assays of endothelial function of lipids in the media. Lipids are important in general cell turnover and function therefore, delipidisation of the media potentially provides a non-optimal growth media and this was investigated. The two concentrations of lipid supplement used were therefore also assessed for their effect on cell viability.

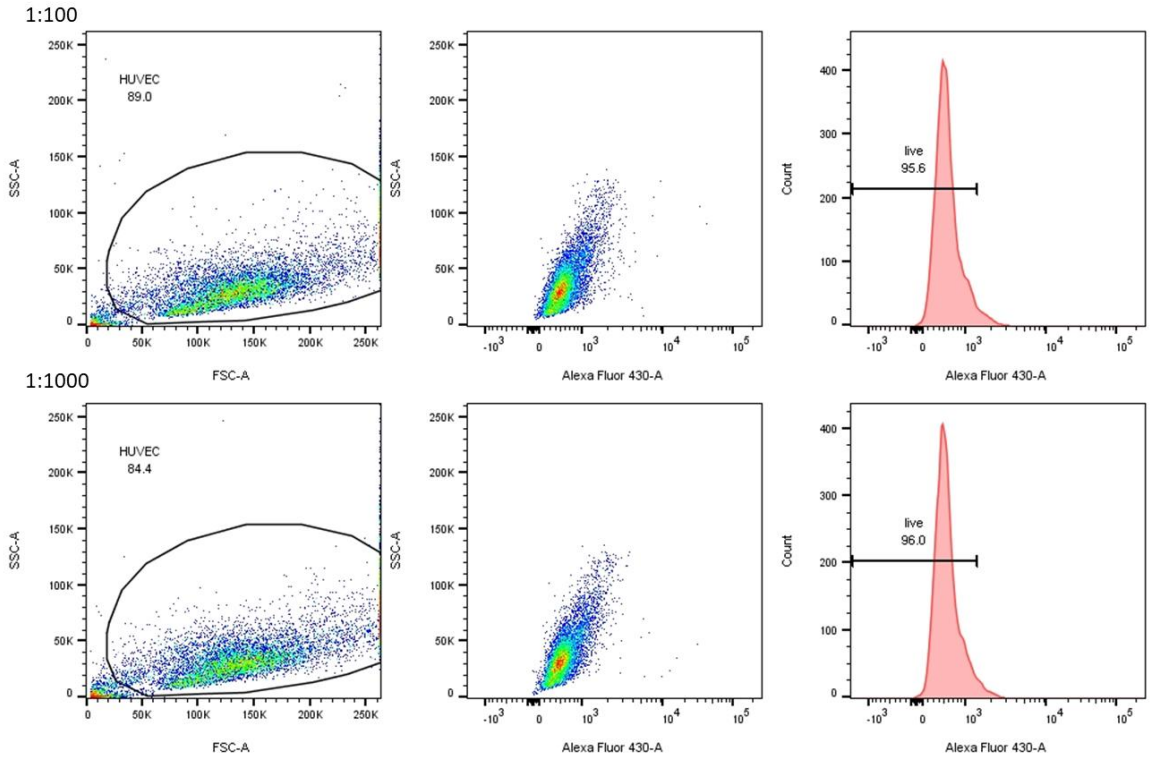

Figure 23 Aqua live/dead staining of a lipid supplement
The left panel shows the total number of events that were recorded for each concentration and the gate from the control that was applied to each sample. The middle panel shows the events within the gate and whether they were positive for the live/dead stain. The third panel shows a histogram of these events determined by the gate from the dead control. Plots shown are representative of three independent experiments.

No significant difference in cell viability was seen between the two lipid supplement concentrations used, with no effect on morphological characteristics observed in the side scatter profile.

Once it had been established that the new live/dead stain was able to differentiate cell viability and that the different variations of media did not result in increased cell death, the compounds of interest could be assessed. As described previously, HUVEC were exposed to varying S1P concentrations in the reduced lipid media for 24 hours and assessed for cell viability using the Aqua live/dead stain.

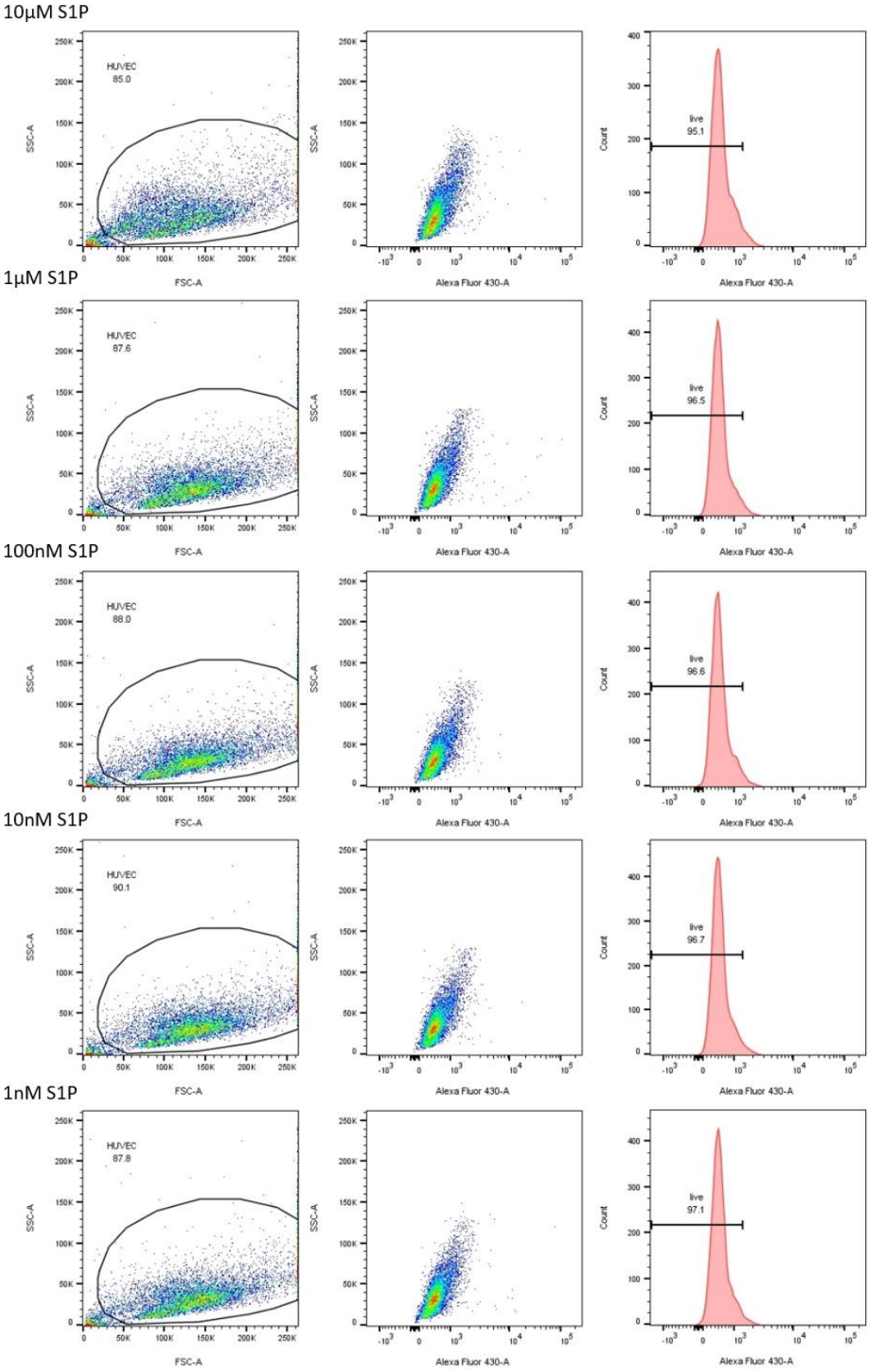

Figure 24 Live/dead FACS plots of S1P in delipidised media

The left panel shows the total number of events that were recorded for each concentration and the gate from the control that was applied to each sample. The middle panel shows the events within the gate and whether they were positive for the live/dead stain. The third panel shows a histogram of these events determined by the gate from the dead control. Plots shown are representative of three independent experiments.

Figure 24 shows that, similarly to the effects of S1P in full media, there is again a slight increase in cell death at the highest concentration of S1P, however as over 90% of cells are still alive this should not have an effect on the functional assays. At this concentration there is also a slight increase in the side scatter, similar to what was seen when 100µg/ml oxLDL was added to the cells in full lipid media.

The effect of the equivalent concentrations of Fingolimod in delipidised media was also investigated and is show below in Figure 25.

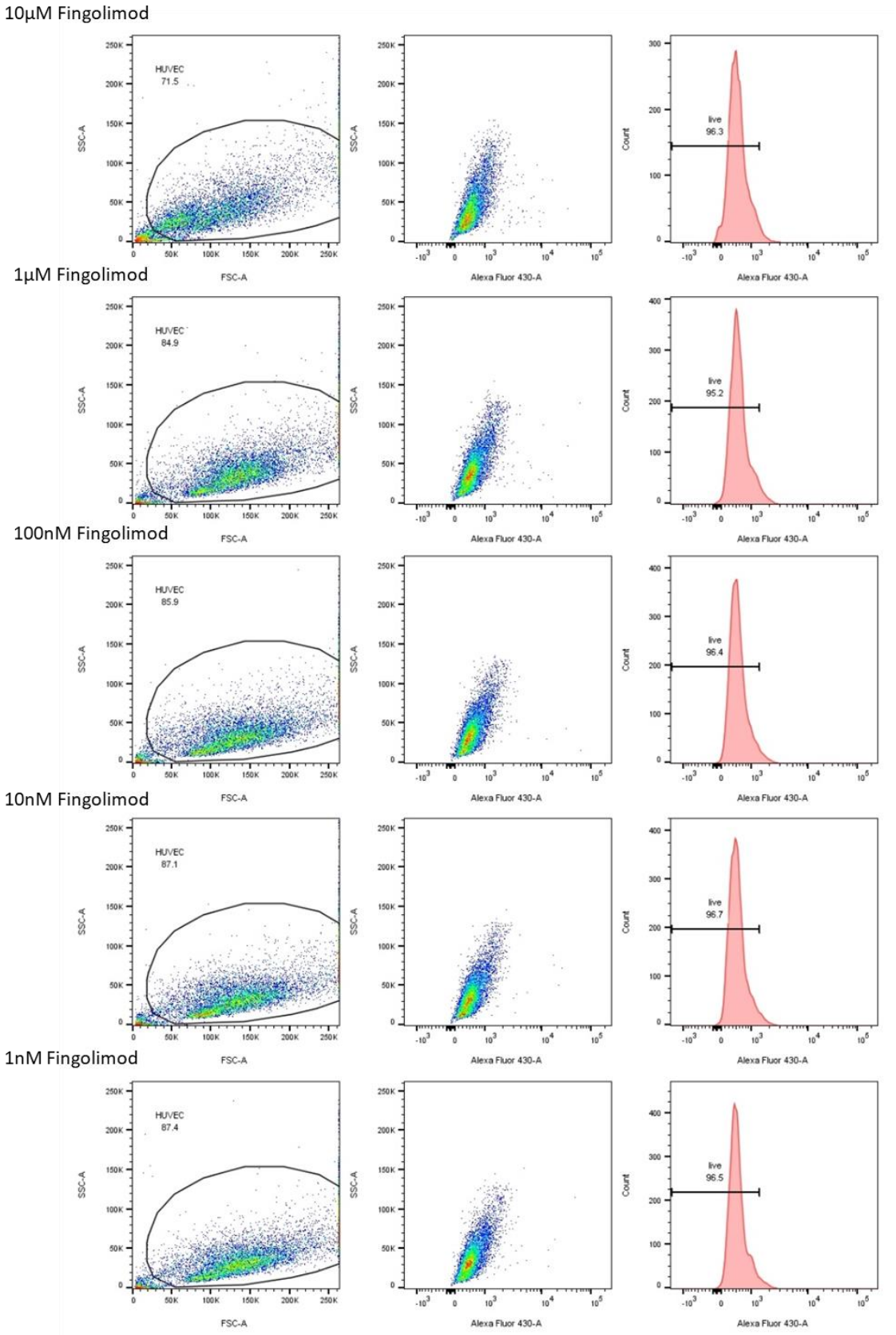

Figure 25 Aqua Live/dead FACS plots of Fingolimod in delipidised media

The left panel shows the total number of events that were recorded for each concentration and the gate from the control that was applied to each sample. The middle panel shows the events within the gate and whether they were positive for the live/dead stain. The third panel shows a histogram of these events determined by the gate from the dead control. Plots shown are representative of three independent experiments.

Fingolimod does not have any effect on the viability of HUVEC in a reduced lipid environment compared with delipidised control and full media control, with >95% viability being recorded for each concentration.

Oxidised LDL was also added in combination with the delipidised media and, as before, LDL was included for comparison.

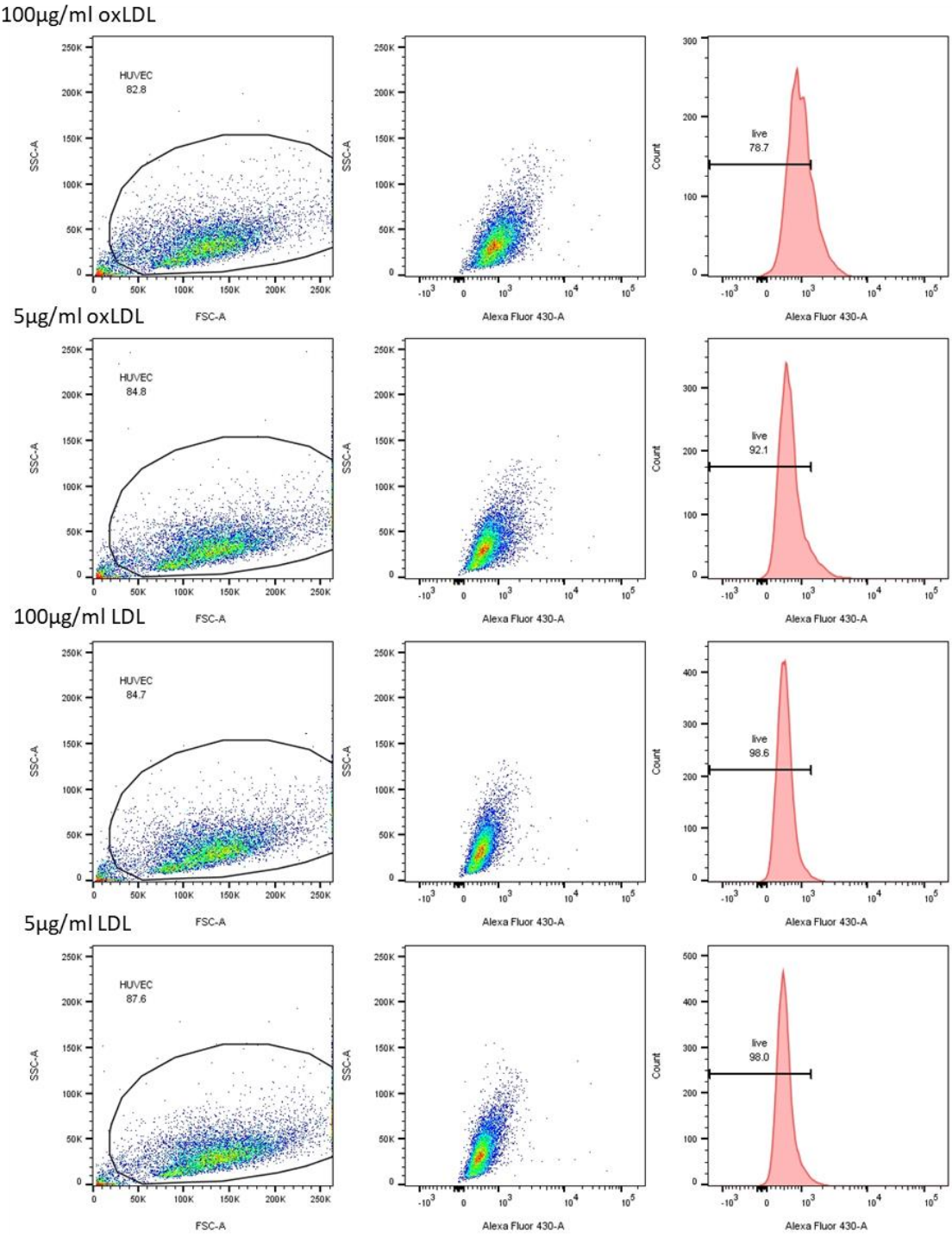

Figure 26 Aqua Live/dead FACS plots of oxLDL/LDL in delipidised media

The left panel shows the total number of events that were recorded for each condition and the gate from the control that was applied to each sample. The middle panel shows the events within the gate and whether they were positive for the live/dead stain. The third panel shows a histogram of these events determined by the gate from the dead control. Plots shown are representative of three independent experiments.

Figure 26 shows that 100µg/ml oxLDL results in around 20% cell death in a reduced lipid environment, while 5µg/ml did not increase cell death above that of the control. Neither concentration of LDL resulted in a decrease in cell viability, suggesting that it is the oxidised portion of the lipid causing the increase in cell death. Interestingly, there does not seem to be the same

increase in side scatter that was seen in the normal media as a result of 100µg/mL oxLDL addition, this may be as a result of the increased cell death.

Albumin and oxidised albumin were also included in the panel of compounds used to assess cell viability in a reduced lipid environment.

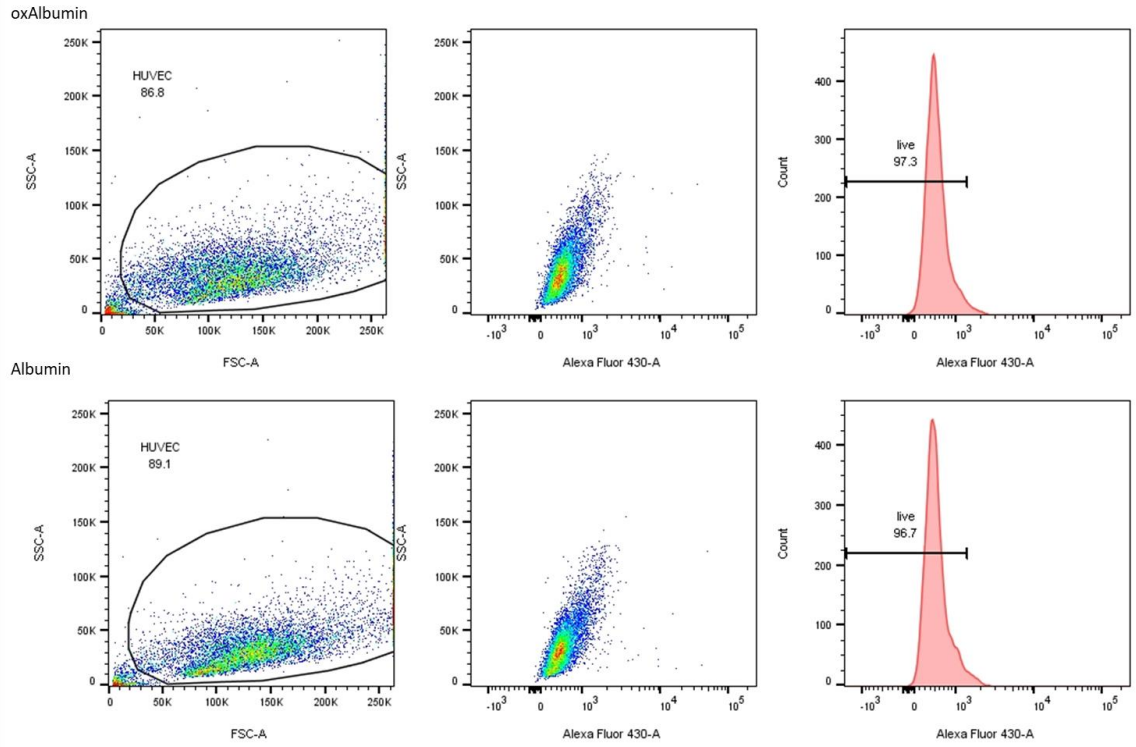

Figure 27 Aqua live/dead staining of ox-albumin and albumin in delipidised media
The left panel shows the total number of events that were recorded for each condition and the gate from the control that was applied to each sample. The middle panel shows the events within the gate and whether they were positive for the live/dead stain. The third panel shows a histogram of these events determined by the gate from the dead control. Plots shown are representative of three independent experiments.

Figure 27 shows that the addition of either ox-albumin or albumin to the delipidised media has no effect on cell viability.

Albumin and ox-albumin were also added to the basic serum free M199 media and the results shown below.

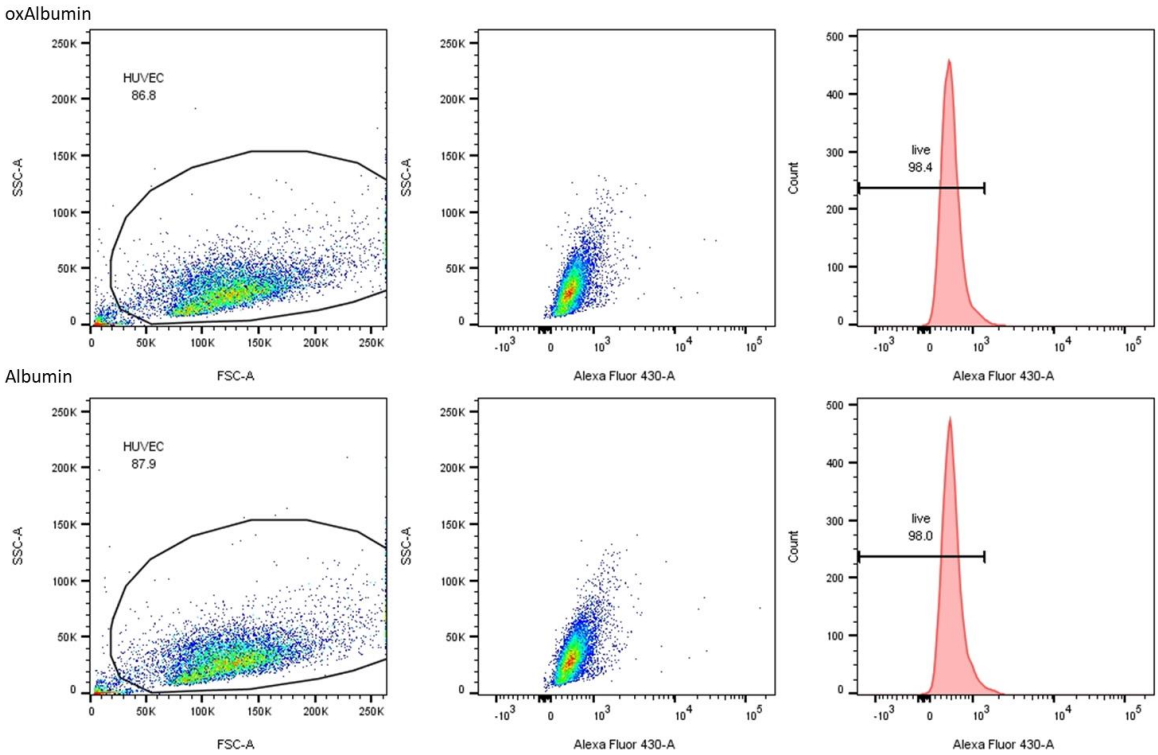

Figure 28 Aqua live/dead staining of ox-albumin and albumin in M199 media
The left panel shows the total number of events that were recorded for each condition and the gate from the control that was applied to each sample. The middle panel shows the events within the gate and whether they were positive for the live/dead stain. The third panel shows a histogram of these events determined by the gate from the dead control. Plots shown are representative of three independent experiments.

These results are similar to those of ox-albumin and albumin in the delipidised media, with no increase in cell death seen when ox-albumin was added to cells in serum free M199 media.

3.1.4.3 S1PR1 expression

So far this chapter has looked at the characterisation of the endothelial lineage using CD31 and CD105, cell viability after the addtition of various compounds and in different lipid conditions and now S1PR1 expression will be studied. The expression levels of S1PR1 were first studied in peripheral blood mononuclear cells (PBMCs) before investigating the levels in endothelial cells in response to the addition of various compounds. The S1PR1 antibody was titrated with the PBMCs to find the best signal, however it was discovered that the antibody could not be titrated much before the signal was completely lost. As with the other graphs presented in the Chapter, each condition was carried out on three separate occasions and representative images are shown.

3.1.4.3.1 Peripheral blood mononuclear cells (PBMCs)

Peripheral blood mononuclear cells (PBMCs) were analysed to determine the expression of S1PR1 on cell types such as lymphocytes, monocytes and neutrophils. Blood was collected from volunteers into EDTA blood tubes and the red blood cells removed as previously described (Materials and Methods section 2.6.3) before being stained with a live/dead stain (APC-Cy7) and S1PR1 (APC).

Firstly, the unstained control was gated in order to separate these three cell types for analysis. Once gated, the live/dead compensation control was gated to show the live cells within each population so that the expression of S1PR1 would only be analysed on live cells. This process is shown below in Figure 29 with dead cells generated as previously described with exposure to 100% ethanol for 10min.

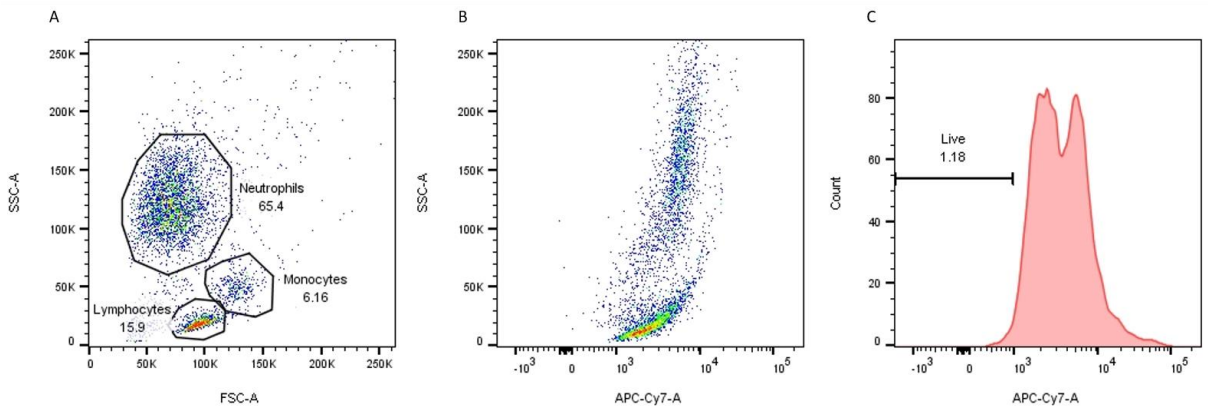

Figure 29 Gating of PMBCs from whole blood
A- Total number of events recorded in the unstained control and showing the gates for lymphocytes, monocytes and neutrophils. **B**- Dead compensation control used to gate for live cells with **C** showing this as a histogram. Plots shown are representative of three independent experiments.

After establishing the population of lymphocytes, monocytes and neutrophils, the live cells were gated and this gate applied to all other samples so that each sample was firstly gated according to cell type and secondly for the live cells within each population. It was this sub-population of live cells that was analysed for S1PR1 expression and the results of lymphocyte expression are shown below. Again, the isotype was used as the control to gate for S1PR1 expression.

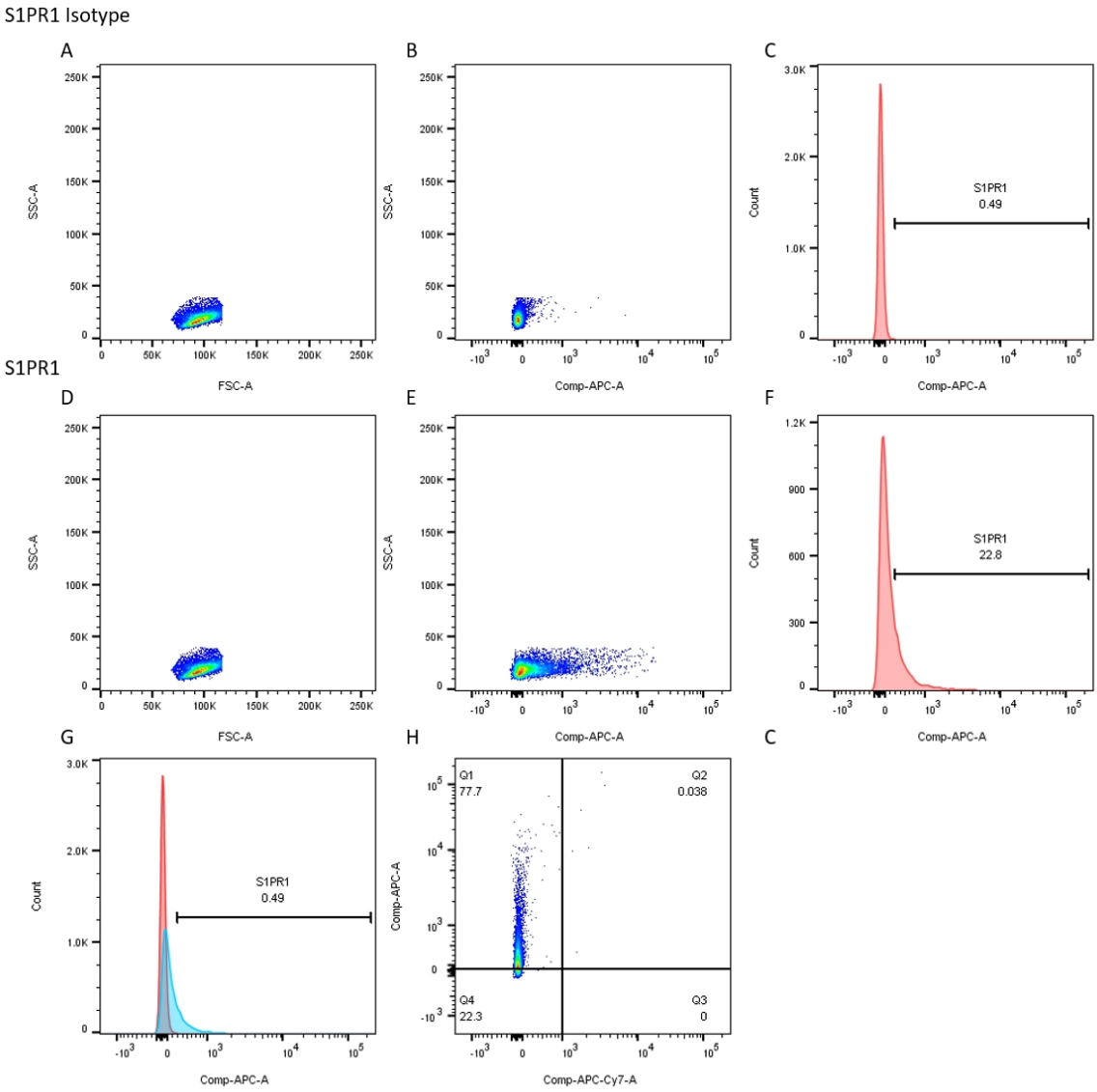

Figure 30 Lymphocyte S1PR1 expression

The top row (**A-C**) shows the results of the live population of lymphocytes in the presence of the S1PR1 isotype, showing the whole population (**A**), cells positive for S1PR1 (**B**) and the gate for S1PR1 (**C**). The middle row (**D-F**) shows the same for the S1PR1 antibody. **G** shows the overlay of **C** (red) and **F** (blue) and **H** shows the combined live/dead and S1PR1 staining. Plots shown are representative of three independent experiments.

Figure 30 shows that the live non-proliferating and unstimulated lymphocyte population has a low expression of S1PR1 with around 25% of the population expressing S1PR1. The MFI for both populations was found to be 20.5 for the S1PR1 isotype (C) and 127 for the S1PR1 stained cells (F).

The monocyte population was also analysed for S1PR1 expression in the same way as described for lymphocytes and the results are shown below.

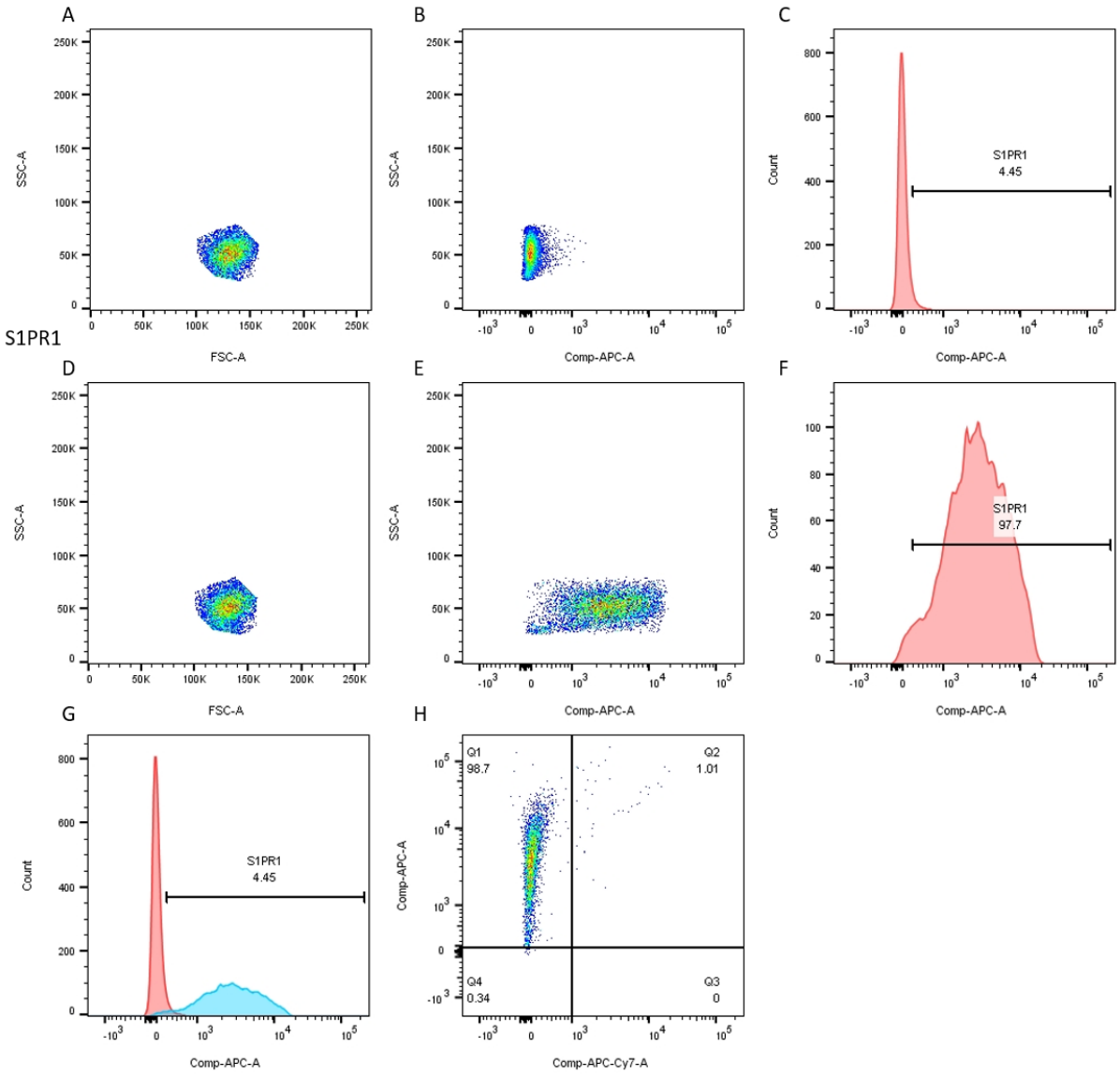

Figure 31 Monocyte S1PR1 expression

The top row (**A-C**) shows the results of the live population of monocytes in the presence of the S1PR1 isotype, showing the whole population (**A**), cells positive for S1PR1 (**B**) and the gate for S1PR1 (**C**). The middle row (**D-F**) shows the same for the S1PR1 antibody. **G** shows the overlay of **C** (red) and **F** (blue) and **H** shows the combined live/dead and S1PR1 staining. Plots shown are representative of three independent experiments.

The monocyte population shows a clear shift to the right indicating the expression of S1PR1 compared to isotype controls indicating that most of the population is expressing the S1P receptor. Again the MFI was calculated and it was found that the isotype had an MFI of 99 while the S1PR1 stained cells had an MFI of 2578, showing a clear difference between the isotype control and the stained cells.

The following figure shows the results of the S1PR1 expression analysis in the neutrophil population as described above for lymphocytes.

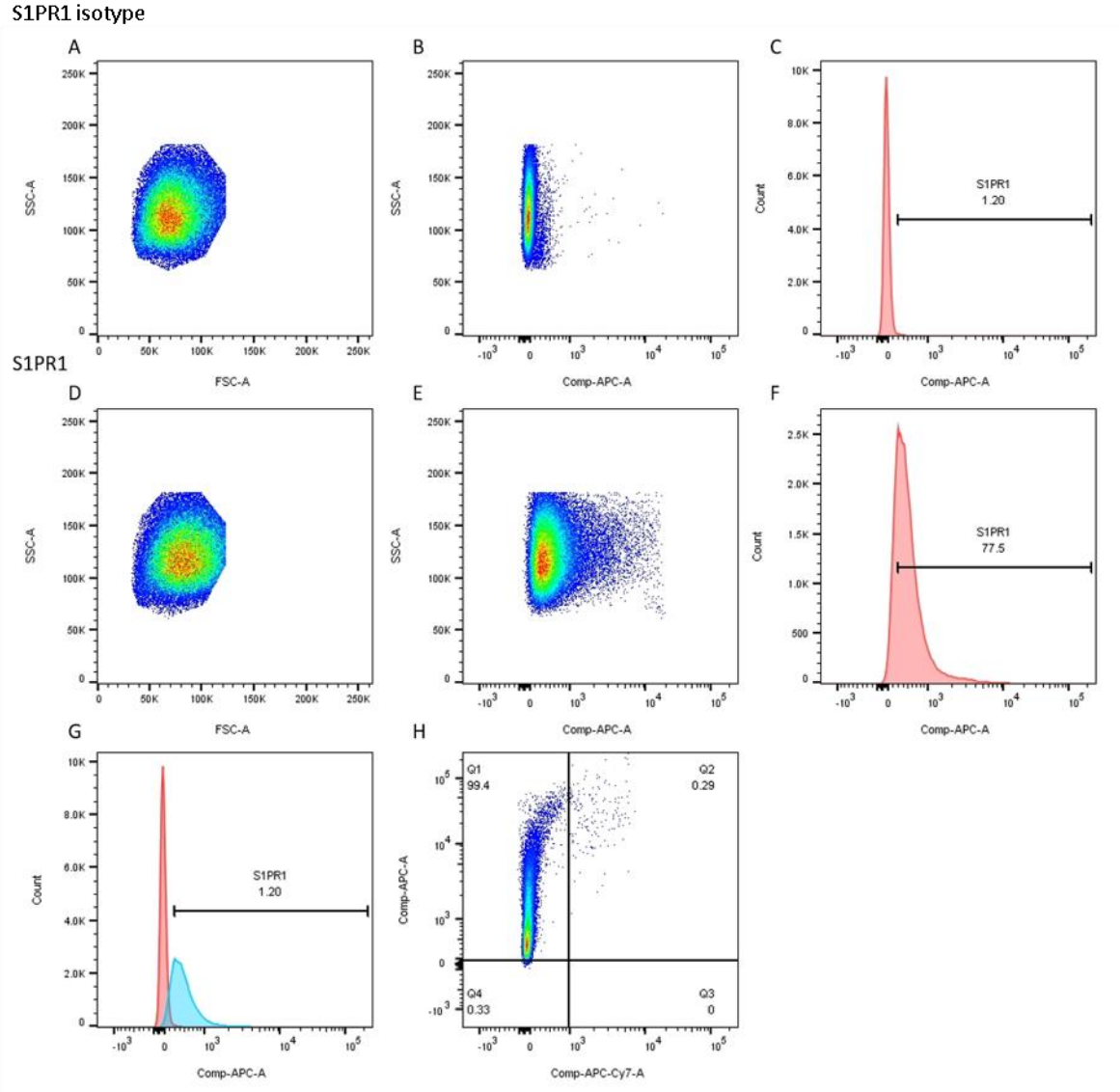

Figure 32 Neutrophil S1PR1 expression

The top row (**A-C**) shows the results of the live population of neutrophils in the presence of the S1PR1 isotype, showing the whole population (**A**), cells positive for S1PR1 (**B**) and the gate for S1PR1 (**C**). The middle row (**D-F**) shows the same for the S1PR1 antibody. **G** shows the overlay of **C** (red) and **F** (blue) and **H** shows the combined live/dead and S1PR1 staining. Plots shown are representative of three independent experiments.

Neutrophil expression of S1PR1 is seen on approximately 75% of the live population with a MFI of 438 compared to 75.8 in the isotype population.

The expression levels of S1PR1 was then compared between the three cell types by subtracting the MFI of the isotype from the MFI of the stained cells. The percentage of S1PR1 positive cells in each group was also compared and the results are shown below in Figure 33.

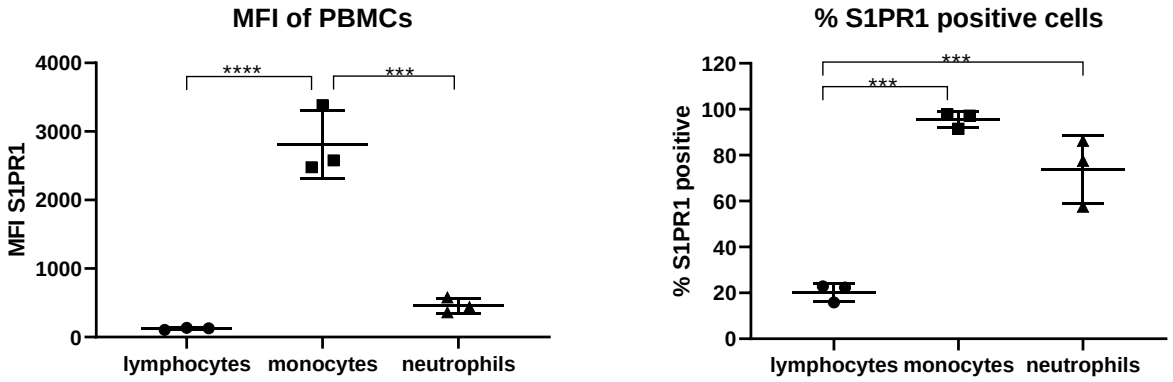

Figure 33 Comparison of MFI and % S1PR1 positive cells
Monocytes have the largest mean fluorescent intensity in response to S1PR1 staining of the PBMCs analysed as well as the greatest number of S1PR1 positively stained cells. Error bar represent the mean +/- SD, n=3.

It was found that monocytes had by far the greatest mean fluorescent intensity out of the three cell types. One way ANOVA gave a p value of <0.0001, with Tukey's multiple comparisons test giving p values of <0.0001 and 0.0002 between monocytes and lymphocytes and neutrophils respectively. No significant difference was found between lymphocytes and neutrophils.

The monocyte population also had the most cells positively stained with S1PR1 which explains the increase in MFI. Interestingly, there was not as big a difference between the number of positive cells in the monocyte and neutrophil populations as there was for the MFI. Lymphocytes had the least number of S1PR1 positive cells of the three populations analysed, which corresponds to the low MFI. One way ANOVA gave a p value of 0.0001, with Tukey's multiple comparisons test showing a significant difference between lymphocytes and both monocytes (p=0.0001) and neutrophils (p=0.0008). No significant difference was seen between monocytes and neutrophils (p=0.0569).

3.1.4.3.2 Endothelial cells

As discussed in the methods section of this chapter, the cells in this section were fixed using 4% (v/v) paraformaldehyde to retain the S1P receptor on the surface and to prevent the antibody being able to bind to intracellular antigens, otherwise no change in profile would be seen. There is also no permeablisation step in this protocol and therefore the only S1P1 receptors avaliable to be stained are located on the surface of the cell. Cells were stimulated with S1P and other compounds for 30 minutes to allow time for the receptor to be activated and removed from the cell surface but not enough time for the receptor to be recycled back to the surface. This time point was chosen based on previous data (unpublished), where cells were stimulated for an hour however no change in receptor expression was observed. It was therefore thought that a shorter timeframe would allow a change in receptor expression to be seen.

The expression of the S1P receptor 1 was studied to determine if the addition of varying concentrations of S1P, Fingolimod or oxLDL had any effect on the expression profile. An isotype of the antibody used to detect the S1PR1 receptor was used to gate the S1PR1 positive cells (see Table 7). 10,000 events were recorded for each sample and the control was gated to show only the HUVEC cells and exclude any debris. This gate was applied to all other samples and only those cells within this gate were included when S1PR1 expression was plotted. Each experiment was repeated on at least three separate occasions and representative images are shown below in Figure 34.

Table 7 Antibody panel used

Marker	**Clone**	**Fluorophore**	**Antibody type**	
CD363 (S1PR1)	SW4GYPP	eFluor® 660	Monoclonal	Mouse/IgG1kappa
Isotype control	P3.6.2.8.1	eFluor® 660	Monoclonal	Mouse/IgG1, kappa

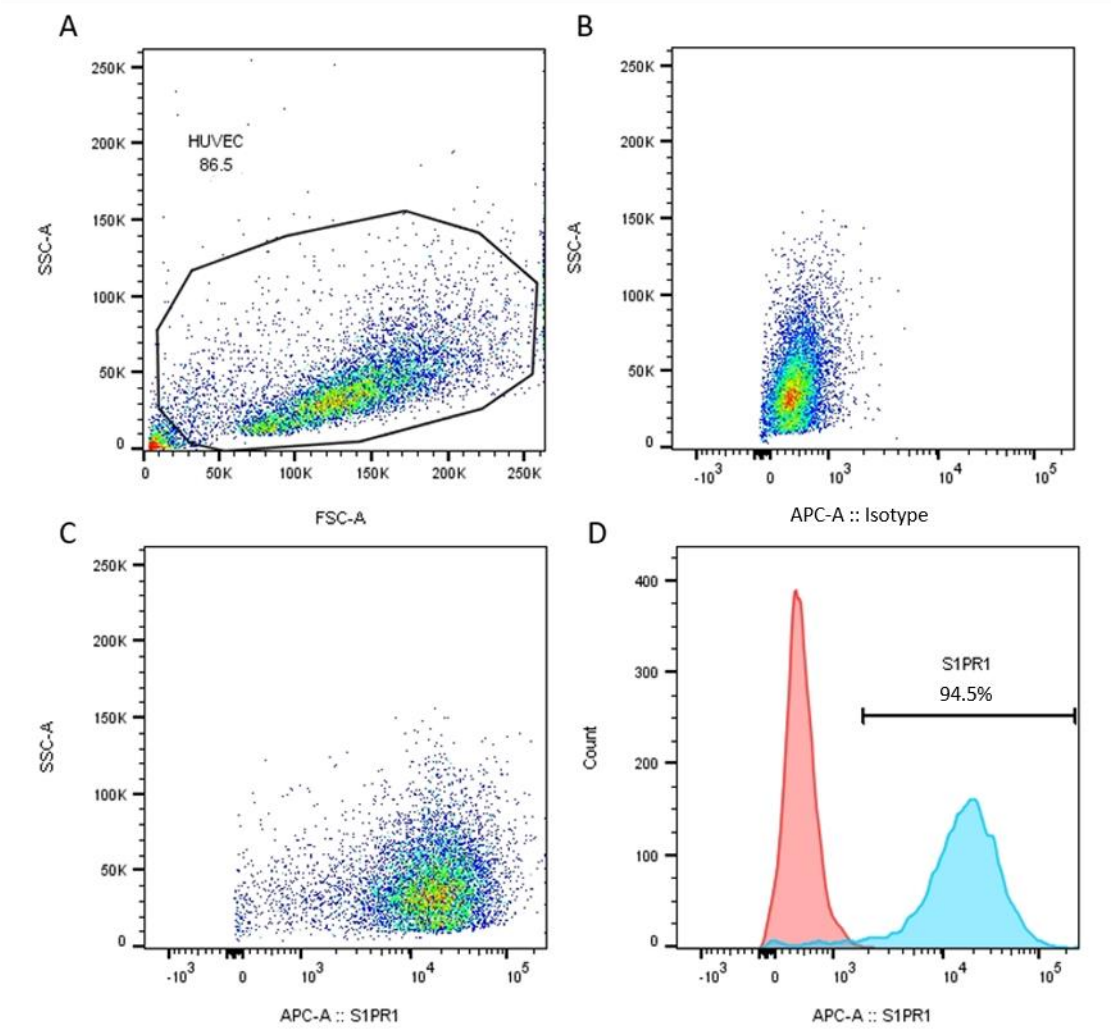

Figure 34 showing the difference between the isotype and the S1PR1 antibody
A- The total number of events recorded and the gated HUVEC cells. **B**- The gated cells showing no signal in the presence of the isotype. **C**- The gated cells showing a positive signal in the presence of the S1PR1 antibody. **D**- Overlapped histogram highlighting the peak separation between the isotype (red) and S1PR1 antibody (blue) and showing the S1PR1 gating using the isotype control. Plots shown are representative of three independent experiments.

Figure 34 shows a clear right shift in signal in cells stained with antibody against S1PR1 compared to isotype control. The isotype control was used to gate cells positive for S1PR1 and this gate was applied to the rest of the samples.

HUVEC cells were exposed to a concentration gradient of S1P (ranging from 10µM-1nM) for 30 minutes before being fixed in 4% (v/v) paraformaldehyde as previously described and antibody labelled ready for analysis by FACS. Representative images are shown below and include the total number of events recorded, S1PR1 expression and a histogram of gated S1PR1 expression.

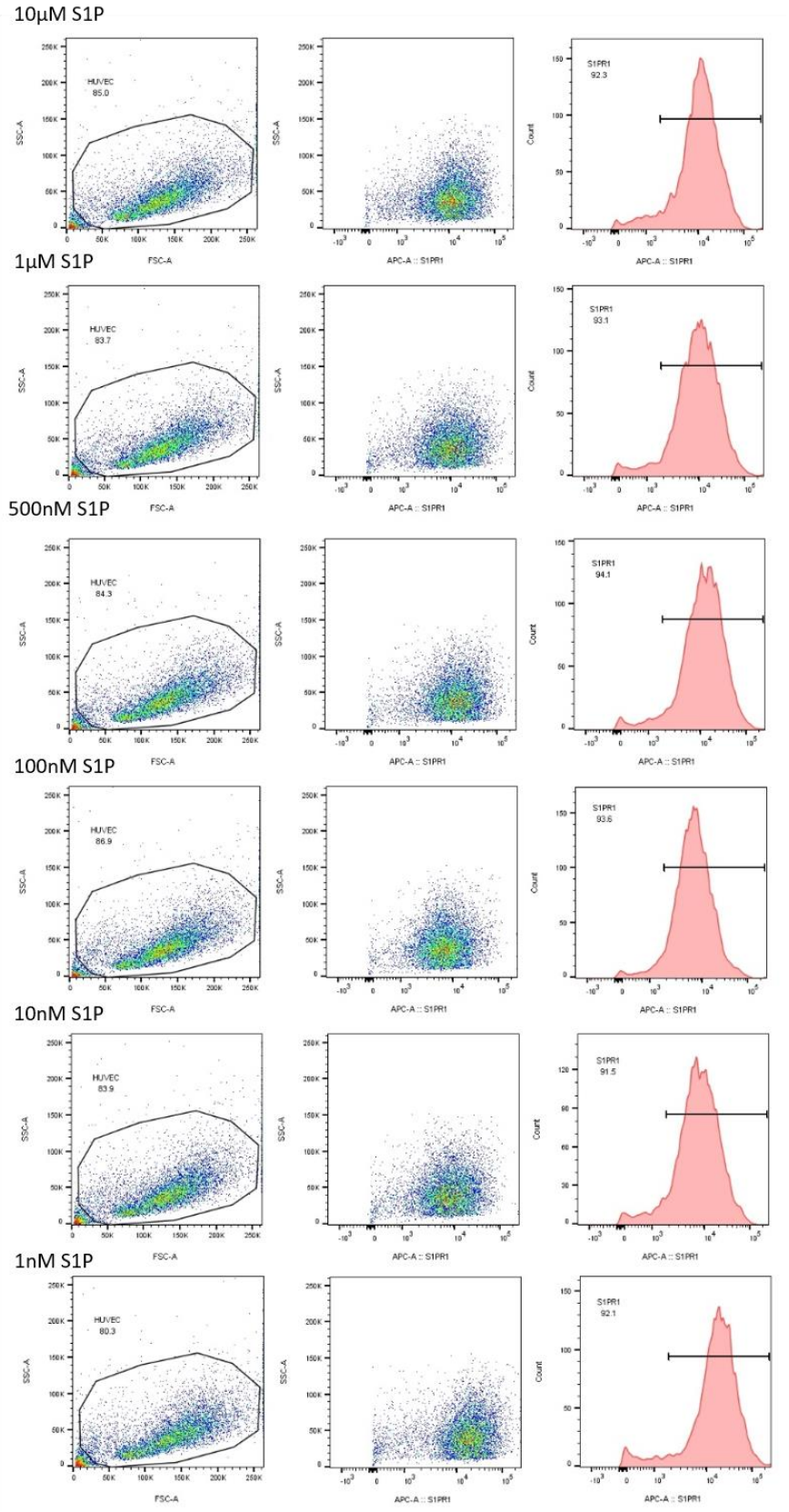

Figure 35 effect of S1P concentration on the expression of S1PR1

The first panel shows the 10,000 events that were recorded for each concentration and the gate for S1PR1 positive cells applied to each sample. The second panel shows the events within the gate and whether they were positive for S1PR1. The third panel shows a histogram of S1PR1 positive events determined by the gate from the isotype control. Plots shown are representative of three independent experiments.

Figure 35 shows that the mean fluorescence intensity (MFI) of the middle concentrations is reduced compared to the extremes at each end. This is highlighted in Figure 36.

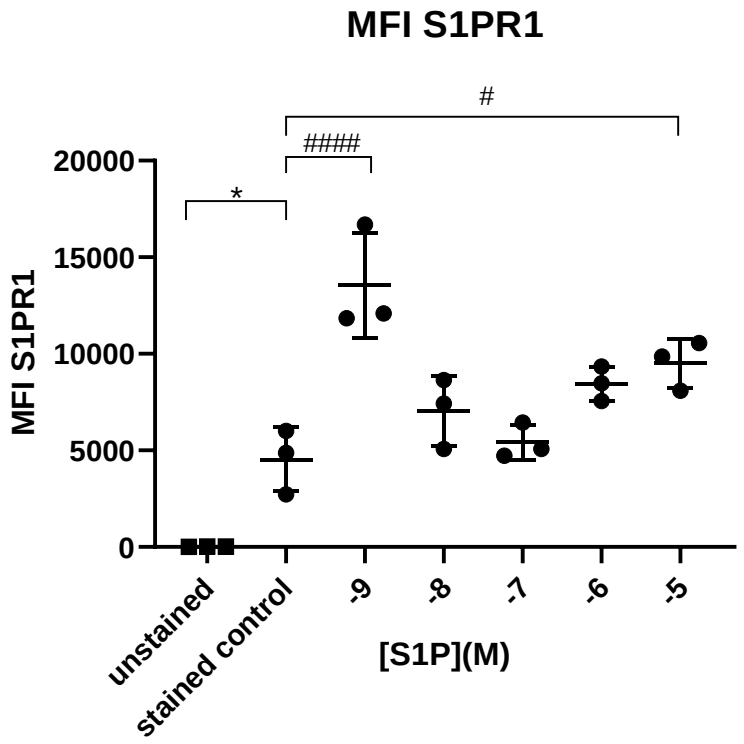

Figure 36 Mean fluorescence intensity of S1PR1 in response to S1P
Receptor expression levels (as determined by the mean fluorescence intensity of APC-A) decrease with increasing S1P concentration before gradually increasing. Error bars represent the mean +/- SD, n=3.

Figure 36 shows that the addition of 1nM S1P increased S1PR1 expression on the surface of EC after 30min incubation compared to unstimulated controls. At intermediate concentrations this effect was absent. However, at 10 µM S1P stimulation, S1PR1 expression is again elevated significantly above that of the unstimulated control. One way ANOVA gave a p value of <0.0001 and the result of Dunnett's multiple comparisons test comparing the stained, unstimulated control to the unstained, unstimulated control gave a p value of <0.05 (shown by * on the above graph). This comparison was repeated, comparing the stained, unstimulated control to the different concentrations of S1P. It was found that there was a significance of p<0.0001 between the control and 1nM S1P and p= 0.0196 between the control and 10µM S1P (shown by # on the graph).

Cells were also exposed to equivalent concentrations of Fingolimod for 30min as described for S1P exposures before fixation and staining with antibody against S1PR1 as described, representative images are shown below in Figure 37.

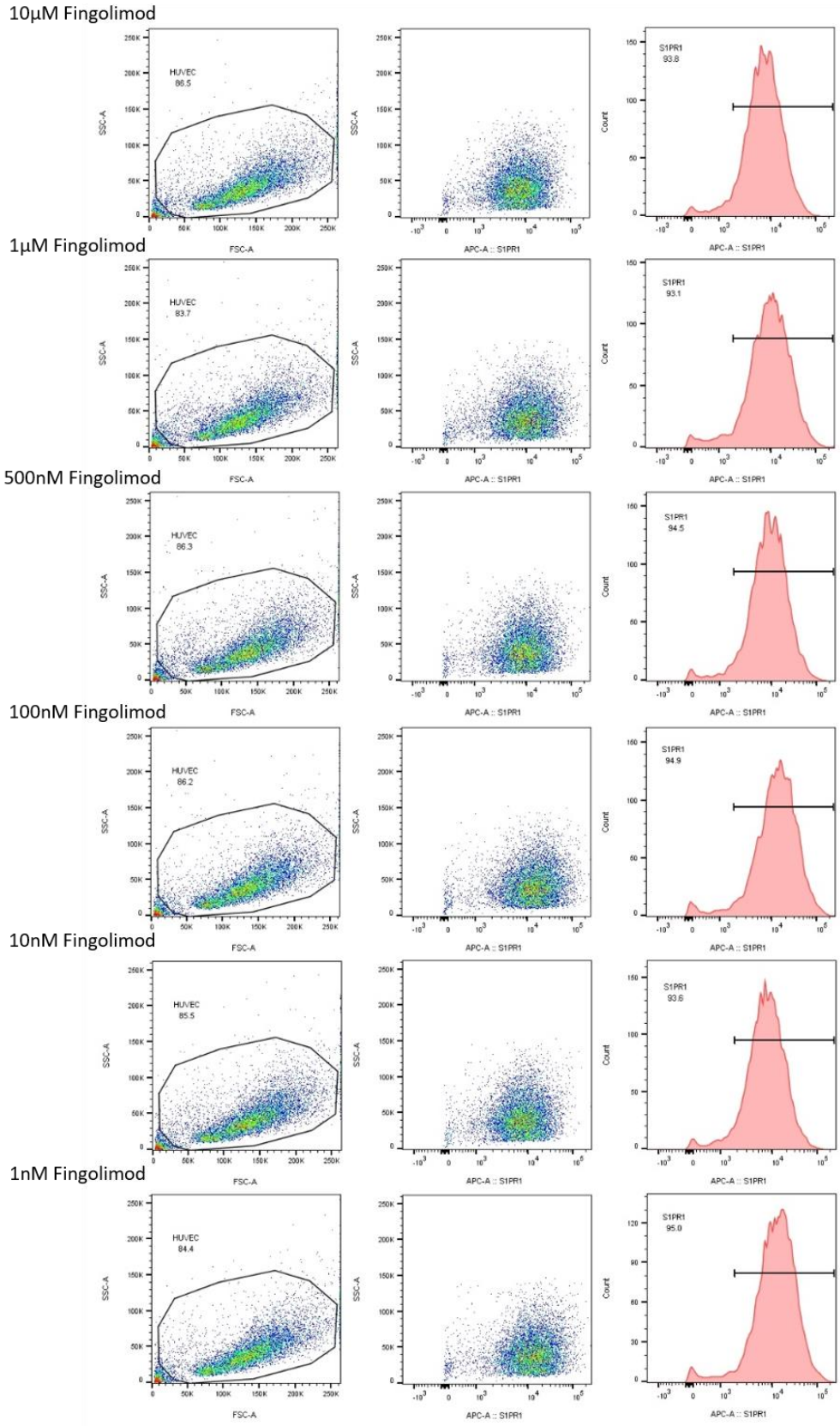

Figure 37 effect of Fingolimod concentration on the expression of S1PR1

The first panel shows all events that were recorded for each concentration and the gate from the control that was applied to each sample. The second panel shows the events within the gate and whether they were positive for S1PR1. The third panel shows a histogram of S1PR1 positive events, including the gate from the isotype control. Plots shown are representative of three independent experiments.

The mean fluorescence intensity (MFI) of each concentration of Fingolimod was calculated and plotted in Figure 38.

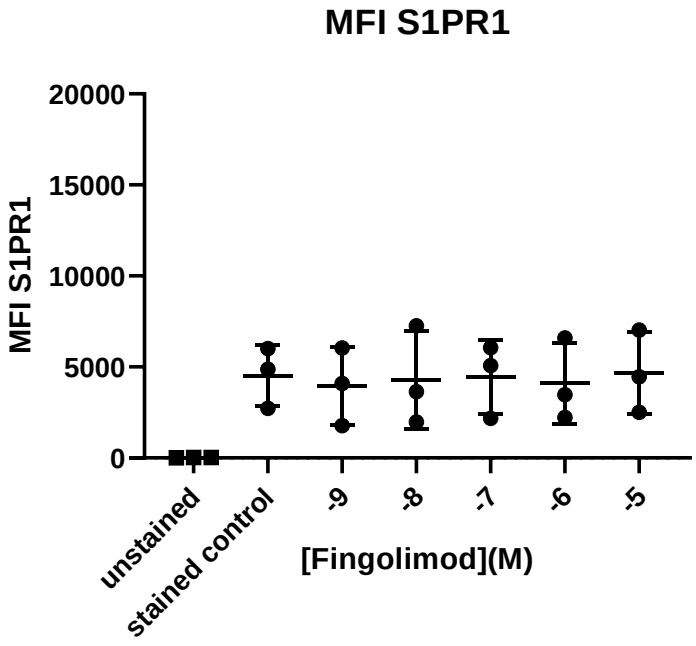

Figure 38 Mean fluorescence intensity of S1PR1 in response to S1P
Receptor expression levels (as determined by the Mean fluorescence intensity of APC-A) were calculated for each concentration of Fingolimod. Error bar represent the mean +/- SD, n=3.

No significant difference was found using one way ANOVA between the Fingolimod concentrations and either the unstained, unstimulated control or the S1PR1 stained, unstimulated control. The same Y axis that was used for the S1P concentrations has also been used here in order for direct comparisons to be made.

The effect of oxLDL on the surface expression of SPR1 was also examined and as before, sample images are shown below in Figure 39.

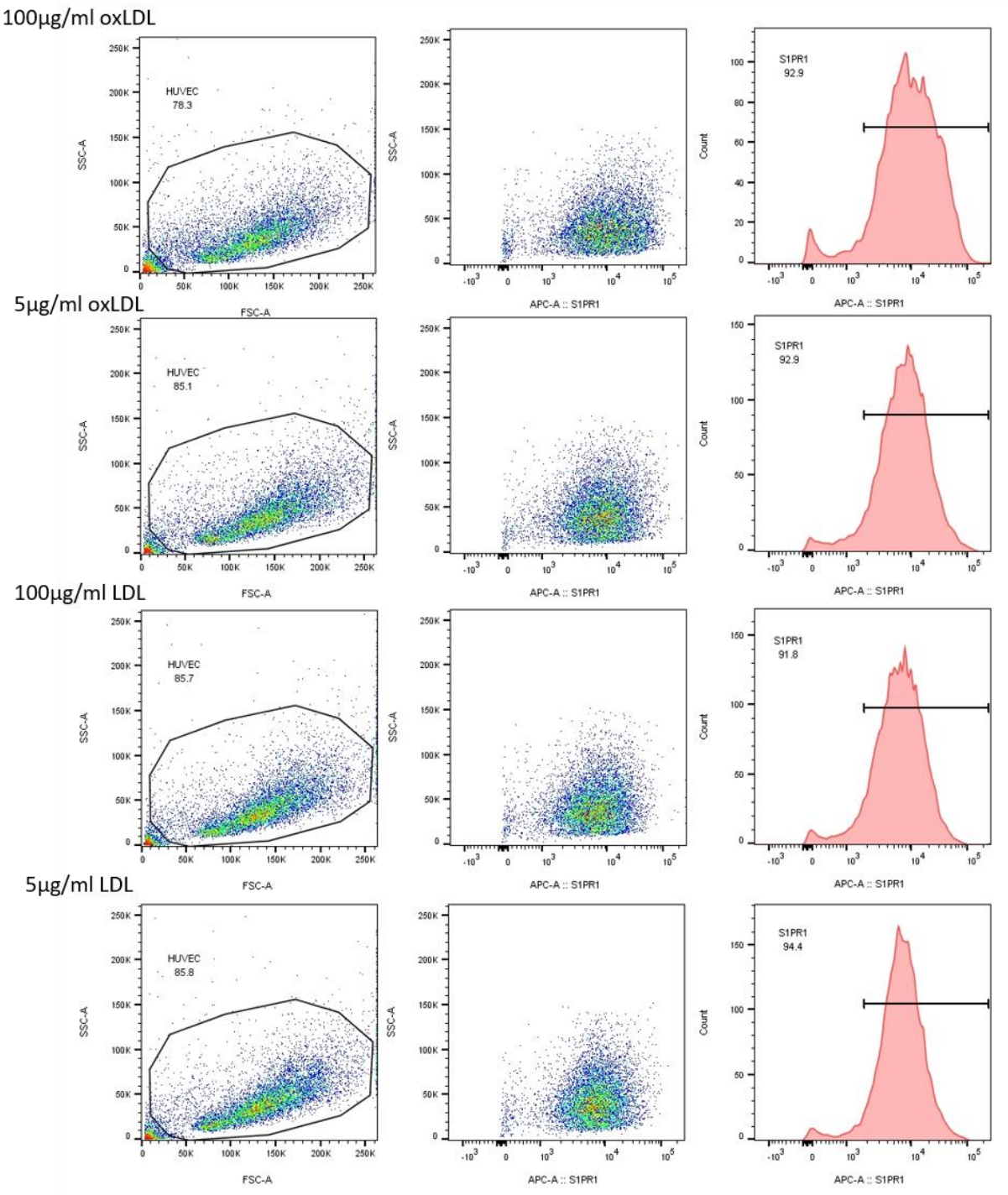

Figure 39 Effect of oxLDL on the expression of S1PR1

The first panel shows all events that were recorded for either oxLDL or LDL and the gate from the control that was applied to each sample. The second panel shows the events within the gate and whether they were positive for S1PR1. The third panel shows a histogram of S1PR1 positive events as determined from the isotype control. Plots shown are representative of three independent experiments.

100µg/ml oxLDL results in a wider peak compared to 5µg/ml or the two concentrations of LDL, suggesting that there is a greater variation in the number of receptors on the surface of cells exposed to this concentration. The total count at this concentration is also lower and this suggests

that there is a downregulation of receptors, which would also account for the variation seen. To investigate this further, the MFI was determined and the results shown below in Figure 40.

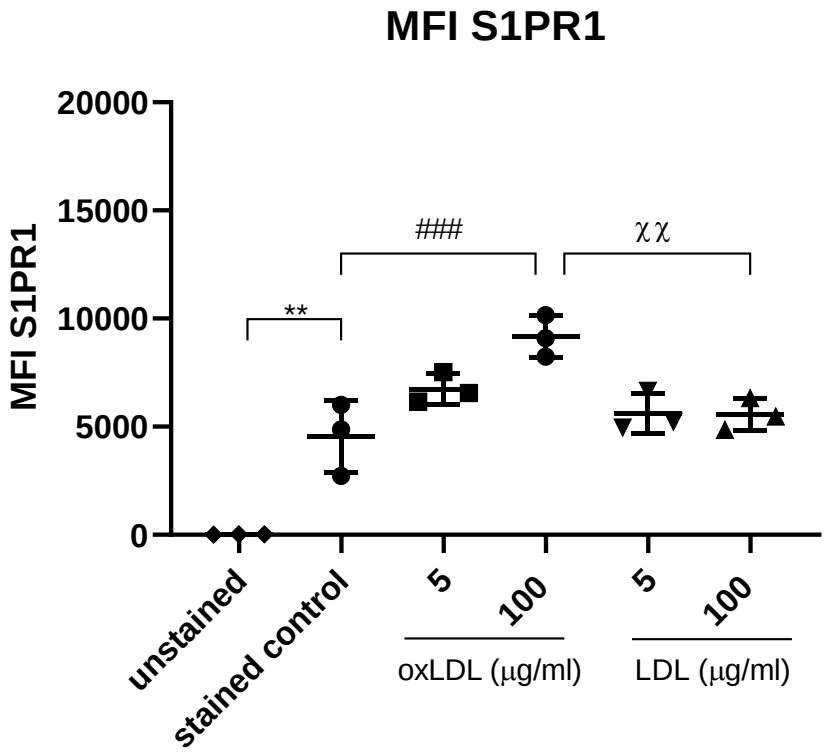

Figure 40 Mean fluorescence intensity of S1PR1 in response to oxLDL and LDL
Receptor expression levels (as determined by the mean fluorescence intensity of APC-A) decrease with decreasing oxLDL concentration whereas LDL concentration has little effect. Error bars represent the mean +/- SD, n=3.

Figure 40 shows that oxLDL concentration has an effect on the level of S1PR1 expression, with 100μg/ml oxLDL causing an increase in the MFI compared to the stained unstimulated control. In contrast, LDL concentration does not have an effect on receptor expression when compared to stained unstimulated controls. Again, the same Y axis that was used for the S1P concentrations (Figure 36) has been used to allow for direct comparisons to be made.

One way ANOVA gave a p value of <0.0001 while Tukey's multiple comparisons test, comparing the unstained, unstimulated control to the stained, unstimulated control gave a p value of <0.01 (* on graph). Comparison testing also compared the stained, unstimulated control and the concentrations of oxLDL/LDL and it was found that only 100μg/ml oxLDL was significantly different (p= 0.0008) as represented by # on the above graph. The two concentrations of oxLDL were also compared to the two concentrations of LDL and it was found that 100μg/ml oxLDL was significantly different from 100μg/ml LDL (p=0.0063), as shown by χ on the graph, but no significance was found between 5μg/ml oxLDL and 5μg/ml LDL.

In summary, this chapter has shown that the cells isolated from the umbilical cords are endothelial in origin, that they are not killed by the various treatments that will be used in the rest of this thesis and that they express S1PR1 which can be changed upon stimulation.

3.1.5 Discussion

3.1.5.1 Characterisation and cell viability

The cells that were isolated from the human umbilical cords were found to be positive for both endothelial cell markers CD31 and CD105, suggesting that they are endothelial in origin and not smooth muscle cells (Goncharov et al., 2017). This shows that the isolation procedure is effective at isolating HUVEC and that the results of the assays used in this project are applicable to the endothelium. All cells used in this project were used at passage 1 and therefore it was likely that the characteristics of the cells are consistent and not subject to passage effects. Other ways of determining whether cells are of endothelial origin include observing their morphology, for example do they form a confluent monolayer with a cobblestone appearance. Endothelial cells are also known to express lectin receptors and take up acetylated LDL as well as being able to form tubes and undergo angiogenesis when added to a matrigel, all of which point to cells being endothelial in lineage. Cobblestone patterns and angiogenesis was observed in these isolated cells, see Figure 41.

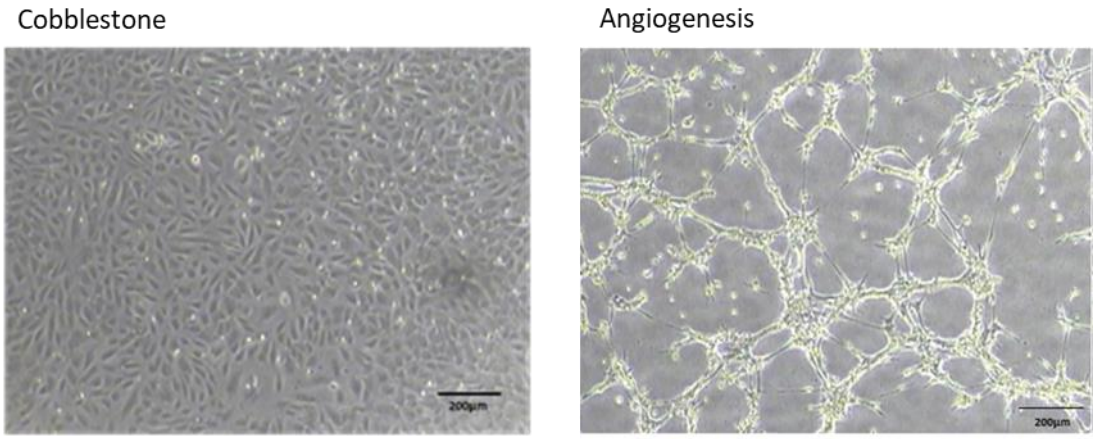

Figure 41 Example of observed cobblestone pattern and angiogenesis
Example images showing the observed cobblestone pattern (when cultured on gelatin coated tissue culture plastic) and angiogenesis (when gown on Geltrex) seen with the isolated cells.

As well as establishing the origin of the cells, it was also important to establish the viability of the cells under various conditions that would be employed in the functional assays. It was found that in the full media, none of the conditions used resulted in a reduction in cell viability, while in the reduced lipid environment, the addition of 100µg/mL oxLDL resulted in a roughly 20% loss of viability as assessed with the live/dead stains. Although relatively small it is noted that interpretation of subsequent assays must be with care and with this in mind as a potential factor.

It was noticed that the addition of 100µg/mL oxLDL to HUVEC in full lipid media resulted in an increase in SSC compared to 100µg/mL LDL. This was not found to be the case in the delipidised media and could be due to reduced uptake under the delipidised conditions. It is possible that the granularity seen in the full media might be due to lipid droplet uptake, a known mechanism in endothelial cells (Kuo et al., 2017), whereas in the reduced lipid environment it could be the oxidation effect causing the death and lack of uptake and therefore granularity.

3.1.5.2 S1PR1 expression

PBMCs were studied for S1PR1 expression and it was found that there was a large difference in expression level between the cell types. Lymphocytes were found to have the lowest expression, with only around a quarter of the population positive for the receptor. It was found that around 75% of neutrophils expressed S1PR1 although at a reduced MFI compared to monocytes. This suggests a lower overall expression of surface receptors. Monocytes however, had by far the greatest expression, with over 95% of the population positive for S1PR1 and with that population showing a high MFI, indicating a high surface expression number of S1PR1.

These results were as expected as it has previously been shown that lymphocyte expression of S1PR1 is reduced when in circulation compared to when they are in the lymphoid organs. This is because S1P signalling through S1PR1 is required for lymphocyte egress from the lymphatic system into the blood, however once in circulation, S1PR1 signalling is no longer as important and the number of receptors drops accordingly (Aoki et al., 2016).

Neutrophil expression of S1PR1 can also vary, in this case it is dependent on whether the neutrophil is activated rather than due to its location within the body. It has also been shown that the expression of S1PR1 is necessary for neutrophil recruitment (Blaho and Hla, 2014). It would therefore be expected that the majority of neutrophils would have some level of S1PR1 expression, with the results obtained supporting this.

Monocytes are important for immune surveillance and S1PR1 expression is important for the migration of the monocyte towards S1P. A high level of S1PR1 expression would therefore be expected and the results support this. It has been shown that the deletion of this receptor causes early inflammation in a psoriatic mouse model by increasing the production of VEGF and its receptor, leading to angiogenesis. Therefore the increased production of S1P by endothelial cells and keratinocytes in psoriasis leads to the recruitment of monocytes to the site of inflammation, potentially resulting in unrequired tissue repair and subsequently contributing to plaque formation (Syed et al., 2019). This could form a potential area of future research in subsequent studies.

The S1PR1 expression of the isolated endothelial cells was assessed by flow cytometry and it was found that endothelial cells express S1PR1 on the majority of primary non activated cells. Previous work in the lab had identified issues with S1PR1 detection following removal of the cells from the culture plastic using trypsin. It is likely that as trypsin is an active protease, either S1PR1 is cleaved from the cell surface as is known for other proteins expressed on the plasma membrane or that because trypsin activates protease activated receptors (PAR 1-4), it is possible that S1PR1 is down regulated from the surface to intracellular stores. This study used Accutase that had previously been shown to preserve surface expression of S1PR1 on endothelial cells and in this study, cells were fixed prior to staining to potentially prevent cycling of receptors once they had been removed from the cell surface. As the down regulation of S1PR1 can be used as a S1P specific activation marker, this assay was therefore used to compare the effects of S1P, Fingolimod and LDL/oxLDL on S1PR1 surface expression.

In these assays, S1P was used as a positive control to show that downregulation of the S1P1 receptor occurred and therefore determine if other compounds such as Fingolimod or oxLDL could do the same. The main aim of studying S1P receptor 1 expression was to determine whether oxLDL signals through S1PR1 in some way, either directly or indirectly via S1P dependent S1P signalling. The addition of increasing concentrations of S1P resulted initially with an increased expression (1nM) followed by a return to unstimulated control levels (10nM-1μM), before a slight increase in MFI was seen at the highest concentration (10 μM). No difference in MFI was seen after the addition of varying concentrations of Fingolimod or LDL however, 100μg/ml oxLDL was found to be significantly different to the unstimulated stained control as well as to 100μg/ml LDL, suggesting that it is the oxidised portion of the lipid having this effect. It is possible that the S1PR1 in the unstimulated cells is still dynamically moving within the membrane and that the effect of adding lipid slows the S1PR1 removal from the surface by changing membrane dynamics as 100μg/ml oxLDL had the highest MFI. This suggests that oxLDL is having a similar effect to either low (1nM) or high (10μM) S1P stimulated cells on the surface expression of S1PR1 although the mechanism of how this occurs is still unknown.

In conclusion, the cells used were characterised and confirmed to be endothelial in nature and were shown to be viable under various conditions, including lipid free and high concentrations of both S1P and oxLDL. The HUVEC cells were also shown to express the S1P receptor 1 and that stimulation of this receptor changes the expression levels. To investigate this, cells were stimulated for 30 minutes and therefore it would be interesting to look at different time points to try and identify how quickly the receptors are recycled back to the surface. Previous work has shown that after an hour and a half there is no difference in expression levels, suggesting that by this time, the receptors

have already been recycled. Future experiments could therefore focus on time points between 30 minutes and an hour and a half.

3.2 Intracellular signalling

3.2.1 Introduction

Intracellular signalling allows cells to receive and respond to internal and external signals and elicit a response. This response can range from altering a certain protein expression to rearranging the cytoskeleton. The extracellular-signal-regulated kinase (ERK) signalling pathway connects a receptor on the cell surface (in this case a tyrosine kinase) to the nucleus. It is an example of a kinase cascade where each component of the pathway phosphorylates and activates the next, until ultimately ERK is activated and can translocate into the nucleus and activate transcription factors to alter gene expression (McCain, 2013). ERK signalling regulates many important cellular processes such as proliferation, differentiation and apoptosis. As mentioned before, vascular endothelial growth factor (VEGF) is required for angiogenesis to occur and it has been found that ERK signalling occurs in response to VEGF in cells undergoing angiogenesis and that inhibition of ERK signalling can prevent endothelial cells sprouting (Shin et al., 2016). ERK signalling is therefore an important marker of intracellular signalling and is relevant to this study.

Second messengers are vital components of signalling pathways and are released in response to the activation of receptors. Calcium is an example of a second messenger and regulates gene transcription as well as cell migration and proliferation. Calcium is stored by the cell in a variety of organelles and can be rapidly released in response to an external signal. An example of this is the activation of G-protein-coupled receptors which can activate phospholipase C enzymes that in turn release the stored calcium (Werry et al., 2003). As the S1P receptors are G-protein-coupled receptors, calcium flux within endothelial cells would also represent a good measure of intracellular signalling in response to S1P. It would therefore be expected that the addition of S1P would have a concentration dependent effect on calcium flux whereas blockade of S1P signalling via Fingolimod, receptor antagonists and sphingosine metabolism would block calcium flux via downregulation of receptors as well as other S1P dependent mechanisms.

It has previously been shown that oxLDL causes an increase in ERK phosphorylation and therefore to determine if oxLDL and S1P share a signalling pathway, the effect of S1P on ERK phosphorylation was investigated.

It was decided to investigate the levels of phosphorylated ERK in response to certain external signals to try and further understand which signalling pathways S1P may activate. As MEK is the kinase that phosphorylates ERK, inhibiting MEK essentially inhibits ERK phosphorylation and therefore prevents the phosphorylation of various transcription factors and subsequently the transcription of genes. The ERK signalling cascade is known to be involved in a number of mitogenic processes such as

migration, cell adhesion and overall cell survival (Roskoski, 2012). S1P can activate this pathway by binding to any of the five S1P receptors and therefore it is expected that the addition of S1P to HUVEC will result in increased levels of phosphorylated ERK and therefore increased signalling. The addition of the S1P receptor inhibitors (W146, JTE and TY) should therefore prevent the S1P dependent phosphorylation of ERK and the S1P lyase and kinase inhibitors were also included to try and gain a better understanding of the role of S1P. The effect of three cytokines (TNF, IL-17 and IFNγ) on the phosphorylation of ERK was also investigated as they are associated with inflammation and psoriasis, in particular (IL-17), with the predicted outcome being that they would cause an increase in the amount of phosphorylated ERK.

3.2.2 Hypothesis and Aims

It is hypothesised that the addition of exogenous S1P will cause an increase in intracellular signalling (ERK phosphorylation and calcium flux).

Specific aims of this section are:

- to investigate the change in levels of phosphorylated ERK in response to the addition of exogenous S1P, Fingolimod and various pathway and S1P receptor inhibitors
- to investigate the change in calcium flux in response to the addition of exogenous S1P and Fingolimod

3.2.3 Method

Western blots were used to examine the effect of exogenous S1P and various inhibitors on the phosphorylation state of ERK as described in methods sections 2.10 and 2.11 in primary endothelial cells. Briefly, S1P and inhibitors were added to confluent 12 well plates of HUVEC, incubated for either 10 minutes or 1 hour and lysed directly in Laemmli buffer + DTT. Equal numbers of cells were plated in each well to gain confluency overnight and generate the same amount of protein for each treatment. The samples were then either frozen at -20^{0}C or run immediately on 7.5% SDS-PAGE gels followed by Western blotting onto PVDF membranes. Antibody staining for total and phosphorylated ERK was carried out with specific antibodies as described and detected by chemiluminescence. The results shown below are of the developed light sensitive X-Ray film for phosphorylated ERK (p-ERK) and total ERK and are accompanied by the corresponding densitometry graphs. To generate these, each film was quantified using Fiji where the band intensity for each condition was measured following background subtraction which acted as an internal control across all experiments. The intensity of each band was then expressed relative to the control band intensity (i.e. where the p-ERK control= 1) and this is the result plotted on the graph.

Studying the calcium flux within the cell is a further method to evaluate intracellular signalling within HUVECs as calcium is a well-known second messenger linked to G-protein coupled receptor signalling (Tiruppathi et al., 2002). Therefore, the addition of exogenous S1P to cells should induce a calcium flux as S1P signals through one of three GPCRs in endothelial cells. This assay works on the principle that the fluorescent dye (in this case Fluo-4) is able to be taken up by the cell by crossing the plasma membrane in order to reach the cytoplasm. Once in the cytoplasm, the dye can bind to free calcium, an event that leads to an increase in the fluorescence of the dye. Release of calcium from intracellular stores or through opening of plasma membrane calcium channels to allow extracellular calcium in to increase levels in the cytoplasm can then be measured as the fluorescence of the dye increases on binding calcium. This increase in intensity is proportional to the amount of calcium released, therefore an increase in signal caused by the activation of the GPCR at the cell surface will lead to an increase in fluorescence which can be measured.

3.2.4 Results

3.2.4.1 Intracellular signalling via mitogen activated protein kinase

3.2.4.1.1 S1P concentration gradient

In order to determine which concentration of S1P produced a strong positive result for ERK phosphorylation and therefore should be used as the positive control in future experiments, an S1P concentration gradient was set up. A ten-fold dilution series was used from 10µM to 1pM and an example blot is shown in Figure 42.

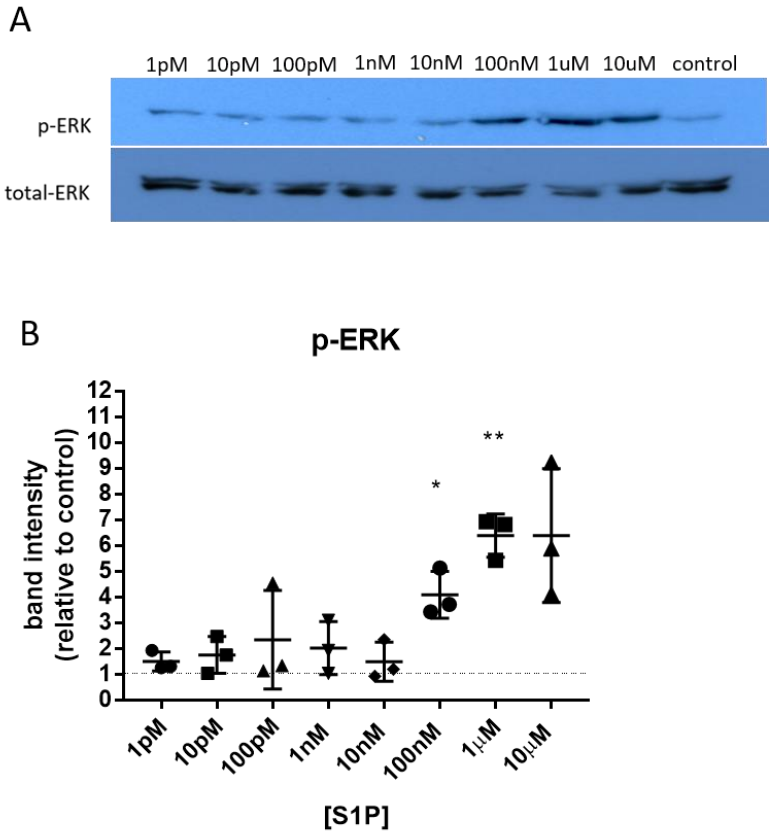

Figure 42 Example of blot investigating S1P effect on p-ERK
Western blots were carried out as described and the band intensity calculated for increasing concentrations of S1P. **A-** Representative western blot of S1P concentration gradient of endothelial cells stimulated for 10min and stained for P-ERK and Total ERK. **B-** Graph of band intensity relative to the p-ERK control. Error bars show the mean +/- SD, n=3.

ERK phosphorylation occurred in a S1P concentration dependent manner with the highest concentrations of S1P causing the greatest ERK phosphorylation with minimal phosphorylation in unstimulated controls. The three highest concentrations of S1P show a large increase in the presence of phosphorylated ERK compared to the control. There is also no change in the total ERK content within samples following stimulation with S1P for 10min.

The results from the S1P concentration gradient show that concentrations above 10nM induce some level of ERK phosphorylation and as expected the highest concentrations show the greatest effect. 10µM was therefore chosen to be used as the positive control as it shows the strongest phosphorylation. One-way ANOVA analysis revealed an overall p value of p=0.0004 while one sample t-testing showed a significance of p=0.0080 for 1µM S1P and p= 0.0277 for 100nM S1P when the means were compared to a theoretical mean of 1. No significance was seen for 10µM S1P due to the larger variation in results. The p-ERK band intensity was also compared to the corresponding total-ERK band (data not shown) and one-way ANOVA analysis revealed a p value of p= 0.0129, with a p value of p= 0.0201 between the control and the highest concentration of S1P as determined by Dunnett's multiple comparisons test.

3.2.4.1.2 S1PR inhibitors

The effect of S1PR inhibitors (W146, JTE and TY inhibiting S1PR1, S1PR2 and S1PR3 respectively) on ERK phosphorylation was also investigated. The inhibitors were added for 10 minutes, either alone or in all possible combinations and S1P was added either to all cells or just to the positive control in order to show that the inhibitors themselves do not cause phosphorylation. Part of S1PR signalling is that the receptor is removed from the surface. There is potential for the inhibitors to cause downregulation of receptors and therefore affect the ability of S1P to signal through ERK. To investigate this the same inhibitors were also added for an hour preincubation, again either alone or in combination. After the hour incubation, S1P was added either to all samples or just to the positive control for a further 10 minutes. Therefore, in this case the total incubation time of the inhibitors was 1 hour and 10 minutes.

3.2.4.1.2.1 10 minute incubation with S1PR inhibitors

Firstly, the inhibitors were added to HUVEC for 10 minutes, with S1P only being added to the positive control, see Figure 43.

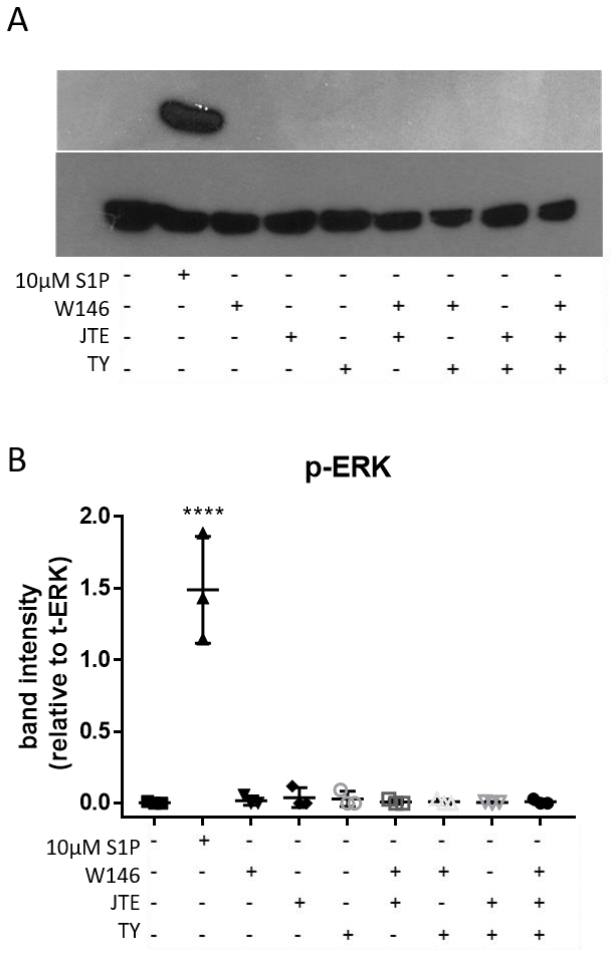

Figure 43 An example of a blot showing phosphorylation is only caused by S1P
A- representative blot, **B-** band intensity relative to total-ERK. Cells were stimulated either with 10µM S1P or incubated with inhibitors for 10 minutes before lysis and Western blotting**.** Analysis was performed by comparing the bands of the samples to the control band, error bars show the mean +/- SD, n=3

This result shows that the inhibitors themselves, either alone or in any combination, do not cause ERK phosphorylation after 10 minutes. Quite a large variation in the levels of phosphorylation was seen between experiments, however the responses seen within experiments were all equivalent. A significance of p=0.0001 between S1P and the control was found by performing multiple comparisons, with ANOVA analysis generating a p value of <0.0001. No significant difference between the inhibitors and the control or between the total-ERK was found.

3.2.4.1.2.2 10 minute incubation with S1PR inhibitors and S1P

Next the effect of adding S1P to the cells at the same time as the inhibitors (again for 10 minutes) was investigated to show if a differential effect of receptor ligation could be observed in the ERK signalling and an example shown in Figure 44.

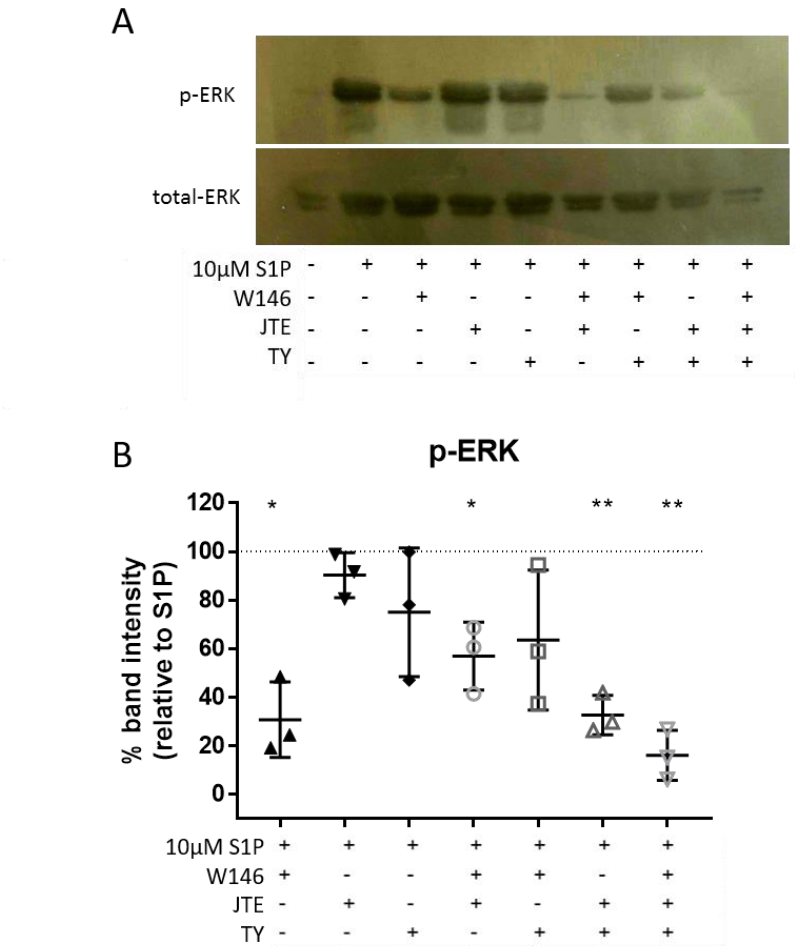

Figure 44 S1P mediated ERK phosphorylation still occurs even with S1PR inhibitors
A- representative blot, **B-** band intensity expressed as a percentage of S1P phosphorylation, n=4 Error bars show the mean +/- SD, dotted line shows the level of ERK phosphorylation by S1P.

From blot A it can be seen that the addition of S1P along with the inhibitors still results in some level of ERK phosphorylation, suggesting that in the presence of 10µM S1P, the S1PR inhibitors individually (at the concentrations used) are unable to prevent all of S1Ps signalling effects and complete inhibition of S1P mediated phosphorylation of ERK. W146 has the greatest inhibitory effect alone as a reduction in the levels of p-ERK is clearly seen. Interestingly, the combination of W146 and JTE ($S1PR_{1\&2}$ inhibitors) results in further reduced levels of ERK phosphorylation. The combination of all three S1PR inhibitors (W146, JTE and TY) has the largest effect at inhibiting ERK

phosphorylation, suggesting that although each inhibitor alone is unable to inhibit S1Ps effects, the combination of all three receptor inhibitors is required to generate the greatest inhibition.

For graph B, the phosphorylation of ERK by 10 minute incubation of cells with 10μM S1P was taken to represent 100% phosphorylation and the phosphorylation of ERK under each condition was compared to this value (within experiments) and expressed as a percentage. One-way ANOVA analysis of this graph revealed a p value of 0.0017 and therefore one sample t-testing was carried out to identify which combinations of inhibitors were significantly different from the theoretical mean of 100% (representing the level of phosphorylation caused by S1P). It is clear that of the three inhibitors, only W146 when used alone was able to prevent S1P stimulated ERK phosphorylation, with a reduction of around 50%. This was confirmed by one sample t-testing yielding a p value of <0.05. Inhibitors then used in combination showed further inhibition of ERK phosphorylation. A p value of <0.05 was found when W146 and JTE ($S1PR_{1\&2}$) were used together and a p value of <0.01 was found for the combinations of both JTE and TY ($S1PR_{2\&3}$) and all three inhibitors together. Again, the variation seen between the results is most likely due to the varying background of the film and would be improved with increasing the n number further.

3.2.4.1.2.3 1 hour incubation with S1PR inhibitors

The same experiments were repeated, this time with the cells being pre-incubated with the inhibitors for 1 hour to examine the effect of prolonged incubation with the inhibitors on the phosphorylation state of ERK i.e. causing a stress response. S1P was added for 10 minutes to the positive control only, see Figure 45.

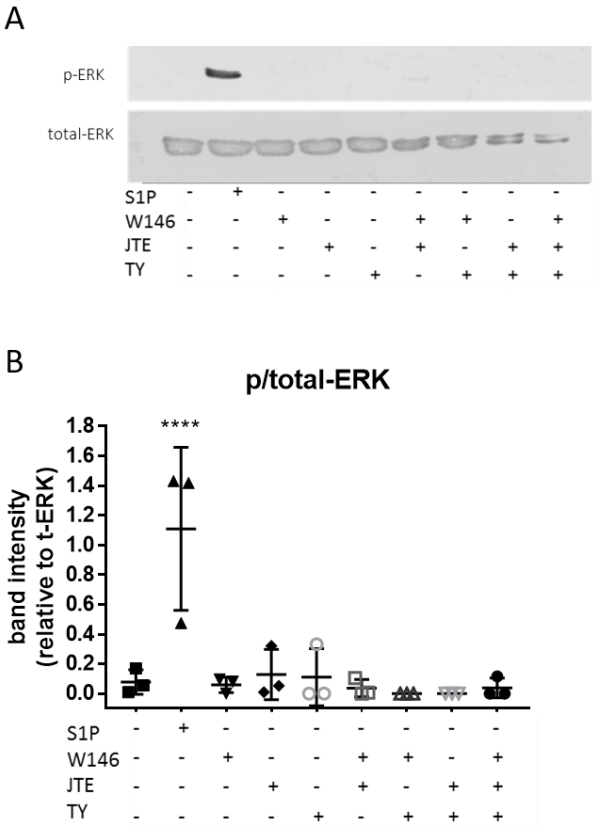

Figure 45 S1PR inhibitors do not cause ERK phosphorylation after 1 hour incubation.
Experiments carried out as previously stated above. **A-** representative blot, **B-** band intensity relative to total-ERK . Error bars show mean +/- SD, n=3

The longer incubation time with the inhibitors does not lead to phosphorylation of ERK, with an increase in p-ERK levels only being seen in the positive control. One-way ANOVA analysis of graph B generated a p value of <0.0001, with Dunnett's post Hoc analysis revealing a p value of p= 0.0001 between the control and S1P. This shows that the S1PR inhibitors do not cause the phosphorylation of ERK after 1 hour of incubation and therefore any change in p-ERK levels seen in the following results are caused by the addition of S1P.

3.2.4.1.2.4 1 hour incubation with S1PR inhibitors and S1P

Part of S1P signalling requires the endocytosis of the receptors. Receptor blockade may therefore lead to the downregulation of receptors from the cell surface as part of their mechanism of action. This was shown in Chapter 3: where flow cytometry was used to investigate S1PR1 expression levels. To determine the effectiveness of receptor blockade, S1P was added for 10 minutes to all wells following an hour pre-incubation with inhibitor cocktails. The results are shown in Figure 46.

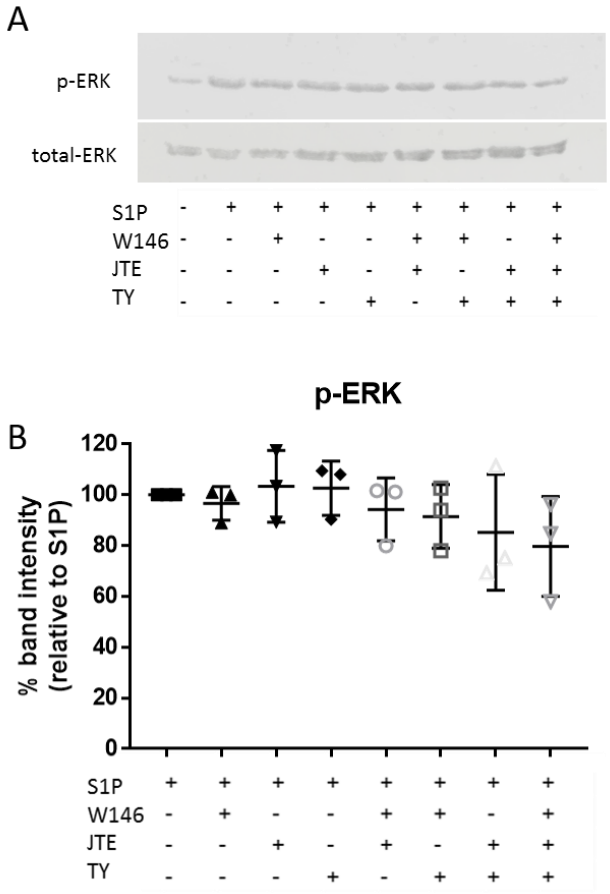

Figure 46 S1PR inhibitors have no effect at preventing phosphorylation after 1 hour
Cells stimulated with S1P following 1 hour pre-incubation with inhibitors, then Western blotted for phosphor- and total ERK. **A-** representative blot, **B-** band intensity expressed as a percentage of S1P phosphorylation, Error bars show mean +/- SD, n=3

An hour incubation with S1PR inhibitors has no effect at preventing ERK phosphorylation stimulated by S1P, unlike the inhibitory effects seen after 10 minutes. This was confirmed using one-way ANOVA analysis which did not reveal any significant differences between the level of phosphorylation seen with S1P alone and any combination of S1PR inhibitors for graph B.

3.2.4.1.3 MEK, p38 and SAPK/JNK inhibitors

Various other inhibitors were also used to study the effect of S1P on ERK phosphorylation, including a MEK inhibitor, the upstream kinase of ERK, and specific inhibitors of two related stress kinases p38 and SAPK/JNK. The inhibitors against the MAPKs, MEK, p38 and SAPK/JNK, are labelled PD(98059), SB(203580) and JNKII respectively.

A similar method was used for these inhibitors to that described above for S1PR inhibitors, i.e. they were added for 10 minutes with and without S1P. They were not however added in combination with each other, see Figure 47.

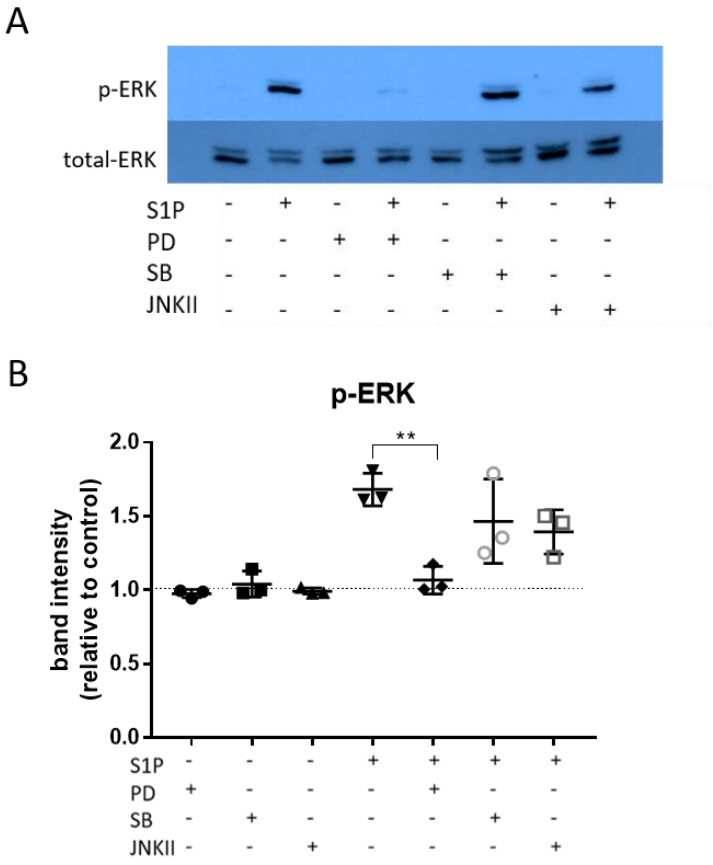

Figure 47 MEK inhibitor prevents S1P dependent ERK phosphorylation
Cells were stimulated with S1P in the absence or presence of a range of inhibitors before being interrogated for ERK phosphorylation via Western blotting as described. **A-** representative blot, **B-** band intensity relative to the control. Error bars show mean +/- SD, n=3

None of the MAPK inhibitors caused ERK phosphorylation alone. A large difference can be seen between the unstimulated control and the phosphorylation caused by the addition of S1P as shown in blot A. In the presence of the MEK inhibitor, S1P was not able to cause ERK phosphorylation. However, the other MAPK inhibitors used here at these concentrations seem to have little or no effect at blocking S1P dependent ERK phosphorylation.

The levels of p-ERK expression were expressed relative to the control expression (shown in graph B) and showed that alone none of the inhibitors cause ERK phosphorylation, however only the MEK inhibitor (PD) is effective at blocking the S1P dependent ERK phosphorylation. One-way ANOVA analysis revealed a p value of <0.0001 and Tukey's multiple comparisons test showed a p value of <0.01 between S1P and S1P+PD. Both SB and JNKII inhibitors appear to slightly lower the levels of p-ERK compared to that seen in S1P alone, although not significantly.

3.2.4.1.4 SKI-I, S1PL, TNF, Il-17 and IFNγ

Inhibitors against S1P formation (sphingosine kinase II SKI-I) and breakdown (S1P lyase S1PL), were also investigated to determine their effect on ERK phosphorylation either alone or in the presence of exogenous S1P. TNF, IL-17 and IFNγ were also investigated to investigate their effect on the phosphorylation state of ERK. Figure 48 shows an example blot and corresponding graph.

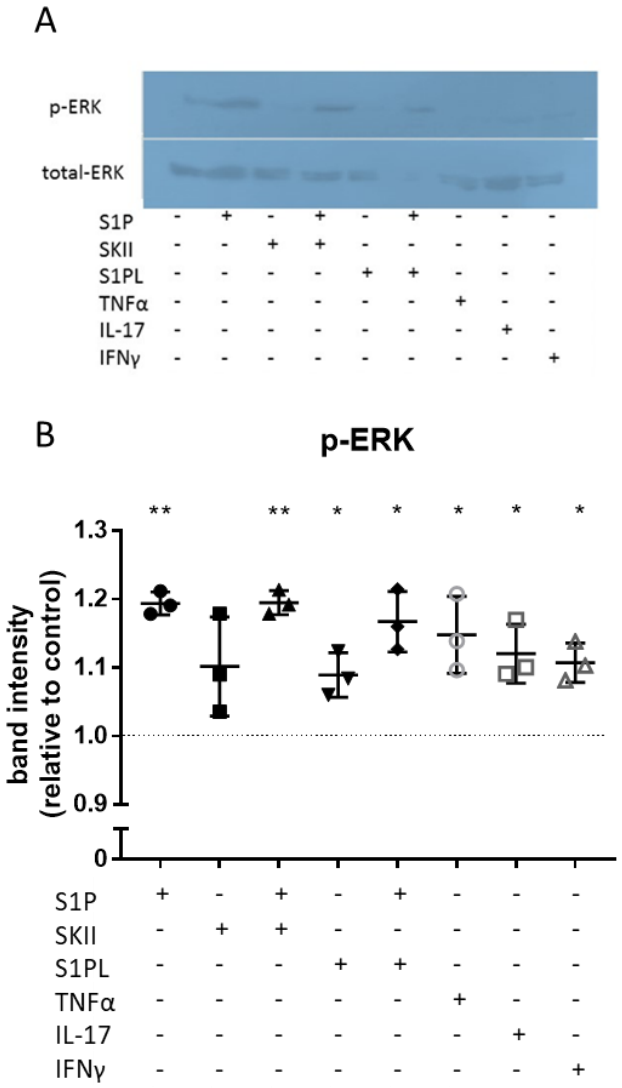

Figure 48 SKI-I and S1PL blockade do not inhibit ERK phosphorylation.
Cells were stimulated with S1P in the absence or presence of a range of inhibitors before being interrogated for ERK phosphorylation via Western blotting as described. **A-** representative blot, **B-** band intensity relative to the control. Error bars show mean +/- SD, n=3

One-way ANOVA gave a p value of $p<0.05$ however Dunnett's multiple comparisons test comparing SKI-I+S1P and S1PL+S1P did not reveal any significance between S1P alone showing that these inhibitors do not inhibit S1P mediated ERK phosphorylation. TNFα, IL-17 and IFNγ were also included as they are important regulators of inflammation, especially in psoriasis. One sample t-testing comparing the levels of ERK phosphorylation in the samples to that of the control showed that there was an increase in phosphorylated ERK in all samples except SKI-I, these results are highlighted on the above graph.

3.2.4.2 Intracellular signalling via Calcium flux

3.2.4.2.1 Histamine

Histamine is known to cause a calcium flux within cells (Ehringer et al., 1996) and therefore was used as a positive control to ensure that a response was detected. The results of a histamine concentration gradient are shown below in Figure 49.

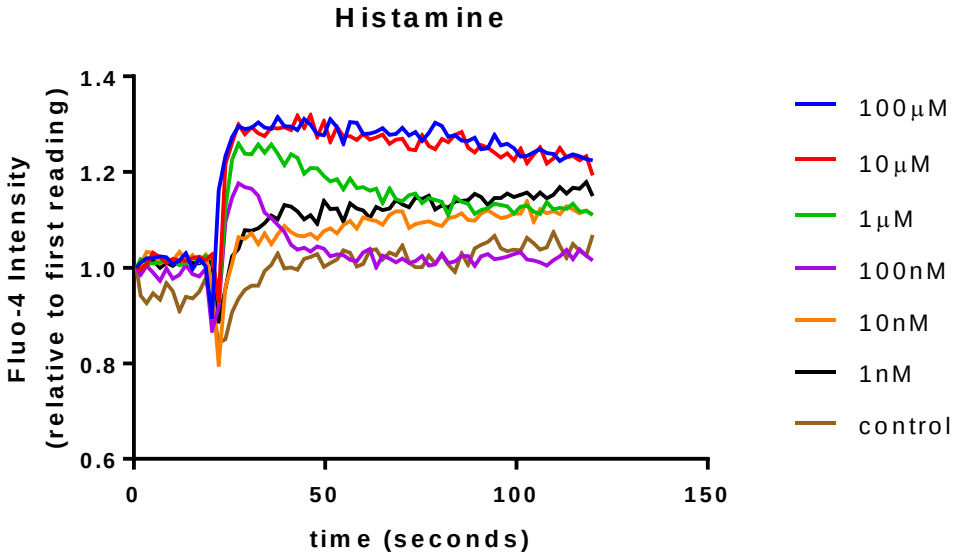

Figure 49 Calcium flux in response to histamine
Endothelial cells were labelled with Fluo-4 as described in Methods being exposed to agonists at various concentrations. Fluorescence was detected over time (Ex 488nm Em 530nm) in an automated multi-well analyser and the relative fluorescence of emitted light plotted against time. The fluorescence intensity measurements were normalised to the first measurement for each data set and the results shown are the mean of three separate assays in triplicate, n=3.

As expected, it can clearly be seen that as the concentration of histamine added to the cells increases, so does the intensity of the fluorescence and therefore calcium flux. In order to try and reduce the variability between experiments, the intensities were normalised to the first reading such that the first reading was equal to one.

There are also other methods for measuring the calcium flux such as calculating the area under the curve (AUC) or the peak height, both of which can be calculated in Prism. These have been shown below as an example for the histamine data and will be used to analyse the S1P data.

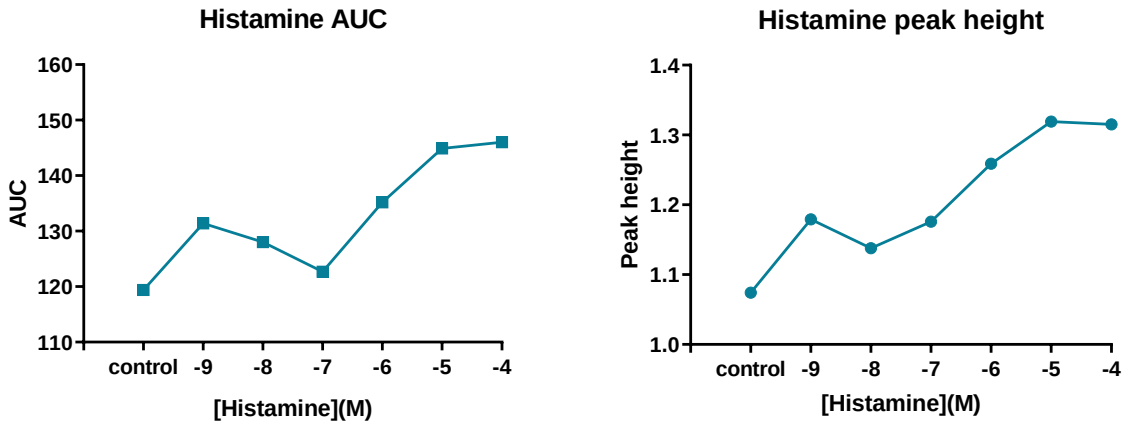

Figure 50 Showing the AUC and peak height for all concentrations for Histamine
Alternative methods of measuring calcium flux are presented here, with both the area under the curve and the peak height showing similar trends.

Figure 50 shows the various methods for measuring calcium flux produce similar results, with all three ways showing that the highest concentration of histamine (100µM) produces the greatest increase in intracellular calcium.

3.2.4.2.2 Sphingosine-1-phosphate

Once it had been established that the assay was working and sensitive enough to be able to pick up the differences in histamine concentration, the assay was repeated using an S1P concentration gradient and the results are shown below.

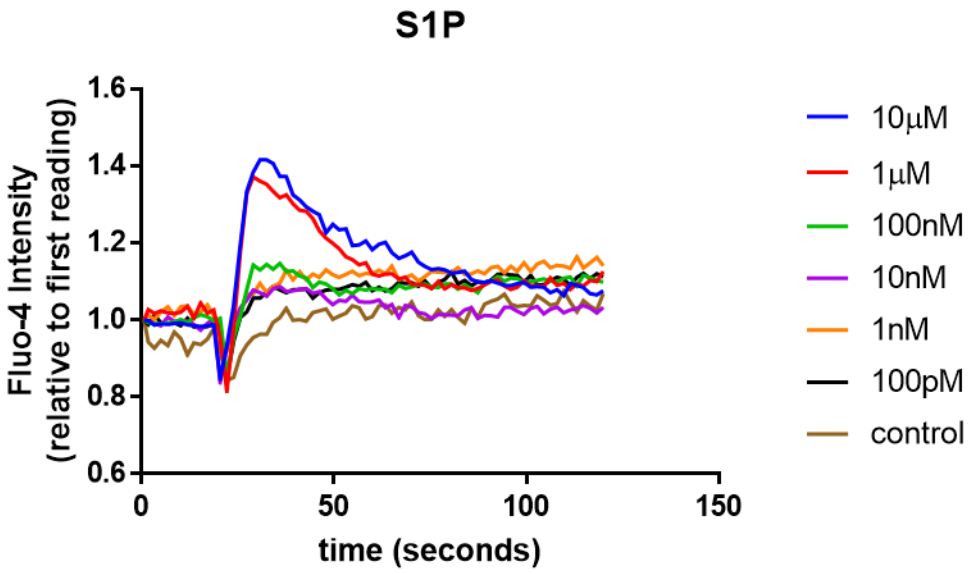

Figure 51 Calcium flux in endothelial cells exposed to S1P
Endothelial cells were labelled with Fluo-4 as described before being exposed to agonists at various concentrations. Fluorescence was detected over time (Ex 488nm, Em 530nm) in an automated multi-well analyser and the relative fluorescence plotted against time. The intensity measurements were normalised to the first measurement for each data set and the results shown are the averages of three separate assays in triplicate, n=3.

The highest concentrations of S1P resulted in a rapid increase in calcium flux. It can clearly be seen that the two highest concentrations of S1P (10µM and 1µM) caused a large peak in calcium flux and this was concentration dependent with lower concentrations showing a more graded response above the control. Comparing this data with the histamine data, the S1P response is much shorter in duration, with levels returning to that of the control at around 100 seconds following stimulation as opposed to still being greatly increase at the end of the time course at 125 seconds. Peak height and area under the curve (AUC) are both methods that can be used to compare the calcium response to agonists.

The area under the curve and the peak height for each histamine and S1P concentration was calculated and is shown below in Figure 52.

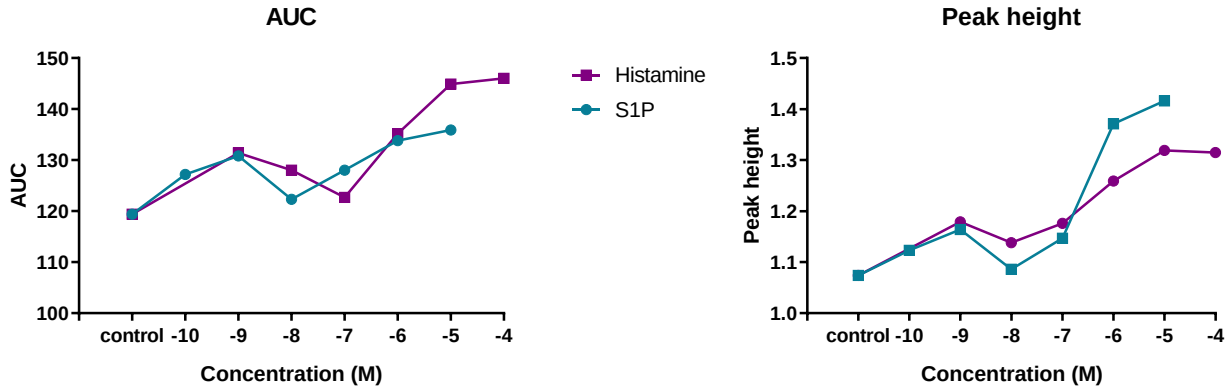

Figure 52 Area under curve and peak height in response to histamine and S1P
The area under the curve and the peak height for each concentration of Histamine and S1P was calculated and plotted against the concentration. The control is included for reference.

The area under the curve for the lower concentrations of histamine and S1P are roughly the same, however at the higher concentrations of histamine it can be seen that there is a larger AUC which would be expected from the differences in the shape of the curves generated in Figure 49 and Figure 51. In contrast, the higher concentrations of S1P are able to produce a greater peak height than the same concentrations of Histamine.

3.2.4.2.3 Fingolimod

The effect of Fingolimod on calcium flux was also examined. Once Fingolimod becomes phosphorylated, it competes with S1P to bind to the S1P receptors, thereby preventing downstream signalling of the S1P signalling cascade. Therefore alone, Fingolimod could potentially elicit a calcium flux and so required investigating in preparation for future work with this compound.

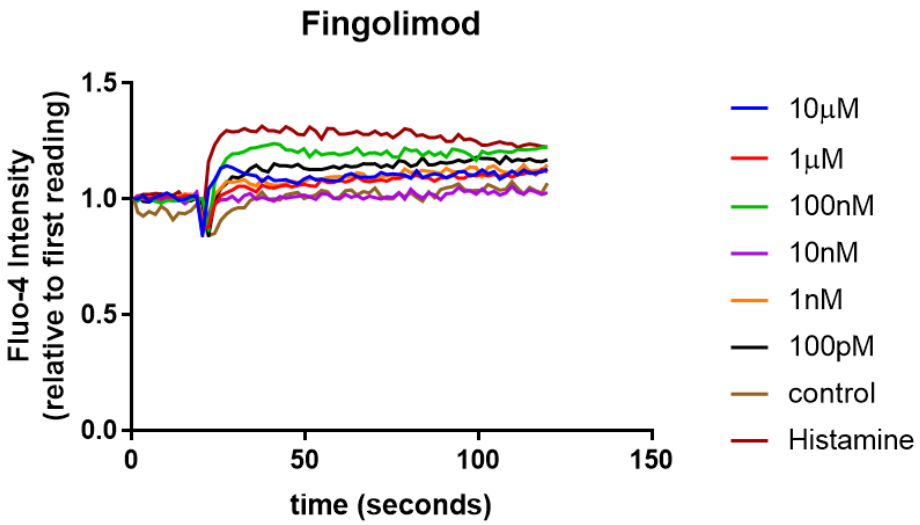

Figure 53 Calcium flux in endothelial cells exposed to increasing concentrations of Fingolimod
Endothelial cells were labelled with Fluo-4 as described before being exposed to agonists at various concentrations. Fluorescence was detected over time (Ex 488nm Em 530nm) in an automated multi-well analyser and the relative fluorescence plotted against time. The intensity measurements were normalised to the first measurement for each data set and the results shown are the averages of three separate assays in triplicate, n=3.

Although there is a slight increase in the calcium flux in response to the addition of Fingolimod, the levels remain around that of the control. Both histamine and S1P were able to produce a definite increase in calcium flux and corresponding peak and therefore it can be assumed that this effect in response to Fingolimod is due to variations in the sensitivity of the assay as no such peak can be seen or that any calcium flux in response to Fingolimod is small, potentially due to artefacts or excitation responses in the cells to the added lipid and not via activation of GPCR.

The area under the curve and the peak height for each concentration of S1P and Fingolimod was also calculated and is shown below for comparison.

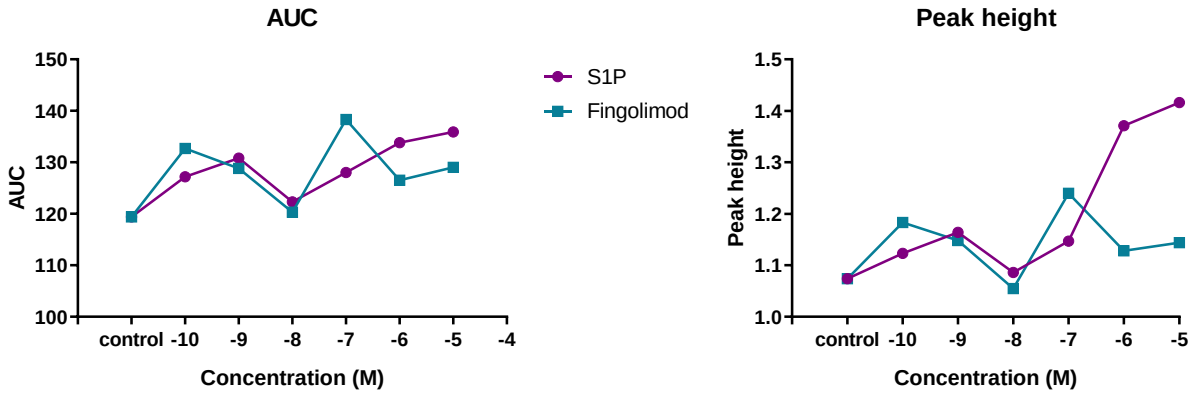

Figure 54 AUC and Peak height of calcium flux in response to S1P and Fingolimod
The AUC and peak height of each concentration of S1P and Fingolimod was calculated and plotted against the concentration.

From the above graphs it can be seen that although there is variation in the peak height across Fingolimod concentrations, it does not follow the regular pattern of an agonist causing a concentration dependent increase in calcium flux at the concentrations used. These graphs also show that high concentrations of S1P result in a much greater peak height compared to Fingolimod.

3.2.5 Discussion

3.2.5.1 Discussion of Intracellular signalling via mitogen activated protein kinase

Western blots were carried out in order to investigate the effect of S1P and associated inhibitors on the phosphorylation of ERK as a way of measuring intracellular signalling within HUVEC. An increase in the levels of ERK phosphorylation can be an indication of cell stress and as it is a known signalling cascade, ERK phosphorylation was therefore investigated to make comparisons in the functional assays as to whether the various compounds used were eliciting this response.

3.2.5.1.1 S1P concentration gradient

The S1P concentration gradient blots produced results as expected, with the higher concentrations causing an increase in the level of ERK phosphorylation above the unstimulated control. The highest concentration (10μM) caused the greatest increase in the levels of p-ERK and therefore this concentration was used as the positive control for the other western blots as it produced the strongest band and the greatest difference from the control.

3.2.5.1.2 S1P receptor inhibitors

The effect on ERK phosphorylation of the S1PR inhibitors was also investigated. This was completed in four separate ways; firstly the effect of the inhibitors alone was studied after a 10 minute incubation. This was to ensure that they did not cause ERK phosphorylation and therefore mask any effects seen after the addition of S1P. No bands were seen and therefore no p-ERK was present, indicating that the inhibitors do not lead to phosphorylation events over this time frame.

Secondly, S1P was added with the inhibitors for 10 minutes and it was shown that none of the inhibitors individually completely prevented the S1P dependent ERK phosphorylation. W146 inhibition resulted in roughly 50% decreased p-ERK levels compared to the control at the concentrations used. JTE also had a small inhibitory effect and the combination of these two inhibitors further decreased p-ERK levels. The $S1PR_3$ inhibitor (TY) appeared to have no effect at blocking S1P mediated ERK phosphorylation alone, however in combination with the other two inhibitors, the greatest effect was observed. The combined effect of the inhibitors suggests that there is some redundancy and that S1P may use all three receptors to stimulate ERK phosphorylation, as well as other potential mechanisms. This may also indicate that there is a difference in functionality, with ERK activation via one receptor causing a different response to ERK activation via one of the other receptors. A review by Wortzel and Seger (Wortzel and Seger, 2011) discusses five main mechanisms by which ERK signalling can be regulated in order to induce the wide range of biological processes known to be controlled by ERK. These include the action of

scaffold proteins, spatial and temporal differences in ERK activation and crosstalk with other pathways. One or more of these regulatory mechanisms may therefore be involved in any differing signal specificity between the S1P receptors.

The S1PR inhibitors were also added for 1 hour to see if this changed the effect on ERK phosphorylation as there was potential for downregulation of the receptors (as seen in the first half of this chapter) which would affect signalling. No increase in the levels of p-ERK were seen when the inhibitors alone were added, indicating that the increased incubation time had no effect on phosphorylation events. However, when S1P was then added after the 1 hour incubation with inhibitors, there was a clear increase in p-ERK levels in the presence of all combinations of inhibitors, suggesting that any inhibition seen after the 10 minute incubation has been lost. This may be due to the short half-life of the inhibitor or possibly that the inhibitor has been used up. This could also be due to receptor recycling, with the inhibited receptor becoming internalised and then either degraded or recycled back to the surface, ready for S1P to bind. In the first part of this Chapter, the expression levels of S1PR1 was measured after 30 minutes of stimulation rather than an hour and changes in receptor expression was observed. This suggests that the receptors are lost from the cell surface after 30 minutes but that they have been recycled back before an hour, therefore receptor loss is transient. This phenomenon could be determined by further assays of receptor expression such as flow cytometry or fluorescence microscopy to track surface expression of receptors in the presence or absence of S1P and receptor inhibitors. Future experiments could also focus on a shorter period of stimulation, such as 30 minutes, with the expectation that results similar to those seen with the flow cytometry data would be obtained.

3.2.5.1.3 Pathway inhibitors

Various other inhibitors were also investigated, including the MAPK inhibitors PD (MEK), SB (P38) and JNKII (SAPK/JNK). Again, these inhibitors showed no increase in ERK phosphorylation when added alone, however a near complete inhibition of S1P mediated ERK phosphorylation was observed with the addition of S1P and PD, while neither SB nor JNKII reduced the levels of p-ERK in response to S1P.

Sphingosine kinase (SKI-I) and S1P Lyase (deoxypyridoxine) inhibitors were also used. As expected, no significant inhibition of ERK phosphorylation was seen either alone or in the presence of S1P for SKI-I however, S1PL alone and in combination with S1P did cause an increase in the levels of p-ERK. This is most likely because endogenous S1P is increasing because it is not being broken down by the lyase. It might have been expected that S1P would build up and cause an increase in ERK phosphorylation compared to that of S1P alone, but it was found not to be the case. The phosphatases that convert S1P to sphingosine will still be active in this system and it may be that in the presence of the lyase inhibitor, the de-phosphorylation of any endogenous S1P formed might reduce its ability to cause ERK phosphorylation. Combined, these results suggest that there is a complex relationship between the addition of exogenous S1P and the resultant intracellular signalling pathways, potentially leading to the formation of de novo S1P, in turn perpetuating its signalling effects.

3.2.5.1.4 TNF, IL-17 and IFNγ

Three cytokines (TNF, IL-17 and IFNγ) known to be involved in inflammation, and therefore important in psoriasis, were also added to HUVEC to assess their ability to increase ERK phosphorylation. It was expected that all three would increase the levels of phosphorylated ERK and this was shown to be the case, with all three showing significantly increased levels above that of the control. These three cytokines are all elevated in psoriasis patients compared to healthy individuals (Bai et al., 2018), it is possible that this increase in ERK signalling is an important part of psoriasis development. This would tie in with the increased proliferation and cell survival seen in the psoriasis plaques as these are both outcomes of ERK signalling.

3.2.5.2 Discussion of intracellular signalling via Calcium flux

Calcium flux within the cell was used as a further method to study the effect of S1P on intracellular signalling. Histamine is a well-known agonist of the second messenger molecule and was therefore used as the positive control. Fluo-4 was used which produced sensitive data and showed good separation between the levels of intensity across the histamine concentration gradient which was in line with the literature (Worthen and Nollert, 2000). Once the measurement of the calcium flux had been optimised, S1P was added to the cells. It was found that the highest concentrations of S1P produced the greatest intensity readings, which was to be expected and also ties in with the results for the western blots looking at the levels of ERK signalling. The effect of Fingolimod on intracellular calcium flux was also investigated, as being a sphingosine analogue, it may be able to activate the S1P receptors because of it being phosphorylated as part of its metabolism. With the addition of varying concentrations, there was no large increase above the control suggesting that Fingolimod was not a direct agonist at least on addition. OxLDL has also been found to increase calcium flux in various cell types (Chen et al., 2009) and therefore it is possible that S1P and oxLDL activate the same signalling pathways but requires further development and the addition of specific inhibitors. Future work would therefore look at calcium flux in response to S1P in the presence of the receptor inhibitors, as well as the effect of oxLDL and receptor inhibitors as a high throughput assay.

3.3 Chapter summary

In conclusion, this chapter firstly aimed to characterise the cells obtained during the isolation procedure as well as determine the viability of the cells when exposed to various conditions that will be used in later parts of this thesis. It was confirmed that the cells were indeed endothelial cells and that they were viable at varying concentrations of S1P and oxLDL as well as in a reduced lipid environment. The HUVEC cells were also shown to express the S1P receptor 1 and that S1P and oxLDL caused changes to the cell surface expression levels.

The second part of this chapter looked at the intracellular signalling of endothelial cells by both pERK levels and calcium flux. It was found that S1P had a concentration dependent effect on intracellular signalling, with high concentrations of S1P producing the biggest change in both the levels of phosphorylated ERK and calcium flux.

Chapter 4: Effects of lipids on the migration and shape of the endothelium

4.1 Introduction

Migration is a method with which cells can move around in their environment and is used by single celled organisms right through to cells of large complex organisms, such as humans, as a fundamental process. In multi-cellular organisms, migration is a vital part of development that enables the formation of organs due to the organisation of the various cell types into functioning specialised tissue. The motility of cells is also vital for the continued survival of the organism, with the immune system relying on this process to resolve potential assaults as well as being essential for the maintenance of homeostasis (Vicente-Manzanares et al., 2005). Migration forms part of the angiogenic process and as such provides a method to dissect the effects of the bioactive lipids.

Migration is a complex process and involves the tight regulation of many individual components of the cellular machinery that have to be precisely controlled and coordinated in order to achieve movement in the desired direction. There are now known to be different models of migration depending on the cell type, such as the gliding-like motion seen with keratinocytes and an amoeba-like motility in leukocytes, and more recently a model for cells migrating in a 3-dimensional environment has been proposed (Borau et al., 2011). Although there are some unique features to these different types of migration, there are a number of similar steps. Endothelial cells undergo the “classical” migration and therefore this model will be described here (Vicente-Manzanares et al., 2005).

For migration to start, the cell needs to receive a signal informing it to move and in which direction. This could potentially be in the form of a growth factor, chemotactic gradient or through another signal such as hypoxic conditions. Upon receiving this signal, the cell becomes polarised through the activation of various factors such as Ras-related C3 botulinum toxin substrate 1 (Rac), leading to the rearrangement of the actin cytoskeleton. Put simply, this rearrangement allows protrusions at the leading edge of the cell to be extended in the direction of travel, while at the lagging edge of the cell, the cytoskeleton is dismantled and actin is transported back to the front of the cell ready to be reused. In this manner the cell is able to effectively pull itself along the extracellular matrix putting down new contacts as it goes (Mayor and Etienne-Manneville, 2016).

Scratch assays (also known as wound healing assays) are commonly used as an easy and inexpensive method to measure the migration of cells into a denuded area. The most common method involves

scratching a single straight line into a monolayer of cells and imaging at various time points (Liang et al., 2007). While this method will allow migration to be measured, it is hard to ensure that the same area is being imaged at each time point unless automated and therefore it is possible that biased or false rates of migration could be obtained. In order to improve upon this method, monolayers of cells were scratched twice at 90^{o} in order to form a cross (see Figure 55), allowing the same field of view to be imaged at each time point, removing the potential for subjective analysis.

It is however possible that there is some damage caused by scratching the monolayer of cells. This may result in the release of factors which may affect migration and therefore other methods of measuring migration could be used to verify the findings. One-way of looking at non-scratch migration is by measuring migration through a porous membrane which is utilised in Boyden chambers. This is an example of a transwell migration assay where cells move from a smaller well towards a chemoattractant through a semi-permeable membrane and into a larger well (Justus et al., 2014).

As mentioned in the introduction, S1P signalling has a wide range of biological effects, including regulating migration. This is achieved through changing the expression of intercellular adhesion molecule 1 (ICAM1) and vascular cell adhesion molecule 1 (VCAM1) on endothelial cells. As an S1P competitive agonist, Fingolimod also effects migration through the same pathways. oxLDL is also able to regulate endothelial migration through the Akt and eNOS pathways. Activation of these pathways results in an increase in the levels of nitric oxide which stimulates the cell to migrate (Chavakis et al., 2001). The effect of these compounds on the migration of HUVEC has therefore been investigated.

4.2 Hypothesis and Aims

It is hypothesised that S1P is important for the migration of HUVEC and that it will have a concentration dependent effect on migration. Various inhibitors of the S1P signalling cascade are also hypothesised to block the effect of S1P on migration.

Specific aims of this chapter are:

- to investigate the effect of S1P and Fingolimod on migration across a range of concentrations (10µM-1nM)
- to investigate the effect of various inhibitors of the S1P signalling cascade on migration, such as inhibitors against the S1P receptors 1-3 and inhibitors of the S1P kinase and lyase
- to investigate the effect of other pathway inhibitors on migration e.g. MEK, p38 and SAPK/JNK inhibitors
- to investigate the effect of oxLDL and ox-albumin on migration
- to determine what effect, if any, S1P, Fingolimod and oxLDL have on a confluent monolayer of cells

4.3 Method

Scratch assays were performed in order to measure the effect that various added stimuli or inhibitors had on the migration of HUVEC. Confluent cells were split into 24 well plates, plated at 100,000 cells per well and incubated overnight. Confluent monolayers were scratched as described in the methods. Images were taken by phase contrast microscopy of each well at 0, 24 and 48 hours and analysed using Fiji (see Figure 55). The edge of the scratch was manually drawn around and the area of the scratch measured for all images. Automated analysis was also tried, however the detected edge of the scratch was not always accurate and therefore it was decided that manual analysis would provide a better representation of migration. In order to account for the variability in the assays and to attempt to correct for the moving background, graphs were plotted of the migration, percentage migration compared to the control, the corrected migration and the corrected percentage migration compared to the control.

To calculate the migration, the area of the scratch was divided by the total area of the field of view while the percentage migration compared to the control values were calculated taking the migration achieved by the control to be 100% (even if the control never achieved full closure of the scratch). This allowed the migration in the presence of the various stimuli/inhibitors to be compared and normalised to the potential achievable migration of those cells. For the corrected migration, 100% represents complete closure of the scratch, as shown in Figure 55 (48 hours), however the denuded area at time 0 is taken to be equal to 0% migration. By comparing each wells migration after 24 and 48 hours to the corresponding starting scratch of that well, the variability in the size of the denuded area due to the scratching process can be negated. Finally, the corrected migration values were obtained by taking these corrected values and comparing them to the migration of the control (again for this calculation the control after 48 hours is equal to 100% migration).

For clarity, only the corrected percentage migration compared to the control graphs are shown here.

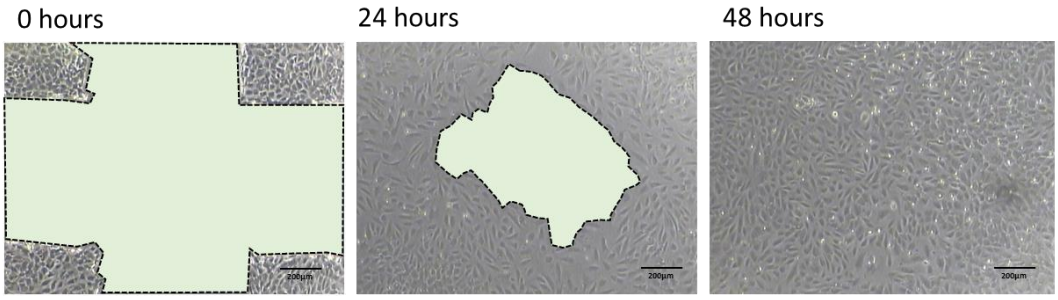

Figure 55 showing a scratch in a monolayer of HUVEC
A monolayer of HUVEC immediately after being scratched (0 hours), after 24 hours and after 48 hours, when cells have migrated into the space created by the scratch to reform a confluent monolayer. The area measured at each time point (0 and 24 hours) is highlighted in green and outlined by a dashed line.

The effect of S1P on the migration of HUVEC was assessed using a $\log_{10}$ range of S1P concentrations (10µM-1nM) to create a concentration gradient that mimicked physiological levels of S1P as well as various inhibitors against components believed to be important in the S1P signalling pathway.

Fingolimod, an analogue of sphingosine, was also used at equivalent concentrations to S1P as a different method of assessing the importance of S1P in endothelial migration. TNFα was used in a range from 10nM-1pM to create a concentration gradient as this cytokine is involved in psoriasis. S1P receptor antagonists (W146, JTE, TY) against the three S1P receptors found in endothelial cells ($S1PR_{1-3}$ respectively) were used to try and gain a clearer understanding of the mechanism through which S1P exerts its effect. The concentrations used were 1µM for W146 and JTE and 10µM for TY as this was equivalent to 100x the IC50 or Ki as reported in the literature. The sphingosine kinase inhibitor (SKII) was used at 10µM while the lyase inhibitor was used at 1mM. The MEK, p38 and SAPK/JNK inhibitors (PD, SB and JNKII respectively) were used at 10µM. oxLDL and LDL were used at both 100µg/mL and 5µg/mL and a lipid supplement was used at 1:100 and 1:1000 dilution. Albumin and oxidised albumin were used at 1% w/v. S1P bound to albumin and oxidised albumin was also used (10µM S1P was added to 10% (w/v) albumin or 5% (w/v) ox-albumin as described in methods section 2.7.3).

In order to provide a baseline migration for HUVEC under various conditions, the following scratch assays were first performed in media containing 20% (v/v) full human serum. The effect of lipids on migration was then assessed by repeating the scratch assays, this time performed in media containing delipidised human serum (see 2.4).

4.4 Results

4.4.1 S1P concentration gradient

Sphingosine-1-phospate is known to have a role in the migration of endothelial cells and oxLDL may potentially signal through this bioactive lipid to exert its effects on the endothelium. The aim of the following assays was therefore to discover if S1P caused a similar bi-phasic response that was previously seen with oxLDL migration.

4.4.1.1 S1P concentration gradient in normal media

In order to study the effect various concentrations of S1P have on migration, a ten-fold dilution series of S1P from 10µM-1nM was set up. Each concentration was performed in duplicate and the mean value calculated. Five separate scratch assays from five individual umbilical cords were performed and plotted as separate points. To provide a clearer picture of the effect of S1P on migration by correcting for the inherent variability in the assay due to the moving background, several normalisation steps had to be performed. For simplicity, the results in Figure 56 show only the final corrected results expressed as a percentage of the control, with the dotted line representing the migration achieved by the control (100%) and the error bars showing the mean and standard deviation.

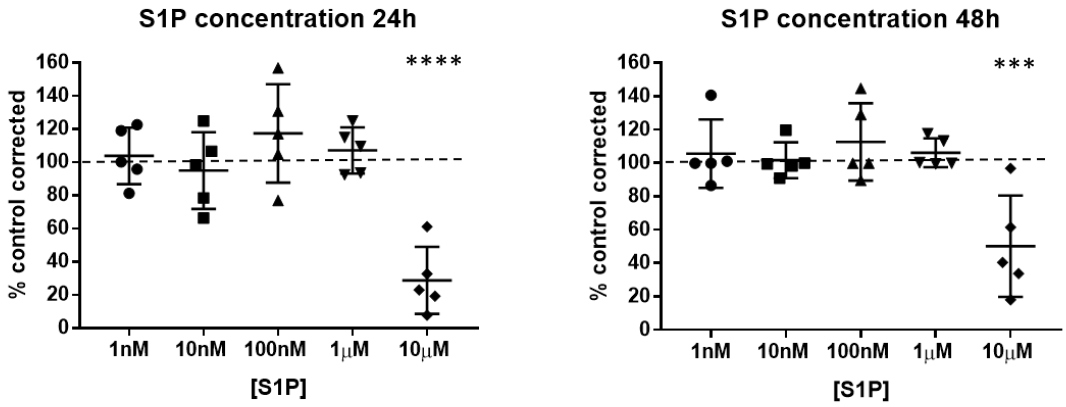

Figure 56 Effect of various S1P concentrations on migration normalised to control.
Cells were scratched as described and cell migration into the denuded area calculated for increasing concentration of S1P. The graphs show the corrected values of the migration achieved at 24 and 48 hours normalised to the control. The error bars represent the mean percentage cover +/- SD, n= 5.

One-way ANOVA analysis was used to ascertain if there was a significant difference between the means of the various S1P concentrations. At 24 hours a p value of <0.0001 was found, showing that there is significance between the concentrations. One-sample t-testing was therefore used to compare the migration achieved by each concentration to the migration of the control, allowing

the significant concentration to be found. This analysis showed that at 24 hours 10µM S1P was significantly different from a hypothetical value of 100%, with a p value of 0.0014. At 48 hours one-way ANOVA analysis reveals a p value of 0.0006, and again the significant difference highlighted by the one-sample t-test was for 10µM with a p value of 0.0215. Combining these results, it can be concluded that 10µM S1P has an inhibitory effect on the migration of HUVEC in full media.

4.4.1.2 S1P concentration gradient in delipidised media

A slight variation in the concentrations of S1P used in 4.4.1.1 was used to assess the effect of the removal of exogenous lipids on migration. This was in part because it was noted that in the normal media, 100nM S1P appeared to have a potential stimulatory effect although this was not significant and that it was expected to see an enhancement in migration stimulated by S1P. It was therefore hypothesised that the concentration that stimulated migration might fall between those already in use. Previous work had also shown that oxLDL had a narrow concentration range over which migration was stimulated before inhibitory effects were seen. Therefore, a concentration of 500nM S1P was added for comparison.

Again the results shown below in Figure 57 show only the corrected results expressed as a percentage of the full lipid control, with the dotted line representing the migration achieved by the control (100%).

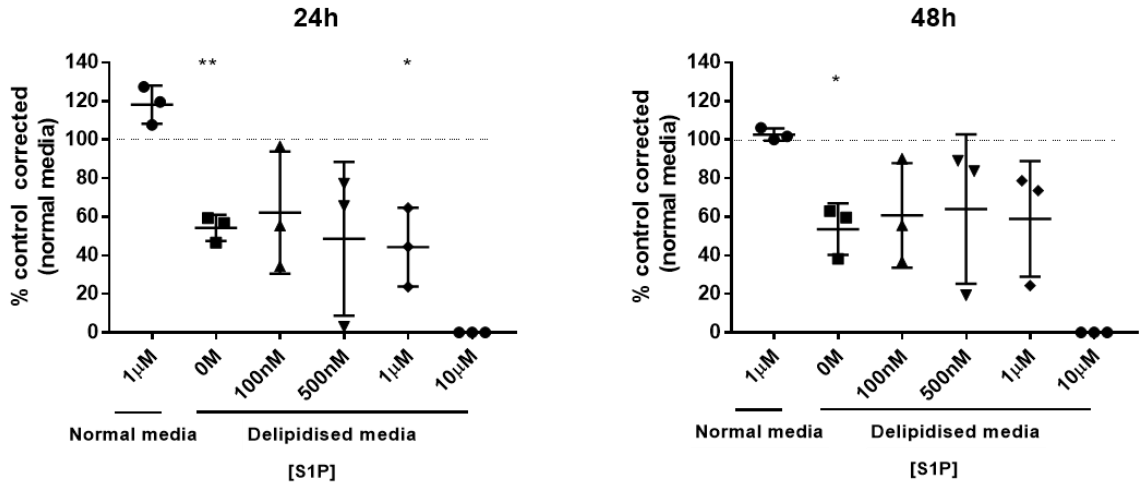

Figure 57 showing the normalised S1P concentration effect on migration in delipidised media
Cells were scratched as described and cell migration into the denuded area calculated for increasing concentration of S1P in either normal or delipidised media. These graphs show the corrected values that have been normalised to the control in normal media. The error bars represent the mean percentage cover +/- SD and n= 3.

Figure 57 shows that, although not significant, 1µM S1P in the full lipid environment is able to stimulate migration above that of the control and that the removal of lipids from the media has an inhibitory effect on the migration of HUVEC. These results also show that the addition of S1P to the reduced lipid environment is not able to recover the migration levels back to that of the control in normal media and indeed at the highest concentration, S1P completely blocks migration. This is however not as a result of total cell death as shown previously by live/dead staining (Chapter 3:).

These graphs show the results as a percentage of the control under normal conditions and highlight the difference between the two types of media used. One-way ANOVA was first used to ascertain if there was a significant difference between the calculated means of the samples. At 24 hours, a p value of $p= 0.0014$ was found, while after 48 hours the $p= 0.0058$, showing that there is indeed a significant difference. Dunnett's multiple comparisons test was then used to compare the delipidised control with the S1P concentrations under the same conditions however this did not reveal any significance, suggesting that under these conditions S1P is not able to stimulate migration. Therefore in order to find out which concentrations of S1P were significantly different from the full lipid control, a one sample t test was used. This test compared the mean of each concentration with a hypothetical value of 100%, representing the migration achieved by the control. It was found that the delipidised control inhibited migration with a p value of $p<0.01$ at 24 hours and $p<0.05$ at 48 hours and that 1µM S1P in delipidised media inhibited migration with a p value of $p<0.05$ at 24 hours.

4.4.1.3 Combined results of S1P concentration gradient

The following graphs show the combined data for S1P in both normal and delipidised media over 48 hours in order to highlight the effect removing lipids from the system has on migration. The data plotted has been normalised and is shown as a percentage of the control (i.e. normal media with no S1P) which is taken to be 100%. The error bars show the standard error of the mean to provide a clearer view of the two lines, however the data is the same as plotted in the above graphs.

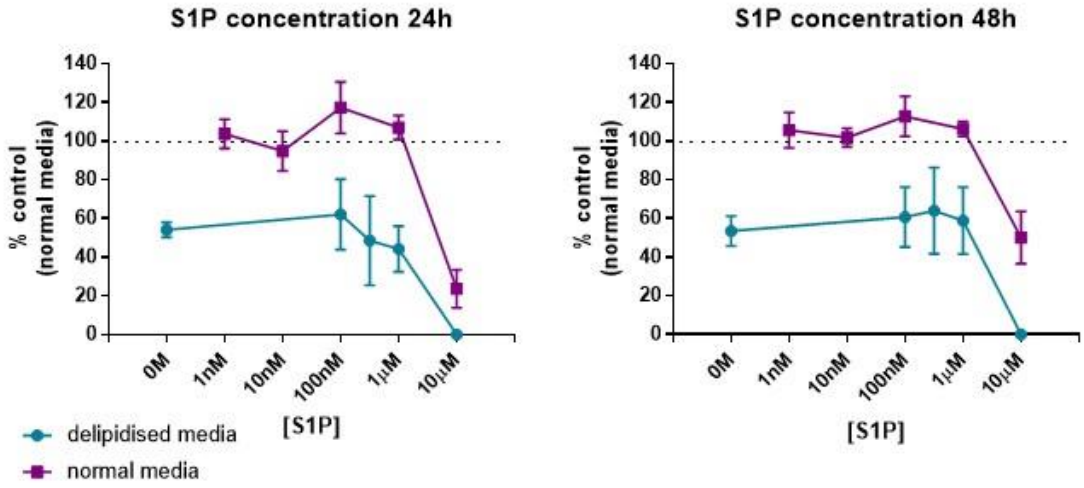

Figure 58 The effect of S1P on endothelial cell migration in normal and delipidised media over time.

Cells were scratched as described and cell migration into the denuded area calculated for increasing concentration of S1P in either normal or delipidised media. The dotted line represents the control under normal conditions, the error bars represent the mean percentage cover +/- SEM, n=5 for normal media and n=3 for delipidised media

From Figure 58 it can clearly be seen that the removal of lipids from the media causes a reduced rate of migration to approximately half of that seen under normal conditions (see the delipidised control). While a slight stimulation in migration (i.e. greater than 100% of the control) due to the addition of S1P can be seen in normal media, the addition of S1P to delipidised media is not able to fully recover the rate of migration. For both time points it is clear that the rate of migration of HUVEC in delipidised media is only able to achieve around 50% of that compared to normal media, increasing to around 60-70% with the addition of S1P.

4.4.2 Fingolimod concentration gradient

Fingolimod is a sphingosine analogue and is currently being used as an anti-S1P drug in the clinic to treat multiple sclerosis. It was included in the panel of compounds as a way to study what effect the perturbation of the S1P signalling cascade had on the migration of primary HUVEC. Once phosphorylated by sphingosine Kinase, Fingolimod is able to bind to four of the five S1P receptors (1,3,4 and 5), activating them but ultimately resulting in their downregulation and therefore preventing further signalling via the S1P pathway (see Figure 6) (Chun and Hartung, 2010).

4.4.2.1 Fingolimod concentration gradient in normal media

The equimolar ten-fold dilutions used for S1P were repeated for Fingolimod. Each concentration in each assay was performed in duplicate and the assays were carried out on four occasions with four individual donor endothelial cells at passage one. It was noticed that Fingolimod had a peculiar effect on migration, with cells appearing to move as individuals rather than as a continual front to close the scratch. This made measuring the area of the scratch left in order to access migration very challenging, see Figure 59.

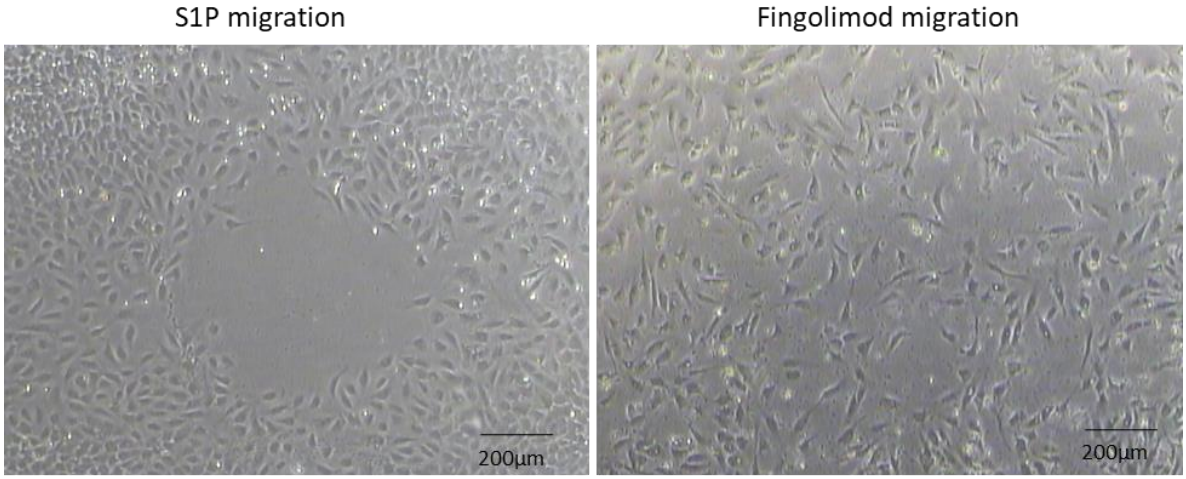

Figure 59 Effect of equimolar (1µM) S1P or Fingolimod on endothelial migration after 24 hours
Cells were scratched as previously described and cultured in the presence of S1P or Fingolimod before being imaged 24 hours following wounding. Cells exposed to S1P show normal migration moving as a front to cover the denuded area, whereas those exposed to Fingolimod lose contact with neighbouring cells and migrate individually.

Compared to the effect that the differing S1P concentrations had on migration, the various Fingolimod concentrations do not appear to markedly affect the cells ability to close the scratch and instead the addition of Fingolimod results in an individual and deranged migration of the cells.

In order to more closely identify the time where the aberrant migration started, a scratch assay was imaged every 2 hours up until hour 8 and another was imaged after 16, 18, 20 and 22 hours.

Example images are shown in the Appendix. It was observed that by 16 hours the cells exposed to 10µM Fingolimod had started to migrate independently but that the other concentrations have a delayed effect on this migration pattern, with cells starting to lose contact with their neighbours at around 18 or 20 hours.

As a result of this scratch assay it was decided that imaging future assays at hours 8, 16 and 24 would provide the clearest picture of HUVEC migration when exposed to Fingolimod. In order to make this more feasible, a single T75 flask of cells was split into two 24 well plates (14 wells used in each) and the assay started at different times, with the 24 hour time point shown coming from the same cells imaged in the 8 hour assay.

Due to the cells having a perturbed migration pattern, a new way to measure the migration also had to be found as it was not practical to draw around every individual cell. The MRI Wound Healing Tool plugin for Fiji was found to give the best representation of the migration achieved and therefore was used to analyse the following assays, examples are shown below in Figure 60.

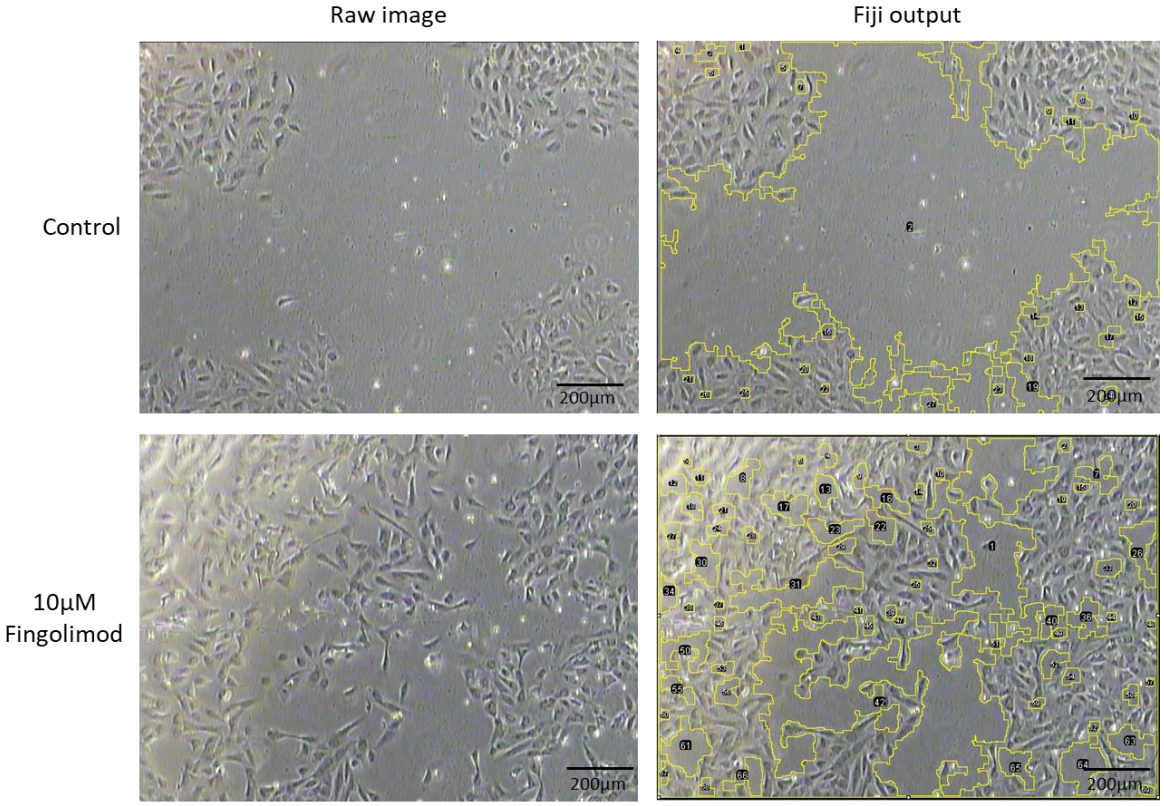

Figure 60 Fiji output after wound healing tool analysis
An example of the output from the Fiji wound healing analysis showing the spaces between the cells outlined in yellow. The same settings were used for both the control and the Fingolimod image and both images were taken 16 hours after the start of the assay.

Using this plugin it is possible to set the various options and careful selection was used to gain the most accurate measurement of migration for each image.

As discussed before, the migration values obtained at each time point were normalised to the starting area of the scratch at time 0 and expressed as a percentage of migration of the control. These graphs are shown below in Figure 61.

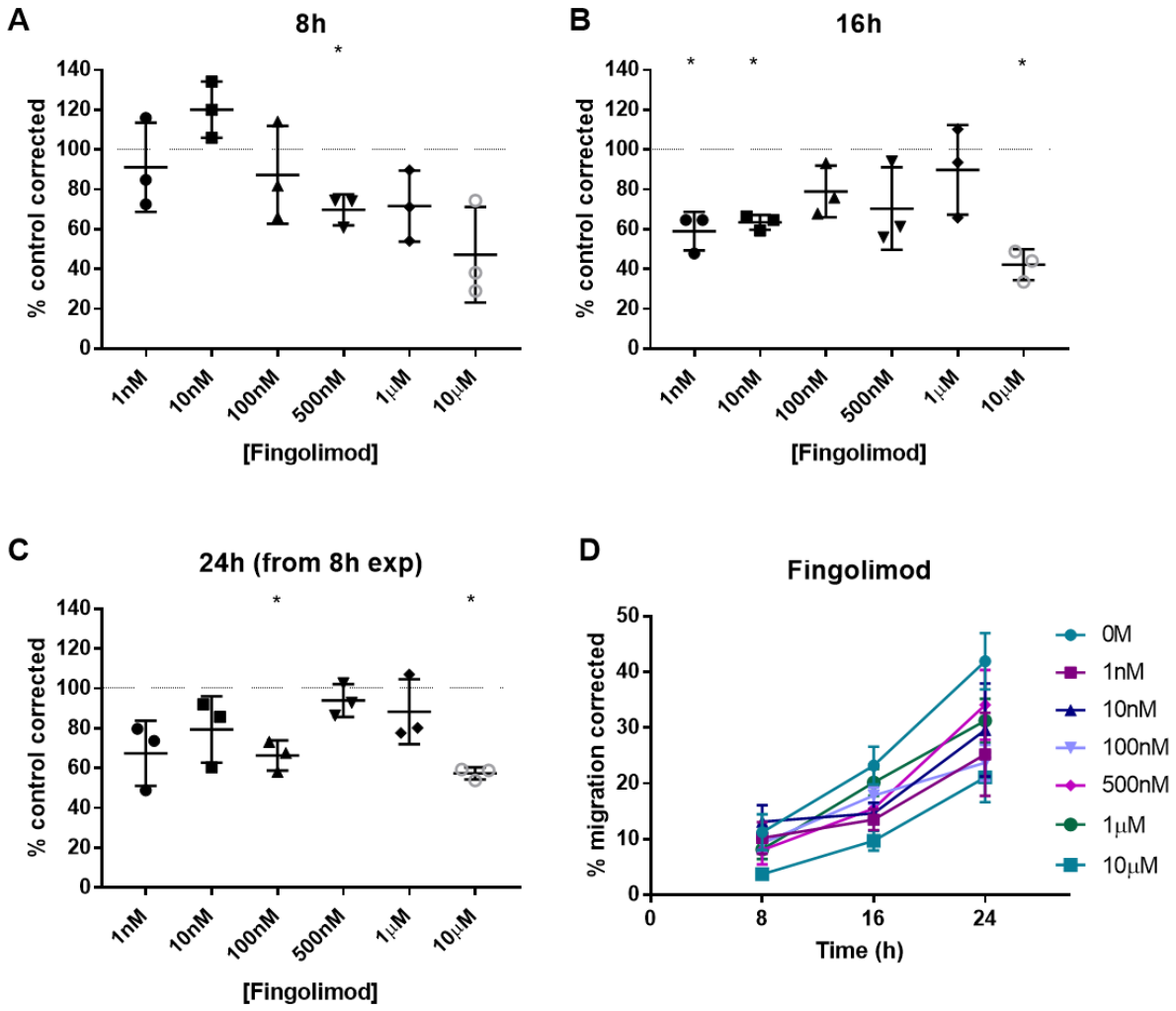

Figure 61 showing the normalised Fingolimod concentration effect on migration
Cells were scratched as described and cell migration into the denuded area calculated for increasing concentration of Fingolimod. **A-C** shows the corrected values of the migration achieved at 8, 16 and 24 hours expressed as a percentage of the control. **D** shows the % normalised migration for all concentrations across the time course. **A-C**: the error bars represent the mean percentage cover +/- SD, with the dotted line showing the migration of the control, **D**: error bars represent the mean percentage cover +/- SEM. n=3.

The results from Figure 61 show that at hour 8 there is a downwards trend across the concentrations but that by 16 hours this is reversed, with the exception of 10µM. One-way ANOVA was used to assess the significance of these results and it was found that at all time points there was a p value of <0.05. In order to identify which concentration of Fingolimod caused a significant change in migration compared to the control, a one sample t test was performed where the results were compared to a hypothetical value of 100%. These results are highlighted on the graphs above, with 10µM having the greatest inhibitory effect.

4.4.2.2 Fingolimod concentration gradient in delipidised media

Fingolimod concentration migration assays were also performed in delipidised media, mainly to find out if the same perturbed effect on the migration of the cells seen in full media would be observed. While this effect seemed to be somewhat lessened in the delipidised media, there also appeared to be a greater proportion of floating dead cells at 48 hours than in the regular media, making the area of migration equally difficult to accurately measure. It was therefore decided to repeat the 8 and 16 hour time point assays in order to try and obtain a migration value for HUVEC exposed to Fingolimod in a delipidised environment. Again the 24 hour time point came from the 8 hour plate of cells and the results are shown below in Figure 62.

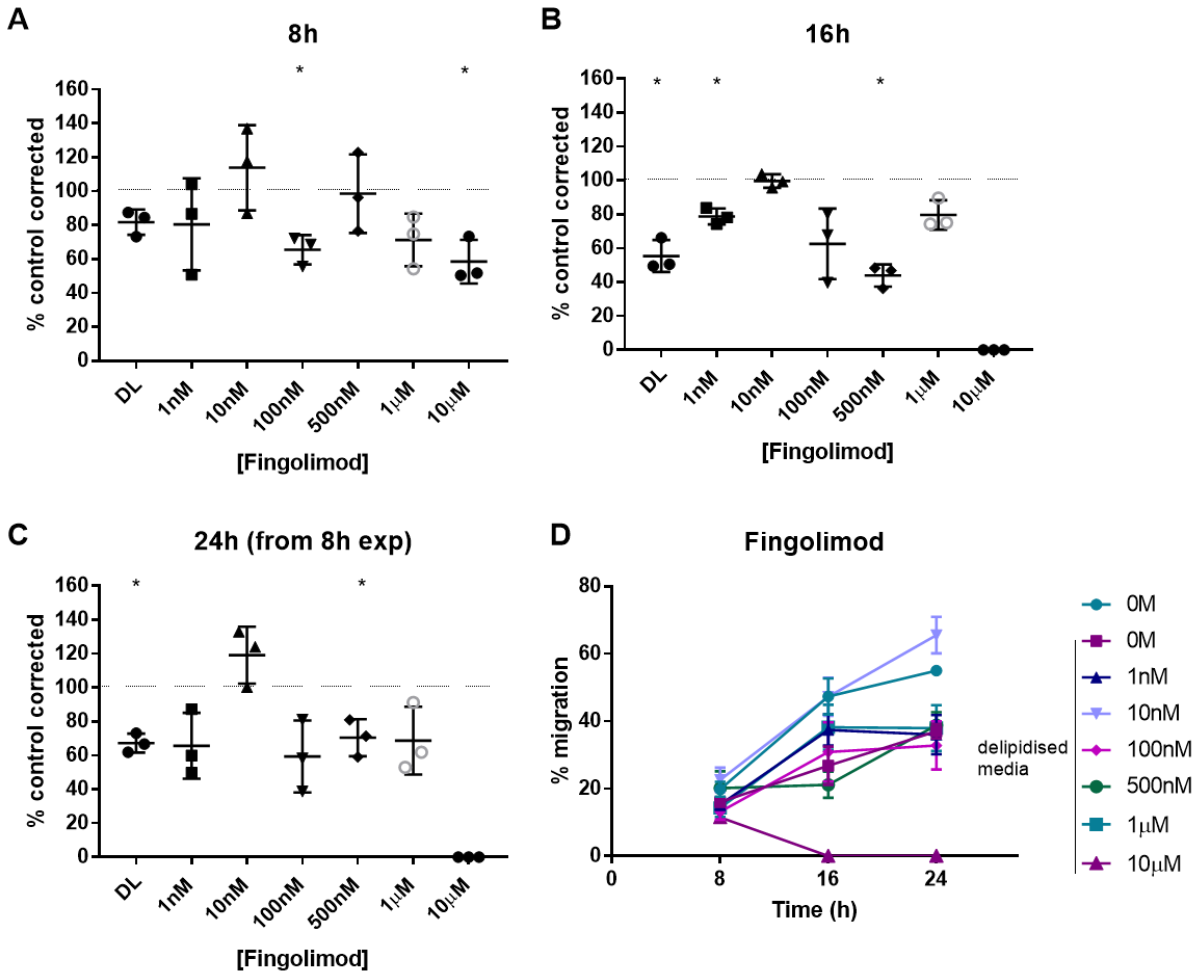

Figure 62 Effect of Fingolimod on endothelial migration in delipidised media

Cells were scratched as described and cell migration into the denuded area calculated for increasing concentration of Fingolimod in delipidised media (DL). **A-C** shows the corrected values of the migration achieved at 8, 16 and 24 hours expressed as a percentage of the control. **D** shows the normalised % migration for all concentrations across the time course. **A-C**: the error bars represent the mean percentage cover +/- SD, with the dotted line showing the migration of the control, **D**: error bars represent the mean percentage cover +/- SEM. n=3

One-way ANOVA was used to assess the significance of these results and it was found that there was a p value of <0.05 at hour 8 and <0.0001 at hour 16 and 24. In order to identify which concentration of Fingolimod caused a significant change in migration compared to the control, a one sample t test was performed where the results were compared to a hypothetical value of 100%. These results are highlighted on the graphs above. Dunnett's multiple comparisons test was also used in order to see if any of the concentrations of Fingolimod were significantly different to that of the delipidised control. At 8 hours there was no significance between samples, however after 16 hours there was a difference between the control and 10nM Fingolimod (p=0.005) and 10µM (p=0.0005) and after 24 hours there was a significant difference of p=0.0004 between the control and 10nM, p=0.041 between the control and 1µM and p=0.0001 between the control and 10µM Fingolimod.

4.4.2.3 Combined results of Fingolimod concentration gradient

The following graphs show the combined migration data for Fingolimod in both normal and delipidised media over the time course in order to highlight the effect removing lipids from the system has on migration.

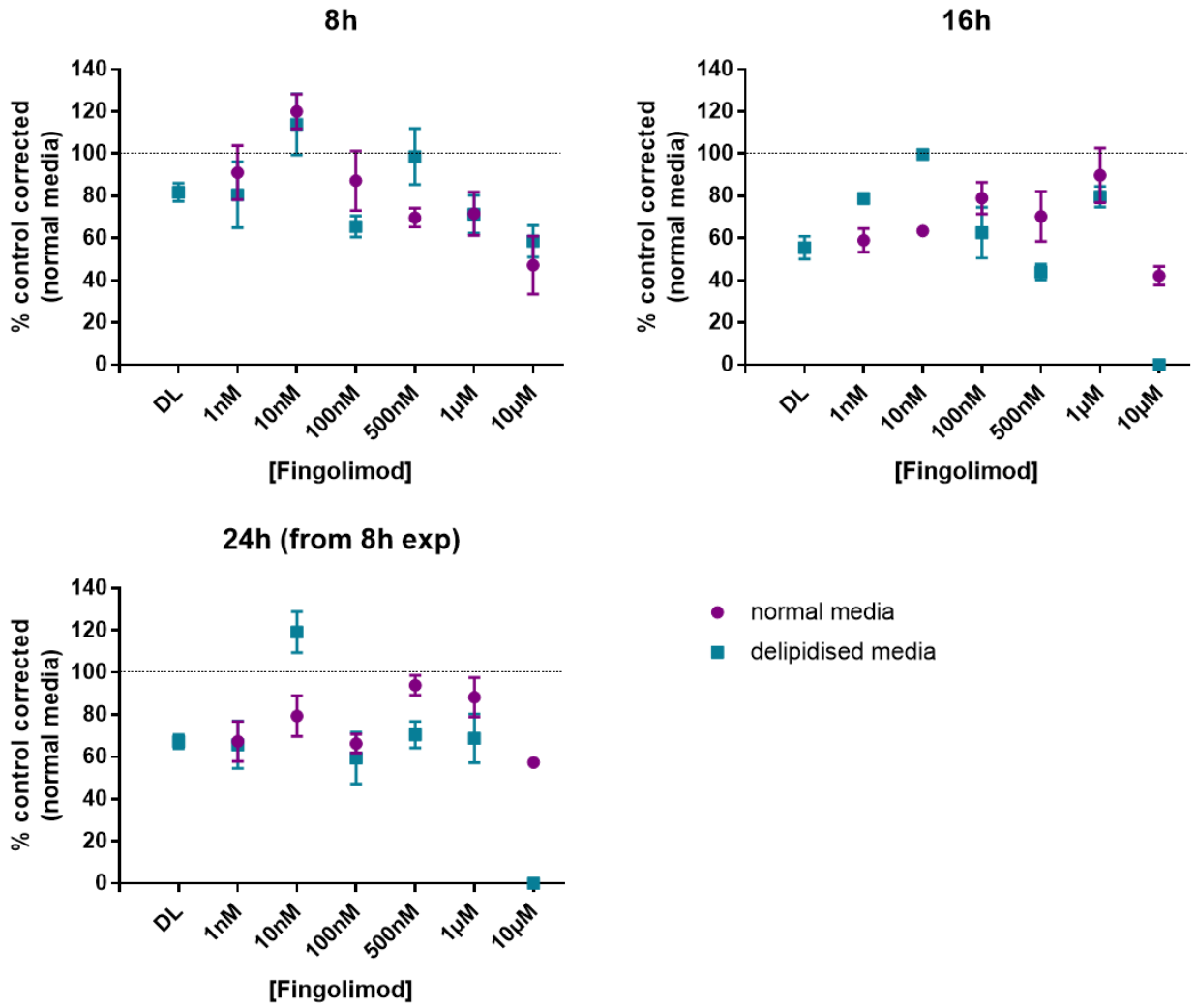

Figure 63 the effect of Fingolimod on endothelial cell migration in normal and delipidised media over time

Cells were scratched as described and cell migration into the denuded area calculated for increasing concentration of Fingolimod in either normal or delipidised media. The dotted line represents the control under normal conditions, the error bars represent the mean percentage cover +/- SEM, n=3 for both conditions.

Figure 63 highlights the difference between the effects of Fingolimod in the two lipid conditions, with 10nM Fingolimod having an inverse effect compared to all other concentrations as the cells were able to migrate more under the reduced lipid conditions.

4.4.3 TNF concentration gradient

TNF is a cytokine elevated in psoriasis and has previously been shown to activate endothelial cells and stimulate migration and may represent a synergistic partner to LDL in regulating endothelial function. Therefore the effect of various TNF concentrations on migration was also determined.

4.4.3.1 TNF concentration gradient in normal media

For the following graphs, ten-fold serial dilutions of between 10ng/mL and 1pg/mL of TNF were used, and for each assay these were performed in duplicate and the mean of three separate assays using three individual HUVEC donors at passage one were plotted.

As previously described for the other scratch assays, the data was normalised and plotted as a percentage of the control and the results are shown below in Figure 64.

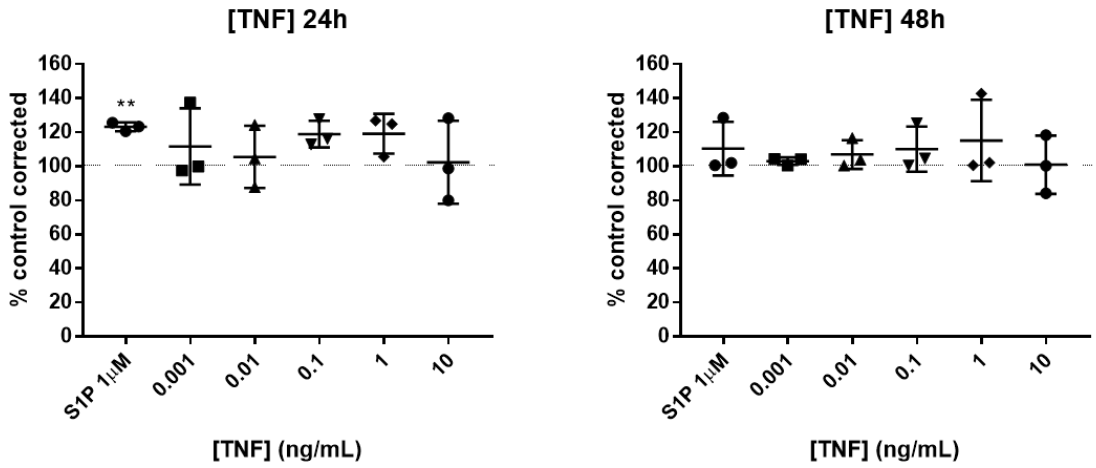

Figure 64 The normalised percentage migration of endothelial cells after TNF exposure over time
Cells were scratched as described and cell migration into the denuded area calculated for increasing concentration of TNF. These graphs show the corrected data that has been normalised to the control. The error bars represent the mean percentage cover +/- SD and the dotted line shows the migration of the control, n=3.

Surprisingly no significant difference in migration was seen across the TNF concentrations, although both 1ng/ml and 0.1ng/ml were able to achieve more than 100% of the control migration at 24 hours. Interestingly, 1μM S1P showed a significance of p= 0.0041 compared to the control at 24 hours whereas in the S1P assays no significance was found.

4.4.3.2 TNF concentration gradient in delipidised media

The same concentrations of TNF used in the full media assays were used to assess the effect of TNF in a reduced lipid environment.

Figure 65 shows the normalised data expressed as migration achieved compared to the control in normal media. The dotted line represents the migration of the control in the full lipid environment.

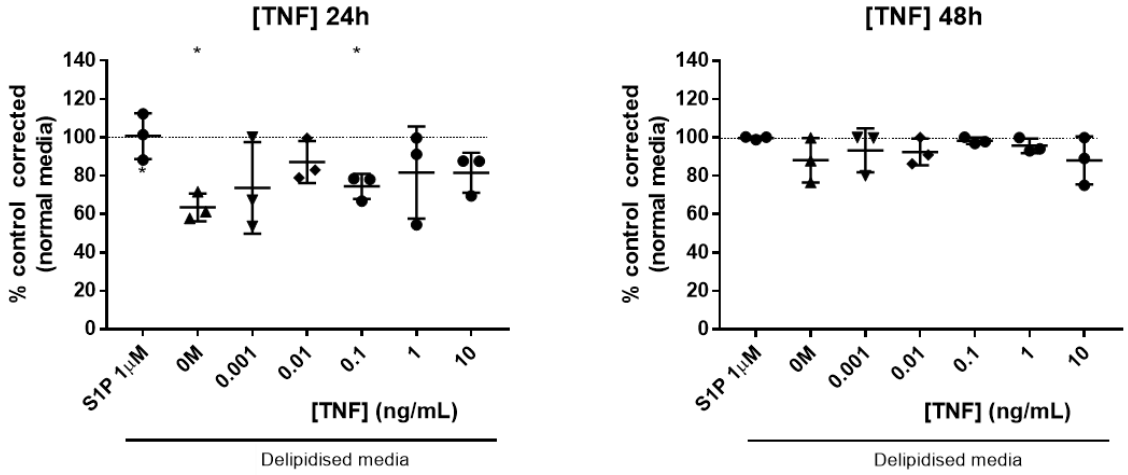

Figure 65 The normalised percentage migration after TNF exposure
Cells were scratched as described and cell migration into the denuded area calculated for increasing concentration of TNF in either normal or delipidised media. The corrected data has been normalised to the control in the full lipid environment. The error bars represent the mean percentage cover +/- SD and the dotted line shows the migration of the control, n=3.

Figure 65 shows both the delipidised control and 0.1ng/ml TNF are significantly different to the control under normal conditions (p= 0.0129 and p=0.0216 respectively). At 24 hours the removal of lipid causes a decrease in migration compared to the migration achieved in a full lipid environment. It also shows that S1P and TNF (all concentrations except 0.1ng/mL) in delipidised media are able to stimulate migration above the level of the delipidised control, with levels being more similar to that of the full lipid control. Interestingly, the inhibitory effects are lost at 48 hours, with all concentrations achieving migration similar to that of the control under normal conditions.

4.4.3.3 Combined results of TNF concentration gradient

The results of TNF migration under normal and delipidised conditions were then combined and the results are shown below in Figure 66.

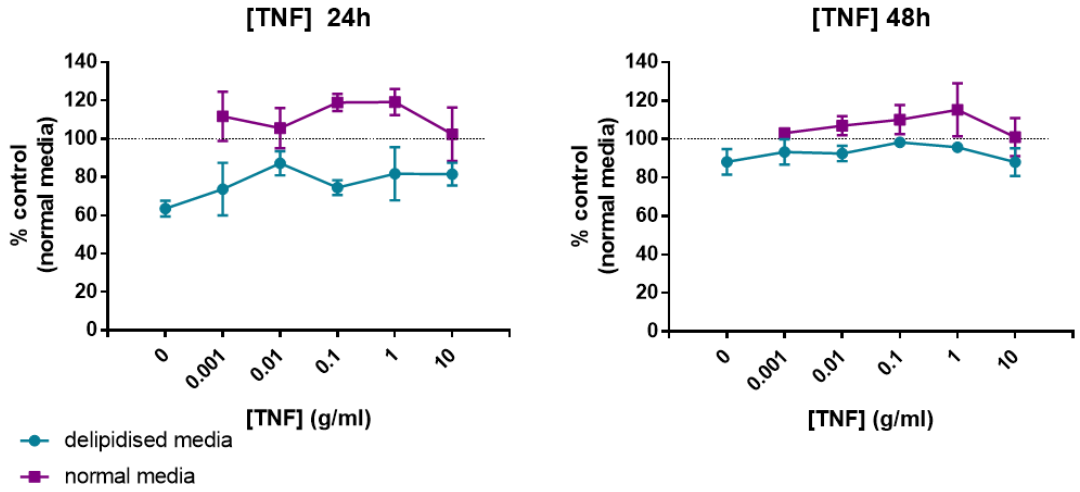

Figure 66 The effect of TNF on endothelial migration in normal and delipidised media
Cells were scratched as described and cell migration into the denuded area calculated for increasing concentration of TNF in either normal or delipidised media. Error bars show the SEM and the dotted line represents the control under normal conditions. n=3 for all samples.

The effect of the removal of exogenous lipids on migration can clearly be seen in Figure 66 (see the delipidised control at 24 hours). The addition of TNF to the reduced lipid environment is able to increase migration to near baseline control levels, especially after 48 hours.

4.4.4 S1P receptor inhibitors

Scratch assays were also used to investigate the effect of S1P receptor antagonists on migration. There are three S1P receptors found in endothelial cells (1, 2, and 3) and these were inhibited by W146, JTE and TY respectively (concentrations are shown in figures below). These inhibitors are known to be specific to their target receptor at the concentrations used, which are equivalent to approximately 100x the IC50 or Ki as reported in the literature.

4.4.4.1 S1P receptor inhibitors in normal media

To assess the receptor antagonists' effects on migration, the three S1P receptor inhibitors were used alone and in combination with S1P. The normalised data from six independent assays with endothelial cells from six donors at passage one are shown.

Figure 67 shows the normalised values for migration expressed as a percentage of the control.

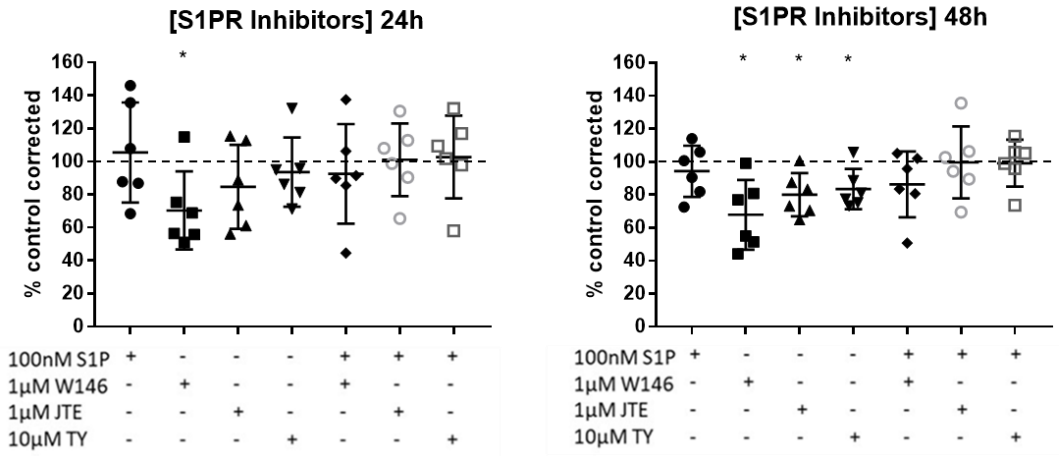

Figure 67 showing the effect of S1P and the S1P receptor inhibitors on migration after normalisation.
Cells were scratched as described and cell migration into the denuded area calculated for the three S1P receptor inhibitors. The graphs show the corrected data that has been normalised to the control. The error bars represent the mean percentage cover +/- SD, with a "+" indicating that the inhibitor has been added, n=6

The addition of the S1P receptor inhibitors has little effect on migration, with some assays showing complete closure of the scratch after 48 hours. ANOVA analysis was used to see if there was a difference between the three inhibitors abilities to inhibit migrations. A p value of p= 0.0324 was found at 48 hours and one sample t testing was therefore used to identify which receptor blockade had the greatest inhibitory effect. This revealed a significance of p= 0.0278 for W146 at 24 hours and a p value of <0.05 for W146, JTE and TY at 48 hours when compared to a hypothetical value of

100% representing the migration of the control. None of the inhibitors were able to significantly reduce the migration of HUVEC in the presence of S1P.

4.4.4.2 S1P receptor inhibitors in delipidised media

The same S1P receptor inhibitors, at the same concentrations, were also used to look at the effect of delipidised media on migration. Again, the antagonists were added either alone or with S1P and the following graphs show the normalised data expressed as a percentage of the control.

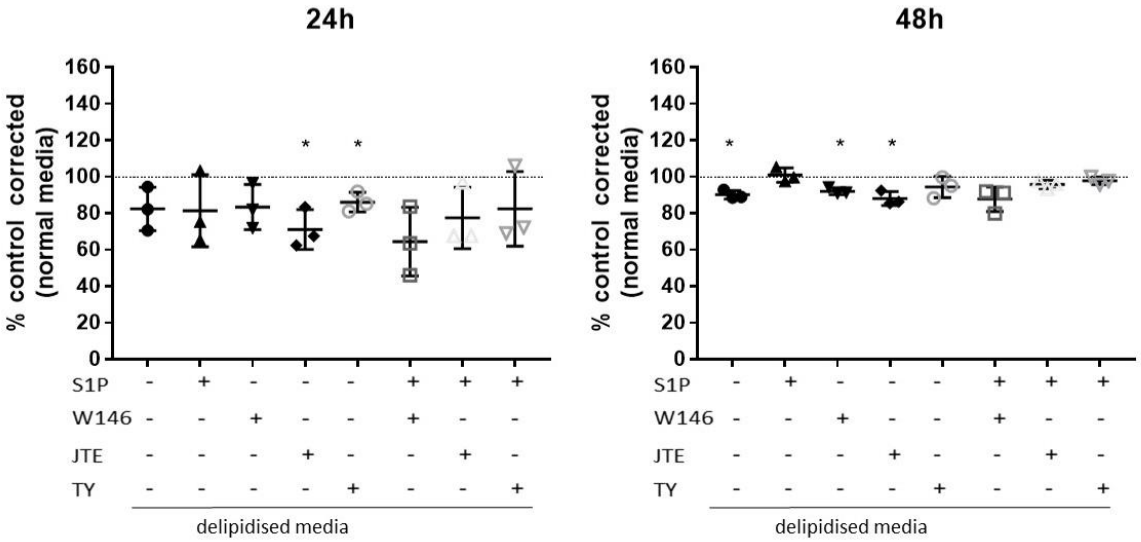

Figure 68 Showing the normalised effect of S1PR inhibitors on migration in a reduced lipid environment
Cells were scratched as described and cell migration into the denuded area calculated for the three S1P receptor inhibitors in delipidised media. These graphs show the corrected data that has been normalised to the control in full media. The error bars represent the mean percentage cover +/- SD, with a "+" indicating that the inhibitor has been added and the dotted line showing the migration of the control, n=3

One-way ANOVA was used to determine if there was a difference between the effect of the three inhibitors on migration in a reduced lipid environment and produced p value of p= 0.0086 at 48 hours. One sample t testing was then used in order to find which inhibitor had a significant effect on migration. This test compared results to hypothetical mean of 100% which represents the migration seen in the control under normal conditions as the results had been corrected to this value. Only JTE had a significant effect on migration at both 24 and 48 hours (p= 0.0445 and p= 0.0172 respectively) while TY had a p value of $p<0.05$ at 24 hours and the delipidised control and W146 had a p value of $p<0.05$ at 48 hours. None of the inhibitors were able to significantly slow the migration of HUVEC when added in combination with S1P, which mirrors the results found in the full lipid environment.

4.4.4.3 Combined results of S1P receptor inhibitors

In order to generate a clearer picture of the effect of the S1P receptor inhibitors on migration, and the potential involvement of lipids, the results under normal and reduced lipid conditions were combined. This is shown in Figure 69.

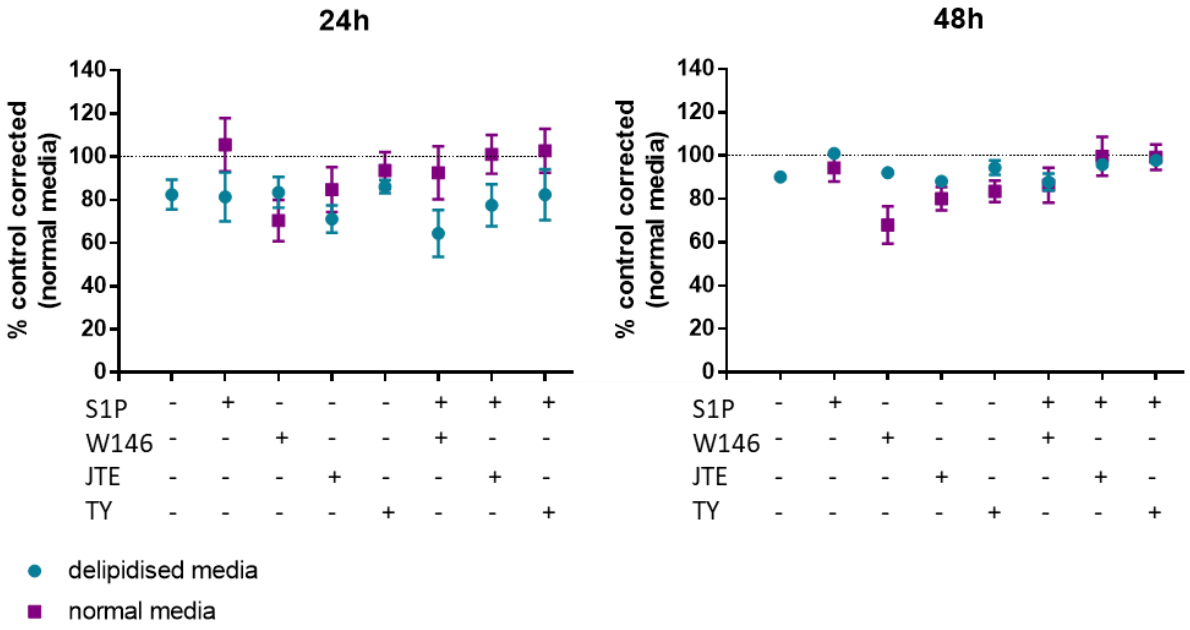

Figure 69 showing the combined results of the S1P receptor inhibitors effect on migration in normal and reduced lipid environments

Cells were scratched as described and cell migration into the denuded area calculated for the S1P receptor inhibitors in either normal or delipidised media. Error bars show the mean +/- SEM, with a "+" indicating that the inhibitor has been added and the dotted line represents the control under normal conditions. n= 6 for normal media and n= 3 for delipidised media.

The combined graphs of the S1P receptor inhibitors in both normal and delipidised media shows some interesting results, with the inhibitors appearing to have more of an effect when exogenous lipids are present, while having a reduced effect at blocking migration when lipids have been removed from the system. The greatest variation between the two different environments seems to be when W146 is added alone with virtually no difference seen after 24 hours when the inhibitors are added in combination with S1P.

4.4.5 Sphingosine kinase and S1P lyase Inhibitors

Inhibitors against two other targets in the S1P signalling pathway (sphingosine kinase II and S1P lyase) were also used as it was expected that interfering with the formation and breakdown of S1P would have an effect on migration.

4.4.5.1 Sphingosine kinase and S1P lyase Inhibitors in normal media

To assess the inhibitors effects on migration, they were used alone and in combination with S1P. The normalised data from four independent assays with endothelial cells from different donors at passage one are shown, and the results are shown below in Figure 70.

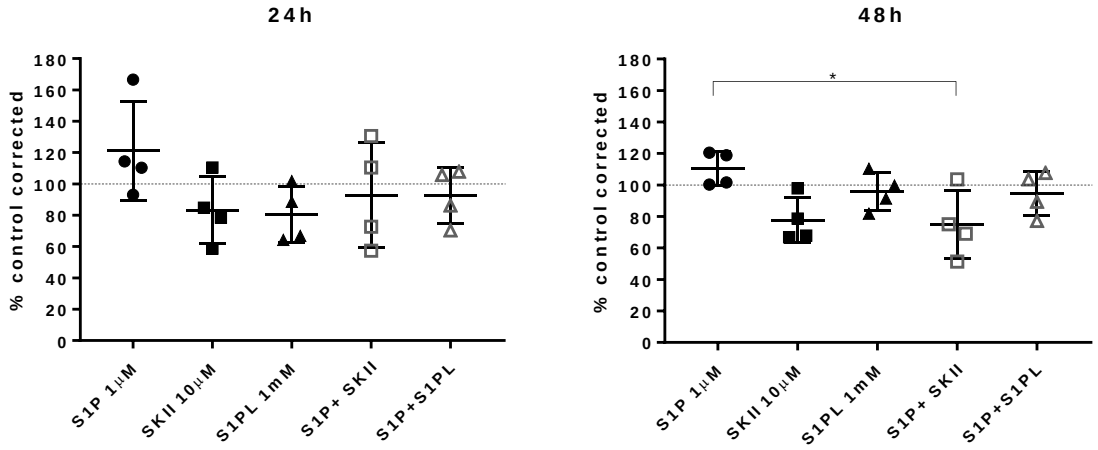

Figure 70 Normalised values showing the effect of SKI-I and S1PL inhibitors on migration
Cells were scratched as described and cell migration into the denuded area calculated for the two inhibitors alone and in combination with S1P. These graphs show the corrected data once normalised to the control. The error bars represent the mean percentage cover +/- SD, n=4.

One-way ANOVA analysis showed no significance at 24 hours however a p value of <0.05 was found at 48 hours. A one-sample t-test comparing the means of the inhibitors to a hypothetical value of 100% representing the migration achieved by the control revealed no significance at either time point however Dunnett's multiple comparisons test showed a significance of <0.05 between S1P and both SKII alone and in the presence of S1P at 48 hours.

4.4.5.2 Sphingosine kinase and S1P lyase Inhibitors in delipidised media

The same inhibitors were also added to HUVEC in a reduced lipid environment to assess their effect on migration once all exogenous lipids have been removed. The corrected data is shown below in Figure 71.

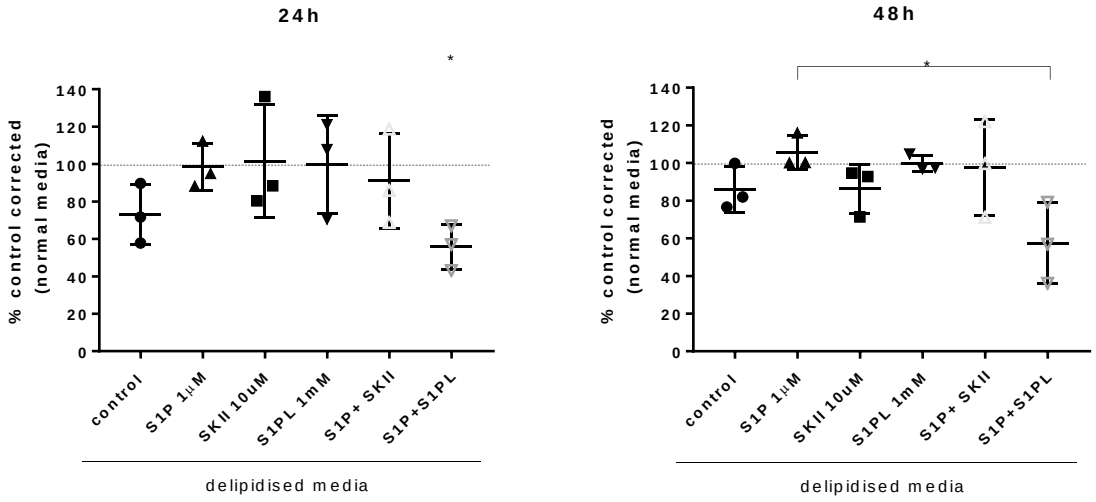

Figure 71 Showing the normalised results of SKI-I and S1PL inhibitors in delipidised media
Cells were scratched as described and cell migration into the denuded area calculated for the inhibitors either in delipidised media. The graphs show the corrected data that has been normalised to the full lipid control. The error bars represent the mean percentage cover +/- SD, n=3.

One-way ANOVA did not produce any significant results at either time point however when the migration of the inhibitors was compared to that of HUVEC in a full lipid environment using a one sample t-test, it was found that after 24 hours S1PL+S1P resulted in a decrease in migration (p= 0.0236), while no difference was found after 48 hours. Dunnett's multiple comparisons test showed that at 48 hours there was a significant difference between S1P and S1P in combination with the lyase inhibitor (p= 0.0288).

4.4.5.3 Combined results of the sphingosine kinase and S1P lyase Inhibitors

The results obtained from the SKI-I and S1PL Inhibitors in both full lipid and reduced lipid environments were then combined and the results are shown below in Figure 72.

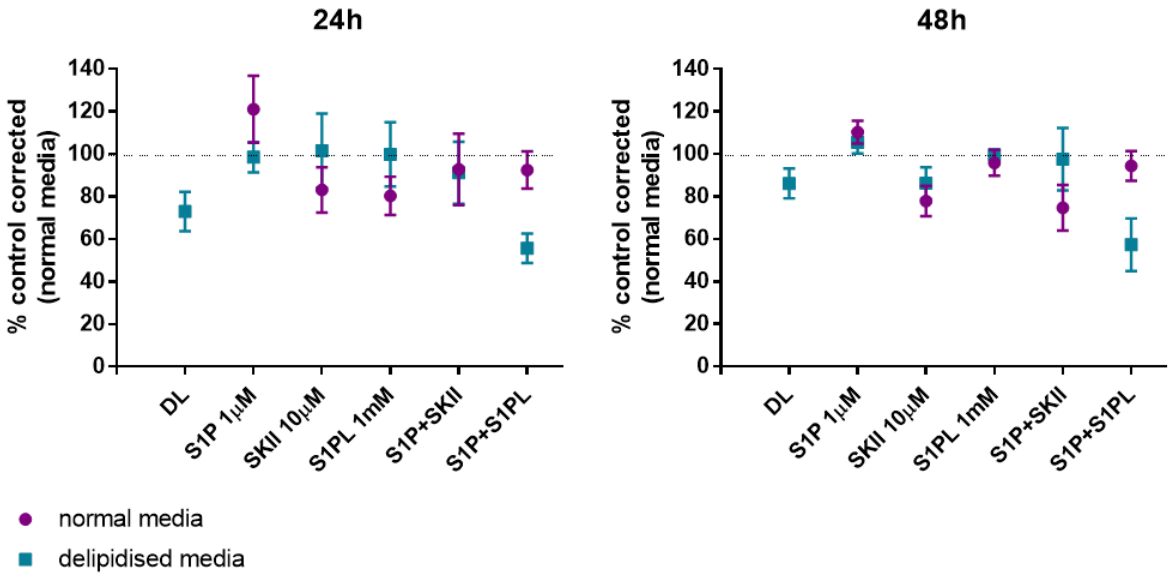

Figure 72 showing the combined results of the SKII and S1PL inhibitors effect on migration in normal and reduced lipid environments
Cells were scratched as described and cell migration into the denuded area calculated for the two inhibitors either in normal or delipidised media. The graphs show the corrected data that has been normalised to the full lipid control. The error bars represent the mean percentage cover +/- SEM, n= 4 for normal media and n= 3 for delipidised media, DL= delipidised control.

Comparing the effect that the sphingosine kinase and S1P lyase inhibitors have on migration in both a full lipid and a reduced lipid environment shows that the removal of the lipids negates the slight inhibition seen in the full media. The greatest difference between these two inhibitors was found to be when S1PL is added in combination with S1P as at both time points there is a clear inhibition of migration in the delipidised environment.

4.4.6 MEK, p38 and SAPK/JNK Inhibitors

Other inhibitors were also used to study the migration of HUVEC and included inhibitors against phosphorylation kinase cascade targets MEK (PD), p38 (SB) and SAPK/JNK (JNKII). This allowed the differences in migration to be determined between interfering with the S1P signalling pathway, as investigated in previous sections and other important signalling pathways known to be involved downstream of S1P signalling and in migration.

4.4.6.1 MEK, p38 and SAPK/JNK Inhibitors in normal media

To assess the inhibitors effects on migration, they were used alone and in combination with S1P. The normalised data, expressed as a percentage of the control, from seven independent assays using endothelial cells from seven donors, is shown below in Figure 73.

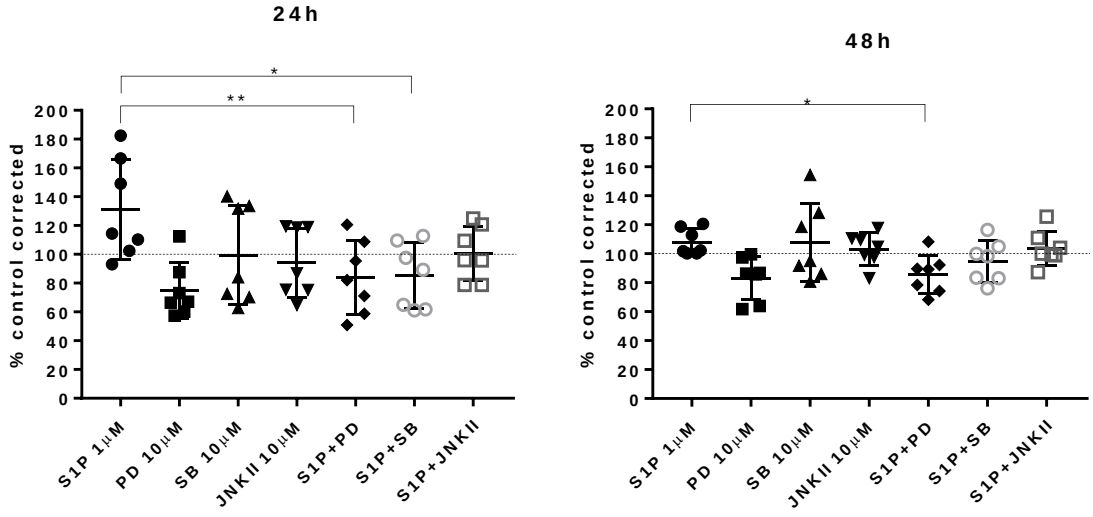

Figure 73 Normalised values showing the effect of MEK, p38 and SAPK/JNK inhibitors on migration

Cells were scratched as described and cell migration into the denuded area calculated for the various inhibitors. These graphs show the corrected data once normalised to the control. The error bars represent the mean percentage cover +/- SD, n=7.

One-way ANOVA was used to determine if there was a significant difference between the inhibitors either alone or in combination with S1P at each time point. At 24 hours a p value of p= 0.0089 was found and a p value of p= 0.0124 was found after 48 hours. A one sample t-test was then used to identify if the means of the inhibitors was significantly different to that of the control (taken to be 100%). After 24 hours, only the PD inhibitor was found to be significantly different showing that this inhibitor has an inhibitory effect on the migration of HUVEC (p= 0.0136). Interestingly, after 48 hours this inhibitor was also found to be able to counteract the effects of S1P as both the inhibitor alone and in the presence of S1P were found to be significantly different from the control (p= 0.0235

and 0.0297). Dunnett's multiple comparisons test was also used to find out if there was a difference in migration when the inhibitors were used in combination with S1P compared to S1P alone. It was found that at 24 hours both PD+S1P and SB+S1P were significantly different from S1P (with p values of <0.01 and <0.05 respectively), however only PD+S1P was found to be significant after 48 hours ($p<0.05$) and is highlighted on the above graphs.

4.4.6.2 MEK, p38 and SAPK/JNK Inhibitors in delipidised media

To try and gain a better understanding of the role of the kinase cascade targets in the migration of HUVEC, the assay was repeated in a reduced lipid environment. Again the inhibitors were used alone and in combination with S1P and the results of three independent experiments are shown below in Figure 74.

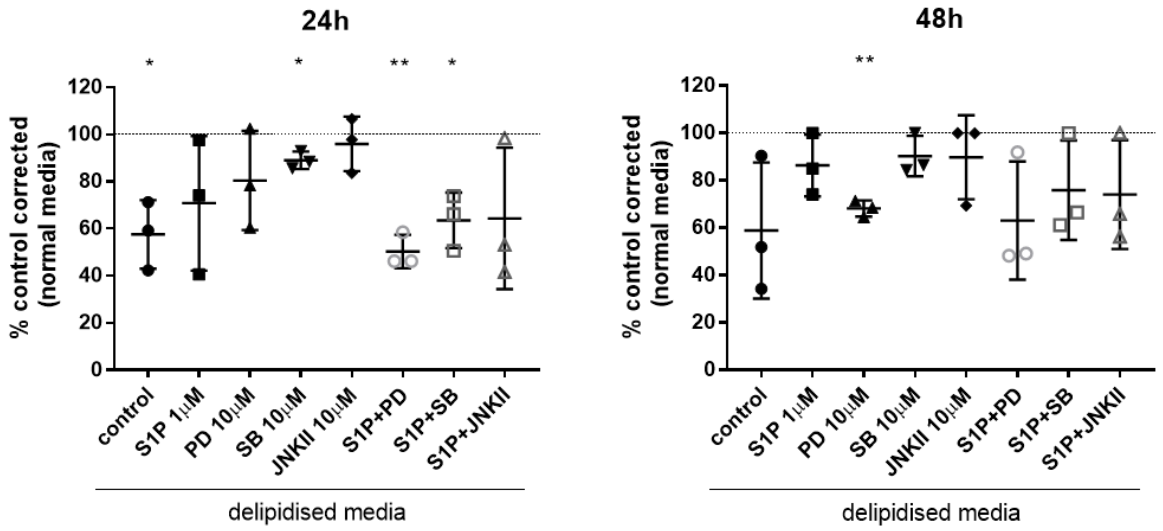

Figure 74 showing the normalised results MEK, p38 and SAPK/JNK inhibitors in a reduced lipid environment

Cells were scratched as described and cell migration into the denuded area calculated for the inhibitors either in delipidised media. The graphs show the corrected data that has been normalised to the control in a full lipid environment. The error bars represent the mean percentage cover +/- SD, n=3.

One-way ANOVA with Dunnett's multiple comparisons test did not produce any significant results at either time point. However one sample t-testing comparing the migration of the inhibitors to that of HUVEC in a full lipid environment found that after 24 hours the delipidised control, SB alone, PD+S1P and SB+S1P all resulted in a decrease in migration relative to the hypothetical 100% migration in complete media. After 48 hours, only PD was found to have an inhibitory effect on HUVEC migration. The results of the one sample t-tests are highlighted by the stars on the graphs above.

4.4.6.3 Combined results of the MEK, p38 and SAPK/JNK Inhibitors

In order to compare the effect of the three inhibitors in both the full and reduced lipid environment, and therefore to see what effect, if any, the removal of lipids has, the results presented in the previous two section were combined and are shown in Figure 75 below.

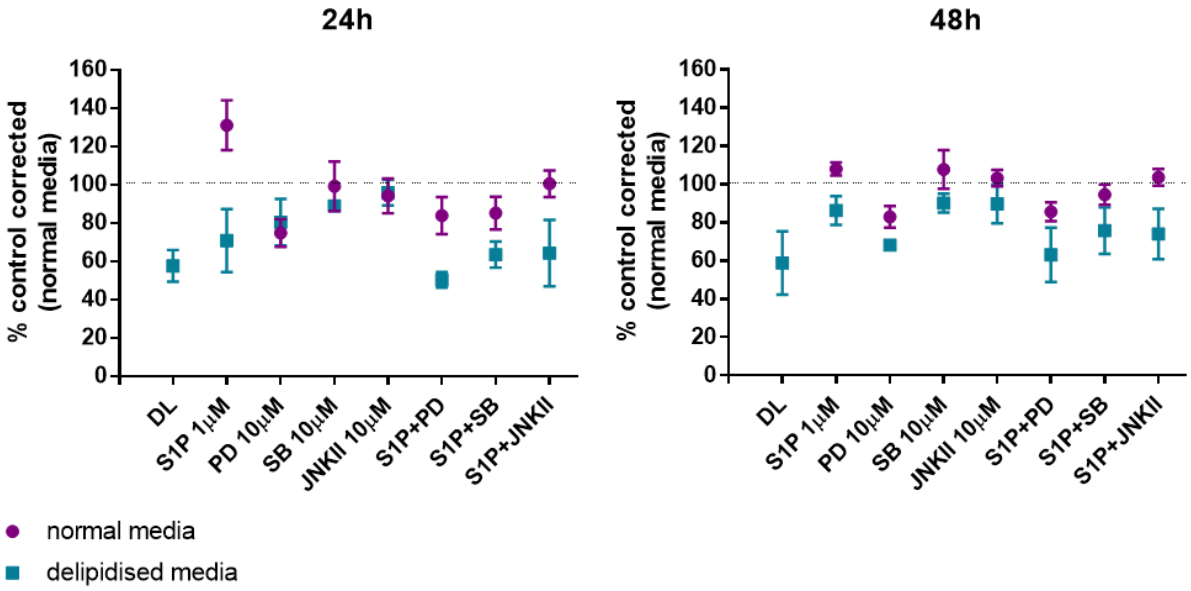

Figure 75 showing the combined results of the MEK, p38 and SAPK/JNK inhibitors effect on migration in normal and reduced lipid environments
Cells were scratched as described and cell migration into the denuded area calculated for the two inhibitors either in normal or delipidised media. The graphs show the corrected data that has been normalised to the full lipid control. The error bars represent the mean percentage cover +/- SEM, n= 7 for normal media and n= 3 for delipidised media, DL= delipidised control.

Figure 75 shows that after 24 hours the inhibitors of MEK, p38 and SAPK/JNK have no effect on the migration of HUVEC between the full lipid and reduced lipid environment when added alone, with only a slight difference being seen at 48 hours. There is however a difference when they are added in combination with S1P at both time points, with an inhibition of migration being seen with PD and SB in the delipidised system compared to the full lipid environment.

4.4.7 Oxidised LDL

The effect of oxLDL on migration has previously been studied using HUVEC and was shown to have a concentration dependent effect, with high concentrations resulting in an inhibition of migration. In order to draw comparisons between the migration of cells exposed to S1P and oxLDL, and potentially establish a link between the two, these experiments were repeated with the expectation that similar results would be obtained.

4.4.7.1 oxLDL concentration gradient in normal media

The same concentrations of oxLDL that had previously been used (5 and 100 µg/mL) were again studied, with the same concentration of LDL being used for comparison. Each concentration in each assay was performed in duplicate and the assays were carried out on four occasions with four individual donor endothelial cells at passage one.

As previously described for the other scratch assays, the data was normalised and plotted as a percentage of the control and the results are shown below in Figure 76.

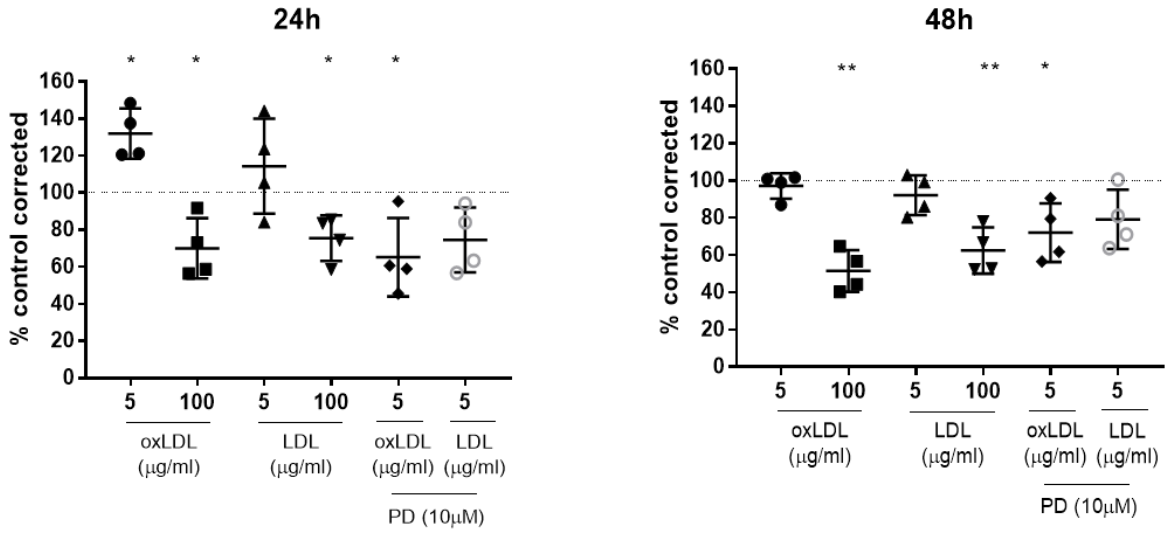

Figure 76 Normalised values showing the effect of oxLDL on migration
Cells were scratched as described and cell migration into the denuded area calculated for the various concentrations of oxLDL and LDL. These graphs show the corrected data once normalised to the control. The error bars represent the mean percentage cover +/- SD, n=4.

One-way ANOVA analysis gave a p value of 0.0002 at 24 hours and 0.0005 at 48h hours. One sample t-testing was used to determine if the means of oxLDL/LDL were significantly different to the mean of the control (100%) and these results are represented by the stars on the above graphs. As expected, it can be seen that 5µg/mL oxLDL stimulated migration above that of the control while 100µg/mL oxLDL inhibited migration. Tukey's multiple comparisons test was also used in order to

compare the means across oxLDL and LDL. It was found that after 24 hours there was no significance between 5µg/mL oxLDL and LDL or 100µg/mL oxLDL and LDL. There was however a significant difference between 5µg/mL oxLDL and 5µg/mL oxLDL + PD (p=0.0008), with no significance being seen between 5µg/mL LDL and 5µg/mL LDL + PD. No significance was found after 48 hours between these groups.

4.4.7.2 oxLDL concentration gradient in delipidised media

As with all other compounds used, the effect of oxLDL on migration in both normal and delipidised media was studied with the theory that the reduced lipid system may provide a clearer picture of this process. The following graphs (Figure 77) show the results obtained in this reduced lipid environment.

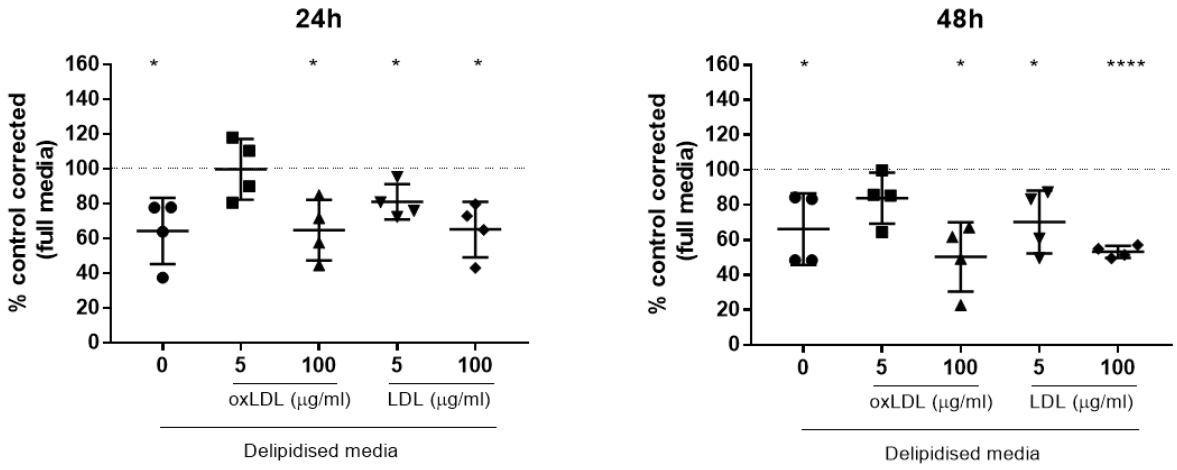

Figure 77 showing the normalised effect of oxLDL on migration in a reduced lipid environment
Cells were scratched as described and cell migration into the denuded area calculated for oxLDL and LDL in delipidised media. The graphs show the corrected data that has been normalised to the control. The error bars represent the mean percentage cover +/- SD, n=4.

One-way ANOVA analysis gave a p value of 0.0288 at 24 hours and 0.0687 at 48h hours. One sample t-testing was used to determine if the means of oxLDL/LDL were significantly different to the mean of the full media control (100%) and these results are represented by the stars on the above graphs. As shown previously in the full lipid assays, 5µg/ml oxLDL is able to stimulate migration, in this case enough to reach the full lipid control levels at 24 hours. Dunnett's multiple comparisons test was then used to compare the concentrations of oxLDL and LDL to that of the delipidised control. At 24 hours, this gave a p value of 0.0251 between the delipidised control and 5µg/ml oxLDL, with no other concentrations being significant and no significance was seen after 48 hours.

4.4.7.3 Combined results of oxLDL concentration gradient

The following graphs show the combined data for oxLDL in both normal and delipidised media over 48 hours to highlight the effect of removing lipids from the system has on migration. The data plotted has been normalised and is shown as a percentage of the control (i.e. normal media with no oxLDL) which is taken to be 100%. The error bars show the standard error of the mean in order to provide a clearer view of the two lines, however the data is the same as plotted in the above graphs.

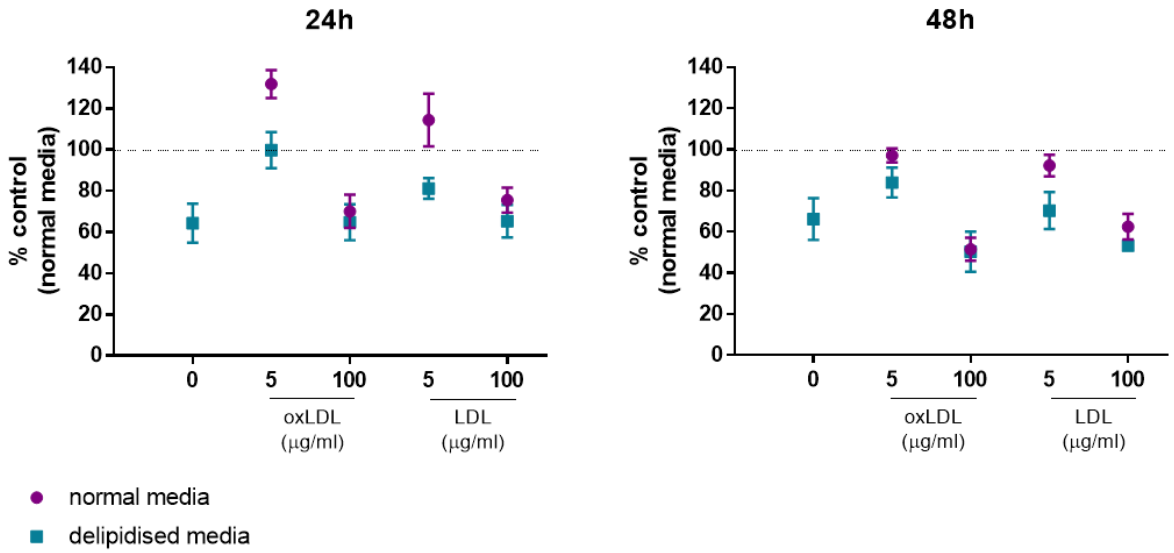

Figure 78 effect of oxLDL on endothelial cell migration in normal and delipidised media over time
Cells were scratched as described and cell migration into the denuded area calculated for oxLDL and LDL in either normal or delipidised media. The dotted line represents the control under normal conditions, error bars represent the mean percentage cover +/- SEM, n=4

Figure 78 shows the difference of endothelial migration in response to oxLDL under normal and reduced lipid environments. After 24 hours there is a clear difference between 5µg/ml oxLDL in normal and delipidised media, however even in the reduced lipid environment this concentration has a stimulatory effect on the migration of HUVEC. As the assay progresses this difference becomes less as the scratch becomes fully closed. In contrast, there is no difference between the two media conditions for 100µg/ml oxLDL, with both points overlapping at both 24 and 48 hours.

4.4.8 ox-albumin and lipid supplement

Albumin is a known carrier of S1P in the circulation and therefore the effect of albumin and oxidised albumin (ox-albumin) on the migration of HUVEC was also investigated. This was achieved by using the basic M199 media without any additives (such as human serum or other proteins) and then either albumin or ox-albumin added at the desired concentration. A lipid supplement was also used in order to see if the levels of migration in a delipidised system could be recovered to that of the full lipid media. Plain M199 media was used with no additives to assess the effect of albumin on endothelial migration. A brief summary of the results is shown in Table 8 below.

Table 8 effect of ox-albumin and lipid supplement on migration

Condition	Result
Full media	Scratch closed after 48h
M199 only	Floating after 24h
M199 + albumin	Rough at 24h, floating at 48h
M199 + ox-albumin	Rough at 24h, floating at 48h
M199 + 1:100 lipid sup.	Floating after 24h
M199 + 1:1000 lipid sup.	Floating after 24h
M199 + albumin + 1:100 lipid sup.	Rough at 24h, floating at 48h
M199 + albumin + 1:1000 lipid sup.	Rough at 24h, floating at 48h
M199 + ox-albumin + 1:100 lipid sup.	Rough at 24h, floating at 48h
M199 + ox-albumin + 1:1000 lipid sup.	Rough at 24h, floating at 48h
M199 + S1P	Floating after 24h
M199 + albumin + S1P	Rough at 24h, floating at 48h
M199 + ox-albumin + S1P	Floating after 24h

Cells were described as “floating” when they appeared as phase bright and spherical and where no trace of the original scratch could be seen. In cases where there were floating cells as well as attached cells, these have been described as “rough”. Due to the number of floating cells at the first time point (24 hours), it was not possible to measure the area of the scratch to compare the different conditions. Therefore the effect of ox-albumin and the lipid supplement at 24 and 48 hours is shown by representative images below.

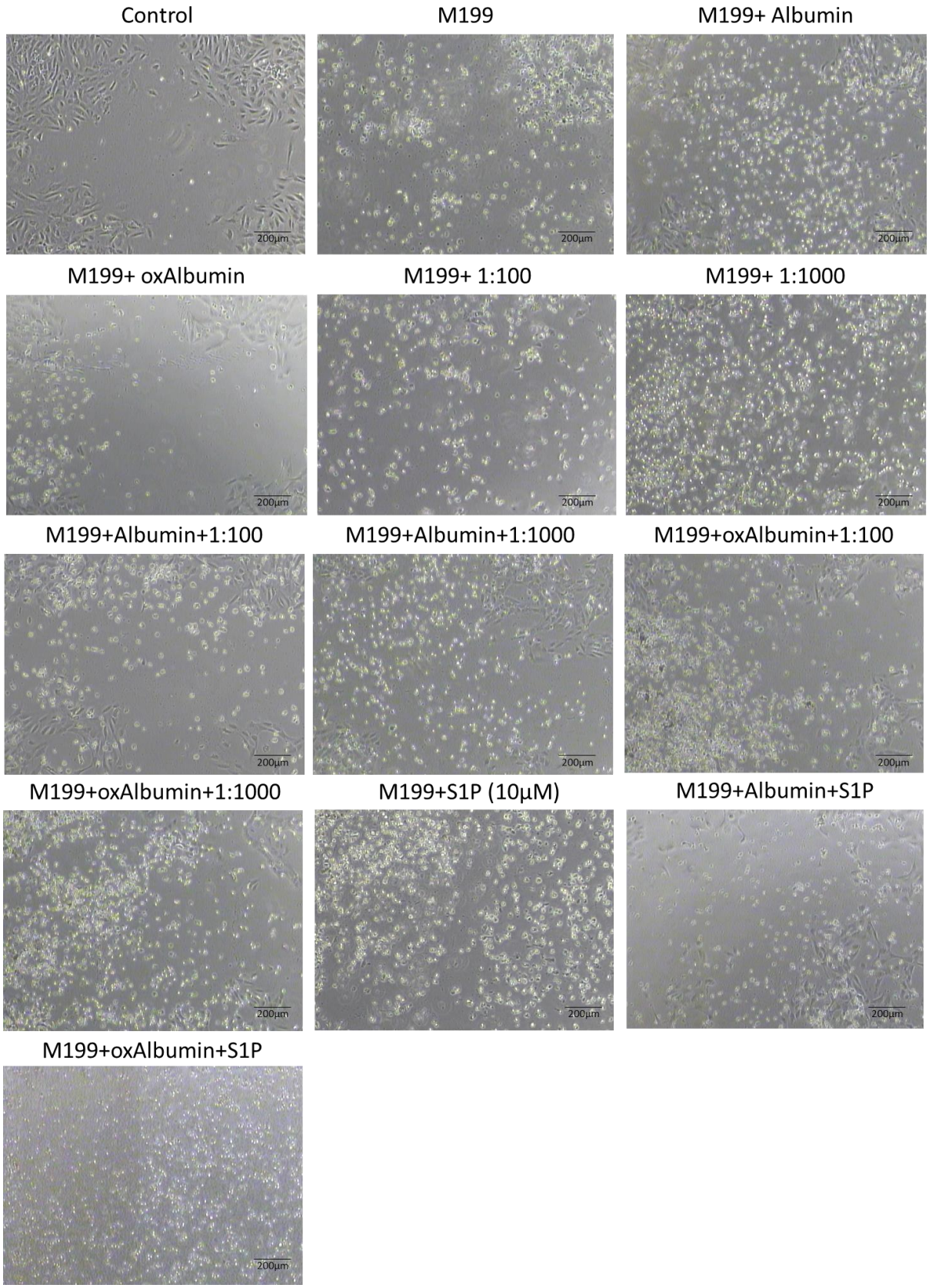

Figure 79 effect of ox-albumin and lipid supplement on HUVEC migration after 24 hours
Cells were scratch as described and representative images shown for the various conditions. Images are in the order listed in Table 8 and highlight the effect of ox-albumin and the lipid supplement (1:100/1:1000) on endothelial cells.

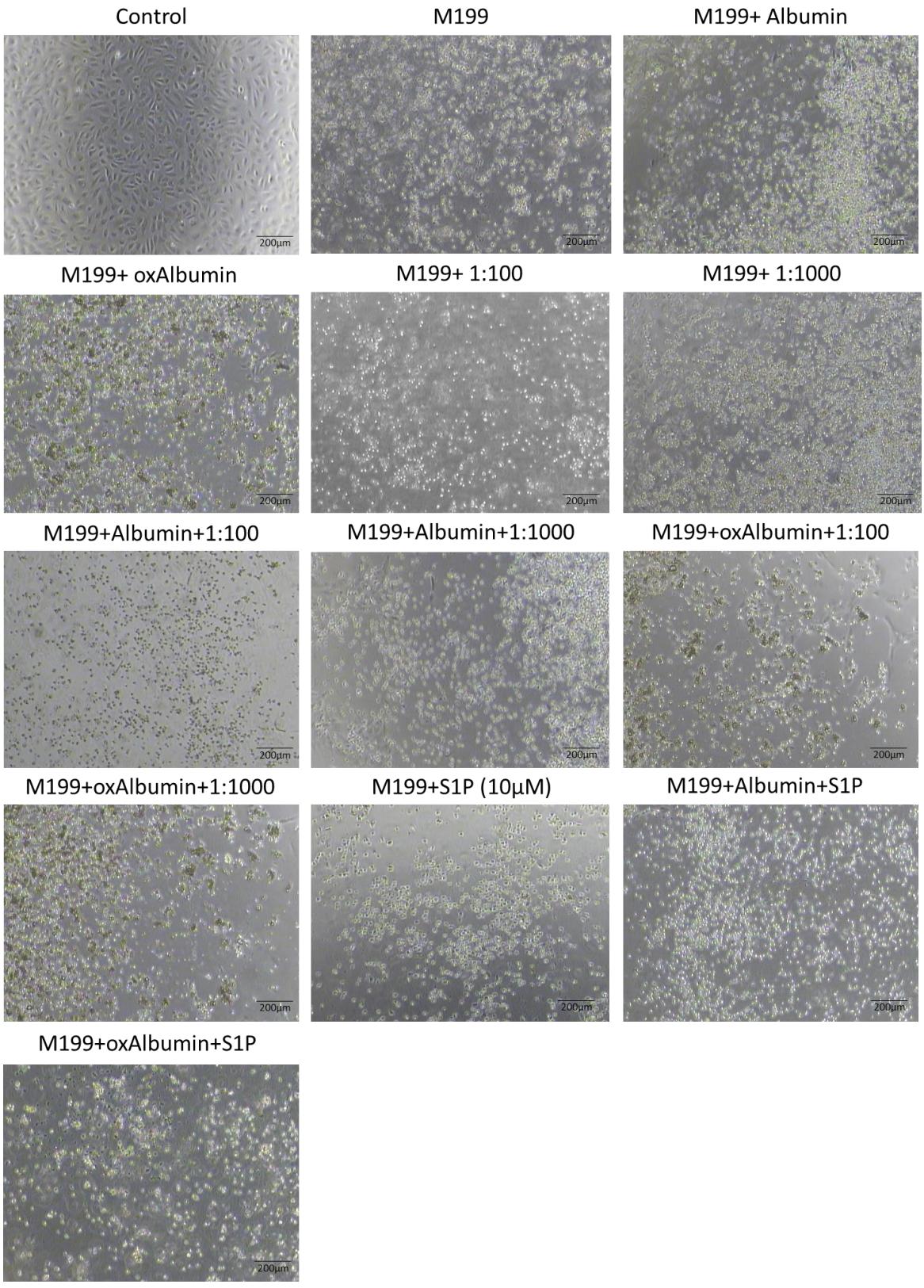

Figure 80 effect of ox-albumin and lipid supplement on HUVEC migration after 48 hours
Cells were scratch as described and representative images shown for the various conditions. Images are in the order listed in Table 8 and highlight the effect of ox-albumin and the lipid supplement on endothelial cells.

From Figure 80 it can be seen that after 48 hours, only the control cells are still attached, with all combinations of albumin, oxidised albumin and lipid supplement resulting in floating cells.

4.4.8.1 S1P bound Albumin

As mentioned previously, albumin is a carrier of S1P and therefore it is possible that when they are added separately in the assays, that S1P is taken up by the albumin. It was decided to attempt to load S1P on to albumin or ox-albumin before then adding them to the assays to see if there was a difference in the migration of endothelial cells between free and bound S1P. This was achieved as described in the methods (2.7.3).

A number of combinations of albumin, oxidised albumin and either bound or free S1P were carried out, however some of the combinations resulted in the cells becoming detached from the plastic and therefore no measurement of the scratch could be taken after 24 hours. Some of the combinations had been used previously and are listed in Table 8, therefore only the new combinations have been listed in Table 9 below. As before, plain M199 media was used unless otherwise stated.

Table 9 effect of S1P bound to albumin on migration

Condition	Result
Full media	Scratch closed after 48h
M199 only	Floating after 24h
10µM S1P in M199	Floating after 24h
S1P bound ox-albumin	Floating after 24h
dialysed BSA+ free S1P	Rough at 24h, floating at 48h

Cells were described as “floating” when they appeared as phase bright and spherical and where no trace of the original scratch could be seen. In cases where there were floating cells as well as attached cells, these have been described as “rough”. Due to the number of floating cells at the first time point (24 hours), it was not possible to measure the area of the scratch to compare the different conditions.

For the combinations that could be measured, the results of the normalised data expressed as a percentage of the control are shown below in Figure 81.

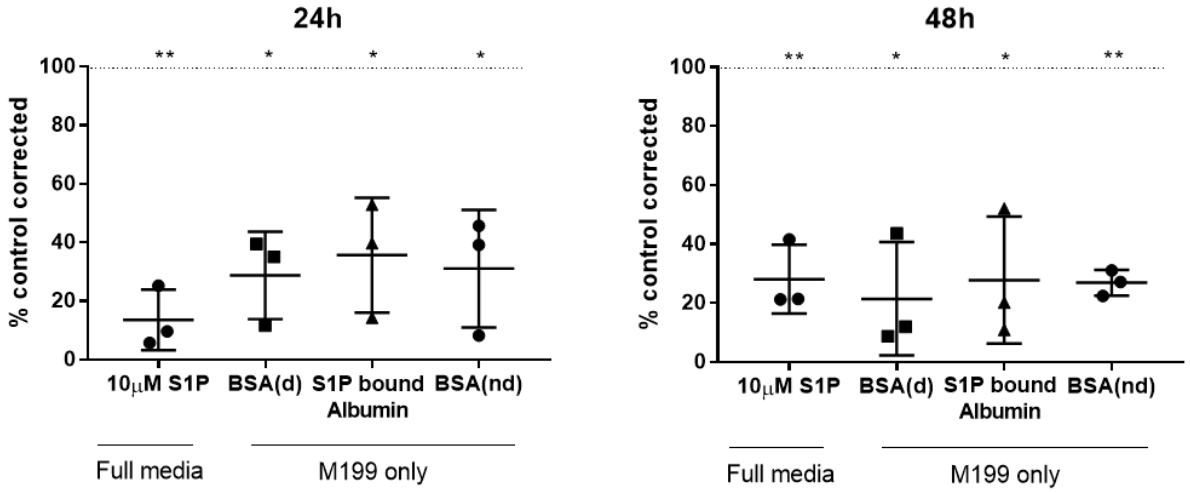

Figure 81 showing the normalised effect of S1P bound to albumin on migration
Cells were scratched as described and cell migration into the denuded area calculated for the various conditions. These graphs show the corrected data once normalised to the control. The error bars represent the mean percentage cover +/- SD, n=3, (d)- dialysed, (nd)- non-dialysed.

One-way ANOVA was used to determine if there was a significant effect on endothelial migration when cells were exposed to albumin and S1P in various combinations, however no significance was found at either 24 or 48 hours. One sample t-testing was then used to determine if the means of the various combinations were significantly different to the mean of the full media control (represented by 100%) and these results are highlighted by the stars on the above graphs. It can be seen that all combinations shown are significantly different from the full media control. It should however be noted that although there is an inhibition of migration compared to the control, that cells exposed to M199 only, quickly detached from the plastic and therefore as the calls were able to remain attached, it could be argued that there is in fact a stimulatory effect.

From Table 9 and Figure 81 it can be seen that there is a difference between S1P bound to either albumin or oxidised albumin, with only the cells exposed to the un-oxidised form of albumin remaining attached to the plastic and able to migrate.

4.4.9 Confluent cells

As a result of observations made during the course of the scratch assays, regarding the change in shape of the cells or their spreading apart in response to some of the compounds, it was decided to see if this effect was also seen when these compounds were added to a confluent monolayer of cells. Fingolimod is known to cause vessel leakiness therefore whether Fingolimod had an effect on an established monolayer was investigated. In order to do this, cells were plated at least 24 hours before the start of the assay and then an image taken 24 and 48 hours after the addition of the compounds of interest. These images were then analysed using the wound healing tool in Fiji, with settings adjusted to: variance filter radius=4, threshold=70, radius open=4 and min. size=100. An example of the results obtained via this method is shown below in Figure 82.

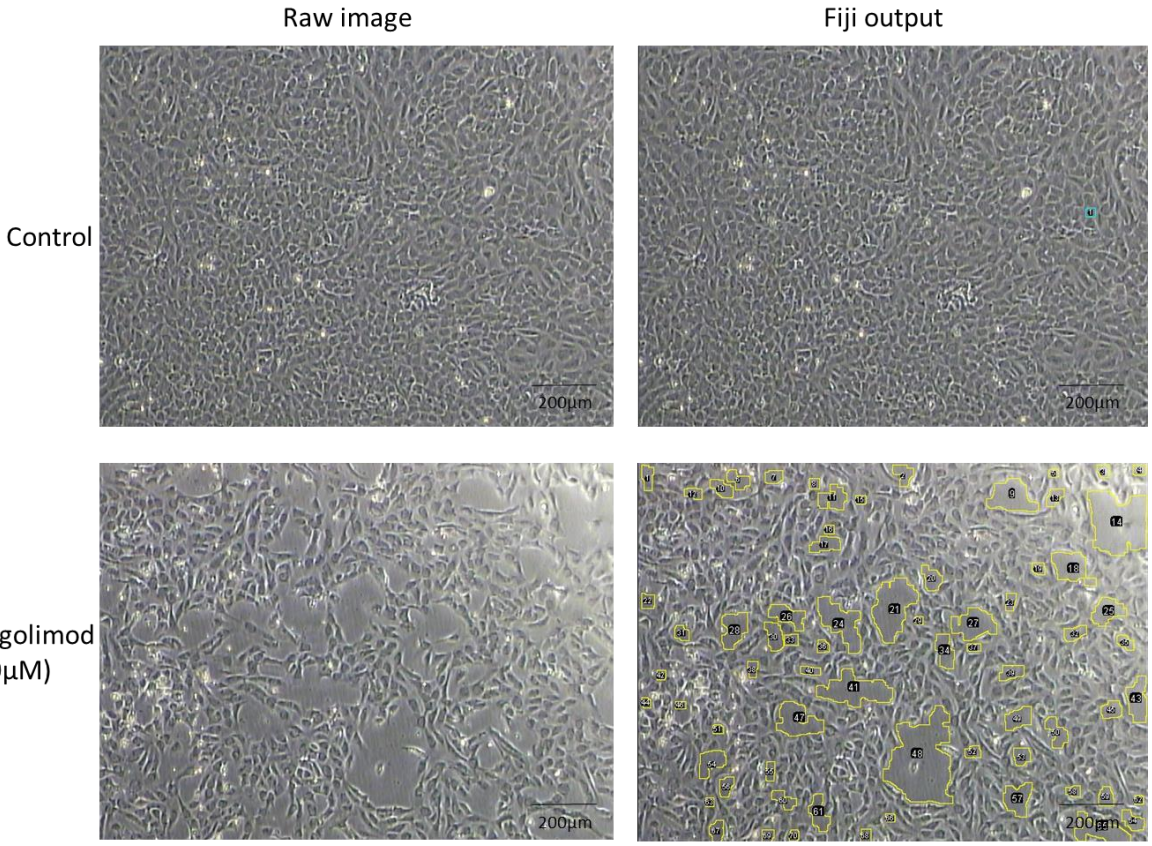

Figure 82 Fiji output after wound healing tool analysis
An example of the output from the Fiji wound healing analysis showing the spaces between the cells outlined in yellow. The same settings were used for both the control and the Fingolimod image and both images were taken 24 hours after the start of the assay.

Once the images were analysed, the total area measured was subtracted from the total area of the image to give an overall percentage cover, i.e. the larger the gaps between cells equals less percentage cover. These results are shown below in Figure 83.

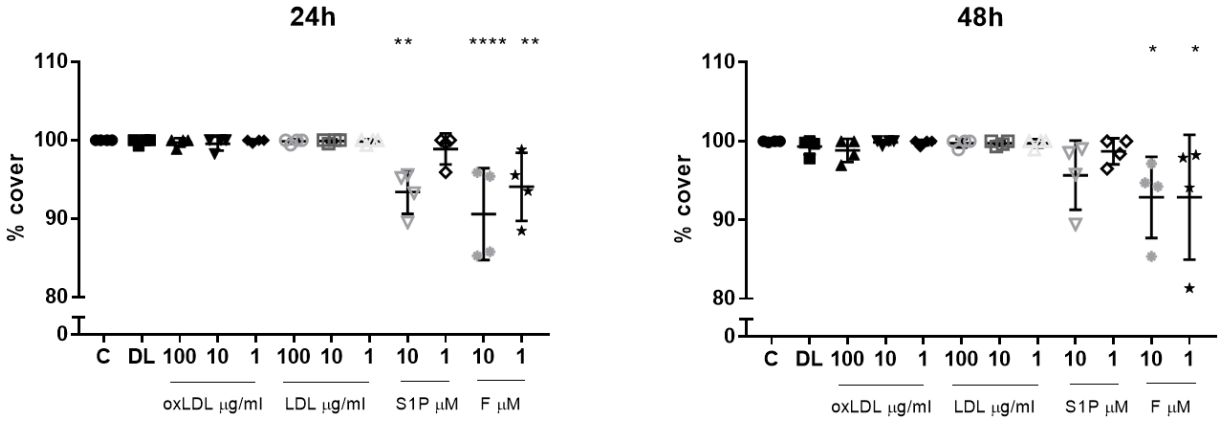

Figure 83 effect of oxLDL, LDL, S1P and Fingolimod on confluent cells
oxLDL, LDL, S1P and Fingolimod were added to confluent monolayers of cells and imaged after 24 and 48 hours. The area of gaps was measured and the overall percentage cover calculated, n=4. DL=delipidised media

It is clear from Figure 83 that delipidised media, oxLDL and LDL do not have any effect on the level of cover of a monolayer of endothelial cells, while S1P and Fingolimod have a small but significant concentration and time dependent effect. One-way ANOVA gave a p value of <0.0001 at 24 hours and 0.0058 at 48 hours. Dunnett's multiple comparisons test was used to see if there was a difference between the control and any of the other conditions and these results are highlighted by the stars of the graphs above. As expected from the results of the scratch assays, Fingolimod (particularly 10µM, p=0.0001) produced the greatest increase in area between the cells, while only the highest concentration of S1P produced a response at 24 hours, which was negated after 48 hours.

4.5 Discussion

Scratch assays were used to assess the migration of HUVEC under various conditions including the addition of lipids such as S1P and numerous inhibitors as well as the effect of a delipidised environment. One of the limitations of this assay is that it becomes less sensitive as the assay progresses, i.e. the closer to closing the scratch is. It is therefore often not possible to see stimulation above the control at 48 hours as the cells can only reach 100% migration i.e. close the scratch. The use of an additional, earlier time point would be one potential way to see stimulation right up until the scratch is closed and measure the rate of closure (% per unit time of distance migrated per unit time).

4.5.1 Sphingosine-1-phosphate

It is hypothesised that oxLDL signals through S1P to bring about its effects. In order to be able to compare the effects of these two lipids, scratch assays of various concentrations of S1P were used to assess the effect of S1P on migration. It was discovered that the highest concentration of S1P used (10µM) had an inhibitory effect on the migration of HUVEC while all other concentrations had no significant effect on migration. After 48 hours, 10µM S1P has a reduced inhibitory effect. This is as expected as the cells are migrating into a fixed space so after 48 hours the difference between the control and 10µM S1P is not as great due to the control already having reached 100% migration. This suggests that migration is slowed rather than completely inhibited and also that the cells are still alive and that the high concentration of S1P is not cytotoxic. This has been confirmed using live/dead staining previously (Chapter 3:). It was expected that the addition of the lower concentrations of S1P would result in an increase in migration rate above the control as this had previously been observed with S1P and oxLDL and it is hypothesised that oxLDL signals through S1P dependent mechanisms. From the results of the S1P assays this stimulation was not clearly observed, however stimulation with 1µM S1P was seen in other assays e.g. the TNF assay. Both the high concentrations of S1P and oxLDL had a similar inhibitory effect on migration suggesting that there may indeed be a link between these two bioactive lipids. This difference in lack of stimulation seen with S1P may be due to differences in signalling pathways between S1P and oxLDL but also the conditions under which the assays have been performed. Previously, serum dilutions where both protein and lipid have been reduced have shown a slower migration response in control cells above which S1P could stimulate an accelerated migration (data unpublished).

It is interesting to note the difference between the migration results and the p-ERK results as the migration results showed a more bell shaped curve with some stimulation and inhibition seen whereas the p-ERK data suggest a more sigmoid curve. It is therefore possible that ERK forms only

part of the signalling cascade for migration or that hyperphosphorylation leads to alter functional outcomes.

Again in the delipidised system, the addition of S1P did not cause a significant stimulatory effect on migration above control, however the higher concertation (10μM) was observed to have a much more pronounced inhibitory effect than was seen in normal media. At this concentration the cells were unable to migrate as they were no longer attached and were floating as individual cells, however they have been shown to still be alive by live/dead staining. This may be due to the removal of the S1P chaperone HDL as it is not present to mop up the excess S1P, resulting in a potentially hyperstimulation being administered to the cells.

It is also interesting to see that the rate of migration under delipidised conditions was never able to be recovered to that under normal serum lipid conditions. It was initially thought that the removal of exogenous lipids would initially slow migration but that by 48 hours, similar levels to the normal media would be seen, especially after the addition of S1P as exogenous levels would potentially be replenished. This may also be due to the lack of an effective carrier for S1P as HDL would have been removed from the system by delipidisation. The concentration of S1P in human serum varies between individuals but has been reported to be in the range of 200nM-1μM, with around 65% being bound to lipoproteins (Hammad et al., 2012). Therefore, S1P may not be able to carry out its functions as it is still unknown whether HDL is needed to help S1P bind to the S1P receptors or whether S1P has to first leave the HDL complex. While albumin has been shown to be a carrier of S1P, it does not appear to bind S1P in the same way as HDL, with the S1P existing in a more free state able to be metabolised and carry out signalling functions (Bode et al., 2010). Therefore albumin may not play such a key role in this system for mopping up the excess S1P as HDL appears to, despite not being removed in the delipidisation process. It is possible that the remaining albumin is either already saturated with S1P or rapidly so when excess exogenous levels are added. It has also recently been found that the S1P chaperones, in particular ApoM on HDL, confer an anti-apoptotic effect to endothelial cells as S1P is needed to promote cell survival in times of apoptotic signals (Ruiz et al., 2017b). It would therefore be beneficial in the future to test the potential effect of selective HDL removal to study the effect it has on being able to remove the excess S1P from the system and also by adding it back into the reduced lipid environment and measuring migration, with the expectation that migration would recover to some extent.

4.5.2 Fingolimod

The effect of Fingolimod on migration was also investigated as it is an analogue of the S1P precursor sphingosine. Equimolar concentrations of S1P and Fingolimod were used, however it was difficult to determine the effects of Fingolimod as it had a perturbed effect on migration, see Figure 59. Instead of the cells migrating together to close the space as seen under normal conditions and in the presence of S1P, the cells appeared to separate and migrate individually. Therefore, after only 24 hours, some cells had already migrated to the centre of the scratch leaving behind a large gap to the edge of the original scratch and large gaps in between the cells. This made it incredibly challenging to measure every small area in between the cells to get a picture of the effect of Fingolimod on migration. In order to identify when this aberrant migration started, one scratch assay was imaged every 2 hours up until hour 8 and another was imaged after 16, 18, 20 and 22 hours. After 16 hours, signs of the deranged migration could be seen in the highest concentration of Fingolimod (10µM) but not others, however after 20 hours, all concentrations were showing this migration pattern. It would also have been possible to determine when the cells started migrating independently by using time-lapse microscopy. As it was found that the cells began to separate and migrate much earlier than 24 hours, the assay was repeated with new time points at 8, 16 and 24 hours being used. To make this a feasible task, a single confluent T75 flask of cells was split into two 24 well plates instead of one. This allowed the same cells to be used for both the 8 hour and the 16 hour time points so that it was possible to compare the results even though the assays were started at different times.

Overall, these results show that the highest concentration of Fingolimod has the same inhibitory effects as the highest concentration of S1P. It was also found that there were concentration dependent effects across the three time points, with 500nM inhibiting migration at 8 hours, 1nM, 10nM and 10µM being inhibitory at 16 hours and 100nM and 10µM inhibiting migration at 24 hours. Therefore the only concentration which did not inhibit migration was 1µM, which also ties in with the S1P data as although not significant, there does appear to be a slight stimulatory effect on migration when S1P is added at this concentration all of which adds to the complicated picture of multiple concentrations causing a variety of effects.

Delipidised media was also used to look at the effect of Fingolimod on migration. There appeared to be a greater proportion of floating cells across all concentrations of Fingolimod used, however live/dead staining showed that there was only a slight increase in cell death (10%) when cells were exposed to 10µM. Fingolimod may therefore have antiadhesive properties, which could be investigated by looking at ICAM-1 for example. It is interesting to note that at this concentration, S1P also blocked migration when added to delipidised media, suggesting that the lipids present in

the media offer some protective element to the endothelium. As mentioned previously, S1P bound to HDL promotes barrier integrity. It is possible that the human serum used contains HDL and therefore this protective effect is seen in the full media but is lost in the reduced lipid environment. At the lower concentrations of Fingolimod, the deranged migration response appeared to be reduced in the delipidised media, although the cells still did not fully resemble the migration of the control. It is interesting to note that at both 16 and 24 hours, 10nM Fingolimod stimulated migration in the reduced lipid environment compared to the migration achieved in the full lipid system with the same effect being observed with 1nM at 16 hours but not at 24 hours.

The mechanism of action of Fingolimod is to interfere in the formation of endogenous S1P by competing with sphingosine for phosphorylation by the kinase as well as activating the S1P receptors resulting in their internalisation and subsequent downregulation. Therefore its effects on migration suggest that changing endogenous S1P causes a derangement in the otherwise unstimulated migratory response of the endothelium or potentially that phosphorylated Fingolimod has an activity of its own and requires further investigation.

Fingolimod is also able to bind to the S1P receptors 1 and 3 in endothelial cells and downregulate them. As these receptors are important for endothelial barrier function, blood vessel formation and vascular tone, it is possible that as S1P signalling is no longer taking place, cells are not receiving clear signals and therefore don't know in which direction to travel. It is therefore possible that they may be migrating because they have lost contact with each other and it is a different signalling pathway that is dictating their movement. Although the results from the Fingolimod assays suggest that high concentrations inhibit migration, this may be misleading as the cells are able to migrate into the denuded area and away from other cells. Instead this could therefore be thought of as more of an inhibition of cell to cell contacts resulting in an inability to close the space left by the scratch as all the cells in the wells exposed to Fingolimod show this phenotype, regardless of whether they are on the edge of the scratch. It has been noted that Fingolimod increases vascular permeability resulting in macular oedema in some patients (Collins et al., 2010), suggesting that a similar phenomenon may be occurring *in vivo* and the observation of confluent cells becoming separated after the addition of Fingolimod also suggests this.

When cells migrate under normal conditions, all cells respond to a global signal and therefore move in an organised fashion in a coordinated direction. It has been reported that cells migrating individually have a greater initial velocity, however change direction repeatedly, which ties in with the results presented here as those cells exposed to the highest concentration of Fingolimod separate and spread out the quickest (Mayor and Etienne-Manneville, 2016). This in turn suggests that these cells must lose contact with each other the fastest, leading us to believe that Fingolimod

is able to interfere with cell to cell contacts and might possibly be stimulating polarisation of the cell.

A recent study has found that there is a significant decrease in the levels of the circulating tight-junction proteins occludin and zonula occludens 1 in patients treated with Fingolimod, particularly after 12 months (Annunziata et al., 2018). Another study has reported that simply by adding serum from patients with multiple sclerosis to endothelial cells results in a decrease in the expression of VE-cadherin and occludin (Minagar et al., 2003). Taken together, these results suggest that the levels of cytokines and other pro-inflammatory factors such as metalloproteinases that are found in multiple sclerosis serum are able to alter tight-junction proteins resulting in changes to the integrity of the endothelium, which may be exacerbated by Fingolimod.

4.5.3 Tumour necrosis factor

The effect of TNF concentrations on migration was also studied for comparison as TNF is a cytokine associated with psoriasis. It has been well documented that TNF is a pro-migratory signal (Gao et al., 2002) and therefore a greater stimulatory effect than was seen was expected. TNF was able to increase migration above that of the control, with the majority of the concentrations used able to match the migration seen with 1µM S1P, however no significance was found. This is most likely due to the variability between each assay as well as the moving background.

Scratch assays using TNF in delipidised media were also performed and it was found that most of the concentrations used were able to reach the same levels of migration as the control in a full lipid environment at both 24 and 48 hours. The only concentration of TNF not able to achieve this level of migration was 0.1ng/ml ($p=0.024$), however after 48 hours, migration had reached 100% of the control. Looking at the combination of the data obtained from TNF in the full and depleted media, it is clear that while the removal of exogenous lipids did initially reduce the levels of migration, by 48 hours the levels were almost the same as the levels seen in the full media. The removal of lipids therefore has a greatly reduced effect on the migration levels when TNF is present compared to the effect seen with S1P, where at no point were the migration levels achieved in the two environments similar. This lack of effect in the delipidised environment is possibly because TNF does not need lipids to signal and therefore the removal of exogenous lipids might not be expected to have a significant effect on this stimulated migration.

4.5.4 Sphingosine-1-phosphate receptor inhibitors

To further investigate the role S1P plays in migration, various inhibitors against the S1P receptors 1-3 were used to determine the mechanism through which exogenous S1P exerts its effects. It was found that alone, W146 (the $S1PR_1$ inhibitor) has the greatest effect at inhibiting the migration of HUVEC, with the inhibitors against $S1PR_{2\&3}$ (JTE and TY respectively) only having a significant effect on migration after 48 hours. This suggests that S1P may cause its effect on migration by primarily binding to $S1PR_1$, although as migration is not completely inhibited, either partial inhibition of $S1PR_1$ has occurred due to inhibitor concentration or S1P may also act through other mechanisms, possibly by also binding to $S1PR_{2\&3}$. It has been found that $S1PR_1$ is required for lymphocyte egress from the lymph nodes while $S1PR_2$ antagonises cytokine migration and instead retains T cells in the lymph tissue (Baeyens et al., 2015) which supports these findings. Potentially, other non S1P dependent mechanisms are also stimulating migration. This inhibition of migration observed when the inhibitor was added alone without a stimulus could involve endogenous S1P that is being released from the cell or potentially there could be S1P present in the human serum being used in the media. It is however interesting to note that none of the receptor inhibitors were able to block migration in the presence of S1P. It is potentially necessary to block all three receptors at the same time when a stimulus is added to have an effect on migration as there is potentially a compensation system in place between the receptors.

It is also interesting to note that only W146 alone was able to inhibit migration while in contrast, all three inhibitors were able to mediate S1P dependent ERK phosphorylation after 10 minutes, however they had no effect on S1P dependent migration.

These assays were also repeated in a reduced lipid environment and it was found that at 24 hours, W146 was able to block migration in response to the addition of S1P, however after 48h, migration has caught up with the delipidised S1P positive control although it was still significantly lower than that of the control in normal media. This could be because either the inhibitor has been bound to the receptors and then removed from the system or due to a short half life; suggested to be 73 minutes in rat blood according to the product information sheet from Cayman Chemical. It is also possible that as mentioned above, there is S1P present in the human serum which is removed during the delipidisation process, accounting for this effect only being seen and enhanced in the reduced lipid environment. If this was the case, it may be expected that the other inhibitors would also have an effect as they were shown to cause an inhibition in migration when added alone under normal conditions. This discrepancy could be explained if $S1PR_1$ is the receptor that S1P preferentially binds to stimulate migration. This is plausible as $S1PR_1$ appears to be the preferential

receptor *in vivo*, with the other two receptors forming a redundancy system (Kurano and Yatomi, 2018).

4.5.5 Pathway inhibitors- SKI-I, S1PL, PD, SB and JNKII

Other inhibitors of the S1P cascade were also investigated to see whether migration was affected. These included inhibitors of the kinases that phosphorylate sphingosine (SKI-I), S1P breakdown via S1P lyase (deoxypyridoxine) and three inhibitors targeting various proteins in the mitogen-activated protein kinases (MAPK) pathway. In the full lipid environment, the SKI-I inhibitor had an inhibitory effect on exogenous S1P dependent migration after 48 hours, suggesting that this kinase plays a role in the response to exogenous S1P stimulation in migration. It was however expected that any downstream effects of exogenous S1P would not be affected by the blockade of upstream endogenous S1P, suggesting a role for S1P dependent S1P signalling. Similarly to the effects of W146, migration was not completely inhibited, which may be due to the concentration used or how effectively it is able to enter into the cell.

In terms of the MAPK pathway inhibitors, only PD and SB had an effect on migration when added with exogenous S1P, with an inhibition of migration seen at 24 hours compared to the migration of S1P alone. After 48 hours it was observed that only PD+S1P migration was significantly inhibited compared to that of S1P. One possible reason for this could be that the PD inhibitor is longer lasting than the SB inhibitor and that by 48 hours the inhibitory effects of SB have been lost as cells were able to achieve nearly 100% of the control migration or that there is a temporal effect in inhibition. Another reason could be that migration is ERK dependent with a bit of P38 signalling or that there is some crossover between the signalling pathways. All these inhibitors block ATP dependent activity so they may not be completely specific, however it was shown in Chapter 3: that the inhibitors alone (at the concentration used here) did not have an effect on ERK phosphorylation.

In contrast, the inhibitor against SAPK/JNK (JNKII) almost showed a stimulatory effect and produced the tightest clustering of data, with most of the scratches achieving compete closure after 48 hours. It has been reported that 2-hexadecenal (one of the breakdown products formed by S1P lyase) leads to rearrangement of the cytoskeleton and apoptosis in multiple cell types through JNK mediated signalling (Kumar et al., 2011). This may therefore be why inhibition of JNK appears to have a stimulatory effect as the inhibitory effect of 2-hexadecenal may have been negated thereby inhibiting the apoptosis signals.

These assays were also repeated in a reduced lipid environment and in contrast to the full lipid assays, the S1P lyase inhibitor inhibited migration with SKI-I having no effect. S1PL+S1P was found to significantly inhibit migration at 24 hours compared to that of the control and to be significantly

different to S1P alone at 48 hours. It would be expected that by blocking S1PL more S1P would be available and therefore potentially increase migration, however as the phosphatase is still working, S1P is still able to be dephosphorylated back to sphingosine. It is possible that the inhibition in migration observed is due to the phosphatase being unable to increase the rate in which S1P is dephosphorylated and therefore when exogenous S1P is added, the total concentration of S1P in the assay reaches inhibitory levels, similar to those seen with 10μM exogenous S1P causing inhibition.

Similar results to those obtained for the full lipid assays were found when the MAPK pathway inhibitors were used in the delipidised system. At 24 hours it was found that the migration of cells exposed to SB alone, S1P+SB and S1P+PD were all significantly inhibited when compared to the control, while at 48 hours, the migration of cells exposed to PD alone was inhibited. Combining the results between the full and reduced lipid conditions yielded some interesting results, with none of the inhibitors alone showing any difference between the two environments at 24 hours and only a slight difference after 48 hours. The addition of the inhibitors in combination with S1P did show a difference between the two lipid conditions, with an inhibition across all inhibitors being seen at both time points in the reduced lipid assays. This further supports the role of lipids and specifically S1P in the migration of HUVEC as well as hinting at potential pathways S1P may be signalling through, such as ERK as discussed in section 3.2.

4.5.6 Oxidised LDL

The effect of oxLDL on the migration of HUVEC was as expected and in line with previous experiments. It was found that high concentrations (100μg/mL) resulted in an inhibition of endothelial migration, while low concentrations (5μg/mL) stimulated migration above that of the control. This was also found to be the case when the assays were repeated in a reduced lipid environment. One potential reason for this concentration dependent response may be due to the activation of the endothelial cells in response to the activation of LOX-1 and subsequent oxLDL endocytosis. As discussed previously, this leads to the activation of the MAPK p42/44 pathway and therefore an inhibitor against MEK (the kinase that phosphorylates ERK) was used to determine if this pathway is involved in migration. It was found that when this inhibitor (PD) was used in combination with 5μg/mL oxLDL, the stimulatory effect of oxLDL was lost and in fact, more of an inhibitory effect was observed ($p=0.0008$). This suggests that ERK signalling is important for endothelial migration as blocking ERK phosphorylation resulted in decreased motility.

4.5.7 ox-albumin and lipid supplement

The effect of albumin, ox-albumin and a lipid supplement on migration was initially assessed and it was found that all of the conditions assessed resulted in the cells becoming detached from the plastic. Analysis of cell viability using FACS has however shown that these cells are still viable at 24hours. It was thought that the inclusion of the lipid supplement to the delipidised serum would be able to replace the human serum that is routinely added to the basic M199 media, however even at the highest concentration used, the cells had still detached by 48 hours. Interestingly, it was the cells exposed to albumin that appeared to remain attached for the longest, with the addition of the lipid supplement having no apparent effect. From the results of this assay, there was no discernible difference between albumin and the oxidised form until S1P was also included. Cells exposed to both oxidised albumin and S1P were observed to be completely detached at 24 hours, however cells exposed to normal albumin and S1P took longer to become detached, only becoming fully detached after 48 hours. This suggests that there is a difference between the two forms and that it is the oxidative modification of the protein causing this effect. It is well known that albumin is a carrier of S1P and therefore this may explain the difference between the two forms (Fleming et al., 2016a). In these assays, the addition of S1P to M199 media without any additives resulted in floating cells after 24 hours. It is therefore likely that when albumin and S1P are added together that the albumin is able to bind to some of the S1P and therefore acts a buffer to its effects. As the same effects of S1P alone are seen with oxidised albumin, it is reasonable to suggest that the somewhat protective effect of albumin is lost during the oxidation process. It is possible that the oxidised form of albumin is no longer able to bind S1P, perhaps due to a conformational change around the S1P binding site. It has been demonstrated that the oxidation of albumin has an effect on its binding properties (Oettl and Stauber, 2007) and therefore it is reasonable to suggest that the oxidised form of albumin is perhaps unable to bind free S1P, or at least bind as much as the native form. This could be analysed by performing mass spectrometry to determine how much S1P is retained.

In order to test this theory, the assay was repeated using S1P that was potentially bound to either albumin or ox-albumin prior to the start of the assay as well as free S1P and albumin/ox-albumin. As the S1P bound to albumin and ox-albumin samples have been dialysed to remove any unwanted compounds, albumin was also dialysed and included in the assay to ensure that the dialysis process had no effect on migration. It was found that there was no difference between the normal and dialysed versions of albumin when added to the cells alone, with both conditions resulting in migration, although after 48 hours the cells were starting to look a bit rough with a number of floating cells present. Equally there was no difference when added in combination with free S1P as

both combinations caused the cells to lift off from the plastic. It can therefore be concluded that the dialysis does not cause any changes that would interfere and alter the results of the assay.

The biggest difference observed in this assay was again seen between albumin and ox-albumin, this time with bound S1P, further supporting that the oxidative modification has an effect. Cells that were exposed to S1P potentially bound to albumin were able to migrate and the majority were still attached after 48 hours, whereas those exposed to S1P potentially bound (or not bound due to the oxidative modification) to the oxidised form of albumin were observed to be floating after 24 hours. As mentioned previously, it is possible that ox-albumin is not able to bind S1P and that as the samples were dialysed to remove any unbound S1P, effectively only ox-albumin was potentially added to these cells which has been shown to result in floating cells.

It is also interesting to note that there was a difference in migration between when albumin was added with either free or bound S1P. The ability of the cells to remain attached to the plastic and migrate when bound S1P was added, in contrast to lifting off with free S1P, further supports the theory that albumin is offering a protective effect against the action of high concentrations of S1P on the endothelium. It would therefore be expected that a greater effect would be seen with a greater concentration of albumin. Albumin was incubated with 10µM S1P to allow binding before dialysis and therefore this difference between bound and free S1P may be due to the concentration of S1P in the final assay. Albumin has a finite number of S1P binding sites (Simard et al. (2005) have reported that there are at least seven) and so it is possible that a proportion of S1P is removed during the dialysis stage and therefore the final concentration in the assay is lower than when free S1P is added. This is important as it has been shown that in full media, a high concentration of S1P has an inhibitory effect on endothelial migration but lower concentrations do not. This assay also shows that 10µM S1P in M199 media alone results in the detachment of the cells and therefore it is possible that if albumin is only able to bind to some of the free S1P, the cells are still exposed to a high concentration, producing the same results as when S1P is added alone. Although none of the migration seen is comparable to the migration achieved by the control cells in full media, it is important to highlight that these cells were able to remain attached and migrate, as cells quickly detached when M199 media alone was added.

In the future it would be interesting to selectively remove albumin from the human serum used to make the full media and add back albumin/ox-albumin with either free or bound S1P to see if this has any effect on migration compared to the results already obtained. To investigate the binding of S1P to albumin it would also be possible to use fluorescent probes to determine which binding sites S1P preferentially binds to and potentially quantify the total concentration able to bind. Dansylamide and dansylglycine bind to binding sites one and two on albumin respectively and

changes in their fluorescence due to displacement by competitive compounds can be studied using fluorescent titrations (Sudlow et al., 1975). This would allow a better comparison between the migration of the free and bound S1P as the same concentrations could be used for both conditions.

4.5.8 Confluent cells

Due to the surprising effect observed during the migration assays that the addition of Fingolimod had, it was decided to add S1P, Fingolimod, oxLDL and LDL to a confluent layer of cells. It was found that high concentrations of S1P (10µM) resulted in gaps appearing between the cells after 24 hours which subsequently disappeared after 48 hours whereas 1µM S1P and all concentrations of oxLDL and LDL used did not have this effect. 10µM Fingolimod resulted in the largest gaps seen, with 1µM also causing spaces between cells to appear. These results therefore support the findings from the migration assays and are in line with the current literature. In order to analyse this further it may be beneficial to measure the barrier function of the endothelium using other methods such as electrical resistance or by studying the movement of large molecules e.g. albumin across the barrier.

4.6 Chapter Summary

Overall, the most noticeable finding from these migration assays was the effect that the delipidised system had on migration, with cells only able to achieve around 50% of the migration achieved by the control in a full lipid environment. S1P was also found to be inhibitory at high concentrations while oxLDL was found to have a concentrations dependent effect, with low concentrations stimulating migration and high concentrations having an inhibitory effect. This confirms the role lipids play in the migration of HUVEC and supports the hypothesis that the concentration and proportions of lipids are important factors that potentially play a role in mediating both systemic and localised disease such as psoriasis.

Chapter 5: Cell Spreading

5.1 Introduction

Cells need to be able to change their morphology in order to carry out their function. Depending on the cell type this could include processes such as autophagy and phagocytosis (where the membrane needs to be extended and contracted to engulf debris or a pathogen) or migration (where a cell needs to be able to squeeze past other cells, for example an immune cell exciting the circulation). Endothelial cells have a fairly uniform shape in the absence of any stimuli, however they are able to extend protrusions and migrate towards a signal, which is vital in wound healing, angiogenesis and during development (Lamalice et al., 2007).

When a cell first comes into contact with the extracellular matrix (ECM), the initial contact is through integrins which are expressed on the cell surface. After this contact has been made, the cell is able to flatten and form additional connections, such as focal adhesions, with the substrate and neighbouring cells. In order for a cell to be able to spread, and indeed migrate, it must be able to mobilise and restructure its cytoskeleton. The result of this rearrangement is the formation of lamellipodia, or protrusions, at the leading edge of the cell along with contraction at the lagging edge of the cell when there is a directional element to the migration. Through this continuous formation and breakdown of the cytoskeleton, the cell is able to move forwards and make new connections with the ECM (Reinhart-King et al., 2005). Similar processes occur when the cell is dividing or interrogating the local environment and making connections to other local cells.

S1P is known to be involved in the regulation of the barrier function of endothelial cells by reorganising the cytoskeleton and by forming new adherens junctions. It has been found that S1P does this by relocating integrins (α5β1 and αvβ3) from the apical to basal surface of the cell when required (Aoki et al., 2007). Antibodies against αvβ3 have been shown to inhibit the heightened effect of S1P on barrier integrity and this has been attributed to the Rac mediated targeting of αvβ3 to focal adhesions (Su et al., 2012). A separate study has found that in endothelial cells, αvβ3 integrins (particularly those located in the lamellipodia of a migrating cell) are activated via the S1PR1 receptor and Rho GTPases. The addition of S1P was also found to stimulate the association of the cytoskeleton and focal adhesion kinase with integrin αvβ3, as well as stimulate the dimerization of αvβ3 subunits to produce an active integrin, an essential part of migration and spreading (Wang et al., 2008). S1P is therefore able to regulate endothelial adhesion (which is non-energy requiring), spreading (a more coordinated response) and migration through a number of key processes, highlighting the importance of this bioactive lipid signalling pathway.

5.2 Hypothesis and aims

It is hypothesised that the addition of S1P will influence the morphology of HUVEC and will affect their ability to spread. It is also hypothesised that Fingolimod will cause a decrease in cell circularity.

Specific aims of this chapter are:

- to investigate the effect of S1P, Fingolimod, oxLDL and ox-albumin on cell spreading when cells are plated in the compound of interest
- to investigate the effect of inhibitors against S1P kinase and lyase on cell spreading
- to investigate the effect of S1P, Fingolimod, oxLDL and ox-albumin on cell spreading when added to pre-plated cells

5.3 Method

During the course of the migration assays it was noticed that the morphology of the cells changed when Fingolimod and oxLDL were added. It was therefore decided to investigate this further by analysing the shape of cells via a measure of their circularity once they had adhered following seeding (at 40K cells per well) onto a gelatin coated surface at 4 hours and after 24 hours of attachment. The effect of the lipids and certain inhibitors on cell shape was assessed in two separate ways; first, the cells were plated in the compound of interest to see if there was any effect on the attachment of the cells to the surface of the plate and subsequent spreading, and, second, the cells were plated 24 hours prior to the addition of any lipid or inhibitor to see if they were able to change the morphology of cells which were already adhered. Figure 84 shows examples of the difference in cell spreading between the various compounds.

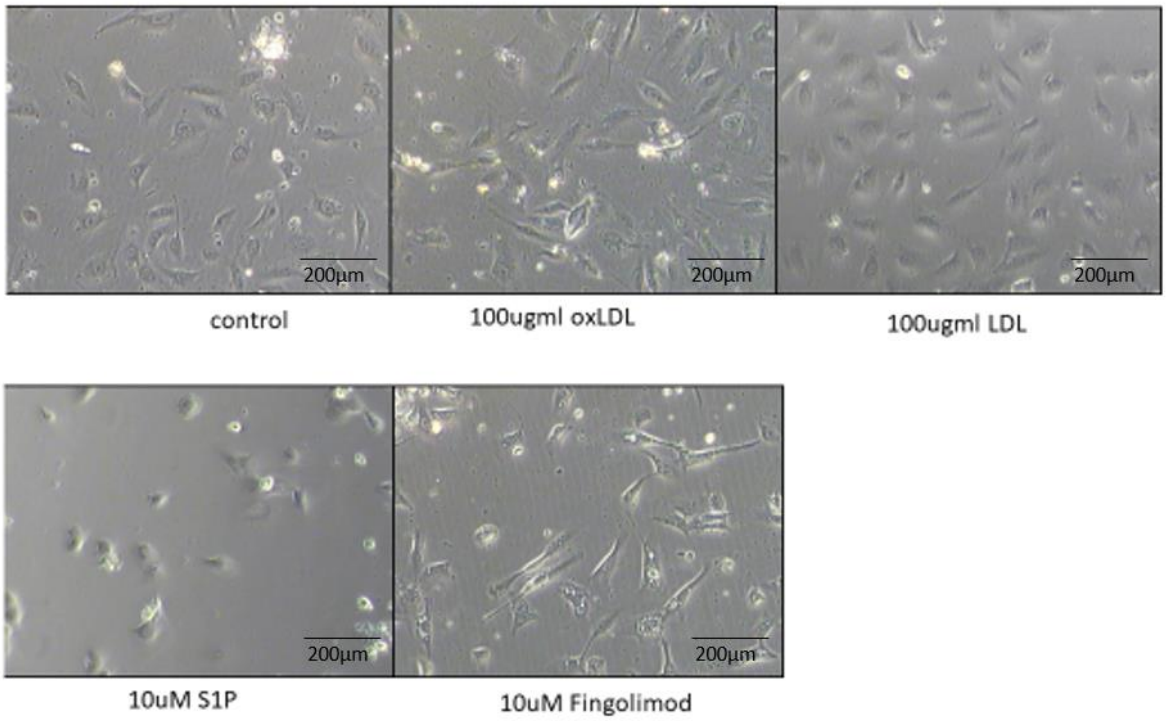

Figure 84 Effect on cell spreading by S1P, Fingolimod, oxLDL and LDL
Plating HUVEC in S1P, Fingolimod, oxLDL or LDL results in varying phenotypes, with high concentrations of S1P preventing spreading and high concentration of Fingolimod resulting in spreading above that of the control.

In both cases, image analysis using Fiji was used to measure the circularity of the cells by using the polygon tool to manually draw around 10 cells from each image so that the average circularity could be calculated. An automated method was also tried using the threshold tool in Fiji with the aim being to analyse all cells in the field of view instead of only 10, however due to the images being grayscale the edges of the cells were not accurately picked up and therefore the manual approach was deemed to provide the most accurate representation of cell circularity.

The values generated for circularity were between 0 and 1, with 0 being a straight line and 1 being a perfect circle. Therefore, the shape of cells can be determined in a time dependent manner. Initially, cells in the first few minutes of attachment are effectively circular with a circularity score of close to 1. As the cells attach and spread, circularity decrease and the cells adopt a more elongated and stretched out shape. As was the case for the migration assays, each condition was performed in duplicate in each assay (therefore the mean circularity of 10 cells in each of two wells was taken) and each assay repeated in triplicate on separate occasions with cells from individual donor umbilical cords. One-way ANOVA was used to ascertain if there was a significant difference in the data sets and Dunnett's multiple comparisons test was used to compare the circularity of the various conditions to that of the control.

5.4 Results

5.4.1 Cells plated in the compound of interest

5.4.1.1 oxLDL, LDL, S1P, Fingolimod

The effect of oxLDL, LDL, S1P and Fingolimod on the shape of freshly plated HUVEC cells was examined as well as the removal of lipids from full human serum, achieved by plating the cells in delipidised media. The results are shown below in Figure 85.

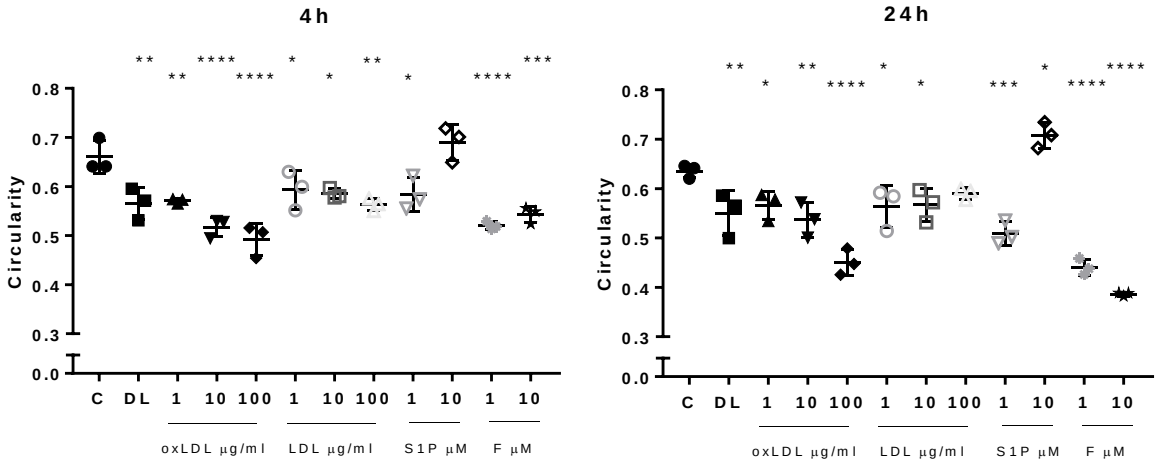

Figure 85 Change in the circularity of HUVEC when plated in lipids
Cells were plated with the lipids as described and imaged after 4 and 24 hours. The error bars represent the mean circularity +/- SD, n=3. C= control, DL= delipidised media, F= Fingolimod. Stars represent significance between the compound and the control as determined by Dunnett's multiple comparisons test.

Figure 85 highlights the change in the morphology of primary HUVEC cells when plated in various lipids, with one-way ANOVA yielding a p value of <0.0001 at both time points. As expected from the results of the migration assays, the cells exposed to Fingolimod were more elongated than the control as were those cells exposed to high concentrations of oxLDL although not LDL. Interestingly those cells exposed to the highest concentration of S1P (10µM) were the most circular, even when compared to the control, however 1µM S1P did not change the circularity compared to the control. The difference between the various concentrations of lipids and the control was analysed using Dunnett's multiple comparisons test and the results are highlighted on the graphs above.

In order to visually highlight these changes in cell shape in response to these lipids, representative images are shown below.

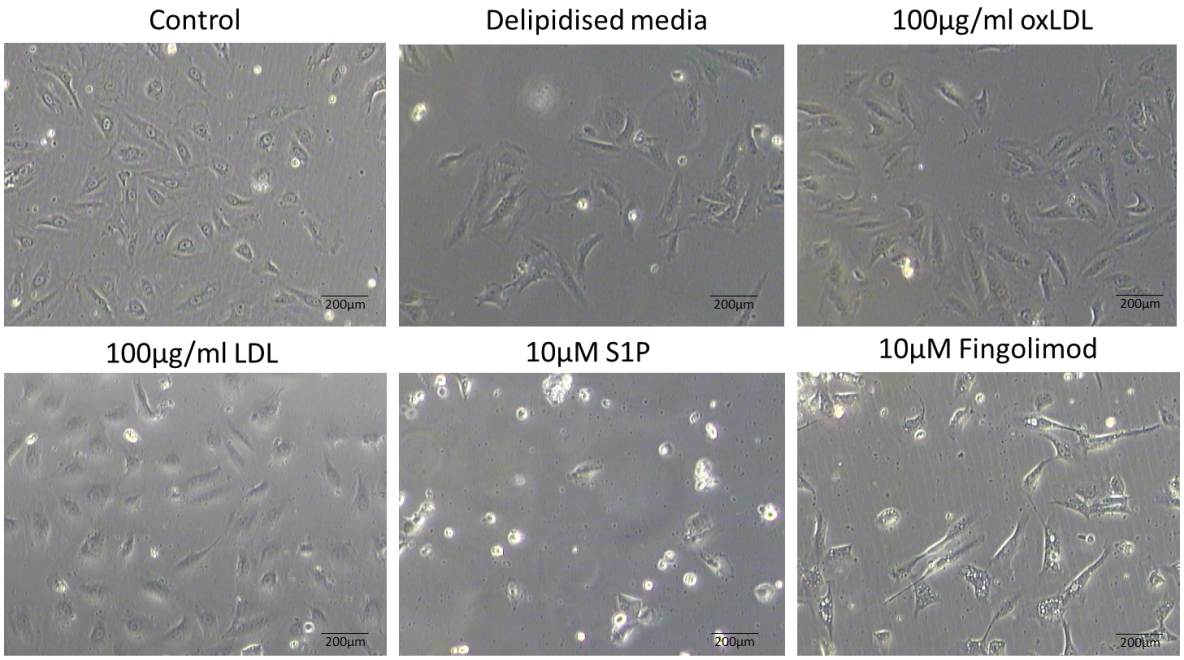

Figure 86 representative images of control, 100µg/ml oxLDL/LDL and 10µM S1P and Fingolimod
Cells were plated in the compound of interest at 40K per well and imaged after 4 and 24 hours. These images are representative of the effect of oxLDL/LDL, S1P and Fingolimod on the spreading of HUVEC after 24 hours.

Figure 86 shows the effect that different lipid conditions can have on the spreading ability of endothelial cells and highlights the different morphologies they can adopt. Visual assessment of the above images clearly show that there is difference between the lipids, with S1P and Fingolimod having the greatest effect.

The following graphs are included in order to show the effect on cell shape over 24 hours as a result of the various lipid conditions, as only comparisons within each time point can be made from the graphs above.

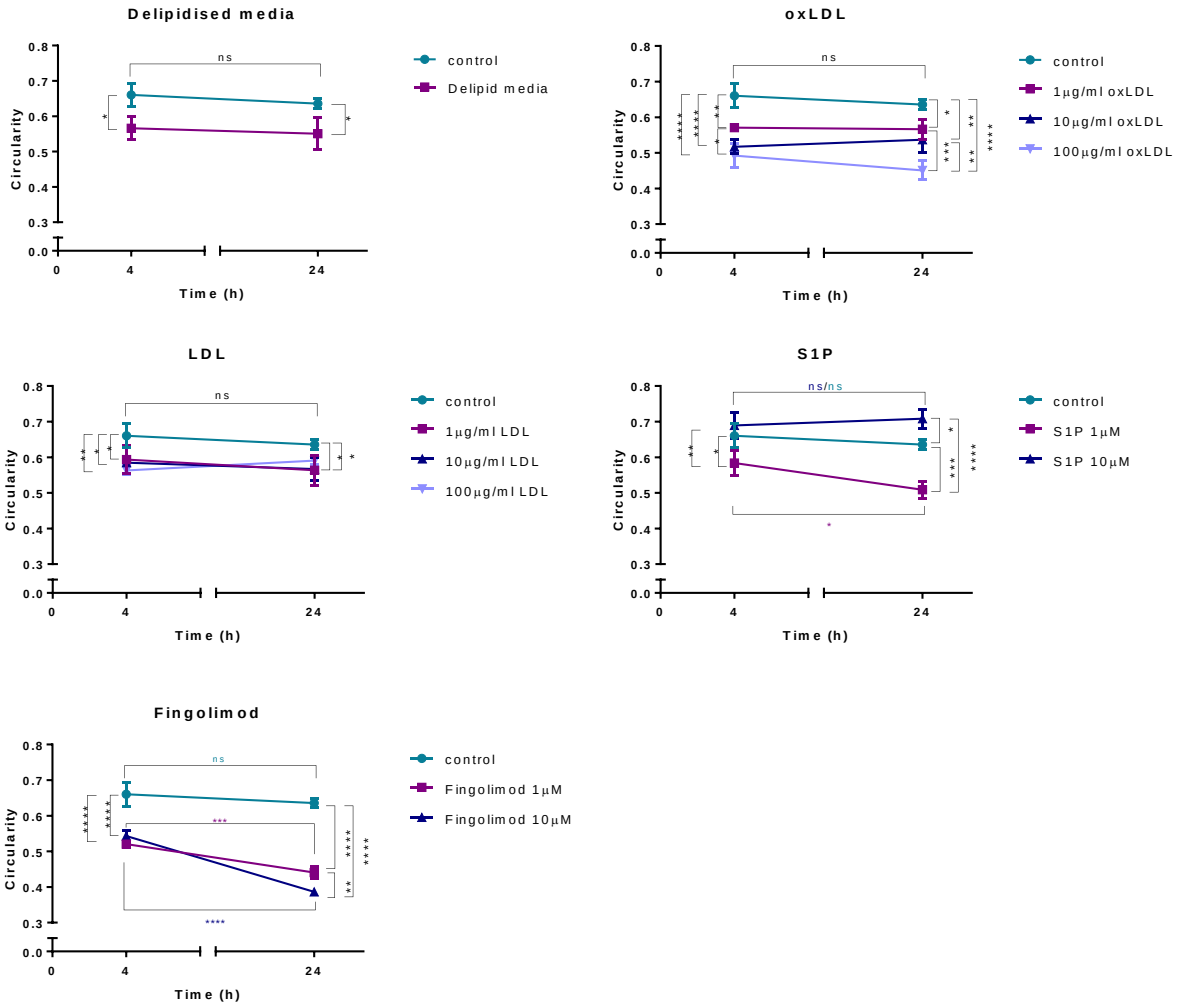

Figure 87 trend of cell shape over 24 hours in response to being plated in lipid
These graphs show the overall trend in cell shape after the cells were plated in lipids (oxLDL/LDL, S1P, Fingolimod). The error bars represent the mean circularity +/- SD, n=3. Significance stars have been colour coded to correspond to the conditions they relate to.

The graphs in Figure 87 show that generally the cells become less circular in response to oxLDL (particularly at the highest concentration), with 10µM S1P being the only lipid to increase the circularity at both 4 and 24 hours above control. The circularity of the control cells and those exposed to LDL does not change significantly over the time period. Two-way ANOVA analysis (comprised of Sidak's multiple comparisons test and Tukey's multiple comparisons test) showed that both 1µM S1P and both concentrations of Fingolimod had an effect on cell shape over time, whereas oxLDL and LDL did not. Differences were also seen between the various concentrations of lipids at each time point. These results are shown on the graphs and where differences in significance were seen between time points, the stars have been colour coded to highlight this.

5.4.1.2 SKII, S1PL, PD, albumin, ox-albumin

The effect of SKII, S1PL, PD, BSA and ox-albumin on cell attachment and spreading was also investigated and the results are shown below in Figure 88. For each independent experiment, each condition was performed in duplicate. The circularity of 10 cells from each well was measured and an average for that well obtained. The average of the two duplicated wells was then taken and this value is represented by each point on the graph as described previously.

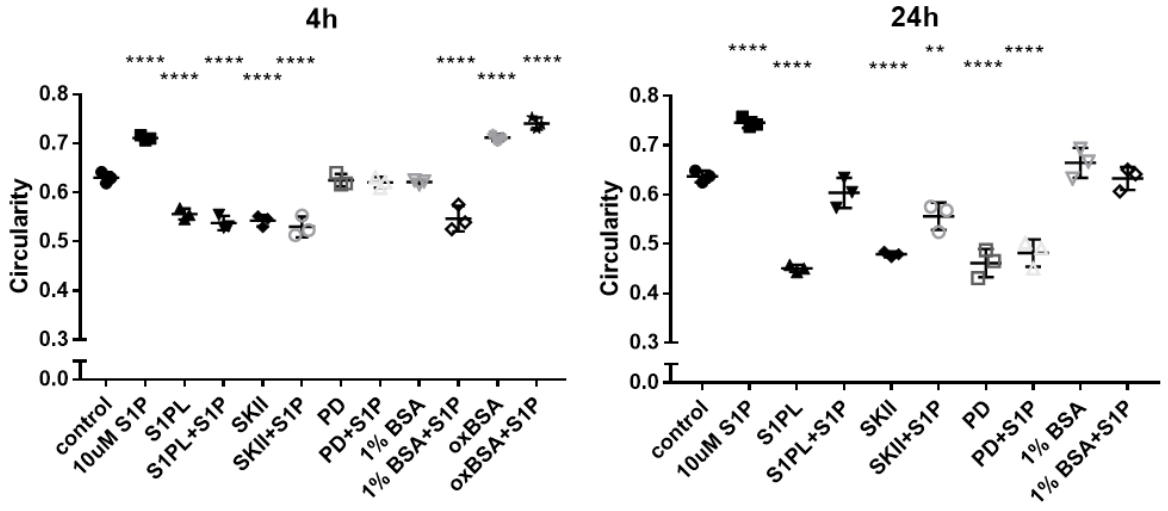

Figure 88 Change in the circularity of HUVEC when plated in SKII, S1PL, PD, albumin and ox-albumin

Cells were plated as described and imaged after 4 and 24 hours. The error bars represent the mean circularity +/- SD, n=3. ox-albumin and ox-albumin+S1P are not included in the 24 hour graph as the cells were floating at this time point.

One-way ANOVA analysis revealed a p value of <0.0001 for both time points and the results of Dunnett's multiple comparisons test comparing the various conditions to the control are shown on each graph. Tukey's multiple comparisons test was also used in order to compare S1P and S1P+PD, giving a p value of <0.0001 at both time points. S1P was also compared to S1P+1% (w/v) albumin which gave p values of <0.0001 and 0.0002 at 4 and 24 hours respectively. 1% (w/v) albumin+S1P and ox-albumin+S1P were also compared and after 4 hours a p value of <0.0001 was found. It was not possible to do this comparison after 24 hours as the cells exposed to oxBSA+S1P were floating and therefore no circularity measurement could be taken. Cell viability was discussed in Chapter 3: and it was found that the addition of ox-albumin had no effect on the viability of the cells, with >95% being found to be alive by live/dead staining.

The following graphs show the circularity of all the cells measured across the three independent experiments.

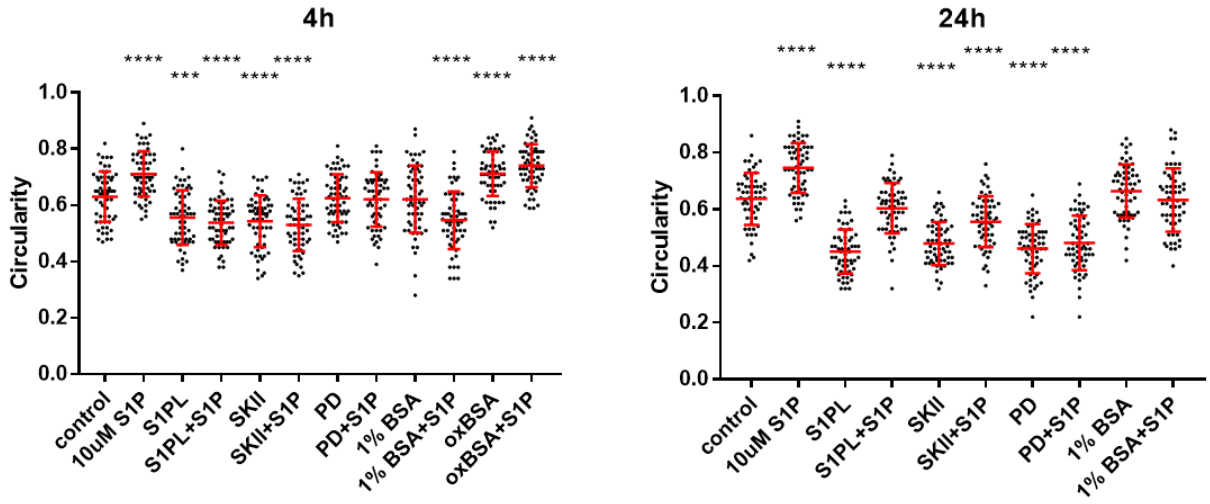

Figure 89 change in the circularity of HUVEC when exposed to SKII, S1PL, PD, BSA and oxBSA
Cells were plated in the compound of interest as described and then imaged after 4 and 24 hours. The error bars represent the mean circularity +/- SD, n=3

One-way ANOVA analysis revealed a p value of <0.0001 for both time points and the results of Dunnett's multiple comparisons test comparing the various conditions to the control are shown on each graph. Tukey's multiple comparisons test was also used to compare S1P with S1P+PD and S1P+albumin. This gave a p value of <0.0001 for both conditions and at both time points. 1% (w/v) albumin+S1P and ox-albumin+S1P were also compared and after 4 hours a p value of <0.0001 was found. As explained before, it was not possible to do this comparison after 24 hours as the cells exposed to ox-albumin+S1P were floating and therefore no circularity measurement could be taken.

The following graphs are included in order to show the cell shape over the 24 hour time course as a result of the various conditions, as only comparisons within each time point can be made from the graphs above.

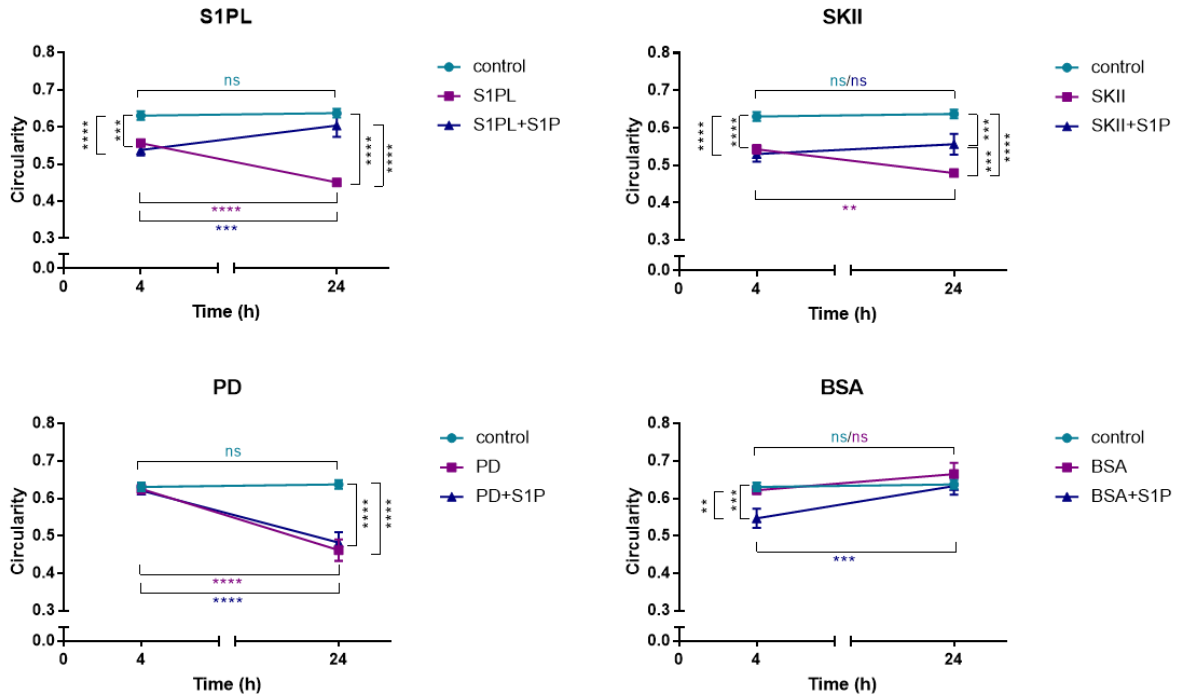

Figure 90 trend of cell shape over 24 hours in response to being plated in SKII, S1PL, PD and albumin

These graphs show the overall trend in cell shape over 24 hours after the cells were plated in SKII, S1PL, PD and albumin. The error bars represent the mean circularity +/- SD, n=3. Significance stars have been colour coded to correspond to the conditions they relate to.

Two-way ANOVA analysis (comprised of Sidak's multiple comparisons test and Tukey's multiple comparisons test) was used to compare the different conditions to each other within each time point as well as across time points to see if there was a change in the morphology of the cells over 24 hours. These results are shown on the graphs above and any differences between time points has been colour coded to correspond to the various conditions. No graphs of ox-albumin are shown as the cells were floating at 24 hours and so no comparison could be made.

5.4.2 Effect of compound addition on cell morphology in established and attached cells

Following the results of plating cells in the presence of lipids, an investigation into the effects of lipids on pre-attached cells was conducted to examine if these lipids had a similar effect on the circularity of cells which had already been plated for 24 hours (as opposed to the cells being plated in the lipids). The following graphs show the results.

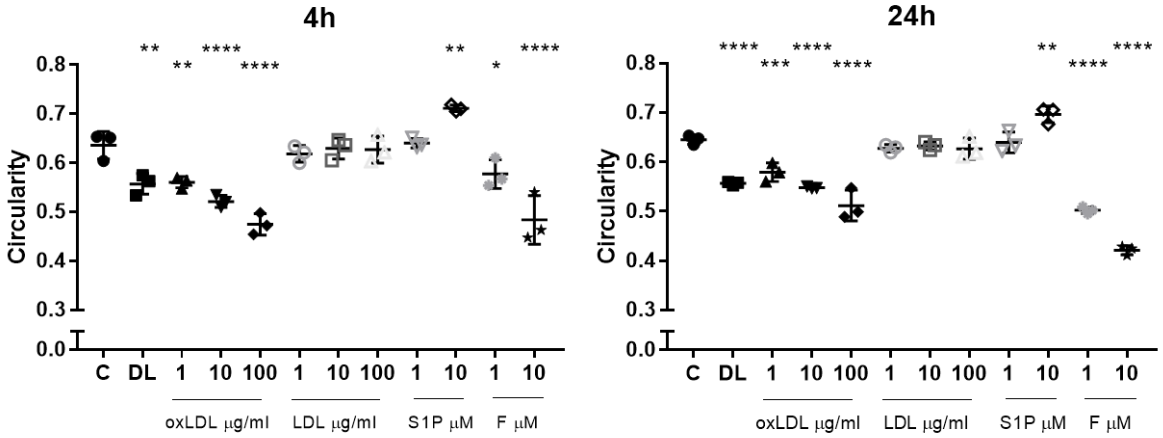

Figure 91 Average change in the circularity of HUVEC when exposed to lipids
Cells were plated at least 24 hours prior to the addition of the lipids and then imaged after 4 and 24 hours. The error bars represent the mean circularity +/- SD, n=3. C= control, DL= delipidised media, F= Fingolimod.

Figure 91 highlights the change in the morphology of primary HUVEC cells when exposed to various lipids, with one-way ANOVA yielding a p value of <0.0001 at both time points. As expected from the results of the migration assays, the cells exposed to Fingolimod were more elongated than the control as were those cells exposed to high concentrations of oxLDL although not LDL. Again, those cells exposed to the highest concentration of S1P (10μM) were the most circular, even when compared to the control, however 1μM S1P did not change the circularity compared to the control cells. The difference between the various concentrations of lipids and the control was analysed using Dunnett's multiple comparisons test and the results are highlighted on the graphs above.

The following graphs show the circularity of each cell measured to generate the averages shown in the above graphs.

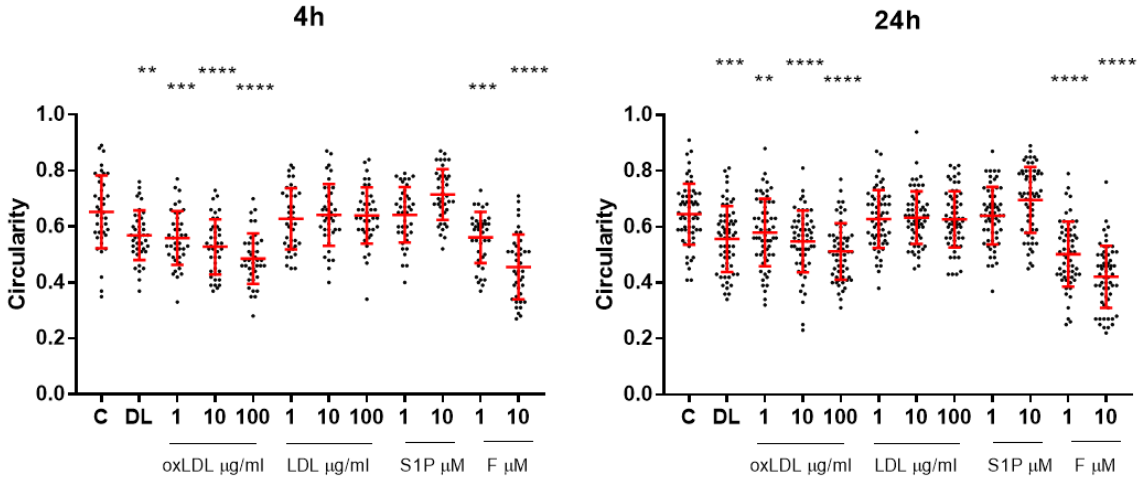

Figure 92 change in the circularity of HUVEC when exposed to lipids
Cells were plated at least 24 hours prior to the addition of the lipids and then imaged after 4 and 24 hours. The error bars represent the mean circularity +/- SD, n=3. C= control, DL= delipidised media, F= Fingolimod.

These graphs show that the lipids have the same effect on the circularity of endothelial cells when added 24 hours after the cells have been plated as they do when the cells are plated at the same time as lipids are added. This suggests that the lipids are not interfering with the process of cells attachment and instead must play an active role in regulating the shape and morphology of the cell. Again, one-way ANOVA gave a p value of <0.0001 at both time points and the results of Dunnett's multiple comparisons test comparing the various lipids to the control are highlighted on the above graphs.

Figure 92 shows the difference between the different lipids and the control at each time point, however there is also a time dependent effect and this was investigated. This was achieved by plotting the following graphs and performing a two way ANOVA to show the change in cell shape over 24 hours as a result of the various lipid conditions.

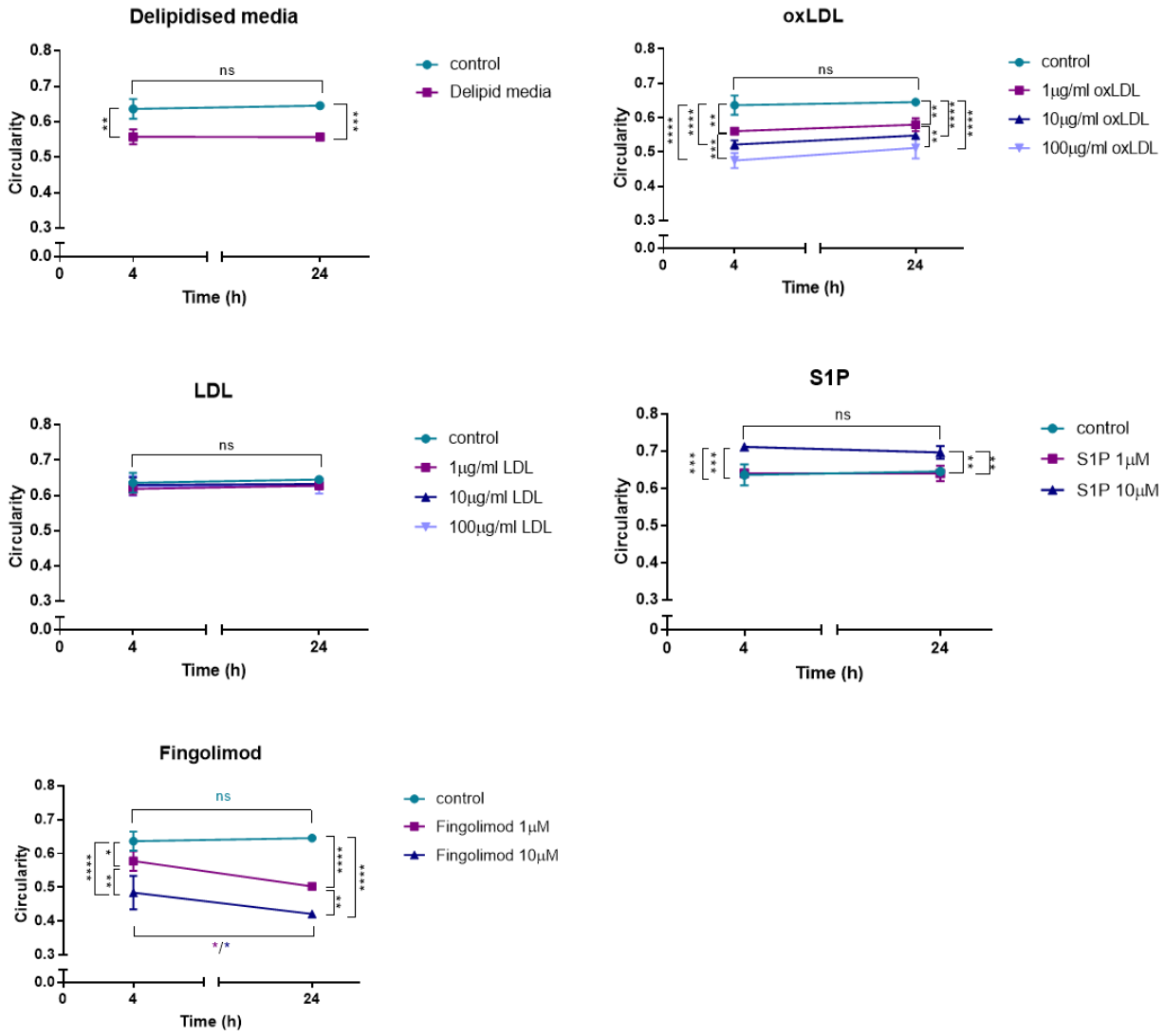

Figure 93 trend of cell shape over 24 hours in response to lipid addition

These graphs show the overall trend in cell shape after the addition of lipids (oxLDL/LDL, S1P and Fingolimod) and highlight the effect of time on cell spreading. The error bars represent the mean circularity +/- SD, n=3.

Two-way ANOVA analysis (comprised of Sidak's multiple comparisons test and Tukey's multiple comparisons test) revealed that there was a significant difference in the circularity between the control and all lipids except LDL at both time points, however only Fingolimod significantly changed the morphology of the cells between the two time points. These results are shown on the graphs above and highlight if there was a difference between the concentrations of lipids used.

5.4.3 Overall effect of compound addition on cell morphology

The combined results of the cell spreading assays are shown below and highlights the difference each lipid has on cell circularity. Cells were plated 24 hours before the addition of the compounds and then the circularity was measured 4 hours (28 hours after plating) and 24 hours (52 hours after plating) after the lipid addition.

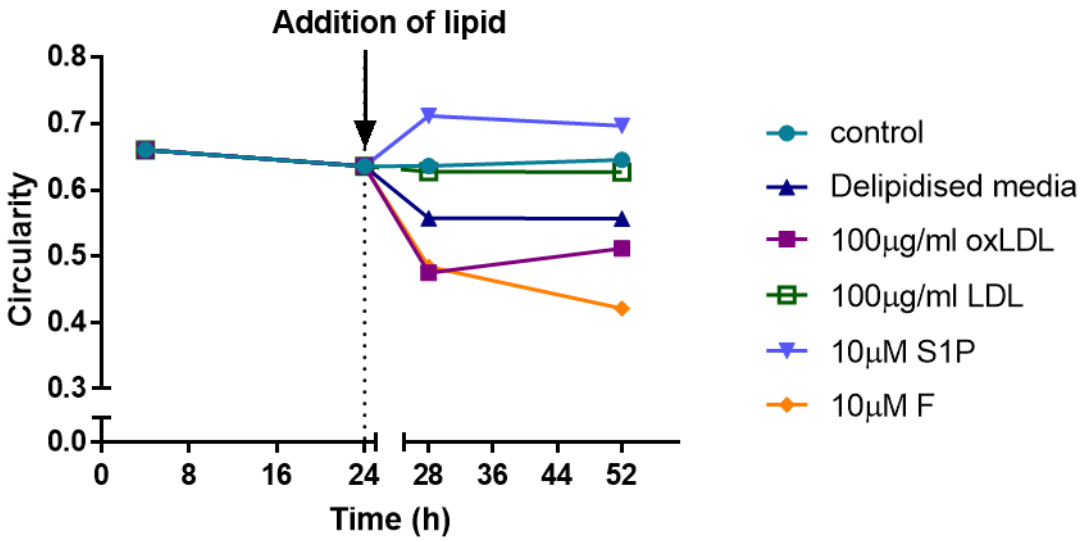

Figure 94 combined effect of lipids on the circularity of HUVEC
Combined cell circulatory data showing the cells plated in normal media 24 hours prior to the addition of lipids as well as the following 24 hours (up to 52 hours total). For clarity only the highest concentrations of each lipid were included. Each point shows the mean circulatory obtained over 3 independent experiments.

Figure 94 shows that the effects of lipids on the shape of endothelial cells is complex, with some stimulating the cells to adopt a more stretched out phenotype (e.g. oxLDL) while others (e.g. S1P) result in an increase in circularity. Interestingly, Fingolimod causes the greatest shape change which ties into the results obtained in the migrations assays.

5.5 Discussion

Cell attachment and spreading are important aspects of migration and, for endothelial cells, functions such as angiogenesis. Using a measure of cell shape, the effect of each compound was investigated in a concentration and time resolved manner. Results showed that cell morphology was changed as early as 4 hours after plating. It is possible that the change in shape at 4 hours is due to an interference with the cells ability to attach to the gelatin coated plastic and that by 24 hours the compound may be either stimulating or inhibiting the migration of the cell and subsequently affecting its shape. It is most likely that in the case of the control and the various LDL concentrations that by the 4 hour time point, the cells have already spread out as much as they are going to and therefore no change is seen between 4 and 24 hours at this seeding concentration. This is not the case with Fingolimod as the cells continue to elongate over the time course studied. The data obtained from 10µM S1P suggesting that S1P has the ability to block this spreading process but not initial attachment. Cell spreading is an average measure of the pseudopodia and filopodia ability, which relates to the sprouting in angiogenesis. A sprouting assay, where cells are embedded in collagen and the number of sprouts that are generated measured, could also be another method to study this process.

Due to the results obtained when the cells were plated in the compound of interest, it was also decided to study the effect of the lipids on the circularity of cells that had been plated for 24 hours in normal media i.e. before the addition of any extra lipids. This was specifically to determine if any of the lipids were able to cause already spread and elongated cells to retract or elongate, that could link into the inhibition in migration previously seen.

5.5.1 Cells plated in the compound of interest

The results of the initial cell spreading assay proved interesting, potentially revealing some insight into how the regulation of the morphology of the cell impacts on the ability of that cell to migrate. For example, in the migration assays it was found that 10µM S1P was inhibitory, with cells on average only able to achieve ~50% of the control migration. This concentration also resulted in the cells adopting a more circular phenotype, even after 24 hours, suggesting that the inhibitory effect on migration might be caused by the cells lack of ability to elongate along a directional axis. The cells appeared as phase bright under the microscope suggesting they were spherical in morphology and likely that they have attached but have not spread. From the data obtained here it is unclear which part of the complex process of migration may be affected, however it would be reasonable to suggest that the cell is unable to become polarised and therefore would not know which direction to travel and so remains circular. S1P is known to be involved in activating Rho GTPases

which are important in establishing the polarity of the cell as well as the Rac and Rho pathways (see Figure 6) which are important in the formation of lamellipodia at the leading edge of the cell and the contraction at the lagging edge respectively. It is also plausible that the addition of high concentrations of S1P result in an inhibition of the PLC pathway which is involved in the rearrangement of the actin cytoskeleton. Therefore, the cell may be receiving but unable to respond to polarisation signals, again resulting in an inhibition of migration and an increase in circularity. It is also possible that this concentration of S1P affects focal adhesions and therefore would stop migration by blocking spreading of the cells via this mechanism.

High concentrations of oxLDL also resulted in a decrease in migration, however, in contrast, these cells were found to be elongated compared to the control suggesting that the cytoskeleton is able to be rearranged and that there is active stimulation to the change in morphology. This inhibition in migration may therefore be due to the cell failing to receive or respond to the necessary signals informing the cell which direction to move or that Rho signalling may have been interrupted, preventing the cell from detaching adhesions at the rear in order to contract and move forward. oxLDL signals through Rho/Akt to exert its effects on endothelial cells and inhibiting either Rho or the phosphorylation of Akt inhibits oxLDL dependent proliferation (Zhang et al., 2017). This effect was not seen with LDL, suggesting that it is the oxidised portion of the lipid that is having the effect, for example it is possible that the oxidised part of LDL is that part that is required for binding to its specific receptor, or that the oxLDL uptake methods are involved in affecting morphology despite the provision of potential further membrane lipids. This could potentially be due to a change in the redox of the cell which may account for the inhibition seen. Both migration and angiogenesis are regulated by a redox system, with VEGF augmenting the activation of Rac-1 and reactive oxygen species from the mitochondria to drive migration (Song and Zou, 2014). It is therefore also likely that spreading may be, at least in part, redox dependent as spreading is important for both migration and angiogenesis.

As discussed in depth previously, Fingolimod might be stimulating cellular polarisation and therefore the cells become more elongated and motile. The results obtained for the cell spreading tie in with those from the migration assays as well as those from the addition of Fingolimod to confluent cells. Combined; Fingolimod causes cells to lose contacts with each other, stimulate polarisation to become more stretched out and subsequently move away from each other. One of the known side effects of taking Fingolimod is macular oedema, caused by a reduction in tight junctions (via S1PR3) between cells allowing the vessels to become leaky (Cugati et al., 2014). This data therefore fits with the current literature and suggests that the formation of tight junctions may also be involved in the inhibition of migration seen with high concentrations of S1P. It would be possible to measure the expression of components of tight junctions such as VE Cadherins,

occludins, junctional adhesion molecules (JAMs), and zonula occludens (ZO) in situ or by western blot to determine if their expression levels and localisation change in response to the addition of S1P or Fingolimod.

The effect of the inhibitor SKII on cell spreading yielded some interesting results and suggests a possibility that it may be blocking an S1P dependent S1P effect. It was expected that inhibition of the kinase responsible for phosphorylating sphingosine would lead to an elongated phenotype as this is the opposite of the effect of high concentrations of S1P and would suggest a role for S1P in cell spreading. It was also seen that when S1P was added back into the SKII inhibited system, the shape of the cells returned back towards that of the control over time, with a significant difference between the inhibitor alone and the inhibitor plus S1P after 24 hours being seen. This suggests that exogenous addition of S1P could negate the endogenous formation of S1P from sphingosine. This could happen in the body if red blood cell derived S1P was generated as red blood cells are turned over quickly so any systemic inhibition of SKII would preferentially affect endothelial cells as they have a longer turn over time.

In contrast, it was hypothesised that S1PL inhibition should increase the circularity of the cells compared to control as by inhibiting the breakdown of S1P, the overall concentration of endogenous S1P increases and this has been shown to result in a more circular, less cell spread morphology. It is however possible that inhibition of S1PL is causing an effect more similar to that of exogenous 1µM S1P addition, as again, addition of further exogenous S1P resulted in the cells retracting and becoming more comparable to the control. It is possible that over a longer time course the cells would continue to retract and could end up appearing more like those seen with 10µM S1P due to the build-up of excess S1P. This may also be dependent of the level of inhibition generated with this concentration of S1PL inhibitor and needs to be further investigated.

The effect of the MEK inhibitor PD showed that ERK is important for cell spreading as PD was able to block the effect of exogenous S1P addition. This inhibition persisted over the 24 hour time course of the assay and suggests that ERK signalling is able to regulate cytoskeleton rearrangement as the cells continued to elongate. It is possible that without ERK signalling, the cells do not know which the leading edge is and therefore continue to stretch out without any directional information. This also ties in with the migration data showing that an inhibition of ERK resulted in decreased migration. It is most likely that as these cells can mobilise their cytoskeleton, the reason they have a slower migration rate is simply because they have lost a directional cue or at least are unable to respond to those cues. This has been shown previously in other studies, with one finding that ERK is required to phosphorylate a Golgi structural protein in order for it to become localised to the leading edge and establish cell polarity (Bisel et al., 2008). The locality of this protein could be

investigated in the presence of S1P and inhibitors to find out if it is similar to MEK inhibited cells. This could provide a potential regulator common to both S1P and ERK.

The albumin/ox-albumin results proved interesting and revealed a number of potential questions. For example, is S1P able to bind to albumin and therefore is albumin able to stop the effect of S1P and protect the cells? Mass spectrometry could be used to test the theory that albumin is able to bind and clear the free S1P. If this was found to be the case, it would be interesting to work out the stoichiometry to ascertain how much S1P albumin can bind and to find out the binding constant. This protective effect was not seen with ox-albumin as the cells appeared spherical like they did with 10µM S1P alone and were floating after 24 hours. It is therefore possible that the oxidised albumin is unable to bind S1P, perhaps the area which is oxidised interferes with the binding sites or maybe there is a conformational change upon oxidation which prevents S1P from binding as it has been reported that albumin oxidation does affect its binding properties (Oettl and Stauber, 2007). This could again be studied using mass spectrometry and would be an interesting topic for future study.

5.5.2 Lipid added to pre-plated cells

As a result of the effect of adding Fingolimod and high concentrations of S1P to confluent cells, it was decided to also analyse the change in circularity of HUVEC which had been plated 24 hours prior to the addition of the compounds. It was found that both the addition of delipidised media and oxLDL had very similar effects on the circularity of HUVEC that was seen when the cells were plated in these compounds. The addition of LDL however did not produce any significant results when added to the pre-plated cells. This was also the case with 1µM S1P, whereas 10µM S1P still resulted in an increase in circularity, suggesting that high concentrations of S1P result in contraction of cellular protrusions and possibly the loss of cell polarity through the signalling pathways discussed previously. As expected, both concentrations of Fingolimod were still able to cause cell elongation, tying in with the results from the migration assays and the literature. As discussed in 4.5.2, Fingolimod increases vascular permeability resulting in macular oedema in some patients (Collins et al., 2010), with another study finding that there is a significant decrease in the levels of the circulating tight-junction proteins occludin and zonula occludens 1 in patients treated with Fingolimod (Annunziata et al., 2018). This suggest that the results found *in vitro* show a similar phenomenon to what may be occurring *in vivo*. Overall, these assays highlight the fluidity of the endothelium, with the cells continually receiving and adapting to external stimuli.

Chapter 6: Effects of lipids on Angiogenesis

6.1 Introduction

Angiogenesis, or the formation of new blood vessels, is a vital part of embryonic development and continues to remain important throughout life. This complex process involves both the migration and differentiation of the endothelium in order to form new capillary networks and is tightly regulated by numerous stimuli. Although essential for life, angiogenesis has also been implicated in a number of diseases, with its role in the metastasis of cancer being arguably one of the most severe and well-studied with over 45 years of continual research being dedicated to this topic (Bielenberg and Zetter, 2015). Psoriasis is also known to include the vasculature and angiogenesis is believed to be important for both the development and progression of the disease.

Angiogenesis occurs through a number of stages that begins with pro-angiogenic factors, such as vascular-endothelial growth factor (VEGF) and fibroblast growth factor (FGF), being released by cells short of oxygen or nutrients. When endothelial cells receive these signals, they change morphology and extend filopodia as well as migrate in the direction of the signal. These cells at the front are termed tip cells while those following behind and elongating the sprout are stalk cells. Tip cells will eventually meet up with other tip cells and the two sprouts will join, forming a new vessel. The vessel is then remodelled to accommodate blood flow and is stabilised by the recruitment of pericytes and a basement membrane is established. Once the hypoxic area is receiving an adequate oxygen supply, the angiogenic signals stop and any remaining tip cells are retracted, returning the endothelium to its quiescent state (Potente and Carmeliet, 2017).

As discussed and shown previously, S1P is involved in the regulation of both cell spreading and migration, which are both involved in the angiogenic process, and therefore it follows that S1P is also able to regulate angiogenesis. S1P does this in both a positive and negative fashion, with S1PR 1 and 3 having a stimulatory effect and S1PR2 inhibiting angiogenesis (Kurano and Yatomi, 2018). Angiogenic stimulation occurs mainly through S1PR1 receptor signalling which results in the activation of the Rho GTPase Rac. Knock-out studies have shown that the ablation of S1PR1 prevents both smooth muscle cells and pericytes from accumulating around blood vessels, subsequently stopping the maturation of new vessels through lack of structural support. Similarly, S1PR2 also exerts its inhibitory effect through the Rac pathway. It has been reported that in senescent cells, S1PR2 is upregulated, thereby inhibiting both migration and angiogenesis in these cells. Inhibitors against this receptor have also been shown to be able to increase S1P mediated angiogenesis, further supporting the inhibitory role of S1PR2 (Takuwa et al., 2010).

This study has focused on the effect of lipids in angiogenesis to try and understand their role in the development of psoriasis. Previous work has shown that oxidised LDL had a concentration dependent effect on angiogenesis and therefore the effect of the bioactive lipid S1P was investigated to show whether oxLDL signals through a S1P dependent mechanism.

6.2 Hypothesis and aims

It is hypothesised that S1P will have a concentration dependent effect on angiogenesis

It is hypothesised that S1P is important for angiogenesis and that it will have a concentration dependent effect. Various inhibitors of the S1P signalling cascade are also hypothesised to block the effect of S1P on angiogenesis.

Specific aims of this chapter are:

- to investigate the effect of S1P and Fingolimod on angiogenesis across a range of concentrations (10μM-1nM)
- to investigate the effect of various inhibitors of the S1P signalling cascade on angiogenesis, such as inhibitors against the S1P receptors 1-3 and inhibitors of S1P lyase
- to investigate the effect of oxLDL and ox-albumin on angiogenesis
- to investigate the effect of adding S1P, Fingolimod and ox-albumin to an established angiogenic network

6.3 Method

Angiogenesis assays were set up using 15 well angiogenesis slides (see Figure 8) and phase contrast microscopy. An example of the images taken of the wells showing endothelial network formation, an indication of the angiogenic process are shown below in Figure 95. The control and 10µM S1P are shown for comparison as they highlight the formation of the hallmarks of angiogenesis in *in vitro* assays namely tubes and nodes and cell network formation in the control compared to the single cells still seen in the presence of 10µM S1P which represents the start point of the *in vitro* angiogenesis assays.

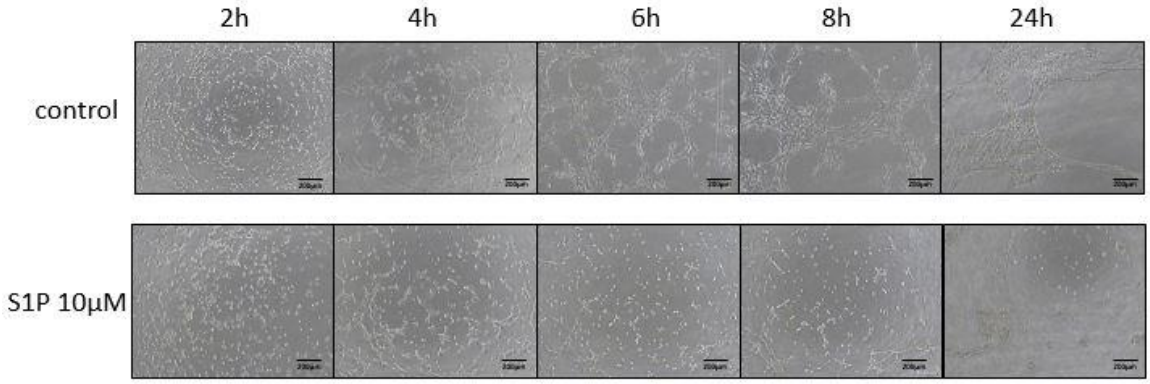

Figure 95 Example of angiogenesis.
Endothelial cells were placed on gel matrix as described and allowed to form networks over time. Representative images from each time point are shown for control cells and in the presence of 10µM S1P. Original magnification x4 using phase contrast microscopy.

To analyse the images, the Angiogenesis Analyser plugin in Fiji was used. This gave a wide variety of values including the total tube length seen in each image as well as the number of nodes or branching points. Figure 96 shows a representation of the results generated using the plugin. For every batch of analysis, the images were checked to ensure that the network detected by the plugin was an accurate representation of the network seen in each image.

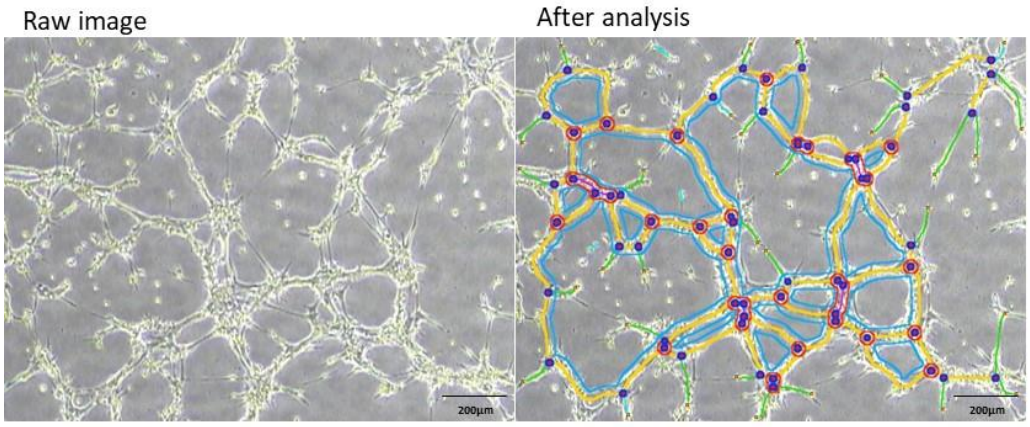

Figure 96 Output of angiogenesis analysis from Fiji

The Angiogenesis Analyser plugin from Fiji provides an accurate representation of the number of nodes and branches seen in each image. Sample images from each batch of analysis were chosen at random and checked so that there was confidence in the data generated.

The angiogenesis plugin works by grouping a number of different functions together so that images can be quickly and autonomously analysed. First of all, the main outline of the network is identified, providing a skeleton of the HUVEC image. This skeleton is then cleaned, with any artificial loops being removed according to pre-set measurements chosen by the user. The Find Extremities function was turned off as this identified the edge of the image as part of the angiogenic network.

Figure 97 shows the features of interest measured by this plugin.

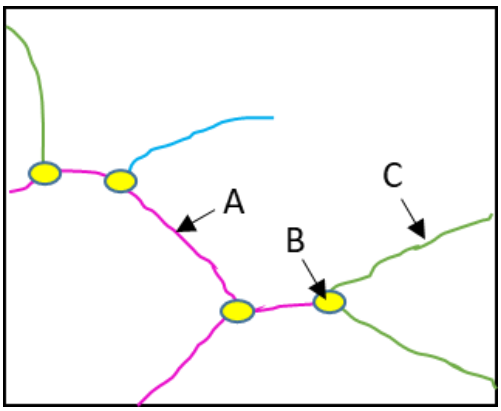

Figure 97 Showing nodes, junctions and branches

The Angiogenesis Analyser plugin from Fiji provides measurements of a number of different features of an angiogenic network. **A** (pink) shows a *segment* (between two junctions), **B** (yellow dots) shows a *junction* (made up of nodes i.e. a pixel with three neighbours) and **C** (green) shows a *branch* (originating at a junction and ending at an extremity). A *twig* (blue) is also shown to highlight the difference between a twig and a branch.

After the skeletal network has been cleaned, nodes and junctions are then identified. A node is defined as a pixel with three neighbours and a junction is a group of touching nodes (see Figure 97). Branches and segments were also identified, with a branch originating at a junction and ending at an extremity (edge of the image) and a segment being between two junctions. Twigs are also identified, and these originate at a junction but do not reach the extremity of the image. The combination of these three measurements provided the total tube length in pixels which was recorded as a measure of the angiogenic potential of HUVEC under various conditions. A range of other functions can also be assessed using this plugin, however only those measurements used here have been described.

In order to provide a measurement for length in a typical length unit rather than in pixels it was necessary to calibrate pixel size for absolute distance. This was achieved by imaging a haemocytometer with known measurements and using Fiji to draw a line to determine how many pixels equated to a known distance measurement. It was found that one pixel was equal to 1µm at the standard 4x original magnification used and therefore any length or area measurements generated could be calculated from the reported pixel number. For example the image shown above in Figure 96 is of 1nM S1P taken at 8 hours after initial seeding and has 175 nodes and with a total tube length of 4525.5 (pixels) which equates to 4.5mm.

The effect of S1P, Fingolimod, the S1P receptor inhibitors, oxLDL and albumin on angiogenesis was studied and the results analysed as described above. The results are shown in the following sections, with both normal and delipidised media being used.

6.4 Results

6.4.1 Sphingosine-1-phosphate

S1P was found to inhibit migration and cell spreading at high concentrations and therefore it was investigated whether it had a similar effect on angiogenesis as both these processes are required for new sprout formation. The same 10-fold concentration gradient of S1P that was used for the previous two assays (migration and cell spreading) was also used to assess the effect on angiogenesis.

6.4.1.1 The effect of S1P on angiogenesis in normal media

In order to ascertain the effects of S1P under normal conditions, the following results are from experiments all performed in full media. A concentration gradient of S1P from 10µM to 1nM was used and the wells imaged every two hours up until hour 8 and then again after 24 hours for a fixed number of cells seeded onto the gel matrix. The mean number of nodes and tube length for the 10-fold dilution series is shown below in Figure 98.

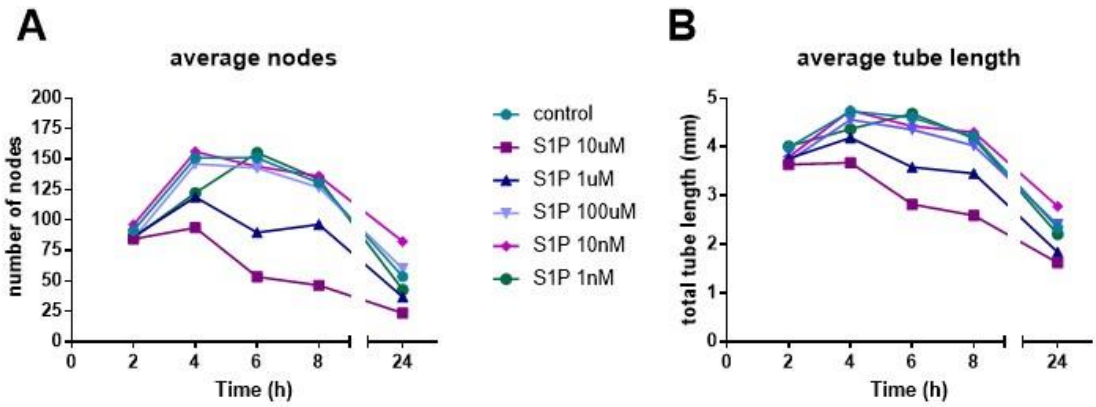

Figure 98 Effect of S1P and time on the number of nodes and tube length over 24 hours
Cells were plated on to Geltrex and allowed develop networks as described. Images were captured and analysed for various parameters related to the angiogenic response. **A-** graph showing the mean number of nodes for each S1P concentration over 24 hours, **B-** graph showing the mean tube length in micrometres across each S1P concentration over 24 hours, n=4

10µM S1P showed the lowest mean tube length and number of nodes across all time points when compared to controls, with 10nM and 1nM concentrations potentially showing an eventual increase compared to the control. The mean tube length and number of nodes at each time point are shown in more detail in Figure 99.

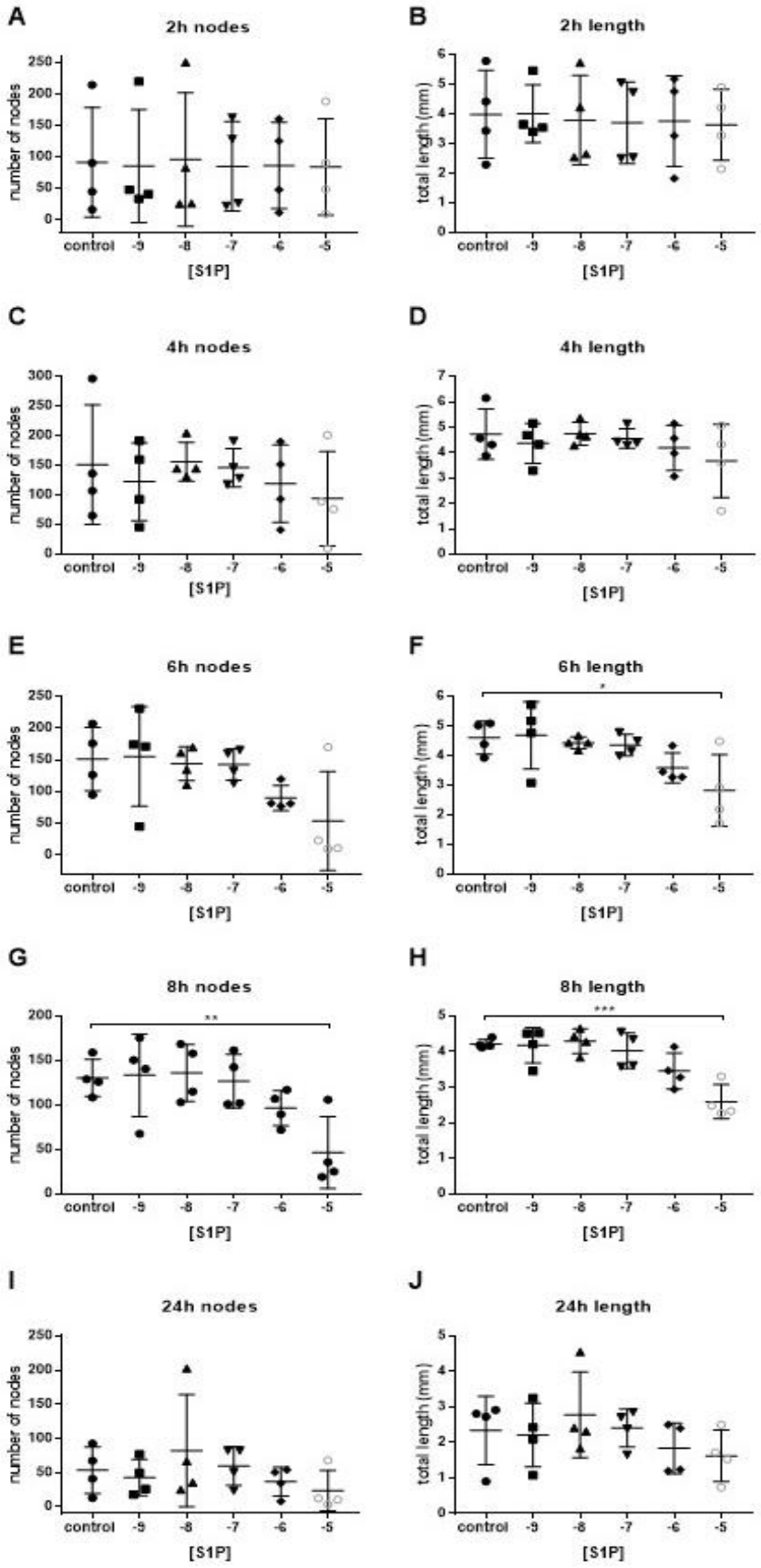

Figure 99 Total tube length and number of nodes at each time point for all concentrations of S1P used

Angiogenesis assays were performed and analysed for node and tube length formation in the presence of various concentrations of S1P and over time as described. Error bars show the mean +/- SD, n=4

Compared to the control and lower concentrations of S1P, 10μM S1P has an inhibitory effect on node formation and total tube length and therefore angiogenesis. One-way ANOVA analysis revealed an overall p value of p= 0.0183 for graph F, p= 0.0076 for graph G and p= 0.0002 for graph H. Any difference between the S1P concentrations compared to the control was tested for using ANOVA with Dunnett's post Hoc tests that revealed a significance of p=0.0161 for graph F, p= 0.0085 for graph G and p= 0.0002 for graph H between 10μM S1P compared to control.

In order to gain a better understanding of the effect of S1P concentrations on angiogenesis as a whole, graphs of the average nodes vs average tube length were plotted for each time point. These are shown below in Figure 100.

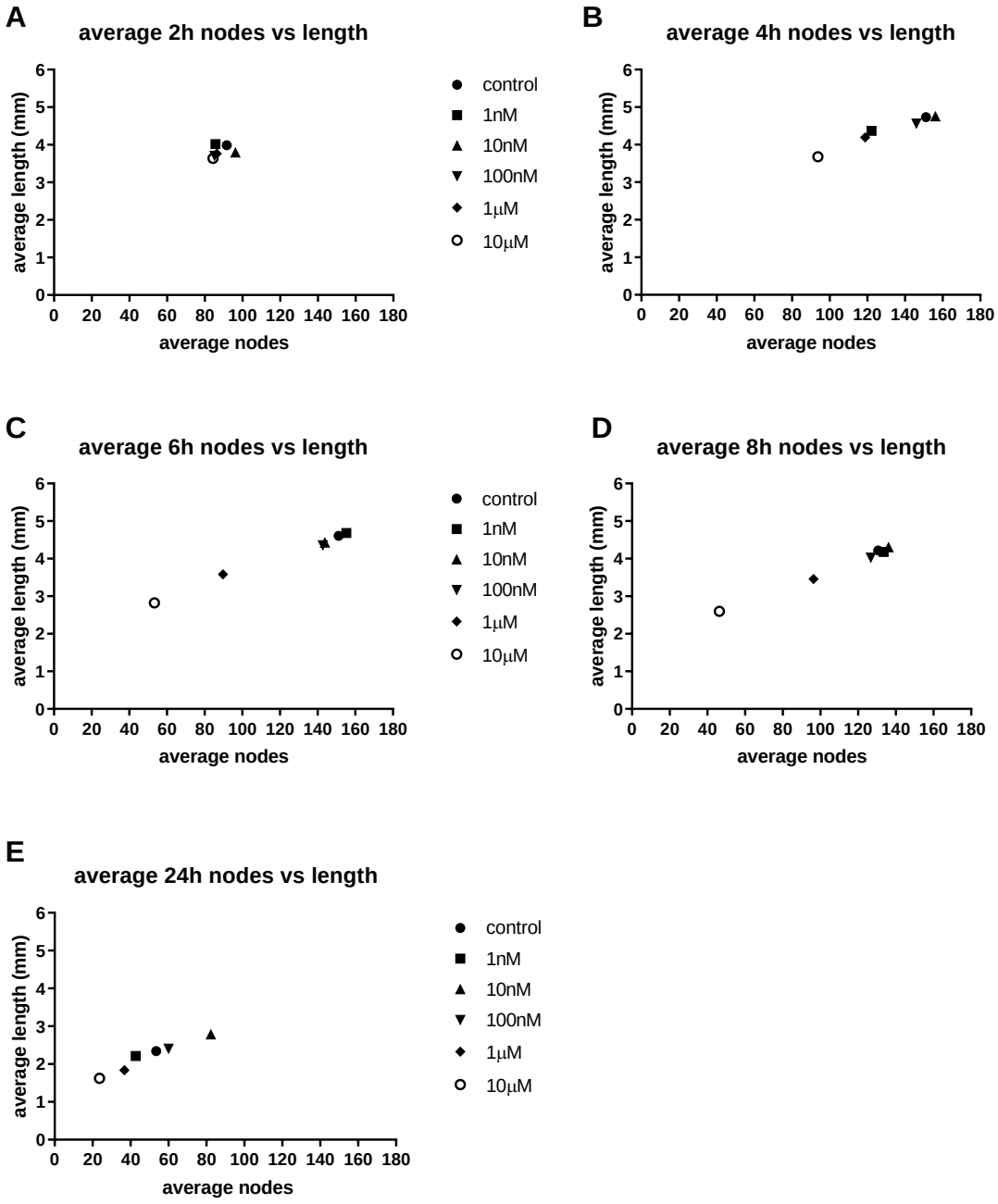

Figure 100 Number of nodes vs total tube length at each time point
Angiogenesis assays were performed and analysed for node and tube length formation in the presence of various concentrations of S1P and over time as described. The average number of nodes against total tube length from four independent assays was calculated and plotted.

From the graphs in Figure 100 it can be seen that all concentrations of S1P start with a similar number of nodes and tube length (graph A). These graphs also highlight that 10μM S1P has an inhibitory effect on both the number of nodes and the tube length, this is especially clear in graphs C and D.

The ratio of the nodes/length over time for the control and 10µM S1P was also plotted to highlight the inhibitory effect that this high concentration of S1P has on angiogenesis. This is shown below in Figure 101.

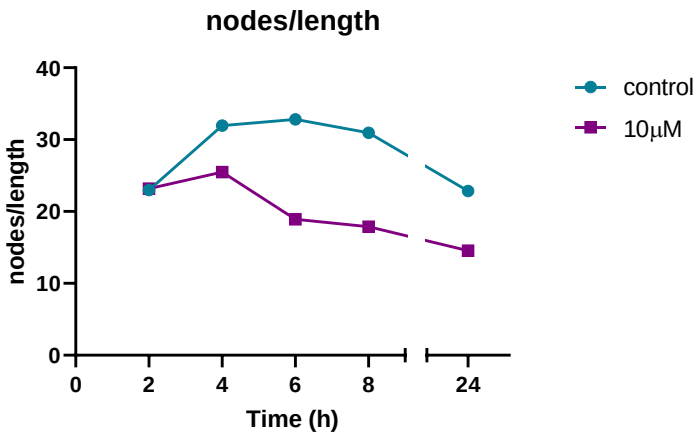

Figure 101 Node/length ratio over time
The node to length ratio was calculated from the average values for each time point and plotted to highlight the effect of high concentrations of S1P on angiogenesis.

Figure 101 clearly shows the inhibitory effect high concentrations of S1P have on the angiogenic potential of HUVEC compared to the control.

From Figure 98 to Figure 101 it can be seen that 10µM S1P has an inhibitory effect on two aspects of angiogenesis mimicking the effect seen in the migration assays. It is interesting to note that even after 24 hours, no angiogenesis is seen for 10µM S1P, suggesting that the inhibitory effects of S1P at this concentration are long lasting.

6.4.1.2 The effect of S1P effect in delipidised media

The experiments from 6.4.1.1 were all repeated in delipidised media in order to gain a fuller understanding of the role of S1P in angiogenesis to compare with the results obtained in the migration studies. By using delipidised media, it was hypothesised that any buffering effect from the lipids in the media would be removed, allowing any effect on angiogenesis by S1P to be more clearly deciphered. Again, the mean number of nodes and the total tube length for the 10-fold dilution series over 24 hours was examined and the results are shown below in Figure 102.

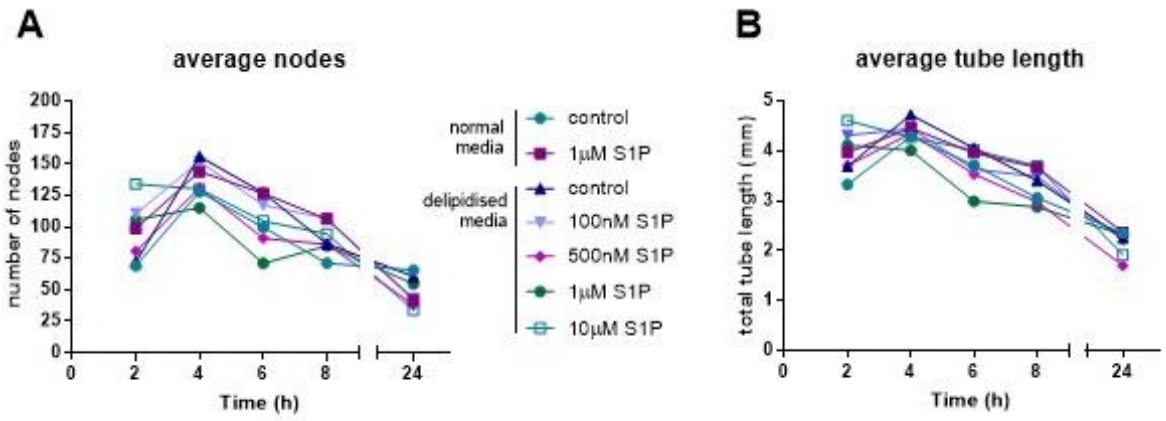

Figure 102 Effect of S1P concentration on the number of nodes and tube length over 24 hours in delipidised media

Angiogenesis assays were performed and analysed for node and tube length formation in the presence of various concentrations of S1P and over time as described. **A-** graph showing the average number of nodes for each S1P concentration over 24 hours, **B-** graph showing the average tube length in micrometres across each S1P concentration over 24 hours, n=3

The results from Figure 102 appear to show that the inhibitory effect seen at the higher concentrations of S1P is not seen when the cells are placed in a reduced lipid environment. For both graphs it can be seen that at the first time point (2 hours) 10μM S1P showed the greatest number of nodes and tube length, however neither of these increased over the remaining time course whereas all other concentrations of S1P did cause an increase at 4 hours. The effect of the various concentrations across all time points was then looked at more closely and the results are shown in Figure 103.

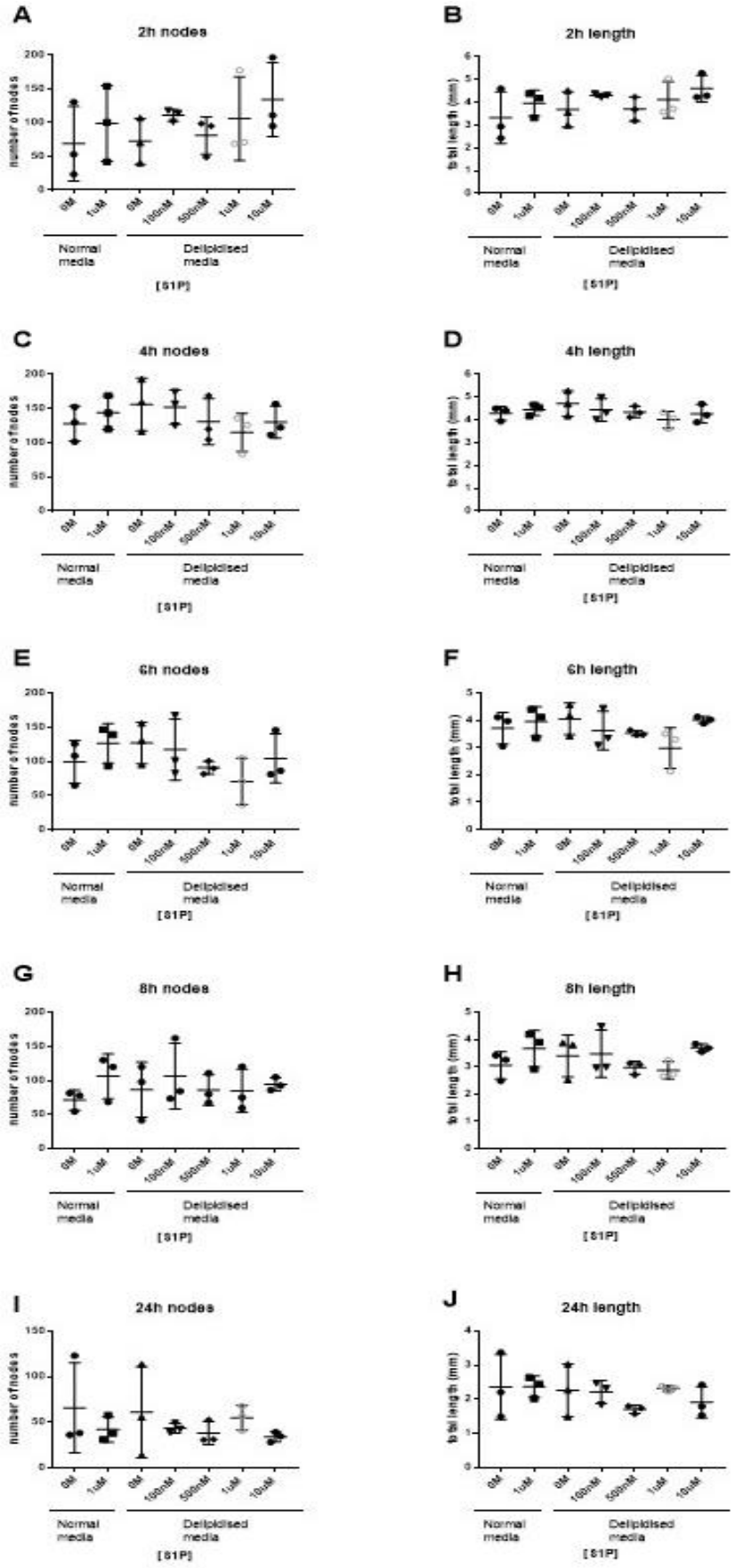

Figure 103 Total tube length and number of nodes at all time points for all concentrations of S1P used

Cells were seeded onto Geltrex and allowed to form networks in the presence or absence of serum lipids over time as previously described. Error bars represent the mean +/- SD, n=3

The inhibitory effect of high concentrations of S1P on angiogenesis seem to be negated in a reduced lipid environment. No significance for any of the time points was found using one-way ANOVA or multiple comparisons testing.

Again, the average results of the number of nodes and the total tube length were combined to show overall angiogenesis and the results are shown below in Figure 104.

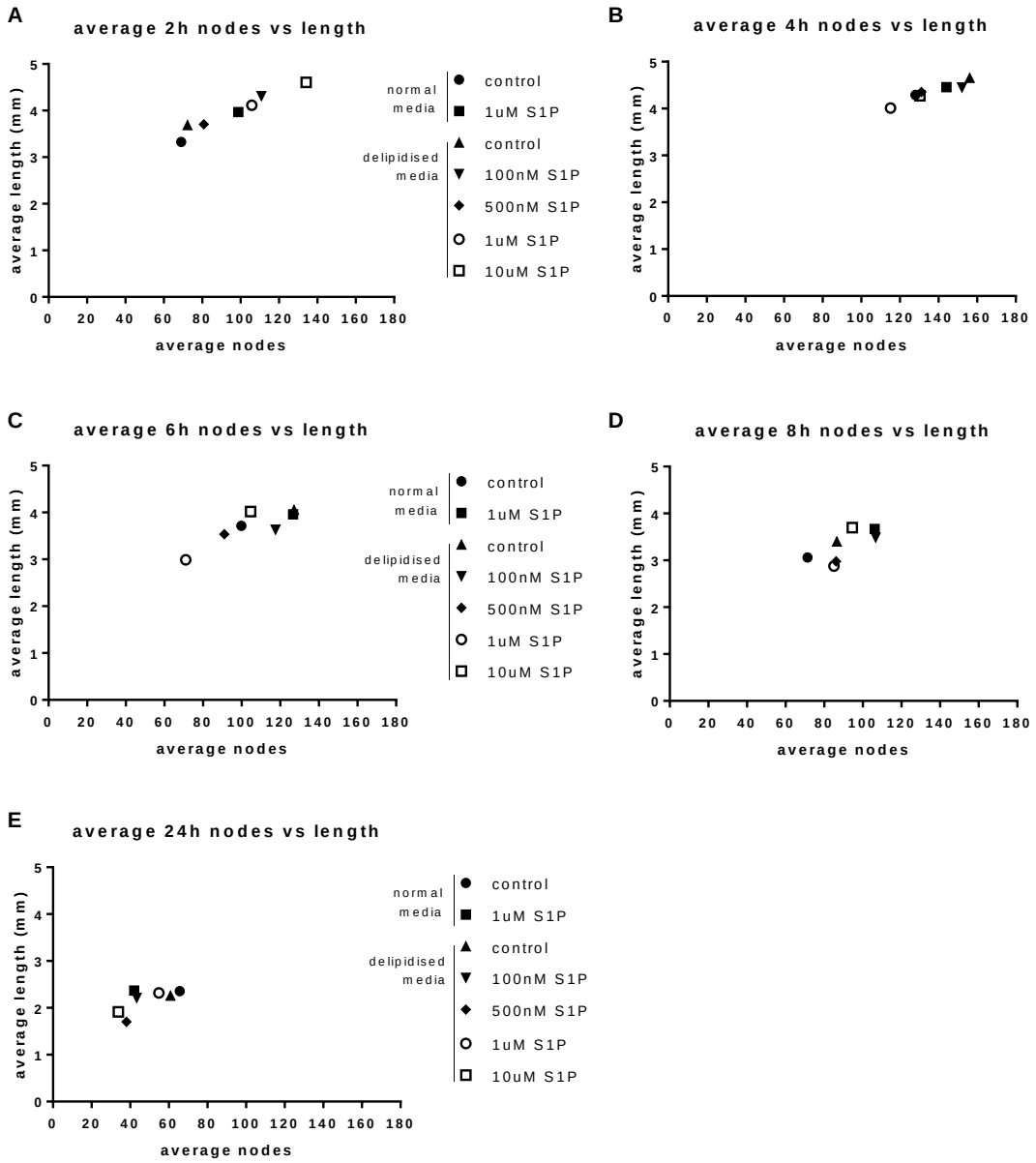

Figure 104 Number of nodes vs total tube length at each time point
Angiogenesis assays were performed and analysed for node and tube length formation in the presence of various concentrations of S1P and over time as described. The average number of nodes and average tube length were plotted, n=3.

Compared to the other concentrations of S1P, the highest concentration of S1P (10µM) does not have the same inhibitory effect in a reduced lipid environment as it does in a full lipid environment, possibly because the angiogenesis of the other concentrations is also reduced.

The ratio of the nodes/length over time for the control, the delipidised control and 10µM S1P in delipidised media was also plotted. This is shown below in Figure 105.

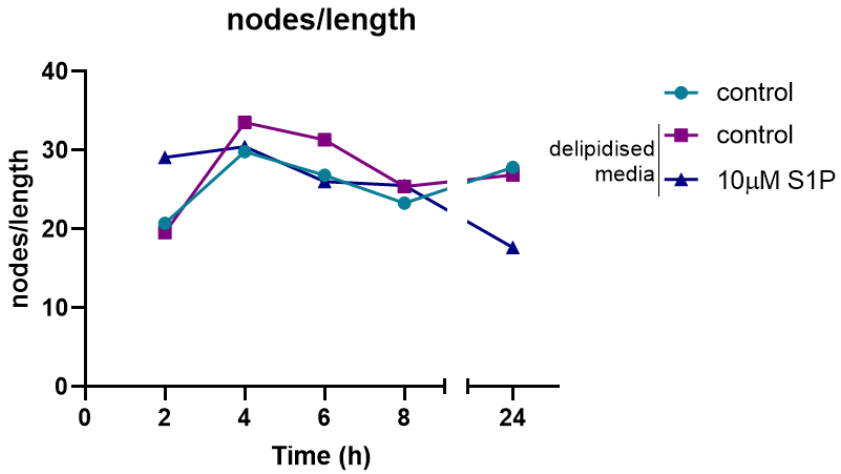

Figure 105 Node/length ratio over time
The node to length ratio was calculated from the average values for each time point and plotted to show the effect of high concentrations of S1P on angiogenesis in delipidised media.

Figure 105 shows the inhibitory effect high concentrations of S1P had on the angiogenic potential of HUVEC in normal media is lost in a reduced lipid environment.

6.4.2 Fingolimod

Fingolimod is a sphingosine analogue and is currently being used as an anti-S1P drug in a clinical setting to treat multiple sclerosis. It was included in the panel of compounds as a way to study what effect the perturbation of the S1P signalling cascade had on endothelial functions and was shown to change the migration and spreading activity of primary HUVEC. Therefore, angiogenesis assays were performed as described above in the presence of Fingolimod.

6.4.2.1 The effect of Fingolimod on angiogenesis in normal media

The results were analysed in the same manner as for S1P stimulation and are shown below.

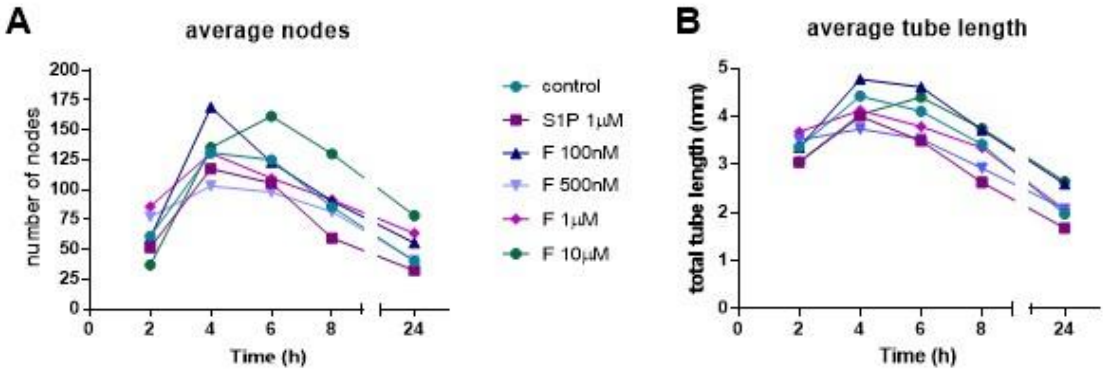

Figure 106 Effect of Fingolimod on the number of nodes and tube length in endothelial angiogenesis over 24 hours
Cells were plated on to Geltrex and allowed to develop networks as described. Images were captured and analysed for various parameters related to the angiogenic response. **A-** graph showing the mean number of nodes for each Fingolimod concentration over 24 hours, **B-** graph showing the mean tube length in micrometres across each Fingolimod concentration over 24 hours, n=3

In normal media, both 100nM and 10μM Fingolimod appear to have a slight stimulatory effect on angiogenesis, in particular the number of nodes seen at 4 hours onwards (graph A). These two concentrations also seem to slightly increase the total tube length above the level of the control (graph B).

The effect of these concentrations on angiogenesis over 24 hours was interrogated in more detail and the results of the raw data are shown below.

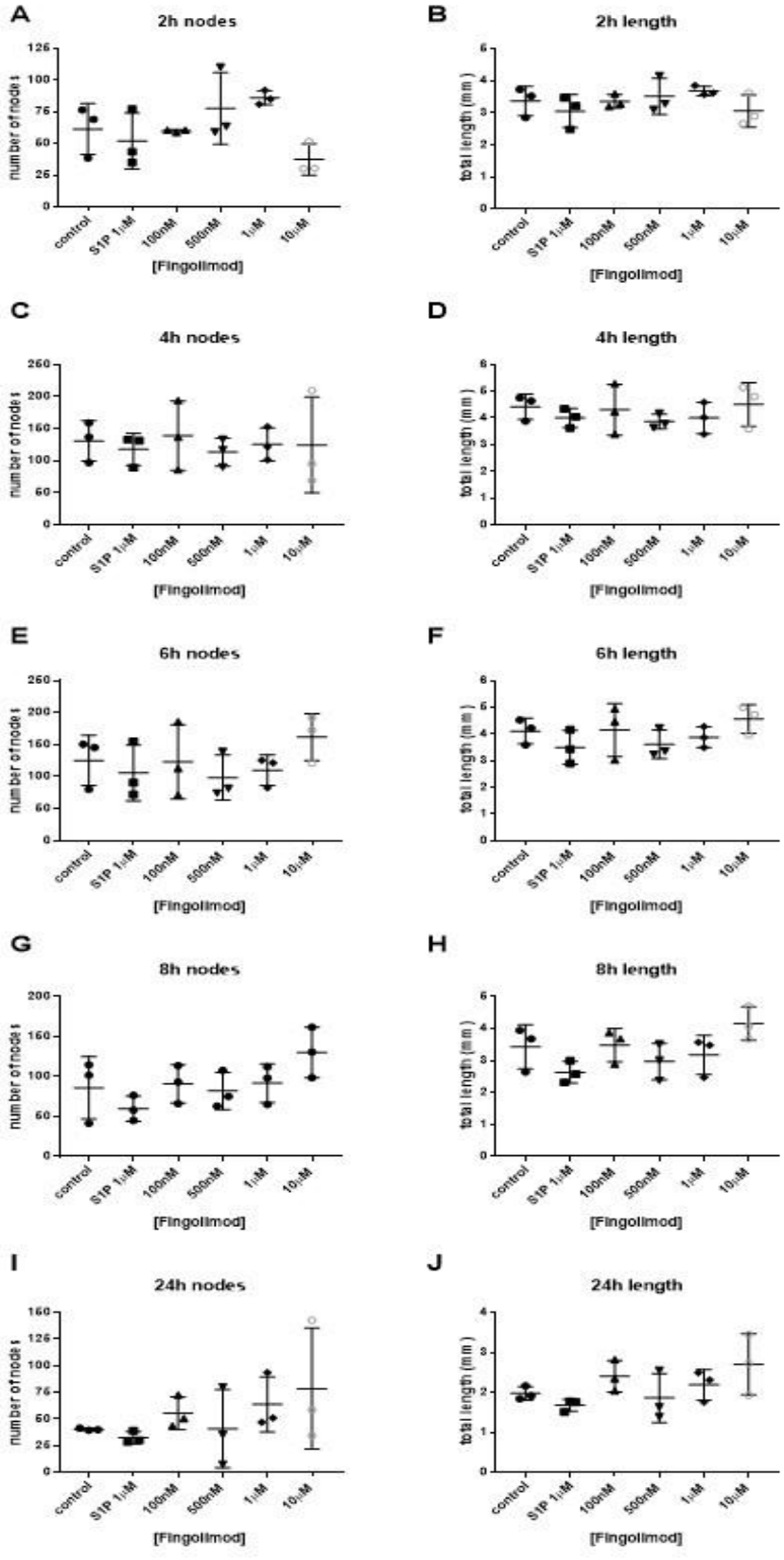

Figure 107 Total tube length and number of nodes over 24 hours for all concentrations of Fingolimod in endothelial angiogenesis assays

Cells were seeded onto Geltrex and allowed to form networks in the presence or absence of Fingolimod at various concentrations over time as previously described. Nodes and tubes length were analysed using Fiji as described and plotted for 8h time point. Error bars represent the mean +/- SD, n=3

Figure 107 shows a potential correlation between the increasing concentration of Fingolimod and both the number of nodes and the total tube length at the 8 hour time point. No significance was found using ANOVA. It is possible that as angiogenesis is a multifactorial process, by using two parameters together it might be possible to describe the effects of each stimulus and inhibitor.

The number of nodes and total tube length were then combined to provide and overall image of angiogenesis. This is shown in Figure 108.

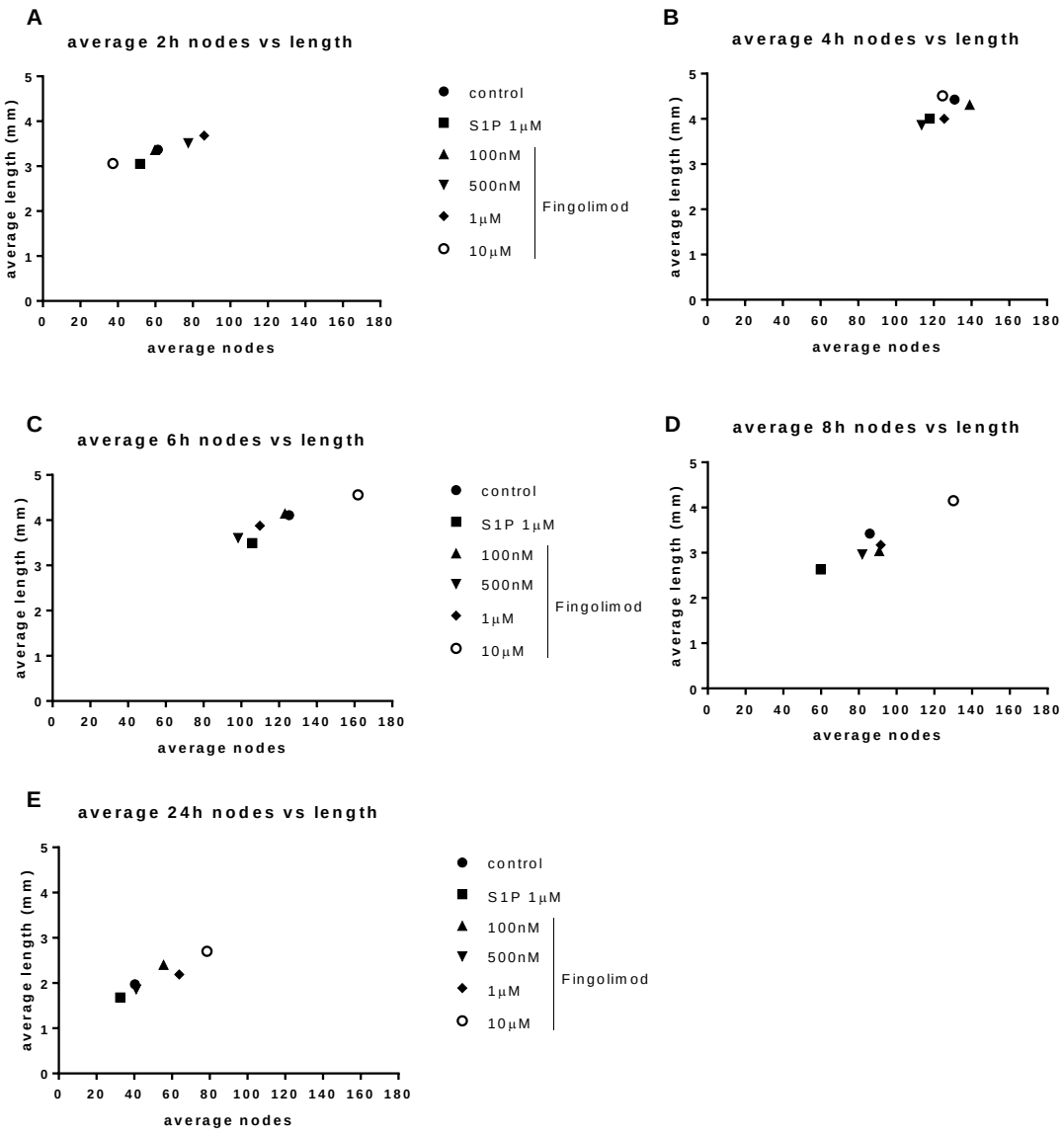

Figure 108 Number of nodes vs total tube length at each time point

Angiogenesis assays were performed and analysed for node and tube length formation in the presence of various concentrations of Fingolimod and over time as described. The average number of nodes and average tube length were plotted, n=3.

In contrast to the results obtained for S1P, the highest concentration of Fingolimod results in an increase in angiogenesis, with the greatest number of nodes and longest tube length being achieved by this concentration.

This is also highlighted on the graph below showing the ratio of nodes to length over time for the control and 10µM Fingolimod.

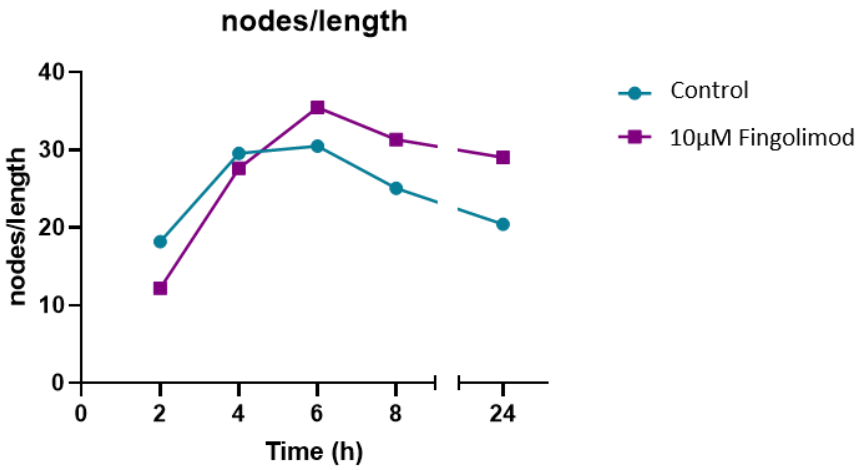

Figure 109 Node/length ratio over time
The node to length ratio was calculated from the average values for each time point and plotted to show the effect of high concentrations of Fingolimod on angiogenesis in normal media.

Figure 109 shows that the highest concentration of Fingolimod stimulates angiogenesis above that of the control.

6.4.2.2 The effect of Fingolimod on angiogenesis in delipidised media

Angiogenesis assays using Fingolimod were also performed in a reduced lipid environment and the results are shown in this section. An overview of the 24 hour time course showing the number of nodes and the total tube length is shown below.

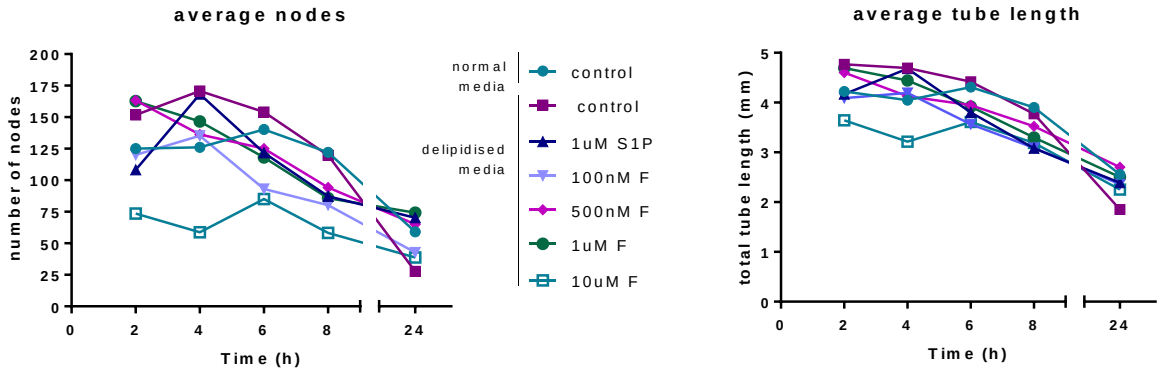

Figure 110 Effect of Fingolimod on angiogenesis in delipidised media on the number of nodes and tube length over 24 hours
Cells were seeded onto Geltrex and allowed to form networks in the presence or absence of serum lipids over time as previously described. Nodes and tubes length were analysed using Fiji as described and plotted against time. n = 3

10µM Fingolimod showed similar results to the S1P assays with the lowest mean tube length and number of nodes across all time points when compared to controls.

When the angiogenesis images were being captured it was noticed that the highest concentration of Fingolimod (10µM) caused the cells to show an altered morphology whereas the cells appeared normal at the lower concentrations (see Figure 111). This difference was the most pronounced after 8 hours, although the difference in the cells started to appear at around 6 hours.

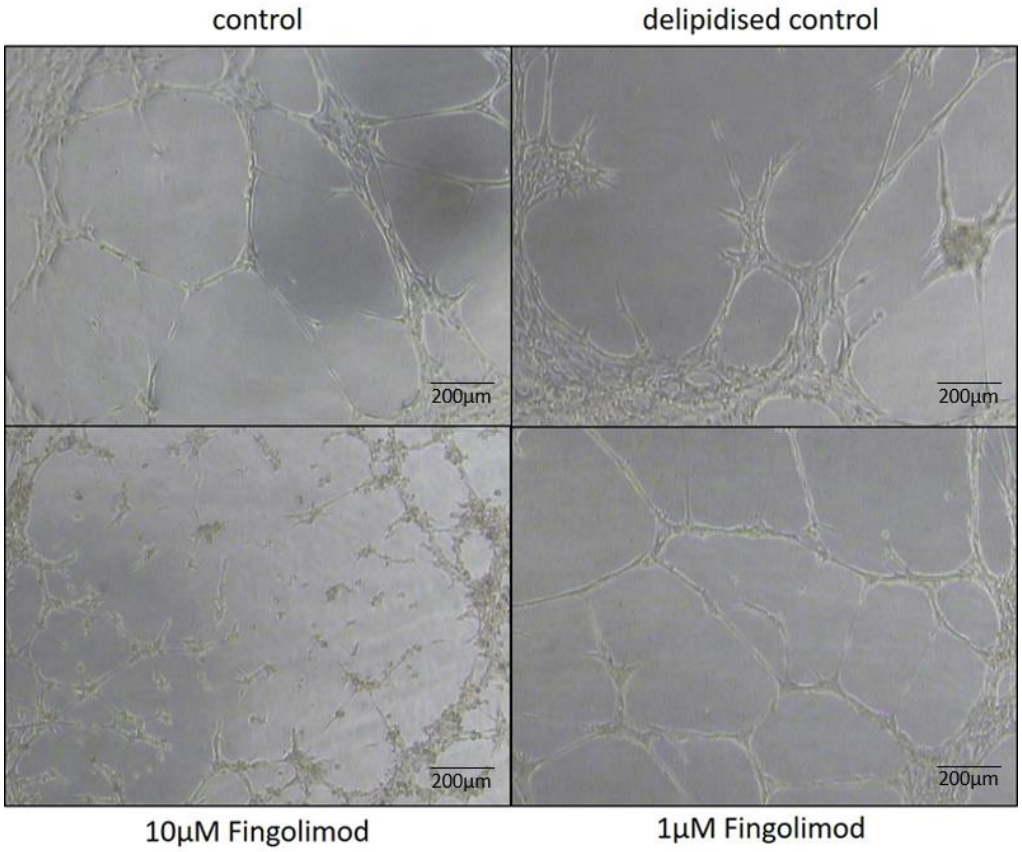

Figure 111 The effect of high concentration of Fingolimod on cells
Cells were seeded onto Geltrex and allowed to form networks in the presence or absence of serum lipids over time as previously described. Images taken after 8 hours.

There is no observable difference between the control and the delipidised control, or indeed 1µM Fingolimod, however the cells that have been exposed to 10µM Fingolimod for 8 hours appear to have an altered morphology. Live/dead analysis showed that there was only a slight increase in cell death at this concentration, therefore this should not have an impact on the results of the angiogenesis assays and instead suggest that Fingolimod may be altering the ability of the cells to form and maintain contacts over time.

The effect of the various concentrations across all time points was then interrogated more closely and the results are shown in Figure 112.

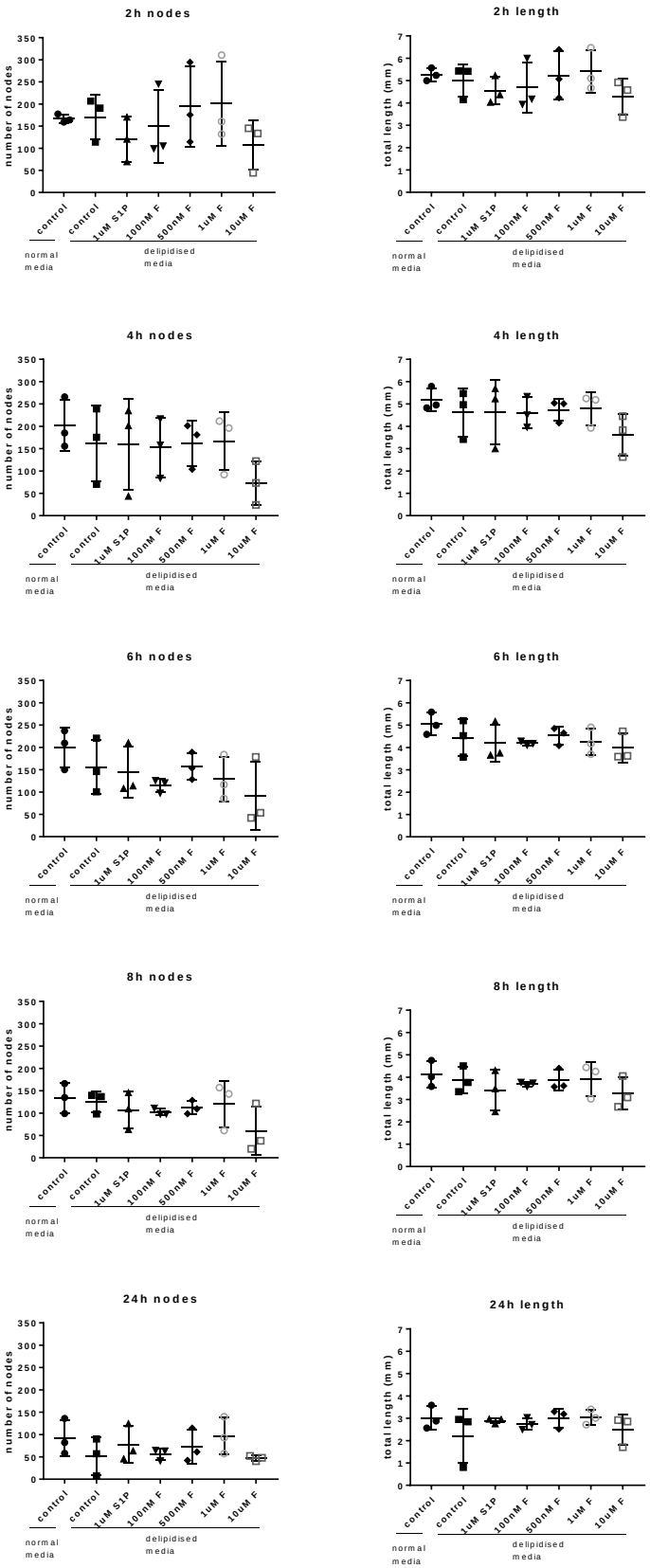

Figure 112 Total tube length and number of nodes over 24 hours for all concentrations of Fingolimod in endothelial angiogenesis assays

Cells were seeded onto Geltrex and allowed to form networks in the presence or absence of Fingolimod at various concentrations over time as previously described. Nodes and tube length were analysed using ImageJ as described and plotted for 8h time point. Error bars represent the mean +/- SD, n=3.

No significant difference was found using either one-way ANOVA or Dunnett's multiple comparisons test for any of the above graphs, showing that the levels of angiogenesis achieved by the various concentrations of Fingolimod was equivalent to control conditions.

The average number of nodes and average tube length for each concentration were then combined to provide an overall image of angiogenesis, the results of which are shown below.

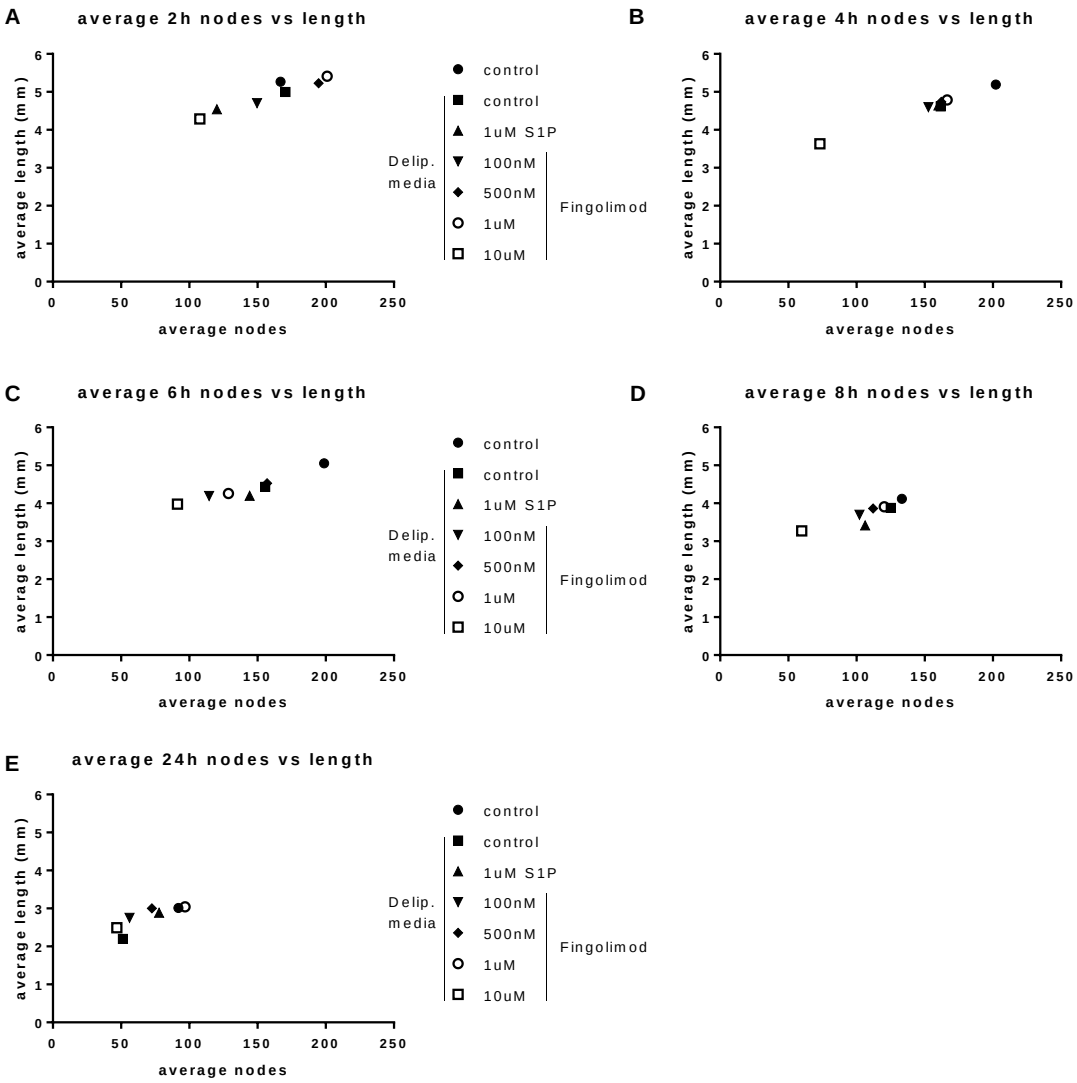

Figure 113 Number of nodes vs total tube length at each time point
Angiogenesis assays were performed and analysed for node and tube length formation in the presence of various concentrations of Fingolimod and over time as described. The average number of nodes and average tube length were plotted, n=3.

Figure 113 shows that in the reduced lipid environment, 10µM Fingolimod inhibits angiogenesis which was as expected due to the rough appearance of the cells (see Figure 111). The lower concentrations of Fingolimod all produce similar levels of angiogenesis compared to the reduced lipid control, with the full lipid control achieving the greatest levels of angiogenesis after 4 hours.

This is also highlighted in Figure 114, showing the ratio of nodes to length over the time course of the assay.

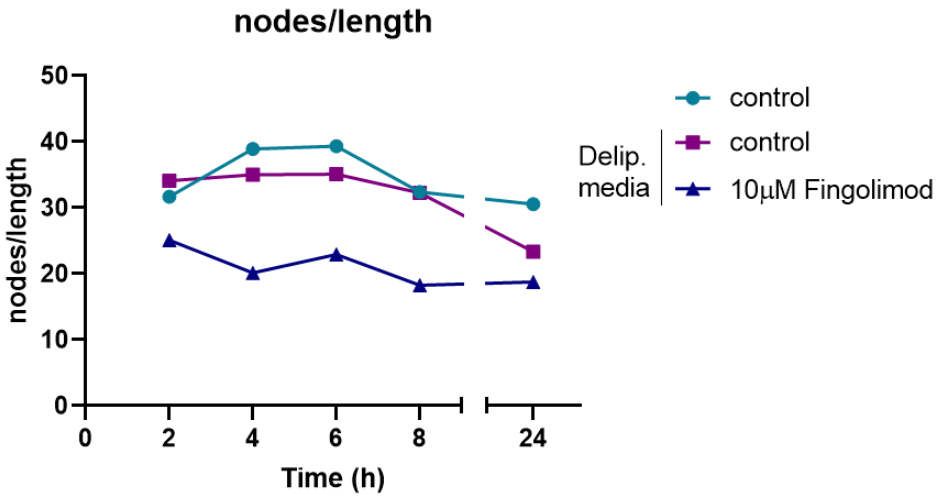

Figure 114 Node/length ratio over time
The node to length ratio was calculated from the average values for each time point and plotted to show the effect of high concentrations of Fingolimod on angiogenesis in delipidised media.

Figure 114 shows that the highest concentration of Fingolimod inhibits angiogenesis compared to both the full lipid control and the reduced lipid control.

6.4.3 S1P receptor inhibitors

The S1P receptor inhibitors that were used in the scratch assays (W146, JTE and TY) have also been used in angiogenesis assays to try to help aid the understanding of the role of S1P in this complex process. As mentioned earlier, S1P has both a stimulatory and inhibitory effect on angiogenesis, with S1P receptors 1 and 3 known to be angiogenic whereas receptor 2 is thought to be anti-angiogenic. Therefore, the hypothesis is that by blocking receptors 1 and 3 this should result in a decrease in angiogenesis and blocking receptor 2 should cause an increase in angiogenesis. The effect of the S1P lyase inhibitor was also studied as a decrease in migration was seen when added in combination with S1P. S1PL also affected the circularity of HUVEC resulting in a more stretched out phenotype compared to that of the control.

6.4.3.1 The effect of S1P receptor inhibitors on angiogenesis in normal media

The effect of the S1P receptor antagonists and the S1P lyase inhibitor on angiogenesis was studied under normal lipid conditions and the mean of the tube length and number of nodes was plotted over the 24 hour time course. As there were so many different combinations of inhibitors, as well as with and without S1P, it was necessary to plot the results on separate graphs and these results are spread over Figure 115 and Figure 116. To clarify, the data is from the same angiogenesis assay and cells obtained from the same umbilical cord were used for all combinations within each experiment. There are a limited number of wells on the angiogenesis slide, therefore not all combinations were able to be performed in duplicate. Therefore only the control, S1P alone, S1PL alone and S1PL plus S1P were performed in duplicate and the average of the two wells used. All the other inhibitors were only added to one well and therefore this result was used. Each point on the following graphs represents the average of three independent experiments.

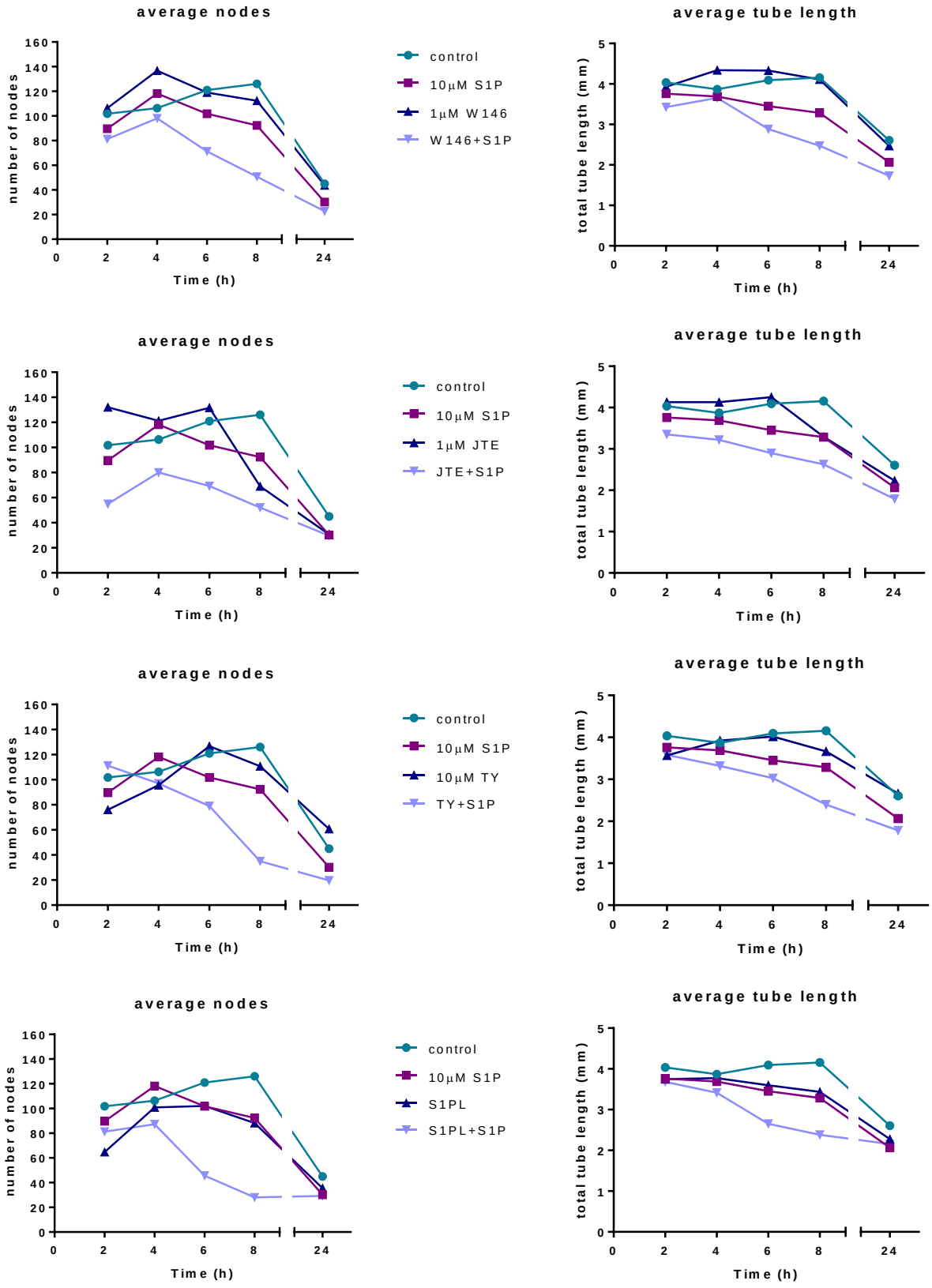

Figure 115 The effect of the inhibitors on the number of nodes and tube length over 24 hours
Cells were seeded onto Geltrex and allowed to form networks in the presence or absence of receptor antagonists or lyase inhibitors over time as previously described. Nodes were analysed using ImageJ as described and plotted against time. All results values are from the same assay using the same cells, n=3.

From looking at the results of the various inhibitors alone, S1PR 1 and 3 do not seem to be important for angiogenesis in the absence of S1P, however S1PR2 is (see JTE alone at 8 hours). In contrast, when exogenous S1P is present this is reversed, with receptor 1 and 3 becoming involved. Similar results were seen for the S1P lyase inhibitor, with the inhibitor alone having no effect on angiogenesis but causing an inhibition in the presence of S1P.

The three receptor inhibitors were also added in combination with each other and the results are shown below.

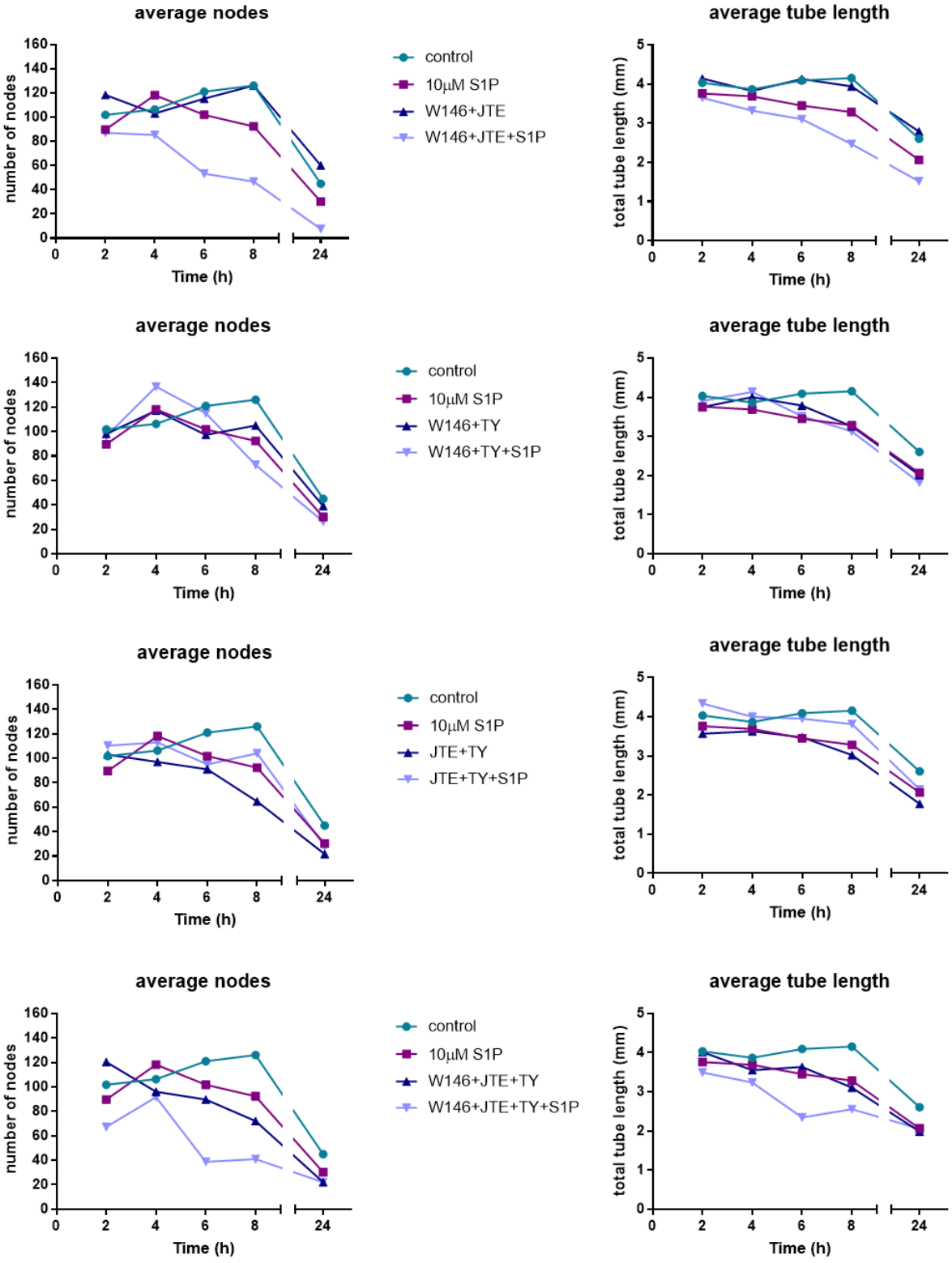

Figure 116 The effect of combined inhibitors on the number of nodes and tube length over 24 hours

Cells were seeded onto Geltrex and allowed to form networks in the presence of combined receptor antagonists as previously described. Nodes were analysed using ImageJ as described and plotted against time. All results values are from the same assay using the same cells, n=3.

The addition of the various inhibitors alone showed that blocking both receptors 2 and 3 and all three receptors slightly decreased angiogenesis compared to that of the control, with the number of nodes affected more that the tube length. The addition of exogenous S1P to inhibitors W146 and JTE showed the greatest inhibition of angiogenesis out of all the combinations used, while addition to JTE and TY resulted in stimulation above the inhibitors alone.

The area under the curve (AUC) for each graph in Figure 115 and Figure 116 was calculated and the results from the number of nodes are shown below in Figure 117 and the AUC for the total length is shown in Figure 118.

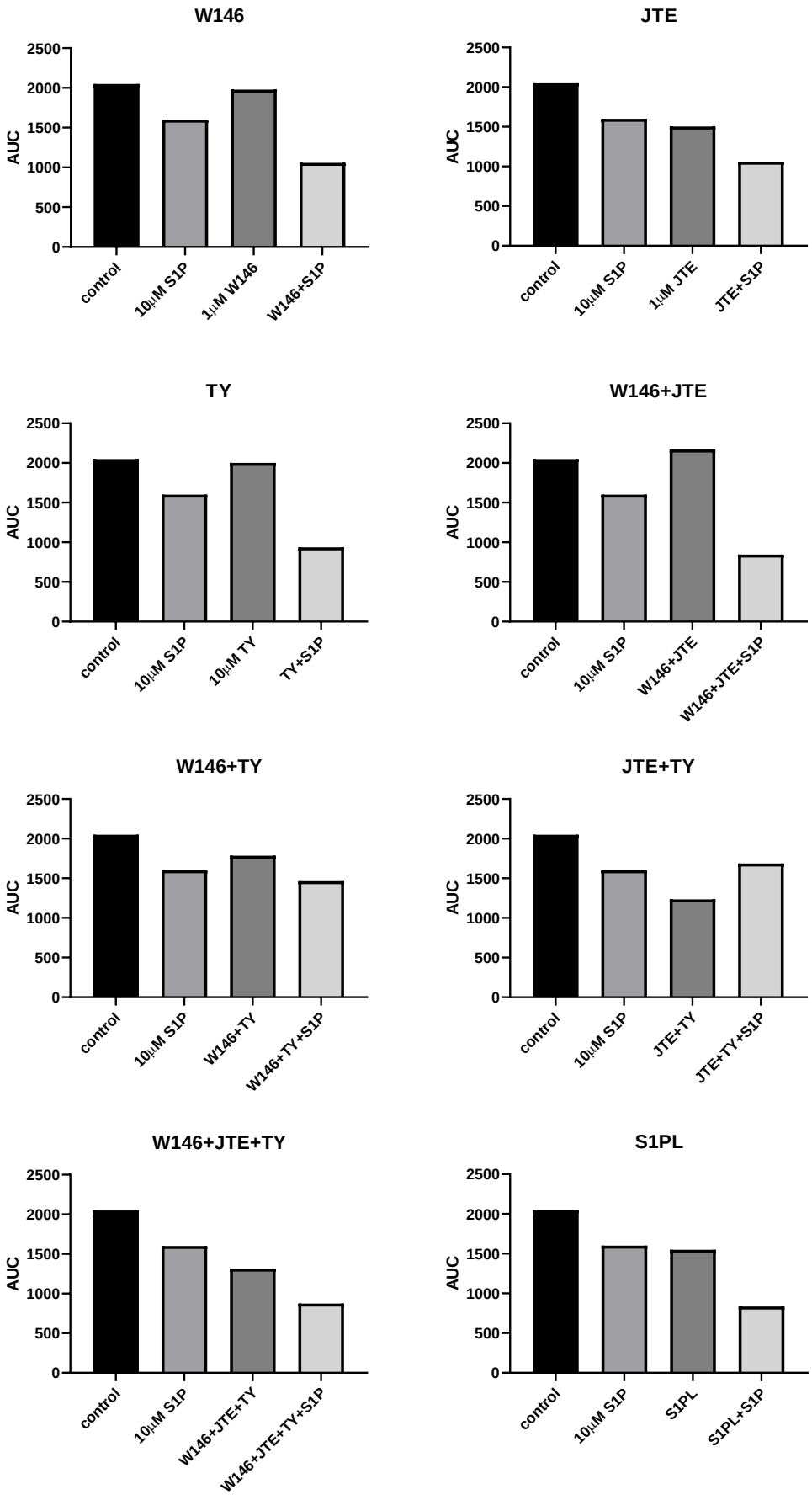

Figure 117 Effect of inhibitors on the AUC for the number of nodes

The AUC for each inhibitor was calculated and plotted to show the effect of the inhibitor on the number of nodes.

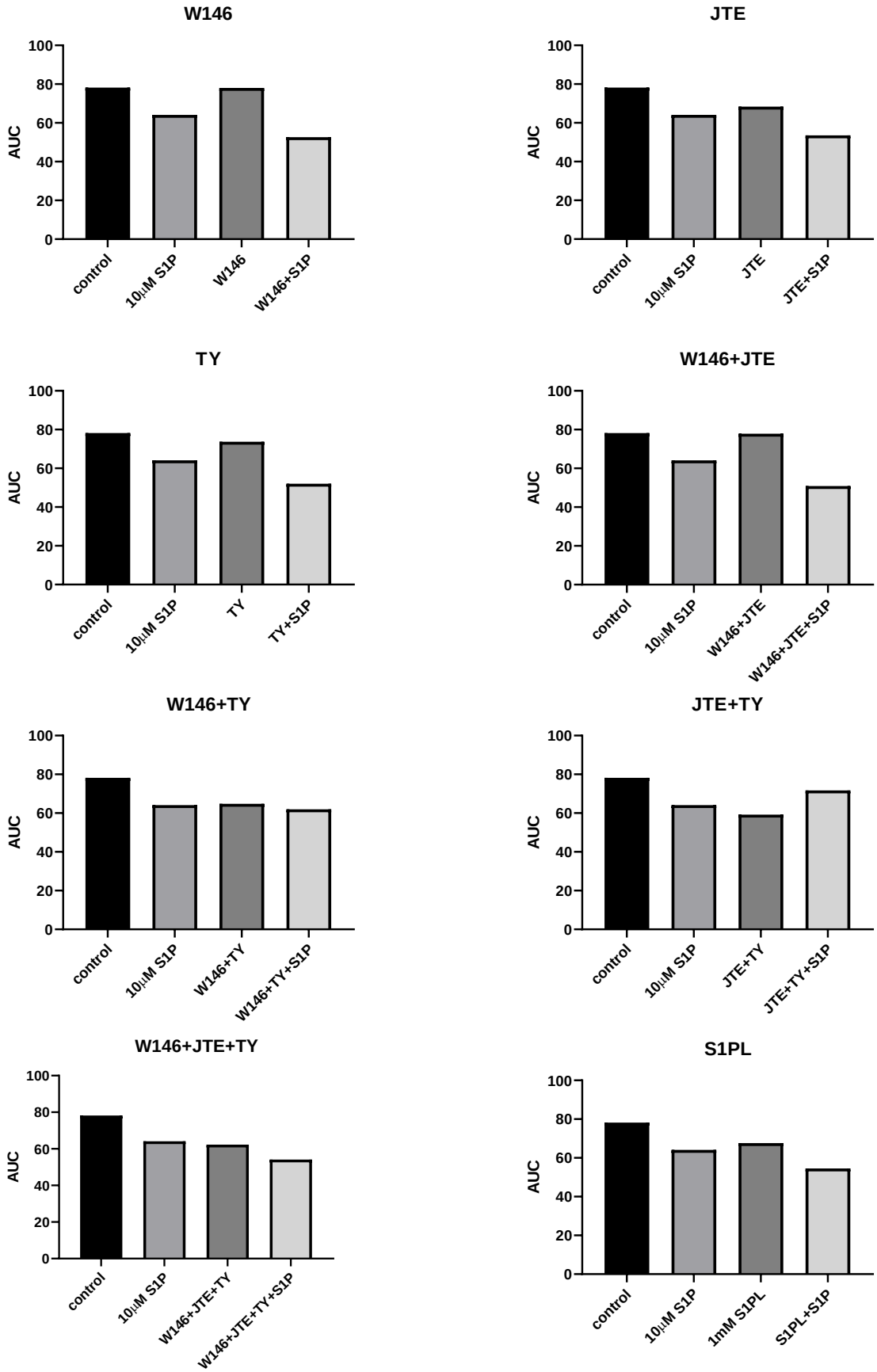

Figure 118 Effect of inhibitors on the AUC for the total tube length

The AUC for each inhibitor was calculated and plotted to show the effect of the inhibitor on the total tube length.

Looking at the AUC for the two average measures of angiogenesis (total tube length and the number of nodes), it is clear that the number of nodes is affected more than the total tube length in response to the S1P receptor inhibitors, especially when they are added in combination with exogenous S1P. This is highlighted in

Table **10**, where the change in the number of nodes or total tube length was calculated as a percentage difference compared to the control, i.e. -20% would mean a reduction of 20% compared to the control.

Table 10 Percentage change of nodes and length (vs control) in response to S1P receptor inhibitors

	-S1P		+S1P	
	Nodes	**Length**	**Nodes**	**Length**
10µM S1P	-	-	-21.85%	-17.99%
W146	-3.51%	-0.24%	-48.44%	-32.71%
JTE	-26.63%	-12.54%	-48.34%	-31.53%
TY	-2.34%	-5.73%	-54.36%	-33.40%
W146 + JTE	+5.80%	-0.45%	-58.75%	-34.95%
W146 + TY	-12.98%	-17.15%	-28.59%	-20.74%
JTE + TY	-39.80%	-24.30%	-17.76%	-8.30%
W146 + JTE + TY	-35.80%	-20.40%	-57.41%	-30.79%
S1PL	-24.49%	-13.53%	-59.32%	-30.31%

Again, the AUC shows that receptors 1 and 3 do not seem to be involved in unstimulated angiogenesis as the inhibitors to these receptors had no effect on the AUC when added alone. JTE (the inhibitor for S1PR2) on the other hand did reduce the AUC when added alone, suggesting that this receptor is involved in unstimulated angiogenesis. The greatest change in AUC in relation to the number of nodes was seen when all three receptor inhibitors were added together. The S1P lyase inhibitor did not have an effect when added alone however caused a reduction in the AUC when added in combination with S1P, while no change in total tube length was seen.

6.4.3.2 The effect of S1P receptor inhibitors on angiogenesis in delipidised media

The S1P receptor antagonists and S1P lyase inhibitor effect on angiogenesis was also investigated in a reduced lipid environment, with the hope that this simplified system may provide a clearer picture of S1P dependent angiogenesis in endothelial cells. Figure 119 shows the results of the inhibitors alone and with S1P over time, with the average of three independent experiments shown.

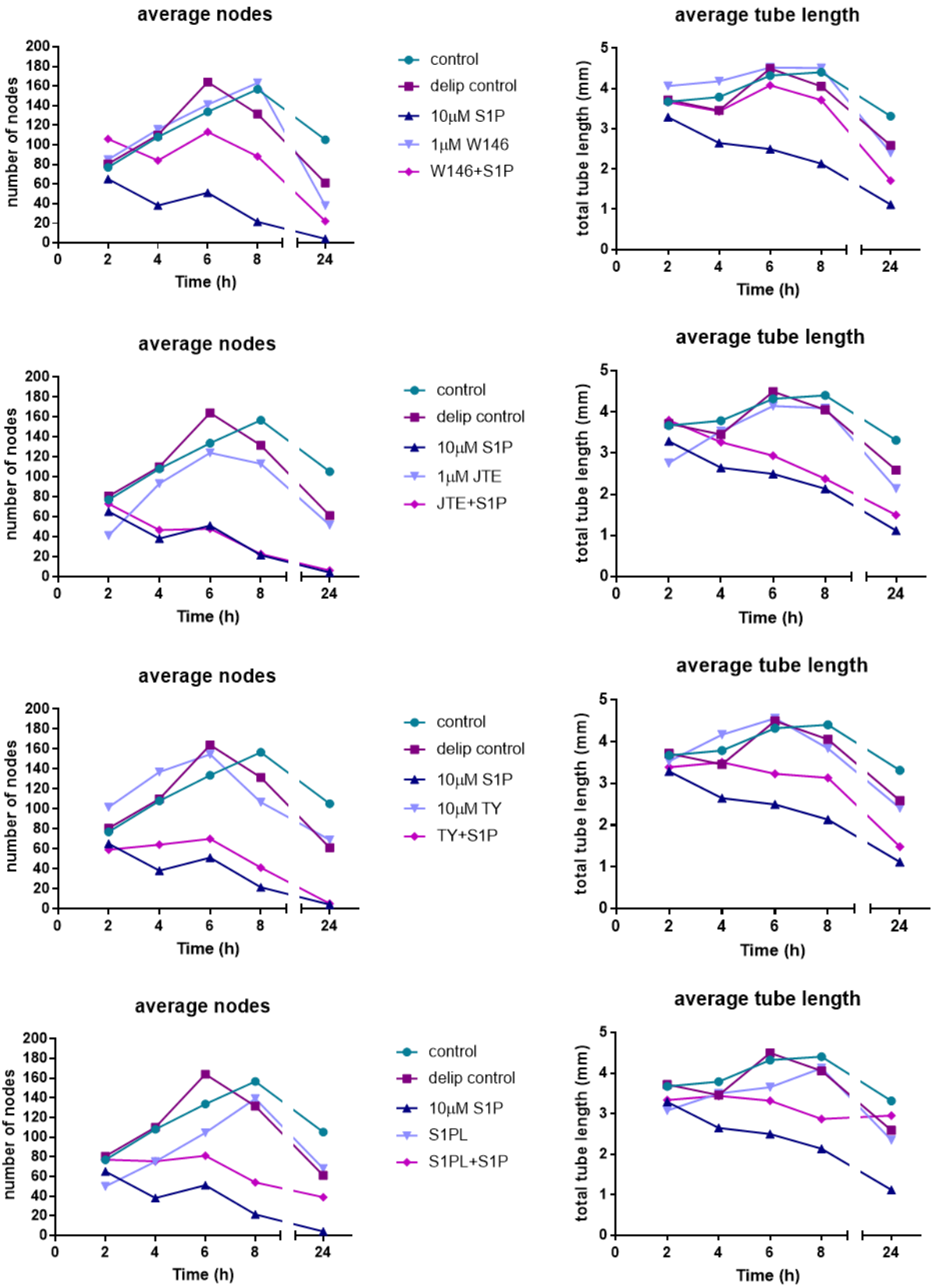

Figure 119 The effect of the inhibitors on the number of nodes and tube length over 24 hours
Cells were seeded onto Geltrex and allowed to form networks in the presence or absence of receptor antagonists or lyase inhibitors over time as previously described. Nodes were analysed using ImageJ as described and plotted against time. All results values are from the same assay using the same cells, n=3.

Figure 119 shows that the addition of the S1PR 1 and 3 inhibitors alone has no effect on angiogenesis, however the addition of the S1PR2 inhibitor and the S1P lyase inhibitor slightly inhibits angiogenesis compared to the control. S1P was added in combination with the inhibitors and it can be seen that the blockade of S1PR1 has a large effect on angiogenesis, with the endothelium still being able to form contacts even in the presence of an inhibitory concentration of S1P, i.e. it rescues the normal angiogenic phenotype to allow tube and node formation. In contrast, inhibitors against receptors 2 and 3 had no effect on angiogenesis and closely mimicked that seen with S1P alone, in particular receptor 2 inhibition. Inhibition was also seen with S1PL and S1P, although not to the same extent as S1P alone.

The three receptor inhibitors were then added in combination with each other and the results are shown below.

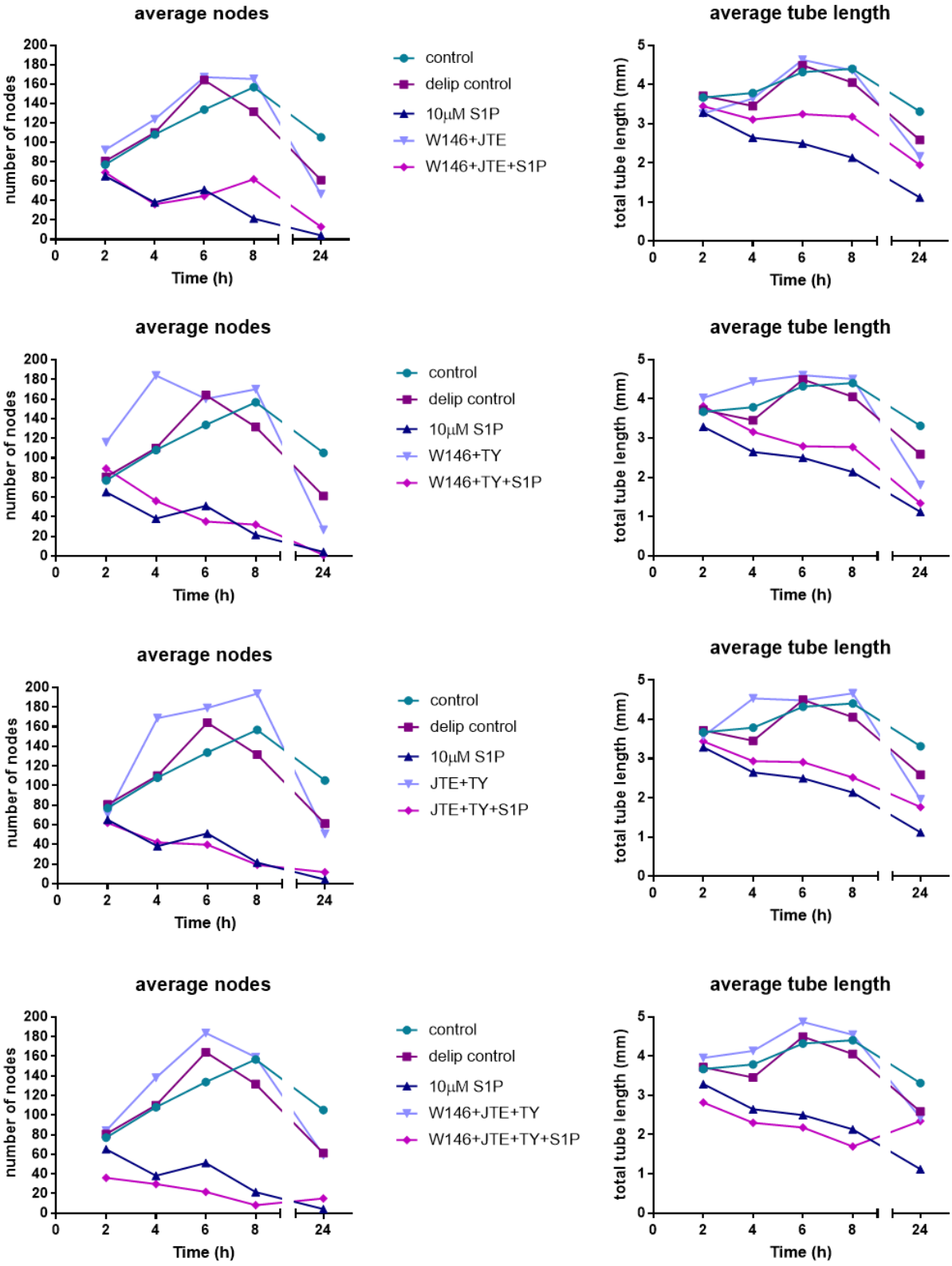

Figure 120 The effect of combined inhibitors on the number of nodes and tube length over 24 hours

Cells were seeded onto Geltrex and allowed to form networks in the presence of receptor inhibitors as previously described. Nodes and tube length were analysed using ImageJ as described and plotted against time, n=3.

Again the combined inhibitors were added alone and with S1P in a reduced lipid environment. The removal of lipids results in a peak number of nodes at 6 hours compared to that of the full lipid control where the number of nodes peaks at 8 hours. It is therefore possible that the removal of lipids is accelerating this angiogenic process. The addition of the inhibitors alone provided some interesting results, with all combinations stimulating angiogenesis above that of the full lipid control, again appearing to accelerate angiogenesis compared to the full lipid control. The addition of S1P to these inhibitor combinations resulted in the opposite effect, with inhibition of angiogenesis seen for all combination.

The area under the curve for each graph in Figure 119 and Figure 120 was calculated and the results are plotted in Figure 121 (showing the AUC for the number of nodes) and Figure 122 (showing the AUC for the total tube length).

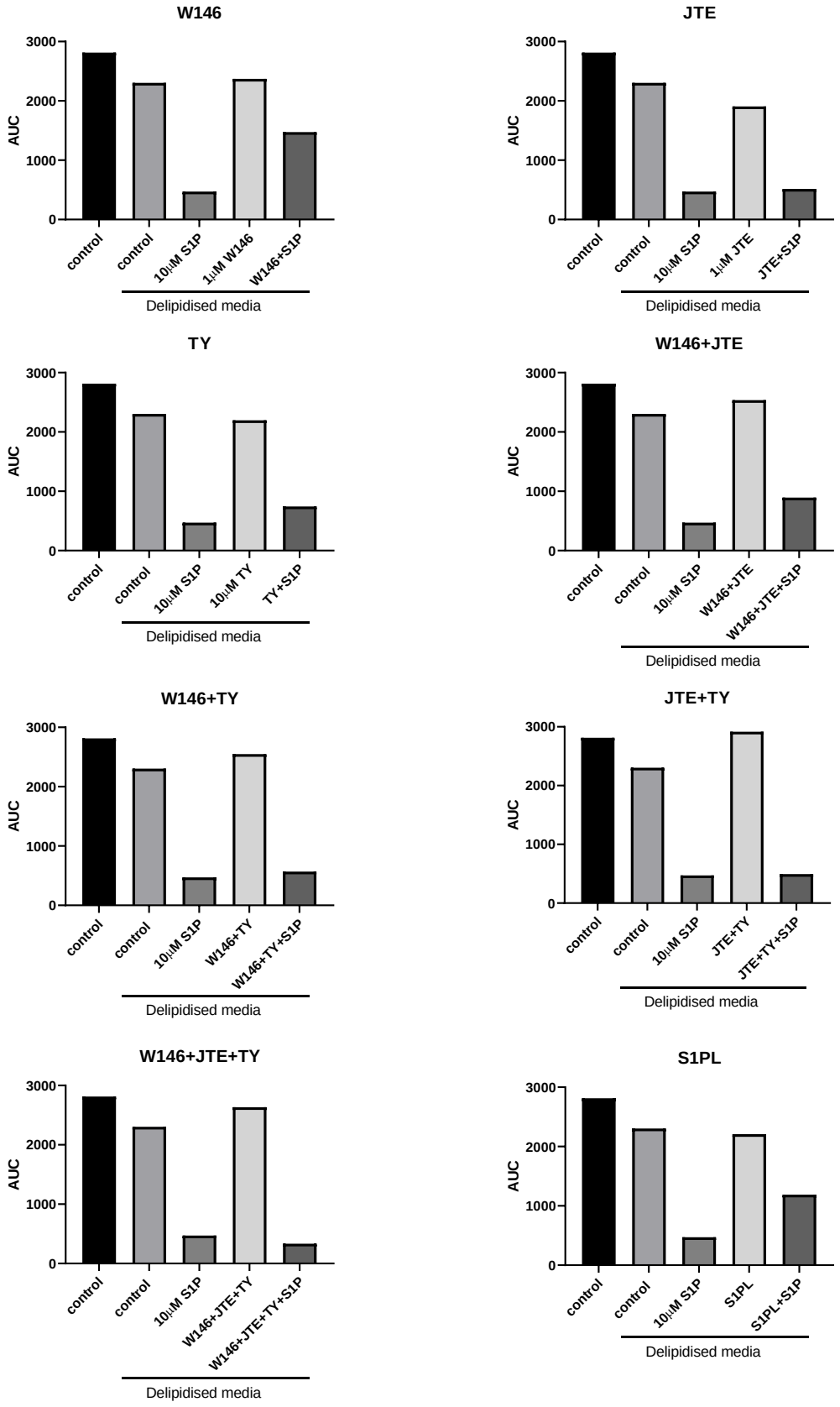

Figure 121 Effect of inhibitors on the AUC for the number of nodes in delipidised media
The AUC for each inhibitor was calculated and plotted to show the effect of the inhibitor on the number of nodes in a reduced lipid environment.

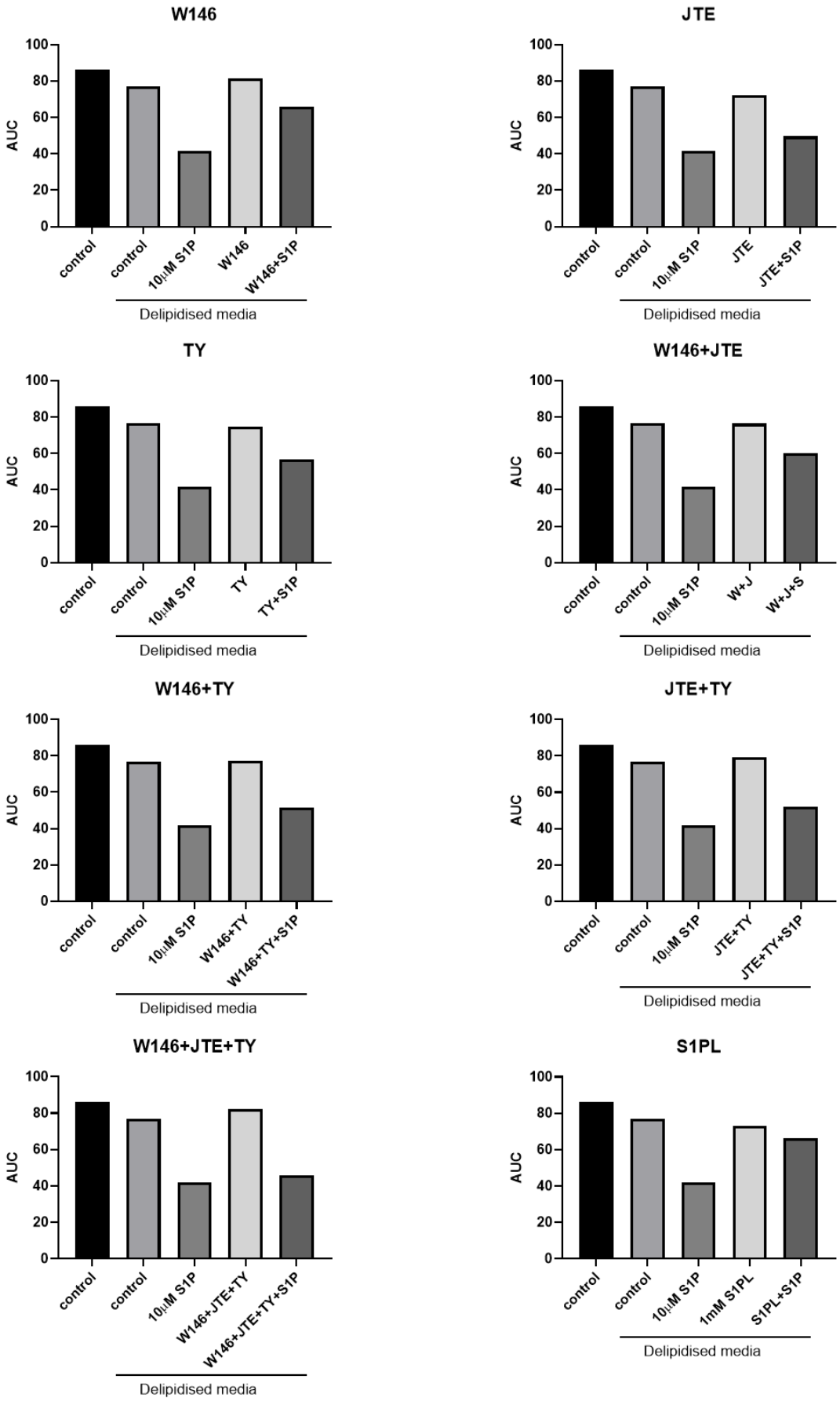

Figure 122 Effect of inhibitors on the AUC for the total tube length in delipidised media

The AUC for each inhibitor was calculated and plotted to show the effect of the inhibitor on the total tube length in a reduced lipid environment.

Similar to the results obtained from the inhibitors in the full media, the AUC for the number of nodes is affected more than that of the total tube length. It can be seen that the AUC for both the number of nodes and tube length is reduced in the delipidised media compared to the full lipid media and that the addition of 10μM S1P causes a large decrease in the AUC, especially for the number for nodes. None of the inhibitors have an effect on the AUC of either the number of nodes or the total tube length when added alone in a reduced lipid environment, however the AUC drops for all inhibitors when added in combination with S1P, with the AUC for the combined receptor inhibitors being even lower than that of S1P alone.

6.4.4 Oxidised LDL

The effect of oxLDL on angiogenesis was studied in order to draw comparisons between S1P and oxLDL, and potentially establish a link between the two. Each condition within each experiment was performed in duplicate and the average of these taken. Three independent assays were carried out using cells from different donors at passage one.

6.4.4.1 The effect of oxidised LDL on angiogenesis in normal media

The same concentrations of oxLDL (and LDL) used in the migration assays was used to study the effect of oxLDL on angiogenesis in HUVEC. The average number of nodes and tube length from three independent experiments is shown below.

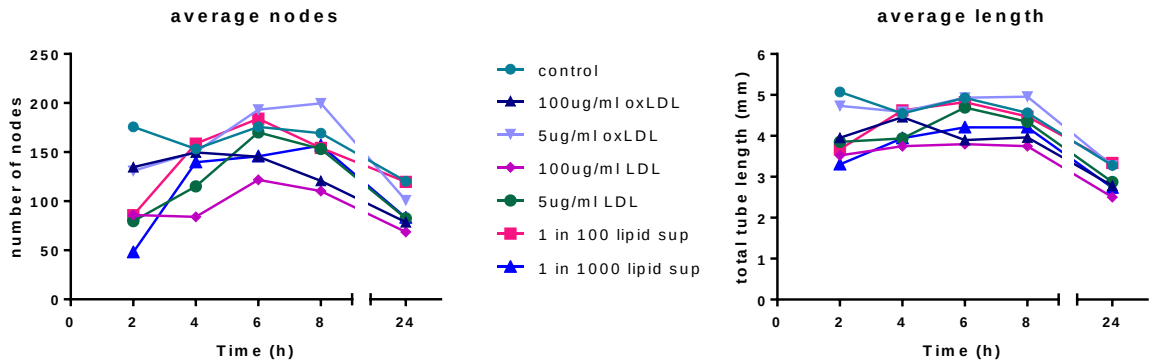

Figure 123 Effect of oxLDL and time on the number of nodes and tube length over 24 hours
Cells were plated on to Geltrex and allowed develop networks as described. Images were captured and nodes and tube length were analysed using ImageJ and plotted against time, n=3.

Figure 123 shows that 5µg/ml oxLDL stimulates angiogenesis compared to the control (see number of nodes at 8 hours) and that, as expected, the lipid supplement has no effect on angiogenesis in a full lipid environment. 100 µg/ml LDL also has an inhibitory effect on the number of nodes compared to the control.

The AUC for the number of nodes and the total tube length was calculated from the graphs above and the results are shown below in Figure 124.

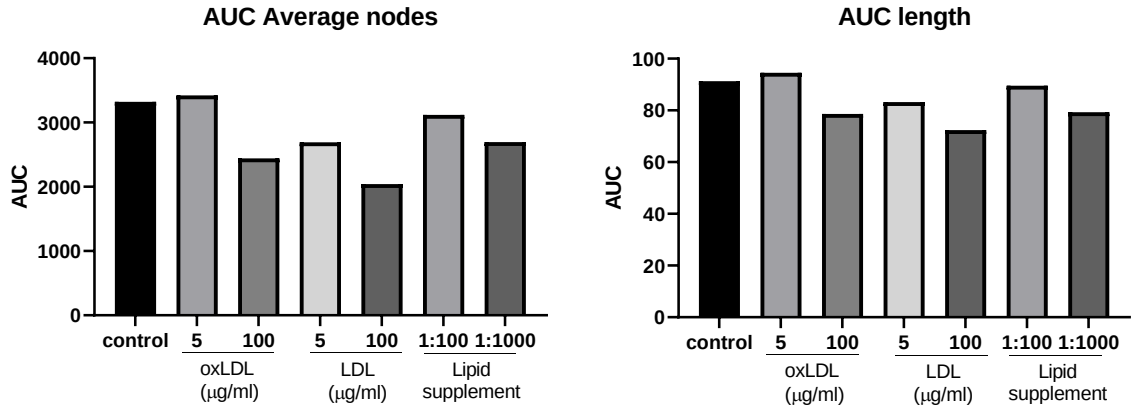

Figure 124 AUC of the number of nodes and tube length for oxLDL
The AUC for oxLDL, LDL and a lipid supplement was calculated and plotted to show the effect on the number of nodes and the total tube length.

It can be seen that 5μg/ml oxLDL has a stimulatory effect on both measures of angiogenesis while 100μg/ml is inhibitory. From these graphs LDL also shows a similar inhibitory effect at both concentrations used.

The number of nodes and the total tube length at each time point was looked at more closely and the results are shown below.

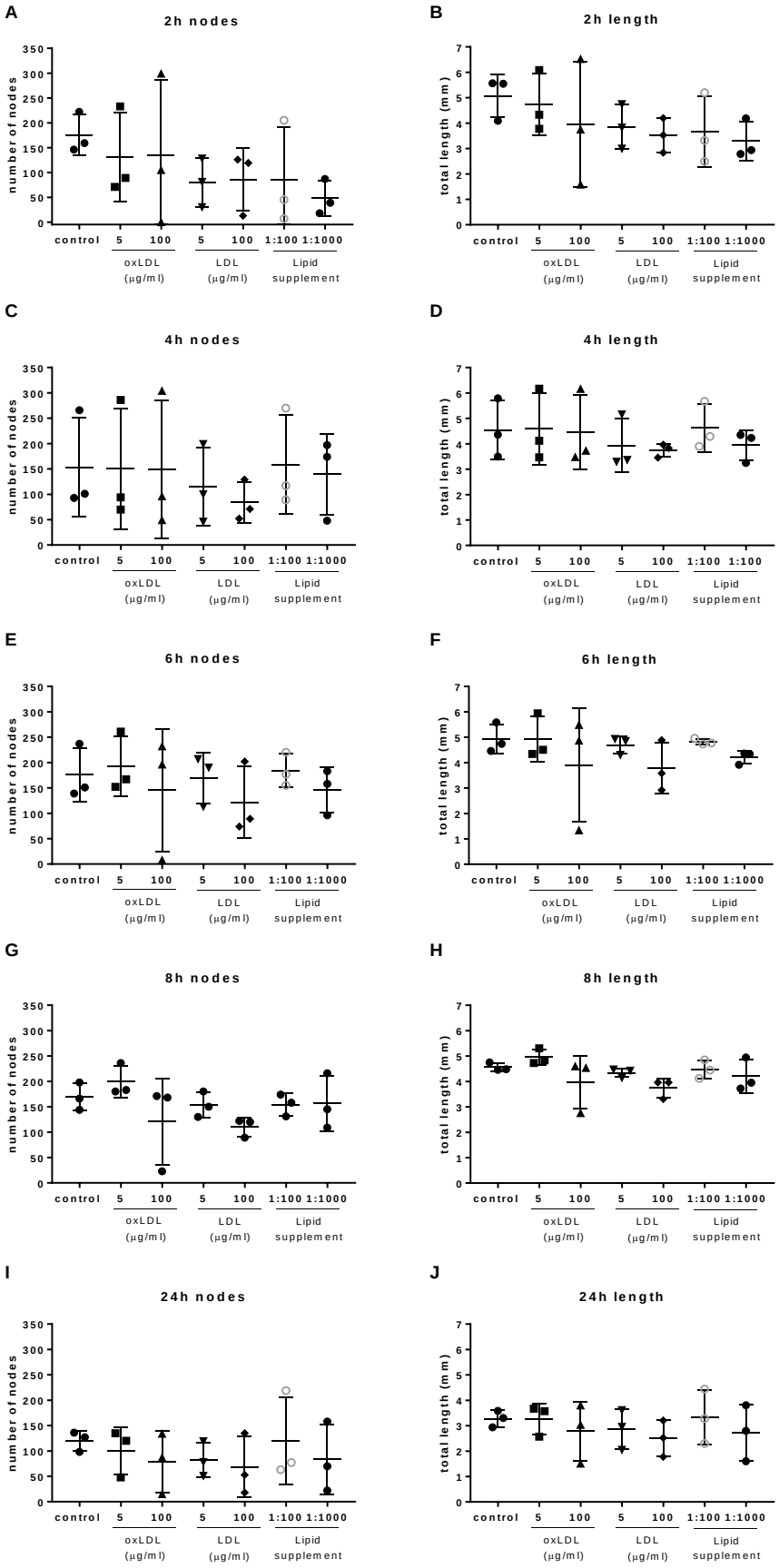

Figure 125 Total tube length and number of nodes over 24 hours for oxLDL

Cells were seeded onto Geltrex and allowed to form networks in the presence or absence of oxLDL over time as previously described. Nodes and tube length were analysed using ImageJ and plotted for each time point. Error bars represent the mean +/- SD, n=3.

One-way ANOVA and Dunnett's multiple comparisons test did not reveal any significant difference between oxLDL, LDL or the lipid supplement at any time point.

The average number of nodes and average tube length for each condition were then combined to provide and overall image of angiogenesis, the results of which are shown below.

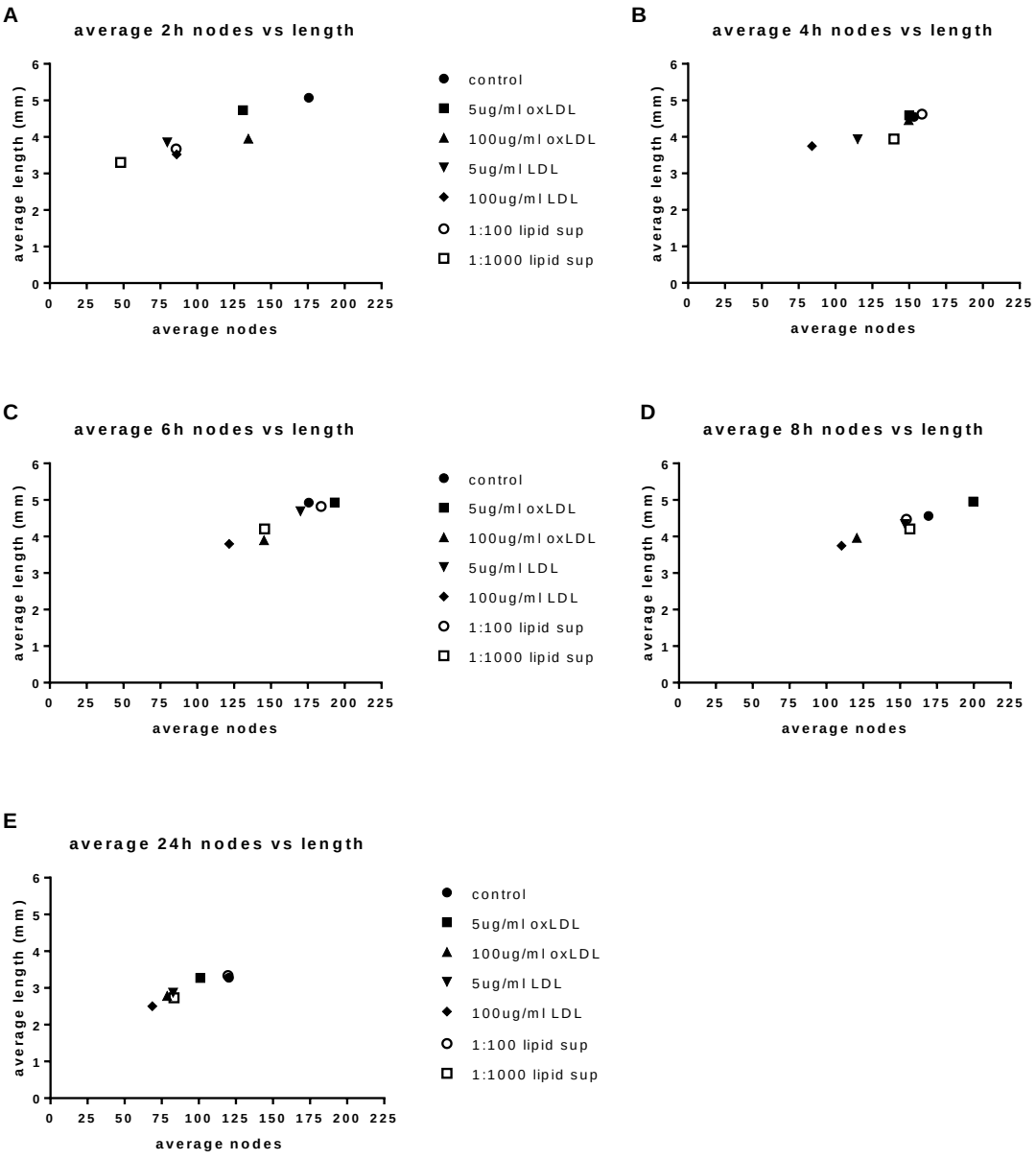

Figure 126 Number of nodes vs total tube length at each time point
Angiogenesis assays were performed and analysed for node and tube length formation in the presence of oxLDL, LDL and a lipid supplement over time as described. The average number of nodes vs average tube length was plotted, n=3.

Figure 126 shows that 5µg/ml oxLDL has a stimulatory effect on angiogenesis, this is especially clear at 8 hours. 100µg/ml oxLDL also shows an inhibitory effect at this time point which is in keeping with previous results.

6.4.4.2 The effect of oxidised LDL on angiogenesis in delipidised media

The effect of oxLDL on angiogenesis in a reduced lipid environment was also studied in order to minimise any buffering effect from the lipids in the full media and the results are shown in this section. An overview of the 24 hour time course showing the number of nodes and the total tube length is shown below.

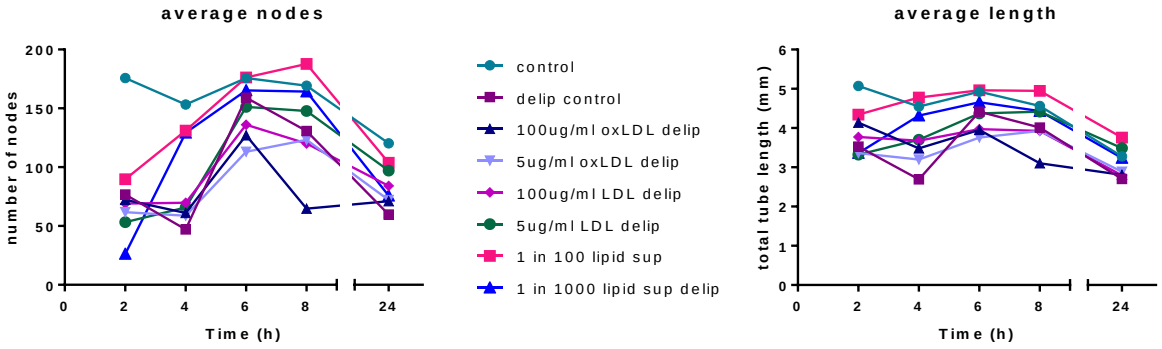

Figure 127 Effect of oxLDL in delipidised media on the number of nodes and tube length over 24 hours

Cells were plated on to Geltrex and allowed develop networks as described. Images were captured and nodes and tube length were analysed using ImageJ as described and plotted against time, n=3.

Figure 127 shows an inhibitory effect on angiogenesis when cells are exposed to 100µg/ml. Both the lipid supplements stimulate angiogenesis compared to the reduced lipid control, with 1:100 lipid supplement also overtaking the full lipid control.

To provide a clearer picture of the effect of oxLDL on angiogenesis, the AUC for the above graphs was calculated and the results are shown below in Figure 128.

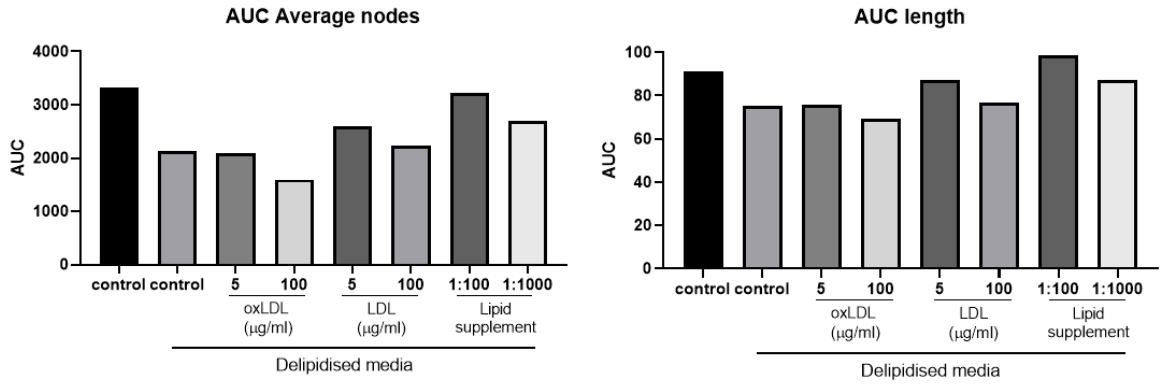

Figure 128 AUC of the number of nodes and tube length for oxLDL in delipidised media
The AUC for oxLDL, LDL and a lipid supplement in a reduced lipid environment was calculated and plotted to show the effect of on the number of nodes and the total tube length. Control cells in full media are represented by the black bar on the left of the graphs.

Figure 128 shows that the AUC is reduced for both the number of nodes and the total tube length in delipidised media, however the lipid supplement at 1:100 is able to return both measures of angiogenesis to that of the full lipid control. No stimulation of angiogenesis is seen with 5µg/ml oxLDL in the reduced lipid environment, however 100µg/ml oxLDL still has an inhibitory effect.

The number of nodes and the total tube length at each time point was looked at more closely to determine if there was a difference between the various conditions and the results are shown below.

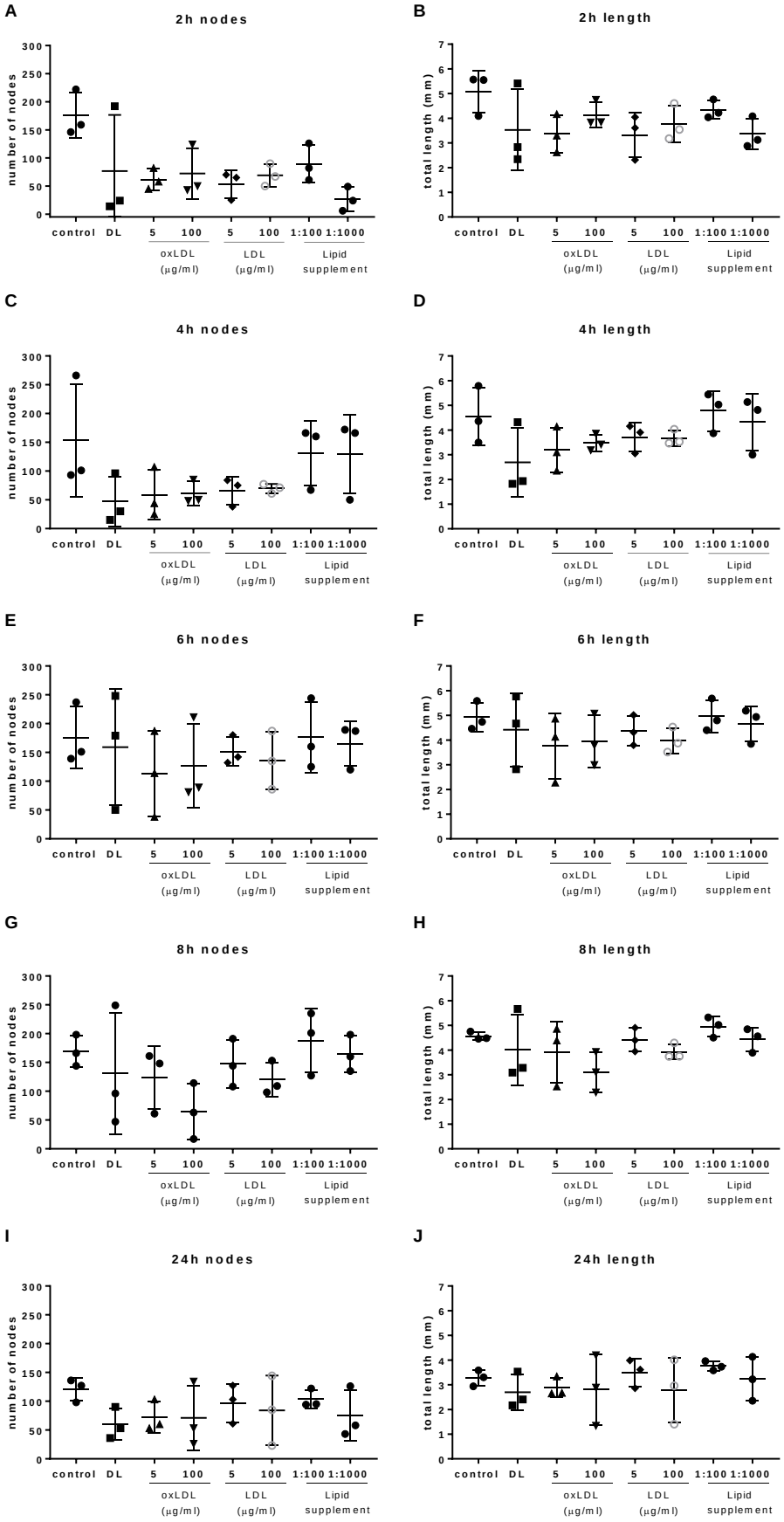

Figure 129 Total tube length and number of nodes over 24 hours for oxLDL in delipidised media
Cells were seeded onto Geltrex and allowed to form networks in the presence or absence oxLDL, LDL and a lipid supplement as previously described. Nodes and tube length were analysed using ImageJ and plotted for each time point. Error bars represent the mean +/- SD, n=3.

One-way ANOVA revealed a p value of $p<0.05$ for graph A with a significant difference ($p<0.05$) between the control and 5µg/mL oxLDL and 5µg/mL LDL and significant difference of $p<0.01$ between the control and 1:1000 lipid supplement. No other significance was found for any of the other treatment.

To provide an overall image of the effect of oxLDL on angiogenesis in a reduced lipid environment, the average number of nodes and average tube length for each condition was combined and the results are shown below.

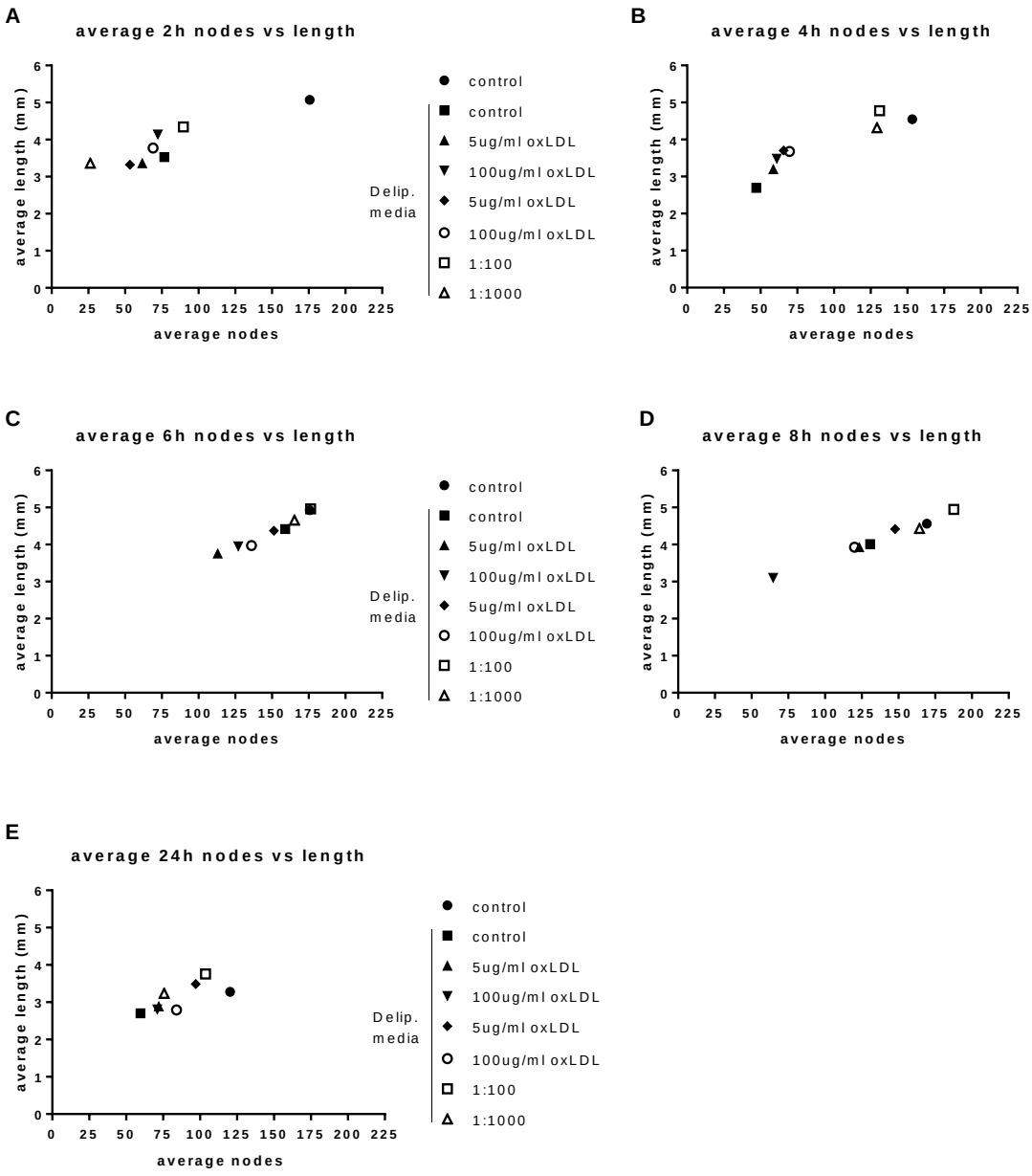

Figure 130 Number of nodes vs total tube length at each time point

Angiogenesis assays were performed and analysed for node and tube length formation in the presence of oxLDL, LDL and a lipid supplement over time as described. The average number of nodes and average tube length were plotted, n=3.

Figure 130 mainly highlights the effect that the two concentrations of lipid supplement have on angiogenesis, with both concentrations increasing both the number of nodes and the total tube length back to that of the full lipid control.

6.4.5 Oxidised albumin

albumin is a carrier of S1P and therefore the effect of albumin and oxidised albumin on angiogenesis was investigated. S1P was also added at the start of the assay with either ox-albumin or albumin to see if this had any effect on angiogenesis.

Angiogenesis assays were carried out as previously described in either full media or the basic M199 media with no serum or additional additives other than standard bicarbonate and Pen/Strep. The results are shown below in Figure 131.

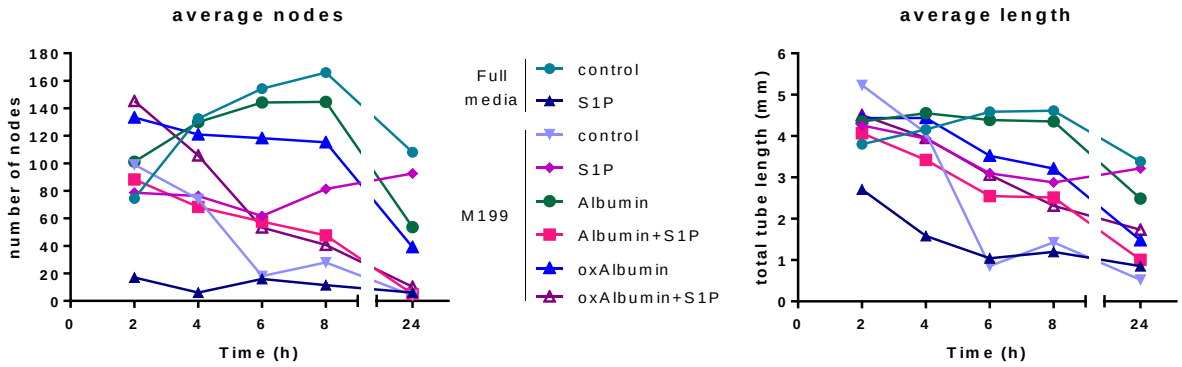

Figure 131 Effect of ox-albumin on the number of nodes and tube length over 24 hours
Cells were plated on to Geltrex and allowed develop networks as described. Images were captured and nodes and tube length were analysed using ImageJ and plotted against time, n=3. S1P was added at 10µM, albumin and ox-albumin were added at 1% w/v.

Figure 131 shows the clear inhibition of angiogenesis previously seen with 10µM S1P and also shows that the cells were not able to maintain connections in the M199 media alone, with a rapid decrease in both tube length and the number of nodes seen right from the start of the assay. Albumin alone is able to replicate the angiogenesis seen in the full media control. On the addition of S1P in albumin supplemented M199, angiogenesis was inhibited in a similar manner to that seen in full media with the addition of S1P. On the addition of ox-albumin, angiogenesis was similar to that seen with albumin alone although not quite to the same extent.

The area under the curve for the above graphs was calculated and the results are shown below in Figure 132.

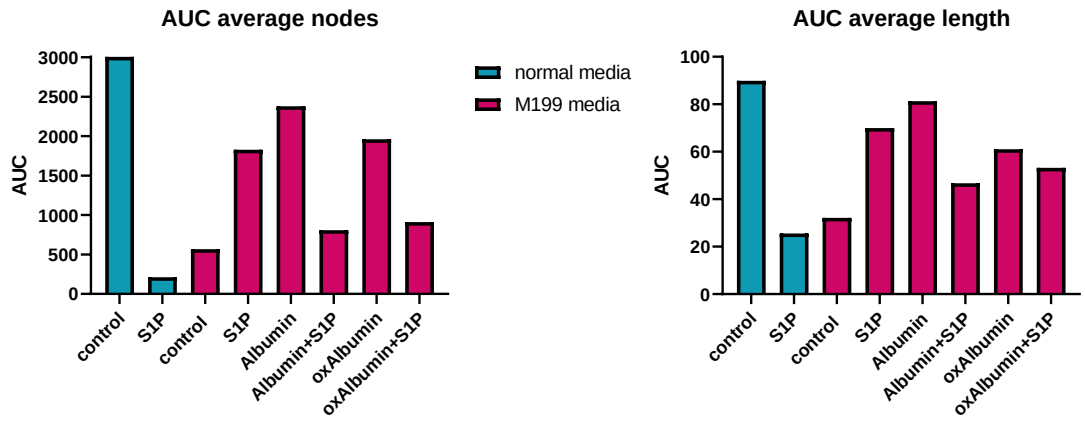

Figure 132 AUC of the number of nodes and tube length for ox-albumin
The AUC for ox-albumin in M199 media (without any additives) was calculated and plotted to show the effect on the number of nodes and the total tube length.

Figure 132 shows that albumin in M199 media without any additives is able to increase the AUC for both the number of nodes and tube length to close to that of the control in full media. ox-albumin is also able to increase the AUC above that of the control in M199, however the AUC for both measures of angiogenesis is less than the AUC for albumin. Interestingly, the addition of S1P to M199 media increases the AUC compared to that of the M199 control and indeed that of the same concentration of S1P in full media. This further supports the role of lipids in angiogenesis.

Both measures of angiogenesis (nodes and tube length) were then combined in order to provide an overall image of the effect of albumin and ox-albumin on angiogenesis.

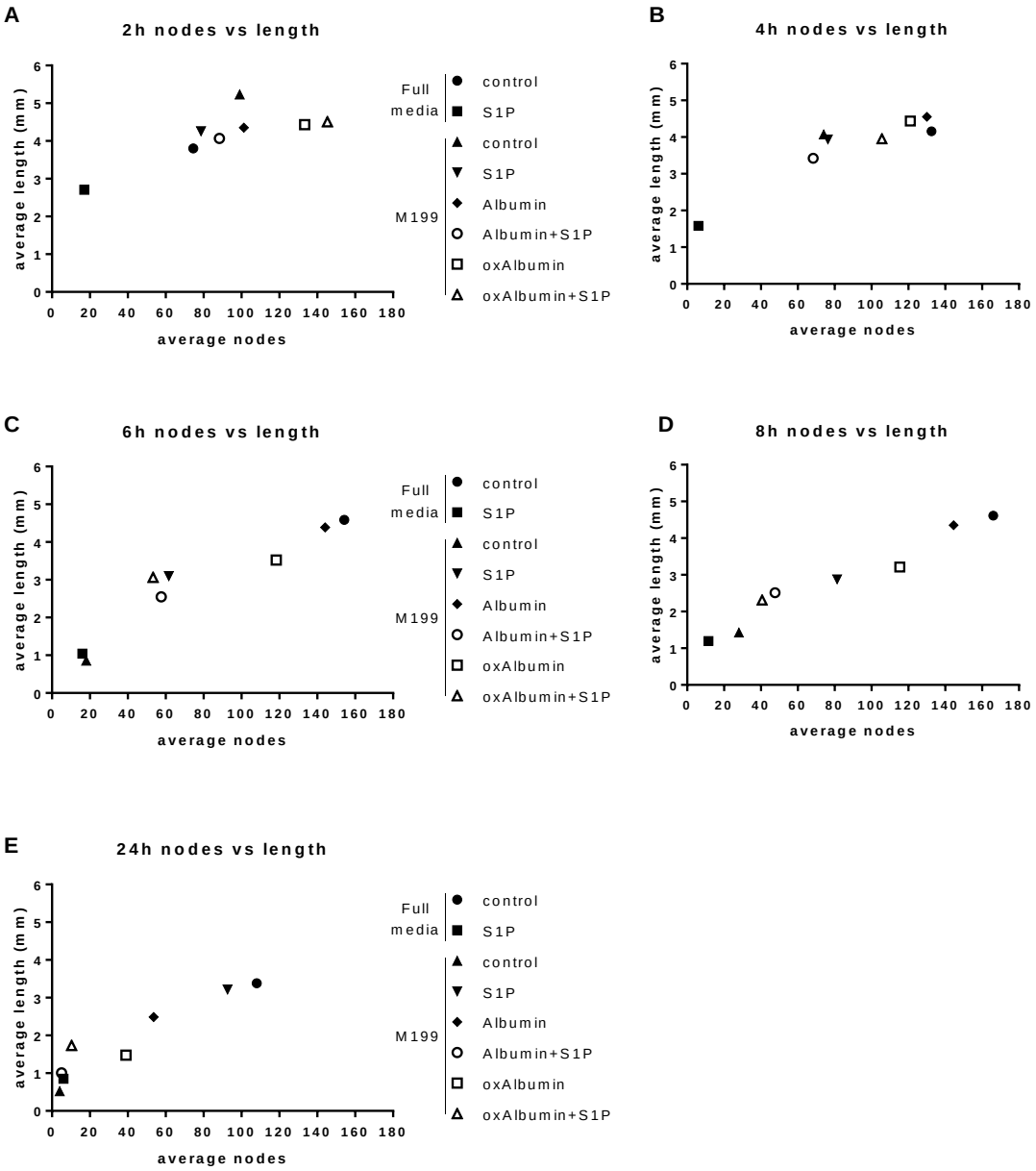

Figure 133 Number of nodes vs total tube length at each time point

Angiogenesis assays were performed and analysed for node and tube length formation in the presence of albumin and ox-albumin in basic M199 media over time. The average number of nodes and average tube length were plotted, n=3. S1P was added at 10µM, albumin and ox-albumin were added at 1% w/v.

Figure 133 highlights the results presented in Figure 131, with 10µM S1P in normal media and the M199 control inhibiting angiogenesis. This figure also emphasises the ability of albumin to supplement for full serum in this assay and that ox-albumin is also able to support angiogenesis although to a lesser extent. The inhibitory effect of S1P in full media is still present when M199 is supplemented with albumin alone.

6.4.6 S1P, Fingolimod and ox-albumin added after 4 hours

To examine the effects of compounds on established endothelial networks, similar to the shape change and established monolayer experiments previously, angiogenesis assays were allowed to develop for four hours in the absence of compounds then allowed to progress following the addition of compounds and monitored. The cells were imaged after 4 hours and then the media aspirated and the compounds added before being imaged after 6, 8 and 24 hours as normal. The results are shown below in Figure 134.

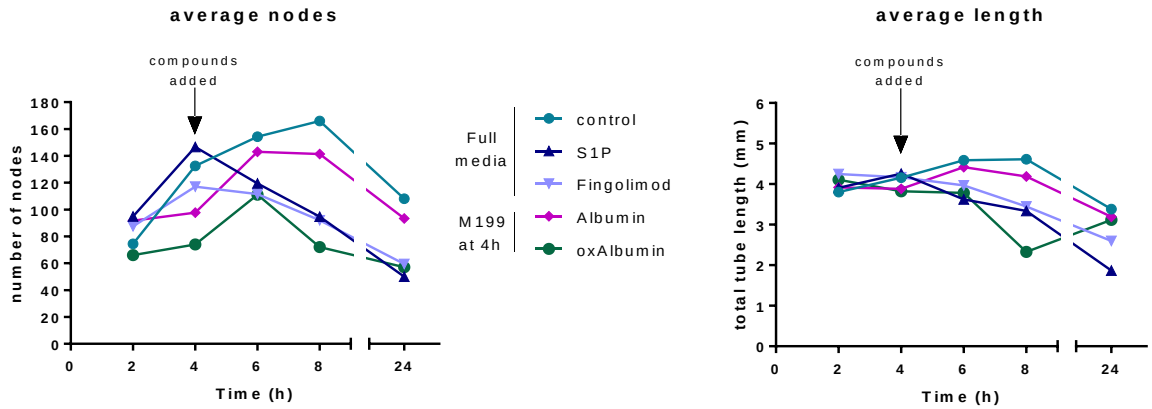

Figure 134 Effect of compounds added at 4 hours on angiogenesis
Cells were plated on to Geltrex in normal media and allowed develop networks for 4 hours as described. After 4 hours, the compounds were added (represented by an arrow on the graphs). S1P and Fingolimod were added in full media at 10µM and albumin and ox-albumin were added in M199 at 1% w/v. Images were captured and nodes and tube length were analysed using ImageJ and plotted against time, n=3.

Figure 134 shows the effect that the addition of S1P has on established angiogenic networks, causing them to rapidly diminish across subsequent time points. Fingolimod also resulted in a decrease in both measures of angiogenesis to almost the same extent as that caused by S1P. The addition of albumin maintained the angiogenic process similarly to that seen in the full media control. ox-albumin had an initial effect by increasing node number although this was lost with time similarly to S1P and Fingolimod.

The AUC for the above graphs was calculated and is shown below in Figure 135.

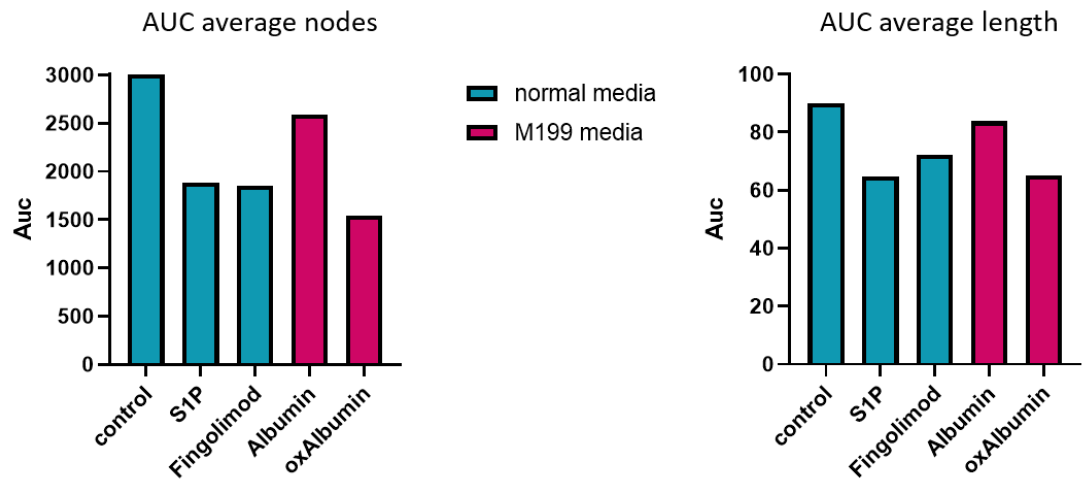

Figure 135 AUC of the number of nodes and tube length for compounds added after 4 hours
The AUC for the various compounds added after 4 hours was calculated and plotted to show the effect on the number of nodes and the total tube length. All cells were started off in full media, with albumin and ox-albumin then being added in M199 at 4 hours.

Figure 135 shows that the addition of S1P and Fingolimod after 4 hours reduces the AUC of both the number of nodes and total tube length compared to the control. The addition of albumin after 4 hours had minimal effect on either the number of nodes or tube length. In contrast, ox-albumin reduced the number of nodes below that of even the inhibitory concentration of S1P, with the AUC for the tube length also reduced to similar levels to S1P.

The data for the number of nodes and the total tube length was then combined to provide an overall measure of angiogenesis. This is shown below in Figure 136.

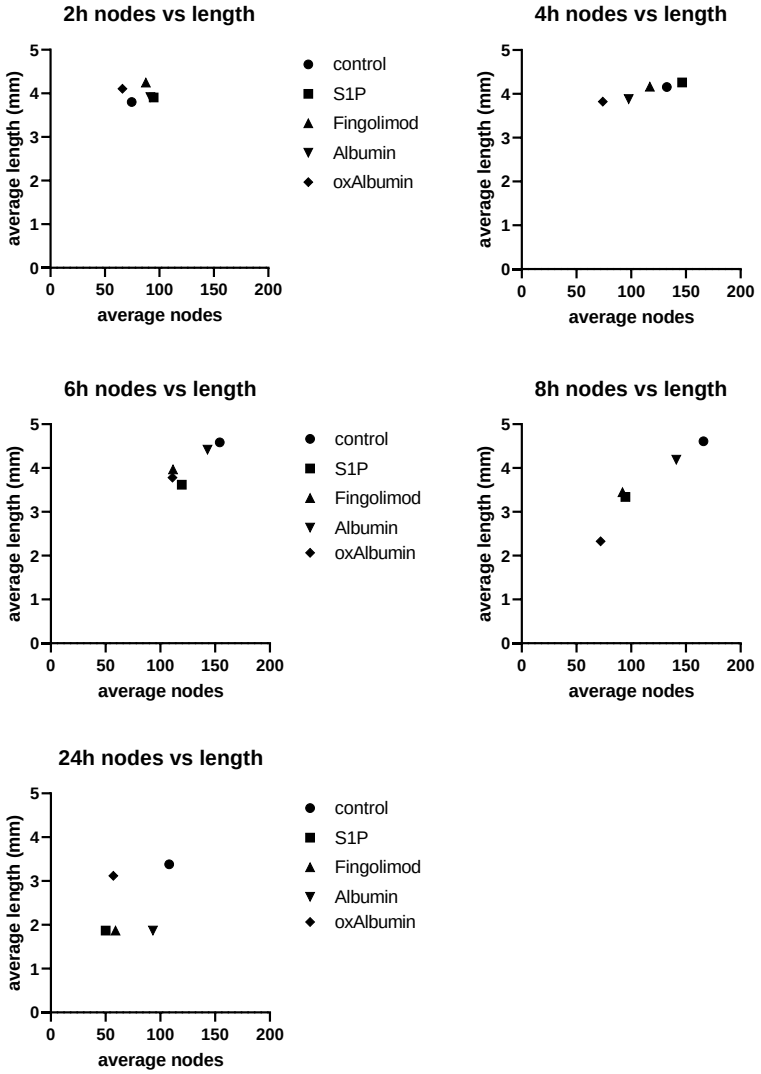

Figure 136 Number of nodes vs total tube length at each time point
Angiogenesis assays were performed and analysed for node and tube length formation over time. Each assay was started in full media and the compounds added after 4 hours. S1P and Fingolimod were added in full media while albumin and ox-albumin were added in M199. The average number of nodes and average tube length were plotted, n=3. S1P and Fingolimod were added at 10µM, albumin and ox-albumin were added at 1% w/v.

Figure 136 highlights the results shown in Figure 134 and Figure 135, with the addition of ox-albumin after 4 hours resulting in a decrease in angiogenesis. This is especially clear after 8 hours and this graph also shows the ability of albumin to support angiogenesis, with levels of angiogenesis being more similar to that of the control in full media than that of ox-albumin which was added in the same media.

6.5 Discussion

Angiogenesis assays were used to explore the response of HUVEC to various lipids. It quickly became clear that the angiogenic response is a more complex function than migration and there were differences between the two assays in the effect of lipids within these processes. One of the main trends seen over all of the angiogenesis assays, irrespective of the lipid condition, was the time dependent nature in the number of nodes and total tube length. This is to be expected as initially, each cell can represent a node from which a branching network will form. The nodes are lost over time due to the cells becoming more organised and some cells taking on other non-branching roles. Tube length also decreases over time as there are only endothelial cells present in the assays. Endothelial cells do not exist in isolation and therefore when angiogenesis occurs *in vivo*, various other cell types such as pericytes and smooth muscle cells provide structural support to the growing tubes. Without this support *in vitro*, the tubes that have formed are not able to maintain their shape and structure and collapse, resulting in the decrease of total tube length seen after around 8 hours (DeCicco-Skinner et al., 2014).

6.5.1 Sphingosine-1-phosphate

Using the same S1P concentration gradient as in the migration assays (10µM-1nM), 10µM S1P showed an inhibitory effect on angiogenesis. It was noted that even after 24 hours, no angiogenesis was seen and as the cells are still attached to the hydrogel and from the previous data on viability suggests that the cells are being prevented from undergoing angiogenesis. Indeed, over 48h in the scratch assay, migration still occurred just at a slower rate suggesting an inhibition of function rather than a toxicity. The lower concentrations used showed a slight stimulatory effect when node formation and total tube length were compared to the control, further supporting the concentration dependent role that S1P plays. This therefore highlights the importance of the receptors and the enzymes involved in S1P signalling and the manipulation of S1P levels and receptor availability as ultimately they will determine the fate of the cell (Kurano and Yatomi, 2018).

Interestingly, angiogenesis progressed in the delipidised media to a similar extent as seen with lipids present, the decrease in lipids almost appeared to enable angiogenesis to occur in the presence of the highest concentration of S1P. However, there does appear to be a decrease in both total tube length and the number of nodes over all time points, whereas the other concentrations of S1P show an increase before an eventual decrease. For all concentrations this decrease also happens sooner in the delipidised media (at around 4 hours) compared to in the normal media (at around 6 hours). There are a number of possible explanations for this; firstly it may be that given enough time the same levels of angiogenesis could be reached in a similar way to the scratch assay where migration

although less at 24 hours had caught up after 48 hours. Secondly it may be that the cells are exhibiting an initial stress response to the reduced lipid environment and that after a certain amount of time the cells are no longer able to respond due to energy requirements for functional responses. It is also a possibility that directional cues are lost. Importantly, angiogenesis requires tip cells to allow branching and the phenotype could be lost and therefore sprouting ceases to occur as the cells are unsure which direction to travel. This could be investigated via Notch signalling and in situ receptor expression as well as the phenotype in the isolated cells as Notch is involved in the direction of migration of the tip cell and the proliferation of the stalk cell (Blanco and Gerhardt, 2013).

6.5.2 Fingolimod

Fingolimod was used in angiogenesis assays in order to see if a similar deranged effect observed with the migration assays was also seen. It was found that this was not the case, with angiogenesis appearing to progress in a similar manner to the controls with some concentrations (100nM and 10μM) able to surpass the angiogenesis seen in the control both in terms of the number of nodes and the total tube length. This suggests that the effect Fingolimod has on angiogenesis is different to the effect it had on migration.

This assay was repeated using delipidised media to see what effect, if any, the removal of lipids had on the ability of Fingolimod to stimulate angiogenesis. In the presence of Fingolimod and absence of serum lipid, angiogenesis resembled that seen in the highest concentrations of S1P, with all concentrations causing a decrease in both aspects of angiogenesis measured over all time points. This was especially noticeable for the total tube length, where there did not appear to be any increase in length after 2 hours. From the migration and cell spreading assays it is known that Fingolimod causes the cells to become more spread out and to migrate differently than the controls. It is therefore possible that this results in fewer nodes and connections being formed and might be a reflection on the way in which the Angiogenesis Analyser plugin in Fiji identifies the nodes. However, the overall decreasing trend in the number of nodes over time is to be expected as the nodes are lost as the cells become more organised.

6.5.3 S1P receptor inhibitors

The three S1P receptor inhibitors (W146, JTE and TY) and S1P lyase inhibitor that were used in the scratch assays were also used in angiogenesis assays. They were added both alone and with S1P to see if they had any effect on node formation and tube length, with the receptor inhibitors also being added in combination. The results shown in Figure 115 and Figure 116 provide some insight into the complex S1P signalling pathway involved in angiogenesis. Similar effects of the inhibitors were seen for both the number of nodes and total tube length, suggesting that different parts of angiogenesis are not controlled separately. It is also possible that without the nodes, tubes are unable to form, and this is therefore a sequential effect. Blockade of receptors 1 and 3 had no effect on control angiogenesis, however inhibition of receptor 2 resulted in decreased angiogenesis in the absence of exogenous S1P. The opposite was true in the presence of added S1P (10μM) suggesting that receptors 1 and 3 are involved in S1P stimulated angiogenesis.

The receptor inhibitors were also combined in the absence of S1P to assess what level (if any) of crossover there was between the receptors. As expected, the combination of all three inhibitors resulted in an inhibition of angiogenesis, with the combination of blocking receptors 2 and 3 also causing a reduction in angiogenesis. This was also expected as it is proposed that receptor 2 is involved in unstimulated angiogenesis.

Out of the S1P stimulated combinations, co-inhibition of receptors 1 and 2 had the biggest effect on angiogenesis, suggesting that stimulated angiogenesis may preferentially signal through S1PR1. In contrast, S1PR2 and 3 co-inhibition had no effect on stimulated angiogenesis, again indicating that S1PR2 is not involved in stimulated angiogenesis and that S1PR3 is not the primary S1P receptor, with S1P potentially preferring to signal though S1PR1.

The results of the S1PL inhibition was also as expected, with S1PL blockade and exogenous S1P addition causing a large decrease in angiogenesis compared to the control or S1PL alone. As S1PL blocks the breakdown of S1P through the lyase, an increase in S1P concentration would therefore be expected, which was shown to decrease angiogenesis in this chapter. This therefore suggests that there is S1P dependent S1P signalling occurring within these cells during this process.

The same conditions were also repeated in a reduced lipid environment with the aim of providing more understanding as to which receptor S1P preferentially signals through. In line with the results obtained in the full lipid environment, inhibiting S1PR2 alone was able to inhibit angiogenesis, providing further evidence that this receptor may signal without the presence of exogenous S1P and suggesting endogenous S1P involvement in the process. This therefore also suggests a role for flippases or ABC transporters and other S1P transporters such as Spinster 2. The addition of S1P

and the S1PR1 inhibitor was also in keeping with the results from the full lipid media assays, with an increase in angiogenesis compared to S1P alone being seen. The addition of S1P in the presence of the other two receptor inhibitors had no effect, with angiogenesis matching that of exogenous S1P addition alone. The S1PL inhibitor again inhibited angiogenesis in the presence of S1P but had no effect when added alone. This is most likely because S1P is not being broken down and therefore the concentration of S1P increases to inhibitory levels. It is also possible that when S1PL is added alone there is a slight increase in stimulation as endogenous S1P is not broken down however this is most likely a small increase and therefore is not statistically significant.

Again the receptor inhibitors were also added in combination with each other and interestingly all combinations stimulated angiogenesis above that of even the full lipid control. It is possible that in the reduced lipid environment, blocking more than one receptor causes stress to the cell and potentially another angiogenic signalling pathway is activated as this stimulation was not seen in the full lipid environment. In contrast, the addition of exogenous S1P to all combinations resulted in decreased angiogenesis, with the combination of all three inhibitors causing an even greater inhibitory effect than that of S1P alone. It would be interesting to add back full media after 4 or 6 hours to see if the full lipid phenotype could be recovered.

Taken together these results suggest that normal angiogenesis is S1P dependent through receptor 2 while stimulated angiogenesis is S1PR1 (and to some extent receptor 3) dependent. This is similar to the results of the migration assays, where it was found that migration is mainly S1PR1 dependent. Combined, these results also further suggest a role for S1P dependent S1P signalling. The contrasting roles of S1PR1 and S1PR2 has also been reported recently by Xiong et al. (2019) who found that S1PR1 stimulated migration through the reduction of VE-cadherin while S1PR2 inhibited migration through ERK signalling, leading to increased VCAM-1 and VE-cadherin expression.

6.5.4 Oxidised LDL

The same concentrations of oxLDL (and LDL) that were used in the scratch assays was also used to assess the effect on the number of nodes and total tube length of endothelial cells undergoing angiogenesis. As migration was inhibited in a reduced lipid environment, it was also expected that angiogenesis would be inhibited. A defined lipid supplement was therefore used to determine whether angiogenesis could be recovered in a delipidised condition.

The assays were first performed in a full lipid environment and it was found that 5µg/mL oxLDL had a stimulatory effect on angiogenesis. This ties in with the results from the migration assays and further supports that this concentration of oxLDL promotes mobilisation of the cell. In contrast to the migration results, no inhibition was seen at the higher concentration of oxLDL, potentially suggesting that there are different mechanisms involved in regulating the two processes as migration is only a part of the angiogenic process. As angiogenesis is a more complicated process than migration, it is possible that this inhibitive effect is lost or that it is compensated, perhaps through a different signalling pathway, during angiogenesis. Neither concentration of lipid supplement was found to have an effect on angiogenesis. This was expected as this was in addition to the serum lipids already contained within the media.

The effect of oxLDL was then assessed in a reduced lipid environment and as predicted, this resulted in a decrease in angiogenesis. In contrast to the full lipid environment, it was found that 100µg/mL oxLDL had an inhibitory effect on angiogenesis whereas 5µg/mL oxLDL did not stimulate angiogenesis nor did it inhibit. This is possibly due to the fact that as all angiogenesis has been reduced in this environment that the addition of 5µg/mL oxLDL is no longer enough to stimulate the cells. It is also possible that the removal of lipids also removes any ability of the cells to compensate when the inhibitive concentration of oxLDL is added. Both concentrations of lipid supplement were able to increase angiogenesis back to the level of the full lipid control and, in fact, 1:100 lipid supplement was actually able to surpass the full lipid control. These results support the hypothesis that lipids are important for normal angiogenesis to occur and in a disease where lipids are dysregulated such as psoriasis patients, it is a possibility that angiogenesis is dysregulated and contributes to the development and progression of the disease.

6.5.5 Oxidised albumin

The results of angiogenesis in response to albumin and ox-albumin provide further insight into the angiogenic process in endothelial cells. Both the albumin and ox-albumin assays were carried out in basic M199 media with no additives (i.e. lipid and protein free) except antibiotics. For a comparison to be made, the assay was also run with M199 alone to see what, if any, angiogenesis was achieved. As expected, it was found that there was a decrease in both the number of nodes and the tube length across all time points, with angiogenesis seeming to stop at 6 hours. One possible reason for this is that the cells have used up any stored energy they had at the start of the assay and therefore as there is no other energy source they are not able to continue to form new protrusions and the existing networks break down.

It has been shown previously that 10μM S1P has an inhibitory effect on angiogenesis and indeed this was confirmed in this assay. Interestingly, when S1P was added to the cells in M199 instead of the full media, angiogenesis was able to progress. This ties in with the results of S1P in a reduced lipid environment, where angiogenesis was not inhibited but neither did it increase. In S1P supplemented M199 media, angiogenesis was able to increase slightly over the course of the assay compared to M199 alone, therefore suggesting that the components of the serum are important for the inhibitory effect the high concentration of S1P exerts on the endothelium. One possible reason for this may be that S1P is not able to bind to its receptors without a chaperone (which would not be present in M199 media but would be in full media that contains serum albumin and HDL) as the mechanism of binding has yet to be described (Proia and Hla, 2015).

The addition of albumin resulted in a dramatic increase in angiogenesis compared to the M199 control, with angiogenesis nearly reaching the levels of the full media control. The addition of S1P however negated this effect, with a decrease in angiogenesis seen across all time points. If, as discussed before, S1P cannot bind to its receptor alone and does indeed need a chaperone, then this would explain the quick inhibition of angiogenesis seen with S1P in the presence of albumin. Similar results were also found with ox-albumin as ox-albumin stimulated angiogenesis, although not to the same extent as albumin. The addition of S1P and ox-albumin also resulted in a decrease in angiogenesis, however it was found that initially, the cells exposed to this condition were able to form branches and that the decrease was not as severe as that of Albumin and S1P. This suggests that the oxidative modification of albumin may be having an effect on the function of the endothelium. It has been discussed previously that S1P may not be able to bind to the oxidised form of albumin (Oettl and Stauber, 2007) . The results of this assay shows that the addition of S1P and ox-albumin was able to inhibit angiogenesis although this was a delayed effect compared to S1P and albumin. This suggests the possibility that S1P is able to bind to ox-albumin, as if this was not

the case, it would be expected that results similar to S1P in M199 alone would be obtained. It is also possible that the oxidation of albumin has other effects on the endothelial cells other than that of affecting S1P binding.

It is therefore proposed that there is either a delay in S1P binding or that the binding stoichiometry has changed which would account for the differences in inhibition seen between albumin and ox-albumin while the addition of albumin in either form enables the cells to undergo the angiogenic process.

6.5.6 S1P, Fingolimod and ox-albumin added after 4 hours

It was decided to add S1P, Fingolimod and albumin at the 4 hour time point in order to see if this had any effect on an established angiogenic network or whether the inhibition seen with S1P was purely as a result of preventing initial branch formation. It was found that all the compounds added at this time point had an effect on angiogenesis, with S1P having the most pronounced effect. S1P caused a rapid decrease in both the number of nodes and the total tube length at 6 hours and this inhibition persisted for the remainder of the assay. This suggests that S1P is continually involved in the angiogenic process and contributes to the re-organisation of the network and is not just important in the early phases of tip cell formation. If this was the case then the addition of S1P to established connections would be expected to have no effect. Fingolimod also had a similar effect although there was a more gradual decrease over time, further supporting the involvement of the S1P signalling pathway throughout angiogenesis.

In contrast to the addition of S1P, albumin addition at 4 hours resulted in a stimulation of angiogenesis being observed at 6 hours. This is in keeping with the stimulation seen in the previous assays. Ox-albumin also had a stimulatory effect however this was not as large, nor as long lived, as that of albumin, again suggesting that the oxidation of this protein is able to differentially regulate functions of the endothelium.

6.6 Chapter summary

Angiogenesis is a complex process which encompasses cell spreading and migration and has many possible regulators. The results presented in this chapter highlight the differences between migration and angiogenesis as many of the effects seen in the migration assays were lost in the angiogenesis assays. This was the case for high concentrations (10μM) of S1P as migration was completely inhibited in delipidised media but in the same reduced lipid conditions angiogenesis was not affected. This might be due to the Geltrex supporting the cells. It was also found that delipidised media alone had no effect on angiogenesis, with both total tube length and the number of nodes being comparable to those formed in full media, whereas the removal of lipids resulted in around a 50% decrease in migration. Fingolimod also had a much greater effect on migration than angiogenesis; angiogenesis occurred at the same level as the control in full media however it resulted in cells becoming elongated and migrating individually.

Angiogenesis is a vital process during development and continues to remain important throughout life. Angiogenesis has also been implicated in a number of diseases and as psoriasis is known to include the vasculature, angiogenesis is believed to be important for both the development and progression of the disease.

Chapter 7: Overall Discussion

Angiogenesis and endothelial migration are both involved in the development of psoriasis, therefore studying these processes further will help to enhance the current understanding of the underlying mechanisms involved. The role of sphingosine-1-phospate in migration and angiogenesis has become a focus of this investigation due to the concentration dependant inhibitory or stimulatory effects that have been observed and the potential mechanism that is utilised by oxidised lipids in the pathogenesis of psoriasis and other diseases showing dyslipidaemia.

The endothelial cells used in this study were all isolated from individual donors and only used at passage one. As each donor was unknown there was a lot of potential genetic variability, which while resulting in more variability in the results, was more likely to provide a truer representation of what happens *in vivo* than if a cell line had been used. The results presented here therefore provide strong evidence for the role of S1P in regulating endothelial function, including processes known to be important for the development and progression of psoriasis.

Western blots and calcium flux experiments were carried out to investigate the effect of S1P and associated inhibitors on intracellular signalling. As expected, S1P caused a concentration dependent effect on both the levels of phosphorylated ERK and calcium flux.

Scratch assays were used to look at the effect on HUVEC migration under a number of different conditions. This included the use of various inhibitors as well as changing the composition of the media in order to remove the exogenous lipids and create a delipidised environment. This allowed the effect of lipids on migration to be assessed as all assays were repeated using delipidated media. It was expected that this would have a significant effect on migration and allow the addition of individual lipids to be investigated in lipid free environment. Exogenous S1P is chaperoned and transported by HDL and albumin therefore there could have been a removal of HDL associated S1P but not of albumin chaperoned lipid. Therefore, if the majority of lipids are removed from the serum, this should also include exogenous S1P as well as the removal of the chaperone HDL that is important for exogenous S1P function. This potentially causes the reduction in the migration seen when compared to that of cells in normal media. Delipidisation appeared to have the greatest inhibitory effect on the migration of endothelial cells compared to normal media containing lipid showing around 50% of that of the control in normal media.

Angiogenesis plays an important role in the development of psoriasis and so angiogenesis assays were used to investigate the effect that S1P may play in this process. As migration is a part of angiogenesis, it was expected that the results of these two functional assays would overlap or act

as surrogate readouts. This was however not the case, with differences in responses to migration and angiogenesis being seen. Angiogenesis is a much more complicated process than migration and this is likely to explain the differences seen.

Combining the data from all the assays performed in this study provides an insight into the mechanism through which S1P exerts its effects. Cell spreading was perhaps the most simple assay carried out, with migration and angiogenesis becoming more complicated and complex in terms of regulation and signalling pathways involved. Therefore, the finding that the addition of 10μM S1P to endothelial cells prevents them being able to spread and form pseudopodia like projections provides an insight into why there was an inhibition of migration at this concentration as the polarisation and spreading of the cell is a vital part of this process. In a similar fashion, migration is important for angiogenesis and therefore the inhibition of these two processes perhaps stems from the endothelial cells inability to spread. This was also confirmed by the addition of S1P to cells which had previously been allowed to spread which resulted in the retraction of the cellular protrusions, an effect that was also seen after the addition of S1P to an established angiogenic network. Again, if the basic process of cell spreading is affected, it makes sense that the more complex angiogenic process which relies on spreading would also be affected. At this point it is not clear through which signalling pathway S1P is having these effects, although it is most likely to be either the Rho GTPases preventing polarisation of the cell, Rac and Rho preventing the formation of lamellipodia or PLC preventing the rearrangement of the cytoskeleton. It is known that S1P stimulates lamellipodia formation (Fu et al., 2018) and therefore the use of specific inhibitors of the various signalling cascades would advance this area of study.

This study has also provided an insight into the S1P receptors. These results suggest that in endothelial cells, receptors 1 and 3 are involved in stimulated S1P signalling, while S1PR2 may be involved in unstimulated signalling. It would also appear that in this system, S1PR1 is the preferred receptor through which S1P signals, which is in line with other reports that this is the preferential receptor *in vivo*. These findings also support the important role of S1P chaperones and potentially suggest that S1P needs a chaperone to be able to bind to its receptors. S1P dependent S1P signalling is also proposed based on the results of inhibitors against S1P lyase and kinase.

This study has aided the understanding of the role S1P plays in regulating the endothelium and how this could contribute to the development and progression of a disease such as psoriasis.

7.1 Study limitations

There are a few limitations of this study that need to be considered. Firstly, due to the source of the cells used throughout this thesis, the n numbers for some of the assays are small, in some instances the assays were only able to be repeated three times. More repeats would also increase the statistical power and perhaps more significance between the conditions used would be seen.

Secondly, the cells used were all from individual donors, which while providing a strong basis on which to compare the results seen with what may be happing *in vivo*, also added an additional complication when it came to comparing results. It would have been beneficial to carry out some of the functional assays such as migration and angiogenesis with a cell line in order to get more reproducible results with less variation. This would have allowed a simpler comparison between the various conditions used in the assays to be made.

Another limitation of the angiogenesis assay in particular, is that the HUVEC cells were in isolation, whereas they would be supported by other cell types such as smooth muscle cells and pericytes. As there was no structural support, the branches and connections that the HUVEC made started to disassemble at around 8 hours and therefore the long lasting effects of the compounds beyond this time point did not yield significant results.

7.2 Future directions

There are a number of different factors that could be investigated in the future. For instance, the effect of S1P and oxLDL on adhesion molecules could be studied. It was seen from the migration data that high concentrations of S1P inhibit migration and this concentration also resulted in an inhibition of cell spreading. One possible reason for this inhibition may be that adhesion molecules are being affected and therefore the expression of adhesion molecules such as intercellular adhesion molecule 1 (ICAM-1), E-selectin and vascular cell adhesion molecule (VCAM-1) in chronic inflammation assays and P-selectin in models of acute inflammation could be assessed, both in lipid rich and poor environments. Fluorescence microscopy could also be used to study focal adhesions to determine if high concentrations of S1P changes the number and location of these complexes and therefore prevents the cells from spreading. This would provide further insight into the regulation of migration by S1P and would allow further comparison between S1P and oxLDL.

A further aspect that may account for the slight differences seen between S1P and oxLDL (such as the stimulation seen only with oxLDL) may be due to changes in energy availability. It is possible that S1P has an effect on glucose uptake via the glucose transporters and therefore a glucose uptake assay could be used. It has previously been documented that the glucose transporter-1 (GLUT-1) is upregulated in the plaques in psoriasis patients and has been positively correlated with PASI score, inflammatory response and the density of the surrounding microvessels (Hodeib et al., 2018). It has also been reported that in myoblasts, S1P activation of S1PR2 causes an increase in levels of intracellular calcium, generating reactive oxygen species. This in turn results in the phosphorylation of the insulin receptor and causes an increase in glucose translocation through GLUT-4 (Fayyaz et al., 2014). Research on cellular energy supply has recently suggested that endothelial cell metabolism drives angiogenesis along with other known factors and the lipid environment is likely to play a role too (Eelen et al., 2018).

Cellular changes due to lipid depletion and/or oxidised lipid addition could also be investigated as it is possible that the addition of oxLDL changes the redox environment of the cell, which may account for differences seen between S1P and oxLDL addition. One way to study this would be to incorporate antioxidants such as n-acetylcysteine into the migration and angiogenesis assays alongside oxLDL and S1P to assess if there are any changes in the results. N-acetylcysteine acts as a reduced glutathione precursor as well as being able to directly act on certain oxidising species (Aldini et al., 2018). N-acetylcysteine is currently used as a mucolytic agent in diseases such as chronic obstructive pulmonary disease (Sadowska et al., 2006) and as it is already approved for use in patients, it may be possible that n-acetylcysteine could be used in redox dependent diseases. It has previously been reported in a pilot study that another glutathione precursor (Immunocal) has

a positive clinical effect on psoriasis (Prussick et al., 2013), suggesting that the redox state of the tissue may be a factor that contributes to the development and progression of the disease. Therefore, oxidative stress in the skin vasculature may either convert LDL to oxLDL in situ and dysregulate angiogenesis or the arrival of oxLDL to the skin might activate the local vasculature to become dysregulated. It is possible that this occurs in an S1P dependent manner in this environment where major inflammatory cytokines are also present.

Using samples from psoriasis patients of involved and non-involved skin would allow immunohistochemical staining of the samples to examine S1P receptor expression and possible differential patterns. These could also be compared to deposition of oxLDL to these skin areas further linking the plaques seen in psoriasis and dyslipidaemia. Tissue analysis would also provide an insight into whether there is elevated or inhibited levels of angiogenesis in psoriasis tissue and correlate with disease severity (PASI). This may therefore lead to the use of lipid modifying therapies in psoriasis that would control underlying cardiovascular disease and benefit the skin pathology.

There is no naturally occurring animal skin disorder that is similar to the complexity seen in psoriasis and therefore genetically engineered animal models have been made. This has typically been achieved through either loss of function mutations or tissue specific gene overexpression. While these models have helped to identify certain inflammatory markers, the difference between human and murine skin poses translational challenges. Perhaps most obviously, mouse hair follicles are closely packed together whereas they are spread out in human skin and therefore there is a large structural difference. Mouse epidermis is also thinner, with increased cell turnover, and is able to regenerate faster than human skin. There is also a difference in the immune cells found in mouse and human skin and therefore makes translating findings from the mouse model to humans challenging (Schön, 2008).

7.3 Concluding remarks

The combined data so far suggests that there is a complex mechanism through which S1P regulates migration and angiogenesis. The results imply that all three S1PR receptors are involved, with potential stimulation of endogenous S1P formation via exogenous S1P activity which may also therefore implicate the involvement of the ABC transporters, and Spins2 in endothelial cells, or as yet unknown receptors or redundancy of effect due to the lack of complete inhibition in any of the assays used. This could be investigated by inhibiting the transporters and therefore preventing the release of intracellular S1P. Sphingosine kinases also appear to be required as well as exogenous lipids.

Combining the data obtained in this thesis, it is possible that oxLDL is affecting S1P signalling indirectly rather than there being a direct interaction between oxLDL and S1P. OxLDL may activate its receptor (LOX-1) in endothelial cells causing downstream signalling, potentially via the MAPK p42/44 pathway leading to gene expression important for processes such as cell adhesion and apoptosis. Results found in this investigation have shown that S1P is able to activate the MAPK p42/44 pathway and therefore this could be a point of cross talk between oxLDL and S1P signalling. It has also been shown that S1P is able to regulate angiogenesis and as this is an important feature of psoriasis, S1P signalling could provide a target for potential therapeutics. It was also found that the S1P receptor 1 was the preferential receptor for S1P signalling and therefore this may prove to be an effective therapeutic target for the treatment of psoriasis. This receptor is already a target for the treatment of diseases such as multiple sclerosis, so it is possible that Fingolimod could also be used for the treatment of severe psoriasis.

There is still a lot to uncover about S1Ps involvement in the processes involved in psoriasis and the key players are starting to be revealed. With this ground work, the role of S1P in the response of endothelial cells to oxidised lipids can now be established and potentially correlated to the mechanism of activation that drives one of the pathologies in psoriasis.

Appendix

A.1 Fingolimod time-point images from scratch assays

In order to more closely identify the time where the aberrant migration started, a scratch assay was imaged every 2 hours up until hour 8 and another was imaged after 16, 18, 20 and 22 hours. Example images are shown below.

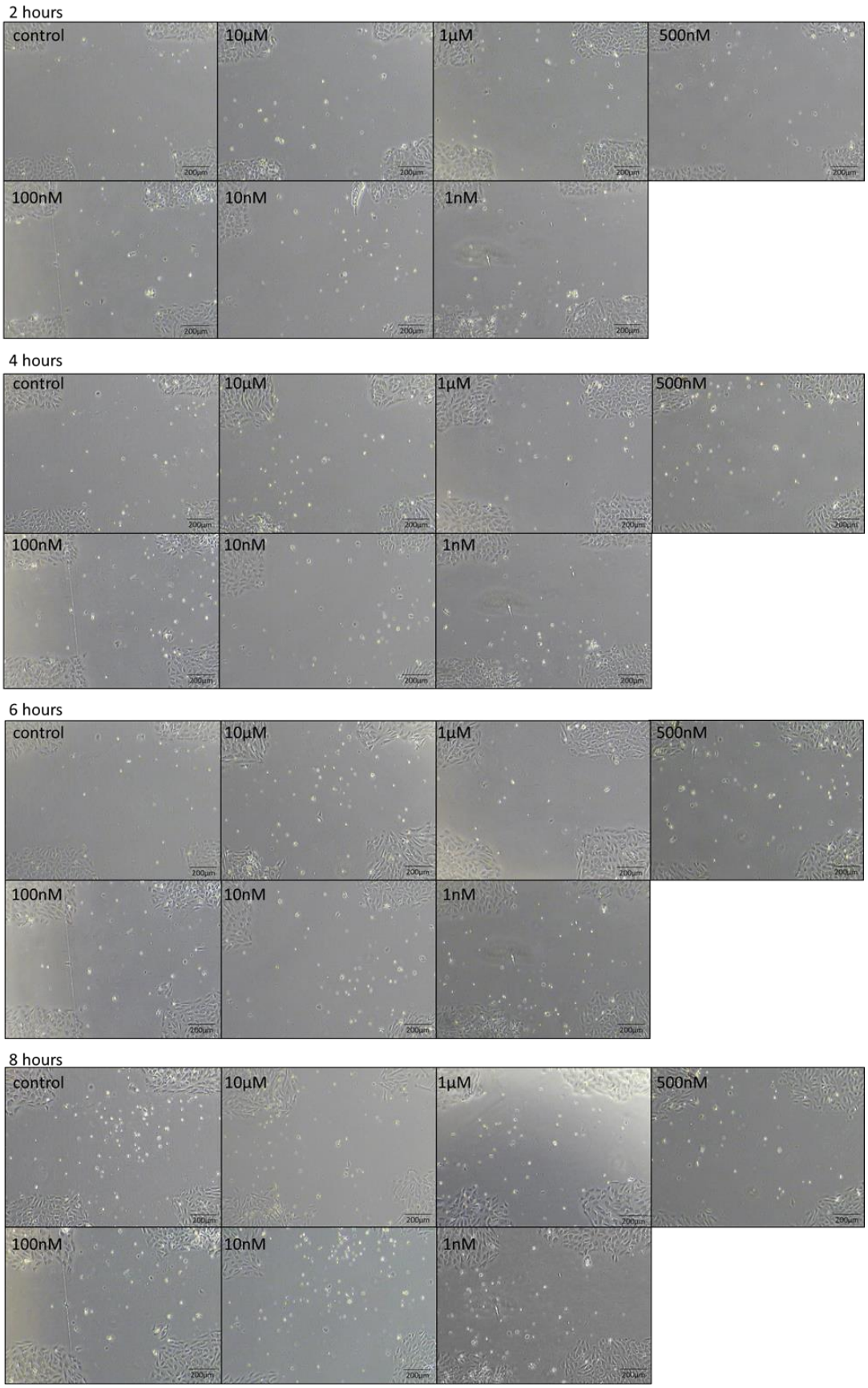

Figure 137 Effect of Fingolimod on endothelial migration

Cells were scratched as previously described and cultured in the presence of Fingolimod before being imaged every 2 hours following wounding

From Figure 137 it can be seen that after 8 hours not much migration is observed, either in the control or in the presence of Fingolimod. The following images are from a different scratch imaged every 2 hours from hour 16 until hour 22.

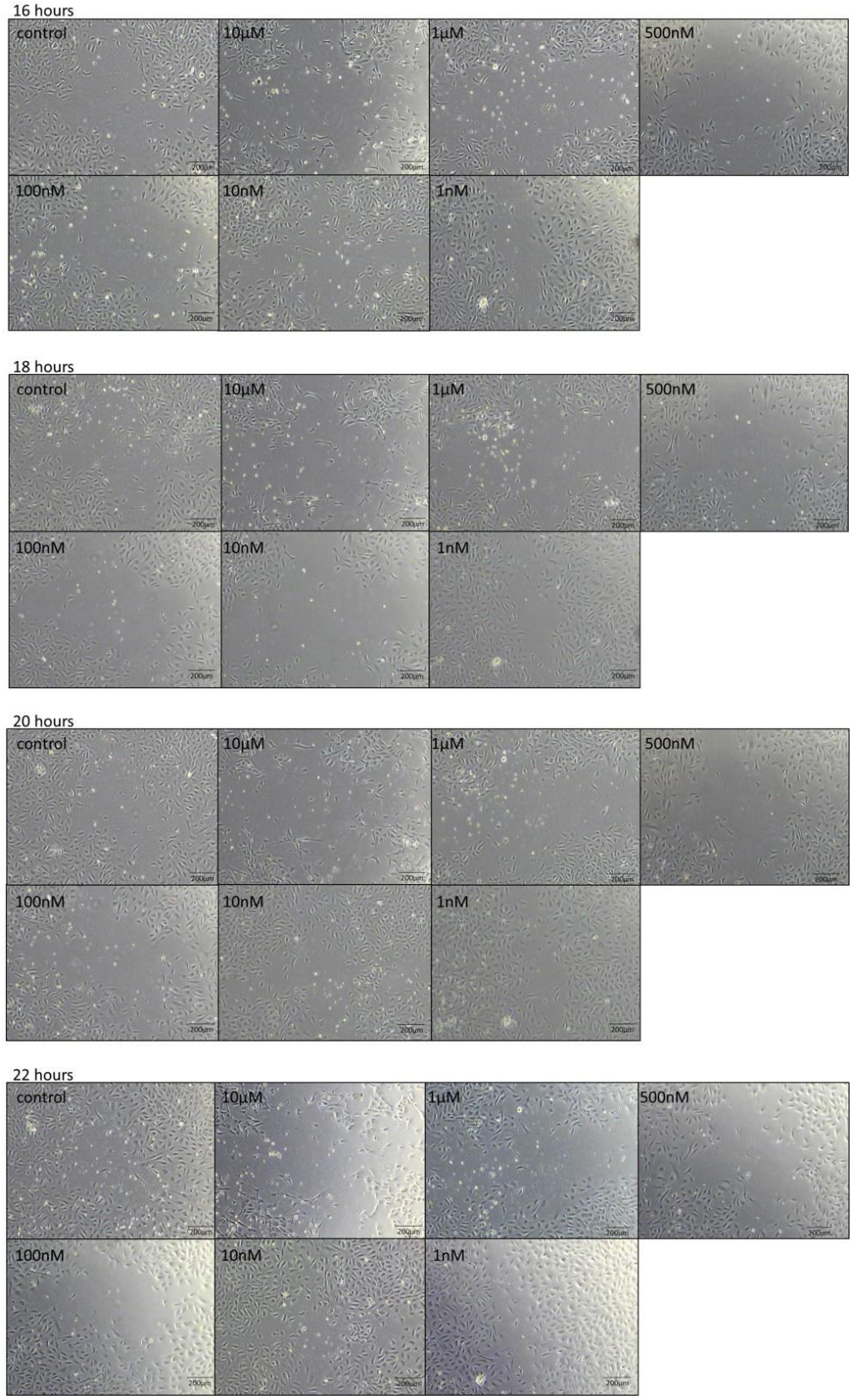

Figure 138 Effect of Fingolimod on endothelial migration

Cells were scratched as previously described and cultured in the presence of Fingolimod before being imaged every 2 hours from hour 16 following wounding

It can be seen that by 16 hours the cells exposed to 10μM Fingolimod have started to migrate independently but that the other concentrations have a delayed effect on this migration pattern. It was therefore decided to image the cells after 8, 16 and 24 hours to provide a clearer picture of when migration was occurring in response to Fingolimod.

A.2 Abstracts/presentations

Posters

"Investigating the role of S1P in angiogenesis and migration" (2017), Southampton university medical conference

"oxLDL Regulated Angiogenesis Is Potentially Mediated via S1P" (2018), British Microcirculation Society annual conference

"oxLDL Blocks Angiogenesis and Endothelial Migration, Potentially via S1P and ERK Mediated Signalling" (2018), World Congress for Microcirculation

"oxLDL Potentially Regulates Angiogenesis and Endothelial Migration via S1P and ERK" (2019), Southampton university medical conference

Presentations

"Not just skin deep: circulating lipids in a "localised" disease and their role in angiogenesis" (2017), Kerkut Charitable Trust annual meeting

"Lipid regulated angiogenesis: the role of oxLDL and sphingosine-1-phosphate" (2018), Kerkut Charitable Trust annual meeting

"oxLDL Potentially Signals via S1P and ERK to Regulate Angiogenesis and Endothelial Migration" (2019), British Microcirculation Society annual conference

"The role of oxLDL and sphingosine-1-phosphate in lipid regulated angiogenesis" (2019), Kerkut Charitable Trust annual meeting

References

ABDALLAH, M. A., ABDEL-HAMID, M. F., KOTB, A. M. & MABROUK, E. A. 2009. Serum Interferon-gamma Is a Psoriasis Severity and Prognostic Marker. *Cutis,* 84**,** 163-168.

ALBINET, V., BATS, M. L., HUWILER, A., ROCHAIX, P., CHEVREAU, C., SEGUI, B., LEVADE, T. & ANDRIEU-ABADIE, N. 2014. Dual role of sphingosine kinase-1 in promoting the differentiation of dermal fibroblasts and the dissemination of melanoma cells. *Oncogene,* 33**,** 3364-73.

ALDINI, G., ALTOMARE, A., BARON, G., VISTOLI, G., CARINI, M., BORSANI, L. & SERGIO, F. 2018. N-Acetylcysteine as an antioxidant and disulphide breaking agent: the reasons why. *Free Radical Research,* 52**,** 751-762.

ALSUFYANI, M. A., GOLANT, A. K. & LEBWOHL, M. 2010. Psoriasis and the metabolic syndrome. *Dermatol Ther,* 23**,** 137-43.

ALVAREZ, S. E., HARIKUMAR, K. B., HAIT, N. C., ALLEGOOD, J., STRUB, G. M., KIM, E. Y., MACEYKA, M., JIANG, H. L., LUO, C., KORDULA, T., MILSTIEN, S. & SPIEGEL, S. 2010. Sphingosine-1-phosphate is a missing cofactor for the E3 ubiquitin ligase TRAF2. *Nature,* 465**,** 1084-U149.

ANAND, S., GUPTA, P., BHARDWAJ, R., NARANG, T., DOGRA, S., MINZ, R. W., SAIKIA, B. & CHHABRA, S. 2017. Is psoriasis an autoimmune disease: Interpretations from an immunofluorescence-based study. *J Cutan Pathol***,** n/a-n/a.

ANNUNZIATA, P., CIONI, C., MASI, G., TASSI, M., MAROTTA, G. & SEVERI, S. 2018. Fingolimod reduces circulating tight-junction protein levels and in vitro peripheral blood mononuclear cells migration in multiple sclerosis patients. *Sci Rep,* 8**,** 15371.

AOKI, M., AOKI, H., RAMANATHAN, R., HAIT, N. C. & TAKABE, K. 2016. Sphingosine-1-Phosphate Signaling in Immune Cells and Inflammation: Roles and Therapeutic Potential. *Mediators Inflamm,* 2016**,** 8606878.

AOKI, S., YATOMI, Y., SHIMOSAWA, T., YAMASHITA, H., KITAYAMA, J., TSUNO, N. H., TAKAHASHI, K. & OZAKI, Y. 2007. The suppressive effect of sphingosine 1-phosphate on monocyte-endothelium adhesion may be mediated by the rearrangement of the endothelial integrins alpha(5)beta(1) and alpha(v)beta(3). *Journal of Thrombosis and Haemostasis,* 5**,** 1292-1301.

ARBISER, J. L., NOWAK, R., MICHAELS, K., SKABYTSKA, Y., BIEDERMANN, T., LEWIS, M. J., BONNER, M. Y., RAO, S., GILBERT, L. C., YUSUF, N., KARLSSON, I., FRITZ, Y. & WARD, N. L. 2017. Evidence for biochemical barrier restoration: Topical solenopsin analogs improve inflammation and acanthosis in the KC-Tie2 mouse model of psoriasis. *Sci Rep,* 7**,** 11198.

ARGRAVES, K. M., GAZZOLO, P. J., GROH, E. M., WILKERSON, B. A., MATSUURA, B. S., TWAL, W. O., HAMMAD, S. M. & ARGRAVES, W. S. 2008. High density lipoprotein-associated sphingosine 1-phosphate promotes endothelial barrier function. *J Biol Chem,* 283**,** 25074-81.

ARMSTRONG, A. W., VENDER, R. & KIRCIK, L. 2016. Secukinumab in the Treatment of Palmoplantar, Nail, Scalp, and Pustular Psoriasis. *J Clin Aesthet Dermatol,* 9**,** S12-S16.

ASGARI, M. M., RAY, G. T., GEIER, J. L. & QUESENBERRY, C. P. 2017. Malignancy rates in a large cohort of patients with systemically treated psoriasis in a managed care population. *J Am Acad Dermatol,* 76**,** 632-638.

AUGUSTIN, M., VIETRI, J., TIAN, H. & GILLOTEAU, I. 2017. Incremental Burden of Cardiovascular Comorbidity and Psoriatic Arthritis among Adults with Moderate-to-Severe Psoriasis in Five European Countries. LID - 10.1111/jdv.14286 [doi].

BAER, A., COLON-MORAN, W. & BHATTARAI, N. 2018. Characterization of the effects of immunomodulatory drug fingolimod (FTY720) on human T cell receptor signaling pathways. *Sci Rep,* 8**,** 10910.

BAEYENS, A., FANG, V., CHEN, C. & SCHWAB, S. R. 2015. Exit Strategies: S1P Signaling and T Cell Migration. *Trends Immunol,* 36**,** 778-787.

BAI, F., ZHENG, W., DONG, Y., WANG, J., GARSTKA, M. A., LI, R., AN, J. & MA, H. 2018. Serum levels of adipokines and cytokines in psoriasis patients: a systematic review and meta-analysis. *Oncotarget,* 9**,** 1266-1278.

BALTA, I., BALTA, S., DEMIRKOL, S., CELIK, T., EKIZ, O., CAKAR, M., SARLAK, H., OZOGUZ, P. & IYISOY, A. 2014. Aortic arterial stiffness is a moderate predictor of cardiovascular disease in patients with psoriasis vulgaris. *Angiology,* 65**,** 74-8.

BALUTA, M. M. & VINTILA, M. M. 2015. PAI-1 Inhibition - Another Therapeutic Option for Cardiovascular Protection. *Maedica (Buchar),* 10**,** 147-152.

BERG JM, T. J., STRYER L. 2015. *Biochemistry,* New York, W H Freeman and Company.

BIELENBERG, D. R. & ZETTER, B. R. 2015. The Contribution of Angiogenesis to the Process of Metastasis. *Cancer J,* 21**,** 267-73.

BISEL, B., WANG, Y. Z., WEI, J. H., XIANG, Y., TANG, D. M., MIRON-MENDOZA, M., YOSHIMURA, S., NAKAMURA, N. & SEEMANN, J. 2008. ERK regulates Golgi and centrosome orientation towards the leading edge through GRASP65. *Journal of Cell Biology,* 182**,** 837-843.

BLAHO, V. A. & HLA, T. 2014. An update on the biology of sphingosine 1-phosphate receptors. *J Lipid Res,* 55**,** 1596-608.

BLANCO, R. & GERHARDT, H. 2013. VEGF and Notch in tip and stalk cell selection. *Cold Spring Harb Perspect Med,* 3**,** a006569.

BODE, C., SENSKEN, S. C., PEEST, U., BEUTEL, G., THOL, F., LEVKAU, B., LI, Z., BITTMAN, R., HUANG, T., TOLLE, M., VAN DER GIET, M. & GRALER, M. H. 2010. Erythrocytes serve as a reservoir for cellular and extracellular sphingosine 1-phosphate. *J Cell Biochem,* 109**,** 1232-43.

BORAU, C., KAMM, R. D. & GARCIA-AZNAR, J. M. 2011. Mechano-sensing and cell migration: a 3D model approach. *Phys Biol,* 8**,** 066008.

BORNFELDT, K. E., GRAVES, L. M., RAINES, E. W., IGARASHI, Y., WAYMAN, G., YAMAMURA, S., YATOMI, Y., SIDHU, J. S., KREBS, E. G., HAKOMORI, S. & ET AL. 1995. Sphingosine-1-phosphate inhibits PDGF-induced chemotaxis of human arterial smooth muscle cells: spatial and temporal modulation of PDGF chemotactic signal transduction. *J Cell Biol,* 130**,** 193-206.

BRINKMANN, V. 2007. Sphingosine 1-phosphate receptors in health and disease: mechanistic insights from gene deletion studies and reverse pharmacology. *Pharmacol Ther,* 115**,** 84-105.

BROWN, M. S. & GOLDSTEIN, J. L. 1987. Plasma lipoproteins: teaching old dogmas new tricks. *Nature,* 330**,** 113-4.

BURDEN & KIRBY. 2016. Rook's Textbook of Dermatology, Ninth Edition, Psoriasis and Related Disorders, Inflammatory Dermatoses

CAMM, J., HLA, T., BAKSHI, R. & BRINKMANN, V. 2014. Cardiac and vascular effects of fingolimod: mechanistic basis and clinical implications. *Am Heart J,* 168**,** 632-44.

CANTRELL STANFORD, J., MORRIS, A. J., SUNKARA, M., POPA, G. J., LARSON, K. L. & OZCAN, S. 2012. Sphingosine 1-phosphate (S1P) regulates glucose-stimulated insulin secretion in pancreatic beta cells. *J Biol Chem,* 287**,** 13457-64.

CHAE, S. S., PAIK, J. H., ALLENDE, M. L., PROIA, R. L. & HLA, T. 2004. Regulation of limb development by the sphingosine 1-phosphate receptor S1p1/EDG-1 occurs via the hypoxia/VEGF axis. *Dev Biol,* 268**,** 441-7.

CHATTERJEE, S., KHUNTI, K. & DAVIES, M. J. 2017. Type 2 diabetes.

CHAVAKIS, E., DERNBACH, E., HERMANN, C., MONDORF, U. F., ZEIHER, A. M. & DIMMELER, S. 2001. Oxidized LDL inhibits vascular endothelial growth factor-induced endothelial cell migration by an inhibitory effect on the Akt/endothelial nitric oxide synthase pathway. *Circulation,* 103**,** 2102-7.

CHEN, J. H., RIAZY, M., SMITH, E. M., PROUD, C. G., STEINBRECHER, U. P. & DURONIO, V. 2009. Oxidized LDL-mediated macrophage survival involves elongation factor-2 kinase. *Arterioscler Thromb Vasc Biol,* 29**,** 92-8.

CHEN, W., LU, H., YANG, J., XIANG, H. & PENG, H. 2016. Sphingosine 1-phosphate in metabolic syndrome (Review). *Int J Mol Med,* 38**,** 1030-8.

CHIESA FUXENCH, Z. C., SHIN, D. B., OGDIE BEATTY, A. & GELFAND, J. M. 2016. The Risk of Cancer in Patients With Psoriasis: A Population-Based Cohort Study in the Health Improvement Network. *JAMA Dermatol,* 152**,** 282-90.

CHO, Y., LEW, B. L., SEONG, K. & KIM, N. I. 2004. An inverse relationship between ceramide synthesis and clinical severity in patients with psoriasis. *Journal of Korean Medical Science,* 19**,** 859-863.

CHUN, J. & HARTUNG, H. P. 2010. Mechanism of action of oral fingolimod (FTY720) in multiple sclerosis. *Clin Neuropharmacol,* 33**,** 91-101.

CHUN, J., HLA, T., LYNCH, K. R., SPIEGEL, S. & MOOLENAAR, W. H. 2010. International Union of Basic and Clinical Pharmacology. LXXVIII. Lysophospholipid receptor nomenclature. *Pharmacol Rev,* 62**,** 579-87.

COIMBRA, S., OLIVEIRA, H., REIS, F., BELO, L., ROCHA, S., QUINTANILHA, A., FIGUEIREDO, A., TEIXEIRA, F., CASTRO, E., ROCHA-PEREIRA, P. & SANTOS-SILVA, A. 2010. Psoriasis therapy and cardiovascular risk factors: a 12-week follow-up study. *Am J Clin Dermatol,* 11**,** 423-32.

COLLINS, COHEN, O'CONNOR, DE VERA, ZHANG-AUBERSON, JIN & KAPPO 2010. Long-term safety of oral fingolimod (FTY720) in relapsing multiple sclerosis: integrated analyses of phase 2 and 3 studies. *Multiple Sclerosis,* 16**,** 295.

COOPER, A. D. 1997. Hepatic uptake of chylomicron remnants. *J Lipid Res,* 38**,** 2173-92.

CRAWFORD, S. E. & BORENSZTAJN, J. 1999. Plasma clearance and liver uptake of chylomicron remnants generated by hepatic lipase lipolysis: evidence for a lactoferrin-sensitive and apolipoprotein E-independent pathway. *J Lipid Res,* 40**,** 797-805.

CUGATI, S., CHEN, C. S., LAKE, S. & LEE, A. W. 2014. Fingolimod and macular edema: Pathophysiology, diagnosis, and management. *Neurol Clin Pract,* 4**,** 402-409.

DALBETH, N., PUI, K., LOBO, M., DOYLE, A., JONES, P. B., TAYLOR, W. J. & MCQUEEN, F. M. 2012. Nail disease in psoriatic arthritis: distal phalangeal bone edema detected by magnetic resonance imaging predicts development of onycholysis and hyperkeratosis. *J Rheumatol,* 39**,** 841-3.

DECICCO-SKINNER, K. L., HENRY, G. H., CATAISSON, C., TABIB, T., GWILLIAM, J. C., WATSON, N. J., BULLWINKLE, E. M., FALKENBURG, L., O'NEILL, R. C., MORIN, A. & WIEST, J. S. 2014. Endothelial cell tube formation assay for the in vitro study of angiogenesis. *J Vis Exp***,** e51312.

DILLMANN, MORA, OLESCH, BRUNE & WEIGERT 2015. S1PR4 is required for plasmacytoid dendritic cell differentiation.

DONNELLY, R. & DAVIS, K. R. 2000. Type 2 diabetes and atherosclerosis. *Diabetes Obes Metab,* 2 Suppl 1**,** S21-30.

DONOVIEL, M. S., HAIT, N. C., RAMACHANDRAN, S., MACEYKA, M., TAKABE, K., MILSTIEN, S., ORAVECZ, T. & SPIEGEL, S. 2015. Spinster 2, a sphingosine-1-phosphate transporter, plays a critical role in inflammatory and autoimmune diseases. *FASEB J,* 29**,** 5018-28.

ECKERT, R. L. & RORKE, E. A. 1989. Molecular biology of keratinocyte differentiation. *Environ Health Perspect,* 80**,** 109-16.

EDSALL, L. C., VAN BROCKLYN JR FAU - CUVILLIER, O., CUVILLIER O FAU - KLEUSER, B., KLEUSER B FAU - SPIEGEL, S. & SPIEGEL, S. 1998. N,N-Dimethylsphingosine is a potent competitive inhibitor of sphingosine kinase but not of protein kinase C: modulation of cellular levels of sphingosine 1-phosphate and ceramide.

EDWARDS, C. J., BLANCO, F. J., CROWLEY, J., BIRBARA, C. A., JAWORSKI, J., AELION, J., STEVENS, R. M., VESSEY, A., ZHAN, X. & BIRD, P. 2016. Apremilast, an oral phosphodiesterase 4 inhibitor, in patients with psoriatic arthritis and current skin involvement: a phase III, randomised, controlled trial (PALACE 3). *Ann Rheum Dis,* 75**,** 1065-73.

EELEN, G., DE ZEEUW, P., TREPS, L., HARJES, U., WONG, B. W. & CARMELIET, P. 2018. Endothelial Cell Metabolism. *Physiol Rev,* 98**,** 3-58.

EHRINGER, W. D., EDWARDS, M. J. & MILLER, F. N. 1996. Mechanisms of alpha-thrombin, histamine, and bradykinin induced endothelial permeability. *J Cell Physiol,* 167**,** 562-9.

FAYYAZ, S., JAPTOK, L. & KLEUSER, B. 2014. Divergent role of sphingosine 1-phosphate on insulin resistance. *Cell Physiol Biochem,* 34**,** 134-47.

FEINGOLD, K. R. & GRUNFELD, C. 2015. Introduction to lipids and lipoproteins.

FERRAZ, T. P., FIUZA, M. C., DOS SANTOS, M. L., PONTES DE CARVALHO, L. & SOARES, N. M. 2004. Comparison of six methods for the extraction of lipids from serum in terms of effectiveness and protein preservation. *J Biochem Biophys Methods,* 58**,** 187-93.

FLEMING, J. K., GLASS, T. R., LACKIE, S. J. & WOJCIAK, J. M. 2016a. A novel approach for measuring sphingosine-1-phosphate and lysophosphatidic acid binding to carrier proteins using

monoclonal antibodies and the Kinetic Exclusion Assay. *Journal of Lipid Research,* 57**,** 1737-1747.

FLEMING, J. K., GLASS, T. R., LACKIE, S. J. & WOJCIAK, J. M. 2016b. A novel approach for measuring sphingosine-1-phosphate and lysophosphatidic acid binding to carrier proteins using monoclonal antibodies and the Kinetic Exclusion Assay. *J Lipid Res,* 57**,** 1737-47.

FLUHR, J. W., CAVALLOTTI, C. & BERARDESCA, E. 2008. Emollients, moisturizers, and keratolytic agents in psoriasis. *Clin Dermatol,* 26**,** 380-6.

FONG, L. G., PARTHASARATHY, S., WITZTUM, J. L. & STEINBERG, D. 1987. Nonenzymatic oxidative cleavage of peptide bonds in apoprotein B-100. *J Lipid Res,* 28**,** 1466-77.

FRY, L., BAKER BS FAU - POWLES, A. V., POWLES AV FAU - FAHLEN, A., FAHLEN A FAU - ENGSTRAND, L. & ENGSTRAND, L. 2013. Is chronic plaque psoriasis triggered by microbiota in the skin?

FRY, L., BAKER, B. S., POWLES, A. V. & ENGSTRAND, L. 2015. Psoriasis is not an autoimmune disease? *Exp Dermatol,* 24**,** 241-4.

FU, P., SHAAYA, M., HARIJITH, A., JACOBSON, J. R., KARGINOV, A. & NATARAJAN, V. 2018. Sphingolipids Signaling in Lamellipodia Formation and Enhancement of Endothelial Barrier Function. *Curr Top Membr,* 82**,** 1-31.

GAO, B., SABA, T. M. & TSAN, M.-F. 2002. Role of α_vβ₃-integrin in TNF-α-induced endothelial cell migration. *American Journal of Physiology - Cell Physiology,* 283**,** C1196.

GAO, X. Y., LI, L., WANG, X. H., WEN, X. Z., JI, K., YE, L., CAI, J., JIANG, W. G. & JI, J. F. 2015. Inhibition of sphingosine-1-phosphate phosphatase 1 promotes cancer cells migration in gastric cancer: Clinical implications.

GELFAND, J. M., NEIMANN, A. L., SHIN, D. B., WANG, X., MARGOLIS, D. J. & TROXEL, A. B. 2006. Risk of myocardial infarction in patients with psoriasis. *JAMA,* 296**,** 1735-41.

GLADMAN, D. D., ANTONI, C., MEASE, P., CLEGG, D. O. & NASH, P. 2005. Psoriatic arthritis: epidemiology, clinical features, course, and outcome. *Ann Rheum Dis,* 64 Suppl 2**,** ii14-7.

GOLDMINZ, A. M., AU, S. C., KIM, N., GOTTLIEB, A. B. & LIZZUL, P. F. 2013. NF-kappaB: an essential transcription factor in psoriasis. *J Dermatol Sci,* 69**,** 89-94.

GOLDSTEIN, J. L. & BROWN, M. S. 2009. The LDL receptor. *Arterioscler Thromb Vasc Biol,* 29**,** 431-8.

GONCHAROV, N. V., NADEEV, A. D., JENKINS, R. O. & AVDONIN, P. V. 2017. Markers and Biomarkers of Endothelium: When Something Is Rotten in the State. *Oxid Med Cell Longev,* 2017**,** 9759735.

GUGLIELMETTI, A., CONLLEDO, R., BEDOYA, J., IANISZEWSKI, F. & CORREA, J. 2012. Inverse psoriasis involving genital skin folds: successful therapy with dapsone. *Dermatol Ther (Heidelb),* 2**,** 15.

HAMMAD, S. M., AL GADBAN, M. M., SEMLER, A. J. & KLEIN, R. L. 2012. Sphingosine 1-phosphate distribution in human plasma: associations with lipid profiles. *J Lipids,* 2012**,** 180705.

HENSELER, T. & CHRISTOPHERS, E. 1995. Disease concomitance in psoriasis. *J Am Acad Dermatol,* 32**,** 982-6.

HERRON, M. D., HINCKLEY, M., HOFFMAN, M. S., PAPENFUSS, J., HANSEN, C. B., CALLIS, K. P. & KRUEGER, G. G. 2005. Impact of obesity and smoking on psoriasis presentation and management. *Arch Dermatol,* 141**,** 1527-34.

HISANO, Y., KOBAYASHI, N., KAWAHARA, A., YAMAGUCHI, A. & NISHI, T. 2011. The Sphingosine 1-Phosphate Transporter, SPNS2, Functions as a Transporter of the Phosphorylated Form of the Immunomodulating Agent FTY720. *Journal of Biological Chemistry,* 286**,** 1758-1766.

HISHIKAWA, D., HASHIDATE, T., SHIMIZU, T. & SHINDOU, H. 2014. Diversity and function of membrane glycerophospholipids generated by the remodeling pathway in mammalian cells. *J Lipid Res,* 55**,** 799-807.

HODEIB, A. A., NEINAA, Y. M. E., ZAKARIA, S. S. & ALSHENAWY, H. A. 2018. Glucose transporter-1 (GLUT-1) expression in psoriasis: correlation with disease severity. *Int J Dermatol,* 57**,** 943-951.

HOLVOET, P., KRITCHEVSKY, S. B., TRACY, R. P., MERTENS, A., RUBIN, S. M., BUTLER, J., GOODPASTER, B. & HARRIS, T. B. 2004. The metabolic syndrome, circulating oxidized LDL, and risk of myocardial infarction in well-functioning elderly people in the health, aging, and body composition cohort. *Diabetes,* 53**,** 1068-73.

IFPA. 2017. Available: https://ifpa-pso.com/our-cause/ [Accessed].

JACOBI, A., MAYER, A. & AUGUSTIN, M. 2015. Keratolytics and emollients and their role in the therapy of psoriasis: a systematic review. *Dermatol Ther (Heidelb),* 5**,** 1-18.

JAPTOK, L., SCHMITZ, E. I., FAYYAZ, S., KRAMER, S., HSU, L. J. & KLEUSER, B. 2015. Sphingosine 1-phosphate counteracts insulin signaling in pancreatic beta-cells via the sphingosine 1-phosphate receptor subtype 2. *FASEB J,* 29**,** 3357-69.

JI, M., XUE, N., LAI, F., ZHANG, X., ZHANG, S., WANG, Y., JIN, J. & CHEN, X. 2018. Validating a Selective S1P1 Receptor Modulator Syl930 for Psoriasis Treatment. *Biol Pharm Bull,* 41**,** 592-596.

JIARAVUTHISAN, M. M., SASSEVILLE, D., VENDER, R. B., MURPHY, F. & MUHN, C. Y. 2007. Psoriasis of the nail: anatomy, pathology, clinical presentation, and a review of the literature on therapy. *J Am Acad Dermatol,* 57**,** 1-27.

JOHNSON-HUANG, L. M., SUAREZ-FARINAS, M., PIERSON, K. C., FUENTES-DUCULAN, J., CUETO, I., LENTINI, T., SULLIVAN-WHALEN, M., GILLEAUDEAU, P., KRUEGER, J. G., HAIDER, A. S. & LOWES, M. A. 2012. A single intradermal injection of IFN-gamma induces an inflammatory state in both non-lesional psoriatic and healthy skin. *J Invest Dermatol,* 132**,** 1177-87.

JUSTUS, C. R., LEFFLER, N., RUIZ-ECHEVARRIA, M. & YANG, L. V. 2014. In vitro cell migration and invasion assays. *J Vis Exp***,** 51046.

KAUR, S., KINGO, K. & ZILMER, M. 2017. Psoriasis and Cardiovascular Risk-Do Promising New Biomarkers Have Clinical Impact? *Mediators Inflamm,* 2017**,** 7279818.

KEUL, P., LUCKE, S., VON WNUCK LIPINSKI, K., BODE, C., GRALER, M., HEUSCH, G. & LEVKAU, B. 2011. Sphingosine-1-phosphate receptor 3 promotes recruitment of monocyte/macrophages in inflammation and atherosclerosis. *Circ Res,* 108**,** 314-23.

KIMURA, T., TOMURA, H., MOGI, C., KUWABARA, A., DAMIRIN, A., ISHIZUKA, T., SEKIGUCHI, A., ISHIWARA, M., IM, D. S., SATO, K., MURAKAMI, M. & OKAJIMA, F. 2006. Role of scavenger receptor class B type I and sphingosine 1-phosphate receptors in high density lipoprotein-

induced inhibition of adhesion molecule expression in endothelial cells. *J Biol Chem,* 281**,** 37457-67.

KITA, T., KUME, N., MINAMI, M., HAYASHIDA, K., MURAYAMA, T., SANO, H., MORIWAKI, H., KATAOKA, H., NISHI, E., HORIUCHI, H., ARAI, H. & YOKODE, M. 2006. Role of Oxidized LDL in Atherosclerosis. *Annals of the New York Academy of Sciences,* 947**,** 199-206.

KLERKX, A. H., EL HARCHAOUI, K., VAN DER STEEG, W. A., BOEKHOLDT, S. M., STROES, E. S., KASTELEIN, J. J. & KUIVENHOVEN, J. A. 2006. Cholesteryl ester transfer protein (CETP) inhibition beyond raising high-density lipoprotein cholesterol levels: pathways by which modulation of CETP activity may alter atherogenesis. *Arterioscler Thromb Vasc Biol,* 26**,** 706-15.

KOWALSKI, G. M., KLOEHN, J., BURCH, M. L., SELATHURAI, A., HAMLEY, S., BAYOL, S. A., LAMON, S., WATT, M. J., LEE-YOUNG, R. S., MCCONVILLE, M. J. & BRUCE, C. R. 2015. Overexpression of sphingosine kinase 1 in liver reduces triglyceride content in mice fed a low but not high-fat diet. *Biochim Biophys Acta,* 1851**,** 210-9.

KRAUSE, A., D'AMBROSIO, D. & DINGEMANSE, J. 2018. Modeling clinical efficacy of the S1P receptor modulator ponesimod in psoriasis. *J Dermatol Sci,* 89**,** 136-145.

KUMAR, A., BYUN, H. S., BITTMAN, R. & SABA, J. D. 2011. The sphingolipid degradation product trans-2-hexadecenal induces cytoskeletal reorganization and apoptosis in a JNK-dependent manner. *Cell Signal,* 23**,** 1144-52.

KUO, A., LEE, M. Y. & SESSA, W. C. 2017. Lipid Droplet Biogenesis and Function in the Endothelium. *Circ Res,* 120**,** 1289-1297.

KURANO, M. & YATOMI, Y. 2018. Sphingosine 1-Phosphate and Atherosclerosis. *J Atheroscler Thromb,* 25**,** 16-26.

LAMALICE, L., LE BOEUF, F. & HUOT, J. 2007. Endothelial cell migration during angiogenesis. *Circ Res,* 100**,** 782-94.

LANGLEY, R. G., KRUEGER, G. G. & GRIFFITHS, C. E. 2005. Psoriasis: epidemiology, clinical features, and quality of life. *Ann Rheum Dis,* 64 Suppl 2**,** ii18-23; discussion ii24-5.

LE STUNFF, H., MILSTIEN, S. & SPIEGEL, S. 2004. Generation and metabolism of bioactive sphingosine-1-phosphate. *J Cell Biochem,* 92**,** 882-99.

LEE, E., KOO, J. & BERGER, T. 2005. UVB phototherapy and skin cancer risk: a review of the literature. *Int J Dermatol,* 44**,** 355-60.

LEE, J. F., GORDON, S., ESTRADA, R., WANG, L., SIOW, D. L., WATTENBERG, B. W., LOMINADZE, D. & LEE, M. J. 2009. Balance of S1P1 and S1P2 signaling regulates peripheral microvascular permeability in rat cremaster muscle vasculature. *Am J Physiol Heart Circ Physiol,* 296**,** H33-42.

LEE, S. Y., HONG, I. K., KIM, B. R., SHIM, S. M., SUNG LEE, J., LEE, H. Y., SOO CHOI, C., KIM, B. K. & PARK, T. S. 2015a. Activation of sphingosine kinase 2 by endoplasmic reticulum stress ameliorates hepatic steatosis and insulin resistance in mice. *Hepatology,* 62**,** 135-46.

LEE, W. K., KIM, G. W., CHO, H. H., KIM, W. J., MUN, J. H., SONG, M., KIM, H. S., KO, H. C., KIM, M. B. & KIM, B. S. 2015b. Erythrodermic Psoriasis Treated with Golimumab: A Case Report. *Ann Dermatol,* 27**,** 446-9.

LEE, Y. M., VENKATARAMAN, K., HWANG, S. I., HAN, D. K. & HLA, T. 2007. A novel method to quantify sphingosine 1-phosphate by immobilized metal affinity chromatography (IMAC). *Prostaglandins Other Lipid Mediat,* 84**,** 154-62.

LEW, B. L., CHO, Y., KIM, J., SIM, W. Y. & KIM, N. I. 2006. Ceramides and cell signaling molecules in psoriatic epidermis: reduced levels of ceramides, PKC-alpha, and JNK. *J Korean Med Sci,* 21**,** 95-9.

LI, D. & MEHTA, J. L. 2005. Oxidized LDL, a critical factor in atherogenesis. *Cardiovasc Res,* 68**,** 353-4.

LIANG, C. C., PARK, A. Y. & GUAN, J. L. 2007. In vitro scratch assay: a convenient and inexpensive method for analysis of cell migration in vitro. *Nat Protoc,* 2**,** 329-33.

LIMA, S., MILSTIEN, S. & SPIEGEL, S. 2017. Sphingosine and Sphingosine Kinase 1 Involvement in Endocytic Membrane Trafficking. *J Biol Chem,* 292**,** 3074-3088.

LIU, Y. J., WADA, R., YAMASHITA, T., MI, Y. D., DENG, C. X., HOBSON, J. P., ROSENFELDT, H. M., NAVA, V. E., CHAE, S. S., LEE, M. J., LIU, C. H., HLA, T., SPIEGEL, S. & PROIA, R. L. 2000. Edg-1, the G protein-coupled receptor for sphingosine-1-phosphate, is essential for vascular maturation. *Journal of Clinical Investigation,* 106**,** 951-961.

LIZZUL, P. F., APHALE, A., MALAVIYA, R., SUN, Y., MASUD, S., DOMBROVSKIY, V. & GOTTLIEB, A. B. 2005. Differential expression of phosphorylated NF-kappaB/RelA in normal and psoriatic epidermis and downregulation of NF-kappaB in response to treatment with etanercept. *J Invest Dermatol,* 124**,** 1275-83.

LONNBERG, A. S., SKOV, L., DUFFY, D. L., SKYTTHE, A., KYVIK, K. O., PEDERSEN, O. B. & THOMSEN, S. F. 2016. Genetic Factors Explain Variation in the Age at Onset of Psoriasis: A Population-based Twin Study. *Acta Dermato-Venereologica,* 96**,** 35-38.

LOWES, M. A., BOWCOCK, A. M. & KRUEGER, J. G. 2007. Pathogenesis and therapy of psoriasis. *Nature,* 445**,** 866-73.

MA, E. A., W, Z., Y, M. A., I, A., M, F., OSMAN, B. & KAABACHI, N. 2014. Serum lipid level in Tunisian patients with psoriasis.

MAJUMDAR, I. & MASTRANDREA, L. D. 2012. Serum sphingolipids and inflammatory mediators in adolescents at risk for metabolic syndrome.

MANSBACH, C. M. & SIDDIQI, S. A. 2010. The biogenesis of chylomicrons. *Annu Rev Physiol,* 72**,** 315-33.

MARANHAO, R. C., CARVALHO, P. O., STRUNZ, C. C. & PILEGGI, F. 2014. Lipoprotein (a): structure, pathophysiology and clinical implications. *Arq Bras Cardiol,* 103**,** 76-84.

MATTIE, M., BROOKER, G. & SPIEGEL, S. 1994. Sphingosine-1-phosphate, a putative second messenger, mobilizes calcium from internal stores via an inositol trisphosphate-independent pathway. *J Biol Chem,* 269**,** 3181-8.

MAYOR, R. & ETIENNE-MANNEVILLE, S. 2016. The front and rear of collective cell migration. *Nat Rev Mol Cell Biol,* 17**,** 97-109.

MCCAIN, J. 2013. The MAPK (ERK) Pathway: Investigational Combinations for the Treatment Of BRAF-Mutated Metastatic Melanoma. *P T,* 38**,** 96-108.

MCGRATH, J. A., R. A. J. EADY & POPE, F. M. 2004. *Rook's textbook of dermatology- Anatomy and organization of human skin.*

MEASE, P. J., GLADMAN, D. D., PAPP, K. A., KHRAISHI, M. M., THACI, D., BEHRENS, F., NORTHINGTON, R., FUIMAN, J., BANANIS, E., BOGGS, R. & ALVAREZ, D. 2013. Prevalence of rheumatologist-diagnosed psoriatic arthritis in patients with psoriasis in European/North American dermatology clinics. *J Am Acad Dermatol,* 69**,** 729-35.

MEHTA, D. & LIM, H. W. 2016. Ultraviolet B Phototherapy for Psoriasis: Review of Practical Guidelines. *Am J Clin Dermatol,* 17**,** 125-33.

MENDELSON, K., EVANS, T. & HLA, T. 2013. Sphingosine 1-phosphate signalling. *Development,* 141**,** 5.

MENTER A, KORMAN NJ , ELMETS CA, FELDMAN SR, GELFAND JM, GORDON KB, GOTTLIEB A, KOO JY, LEBWOHL M, LEONARDI CL, LIM HW, VAN VOORHEES AS, BEUTNER KR, RYAN C & BHUSHAN, R. 2011. Guidelines of care for the management of psoriasis and psoriatic arthritis: section 6. Guidelines of care for the treatment of psoriasis and psoriatic arthritis: case-based presentations and evidence-based conclusions. *Journal of the American Academy of Dermatology*.

MINAGAR, A., OSTANIN, D., LONG, A. C., JENNINGS, M., KELLEY, R. E., SASAKI, M. & ALEXANDER, J. S. 2003. Serum from patients with multiple sclerosis downregulates occludin and VE-cadherin expression in cultured endothelial cells. *Mult Scler,* 9**,** 235-8.

MOON, H., CHON, J., JOO, J., KIM, D., IN, J., LEE, H., PARK, J. & CHOI, J. 2013a. FTY720 preserved islet beta-cell mass by inhibiting apoptosis and increasing survival of beta-cells in db/db mice. *Diabetes Metab Res Rev,* 29**,** 19-24.

MOON, S. H., KIM, J. Y., SONG, E. H., SHIN, M. K., CHO, Y. H. & KIM, N. I. 2013b. Altered levels of sphingosine and sphinganine in psoriatic epidermis. *Ann Dermatol,* 25**,** 321-6.

MYSLIWIEC, H., BARAN, A., HARASIM-SYMBOR, E., CHOROMANSKA, B., MYSLIWIEC, P., MILEWSKA, A. J., CHABOWSKI, A. & FLISIAK, I. 2017. Increase in circulating sphingosine-1-phosphate and decrease in ceramide levels in psoriatic patients. *Arch Dermatol Res,* 309**,** 79-86.

NAGAHASHI, M., KIM, E. Y., YAMADA, A., RAMACHANDRAN, S., ALLEGOOD, J. C., HAIT, N. C., MACEYKA, M., MILSTIEN, S., TAKABE, K. & SPIEGEL, S. 2013. Spns2, a transporter of phosphorylated sphingoid bases, regulates their blood and lymph levels, and the lymphatic network. *Faseb Journal,* 27**,** 1001-1011.

NAGAHASHI, M., TAKABE, K., TERRACINA, K. P., SOMA, D., HIROSE, Y., KOBAYASHI, T., MATSUDA, Y. & WAKAI, T. 2014. Sphingosine-1-phosphate transporters as targets for cancer therapy. *Biomed Res Int,* 2014**,** 651727.

NAGAHASHI, M., YAMADA, A., MIYAZAKI, H., ALLEGOOD, J. C., TSUCHIDA, J., AOYAGI, T., HUANG, W. C., TERRACINA, K. P., ADAMS, B. J., RASHID, O. M., MILSTIEN, S., WAKAI, T., SPIEGEL, S. & TAKABE, K. 2016. Interstitial Fluid Sphingosine-1-Phosphate in Murine Mammary Gland and Cancer and Human Breast Tissue and Cancer Determined by Novel Methods. *J Mammary Gland Biol Neoplasia,* 21**,** 9-17.

NAKAJIMA, M., NAGAHASHI, M., RASHID, O. M., TAKABE, K. & WAKAI, T. 2017. The role of sphingosine-1-phosphate in the tumor microenvironment and its clinical implications. *Tumour Biol,* 39**,** 1010428317699133.

NEIMANN, A. L., SHIN, D. B., WANG, X., MARGOLIS, D. J., TROXEL, A. B. & GELFAND, J. M. 2006. Prevalence of cardiovascular risk factors in patients with psoriasis. *J Am Acad Dermatol,* 55**,** 829-35.

NG, M. L., WADHAM, C. & SUKOCHEVA, O. A. 2017. The role of sphingolipid signalling in diabetesassociated pathologies (Review). *Int J Mol Med,* 39**,** 243-252.

NJAJOU, O. T., KANAYA, A. M., HOLVOET, P., CONNELLY, S., STROTMEYER, E. S., HARRIS, T. B., CUMMINGS, S. R., HSUEH, W. C. & HEALTH, A. B. C. S. 2009. Association between oxidized LDL, obesity and type 2 diabetes in a population-based cohort, the Health, Aging and Body Composition Study. *Diabetes Metab Res Rev,* 25**,** 733-9.

OETTL, K. & STAUBER, R. E. 2007. Physiological and pathological changes in the redox state of human serum albumin critically influence its binding properties. *Br J Pharmacol,* 151**,** 580-90.

OKA, A., MABUCHI, T., OZAWA, A. & INOKO, H. 2012. Current understanding of human genetics and genetic analysis of psoriasis. *J Dermatol,* 39**,** 231-41.

OKAJIMA, F. 2002. Plasma lipoproteins behave as carriers of extracellular sphingosine 1-phosphate: is this an atherogenic mediator or an anti-atherogenic mediator? *Biochimica Et Biophysica Acta-Molecular and Cell Biology of Lipids,* 1582**,** 132-137.

OLIVERA, A., ALLENDE, M. L. & PROIA, R. L. 2013. Shaping the landscape: metabolic regulation of S1P gradients. *Biochim Biophys Acta,* 1831**,** 193-202.

ORMEROD, M. 2015. *Flow Cytometry - A Basic Introduction*, Michael G Ormerod

OSBORNE, N., BRAND-ARZAMENDI, K., OBER, E. A., JIN, S. W., VERKADE, H., HOLTZMAN, N. G., YELON, D. & STAINIERL, D. Y. R. 2008. The Spinster Homolog, Two of Hearts, Is Required for Sphingosine 1-Phosphate Signaling in Zebrafish. *Current Biology,* 18**,** 1882-1888.

OSKOUIAN, B., SOORIYAKUMARAN, P., BOROWSKY, A. D., CRANS, A., DILLARD-TELM, L., TAM, Y. Y., BANDHUVULA, P. & SABA, J. D. 2006. Sphingosine-1-phosphate lyase potentiates apoptosis via p53-and p38-dependent pathways and is down-regulated in colon cancer. *Proceedings of the National Academy of Sciences of the United States of America,* 103**,** 17384-17389.

PATMANATHAN, S. N., WANG, W., YAP, L. F., HERR, D. R. & PATERSON, I. C. 2017. Mechanisms of sphingosine 1-phosphate receptor signalling in cancer. *Cell Signal,* 34**,** 66-75.

PERFETTO, S. P., CHATTOPADHYAY, P. K., LAMOREAUX, L., NGUYEN, R., AMBROZAK, D., KOUP, R. A. & ROEDERER, M. 2010. Amine-reactive dyes for dead cell discrimination in fixed samples. *Curr Protoc Cytom,* Chapter 9**,** Unit 9 34.

PIETRZAK, A., CHABROS, P., GRYWALSKA, E., KICINSKI, P., PIETRZAK-FRANCISZKIEWICZ, K., KRASOWSKA, D. & KANDZIERSKI, G. 2019. Serum lipid metabolism in psoriasis and psoriatic arthritis - an update. *Arch Med Sci,* 15**,** 369-375.

POTENTE, M. & CARMELIET, P. 2017. The Link Between Angiogenesis and Endothelial Metabolism. *Annu Rev Physiol,* 79**,** 43-66.

PROIA, R. L. & HLA, T. 2015. Emerging biology of sphingosine-1-phosphate: its role in pathogenesis and therapy. *J Clin Invest,* 125**,** 1379-87.

PRUSSICK, R., PRUSSICK L FAU - GUTMAN, J. & GUTMAN, J. 2013. Psoriasis Improvement in Patients Using Glutathione-enhancing, Nondenatured Whey Protein Isolate: A Pilot Study.

QUAN, C., CHO, M. K., SHAO, Y., MIANECKI, L. E., LIAO, E., PERRY, D. & QUAN, T. 2015. Dermal fibroblast expression of stromal cell-derived factor-1 (SDF-1) promotes epidermal keratinocyte proliferation in normal and diseased skin. *Protein Cell,* 6**,** 890-903.

RADTKE, M. A., BEIKERT, F. C. & AUGUSTIN, M. 2013. Nail psoriasis - a treatment challenge. *J Dtsch Dermatol Ges,* 11**,** 203-19; quiz 220.

RAMANA, C. V., GIL, M. P., SCHREIBER, R. D. & STARK, G. R. 2002. Stat1-dependent and -independent pathways in IFN-γ-dependent signaling. *Trends in Immunology,* 23**,** 96-101.

REINHART-KING, C. A., DEMBO, M. & HAMMER, D. A. 2005. The dynamics and mechanics of endothelial cell spreading. *Biophys J,* 89**,** 676-89.

ROSEN, P., NAWROTH, P. P., KING, G., MOLLER, W., TRITSCHLER, H. J. & PACKER, L. 2001. The role of oxidative stress in the onset and progression of diabetes and its complications: a summary of a Congress Series sponsored by UNESCO-MCBN, the American Diabetes Association and the German Diabetes Society. *Diabetes Metab Res Rev,* 17**,** 189-212.

ROSKOSKI, R., JR. 2012. ERK1/2 MAP kinases: structure, function, and regulation. *Pharmacol Res,* 66**,** 105-43.

ROZENBLIT, M. & LEBWOHL, M. 2009. New biologics for psoriasis and psoriatic arthritis. *Dermatol Ther,* 22**,** 56-60.

RUIZ, M., FREJ, C., HOLMER, A., GUO, L. J., TRAN, S. & DAHLBACK, B. 2017a. High-Density Lipoprotein-Associated Apolipoprotein M Limits Endothelial Inflammation by Delivering Sphingosine-1-Phosphate to the Sphingosine-1-Phosphate Receptor 1. *Arterioscler Thromb Vasc Biol,* 37**,** 118-129.

RUIZ, M., OKADA, H. & DAHLBACK, B. 2017b. HDL-associated ApoM is anti-apoptotic by delivering sphingosine 1-phosphate to S1P1 & S1P3 receptors on vascular endothelium. *Lipids Health Dis,* 16**,** 36.

SADOWSKA, A. M., VERBRAECKEN J FAU - DARQUENNES, K., DARQUENNES K FAU - DE BACKER, W. A. & DE BACKER, W. A. 2006. Role of N-acetylcysteine in the management of COPD.

SAMAD, F., HESTER, K. D., YANG, G., HANNUN, Y. A. & BIELAWSKI, J. 2006. Altered adipose and plasma sphingolipid metabolism in obesity: a potential mechanism for cardiovascular and metabolic risk. *Diabetes,* 55**,** 2579-87.

SCHON. 2008. Animal models of psoriasis: a critical appraisal. *Experimental dermatology*, 17(8), 703–712.

SCOCCIA, A. E., MOLINUEVO, M. S., MCCARTHY, A. D. & CORTIZO, A. M. 2001. A simple method to assess the oxidative susceptibility of low density lipoproteins. *BMC Clin Pathol,* 1**,** 1.

SETTY, A. R., CURHAN, G. & CHOI, H. K. 2007. Obesity, waist circumference, weight change, and the risk of psoriasis in women: Nurses' Health Study II. *Arch Intern Med,* 167**,** 1670-5.

SHIH, C. M., HUANG, C. Y., WANG, K. H., HUANG, C. Y., WEI, P. L., CHANG, Y. J., HSIEH, C. K., LIU, K. T. & LEE, A. W. 2018. Oxidized Low-Density Lipoprotein-Deteriorated Psoriasis Is Associated with the Upregulation of Lox-1 Receptor and Il-23 Expression In Vivo and In Vitro. *Int J Mol Sci,* 19**,** 2610.

SHIN, M., BEANE, T. J., QUILLIEN, A., MALE, I., ZHU, L. J. & LAWSON, N. A.-O. 2016. Vegfa signals through ERK to promote angiogenesis, but not artery differentiation. *Development*

SHIN, S.-H., , K.-A. C., SOOJUNG HAHN, YOUNGHAY LEE, YU HEE KIM, SO-YOUN WOO, KYUNG-HA RYU, WOO-JAE PARK & PARK, J.-W. 2019. Inhibiting Sphingosine Kinase 2 Derived-sphingosine-1-phosphate Ameliorates Psoriasis-like Skin Disease via Blocking Th17

Differentiation of Naïve CD4 T Lymphocytes in Mice. *Advances in Dermatology and Venerology,* 99.

SILVA, V. R., MICHELETTI, T. O., PIMENTEL, G. D., KATASHIMA, C. K., LENHARE, L., MORARI, J., MENDES, M. C., RAZOLLI, D. S., ROCHA, G. Z., DE SOUZA, C. T., RYU, D., PRADA, P. O., VELLOSO, L. A., CARVALHEIRA, J. B., PAULI, J. R., CINTRA, D. E. & ROPELLE, E. R. 2014. Hypothalamic S1P/S1PR1 axis controls energy homeostasis.

SIMARD, J. R., ZUNSZAIN, P. A., HA, C. E., YANG, J. S., BHAGAVAN, N. V., PETITPAS, I., CURRY, S. & HAMILTON, J. A. 2005. Locating high-affinity fatty acid-binding sites on albumin by x-ray crystallography and NMR spectroscopy. *Proc Natl Acad Sci U S A,* 102**,** 17958-63.

SKOURA, A., MICHAUD, J., IM, D. S., THANGADA, S., XIONG, Y., SMITH, J. D. & HLA, T. 2011. Sphingosine-1-phosphate receptor-2 function in myeloid cells regulates vascular inflammation and atherosclerosis. *Arterioscler Thromb Vasc Biol,* 31**,** 81-5.

SMITH, C.H., ANSTEY, A.V.,BARKER, J.N., et al., 2009. British Association of Dermatologists' guidelines for biologic interventions for psoriasis. *Br J Dermatol*, 161(5):987-1019.

SMITH, R. L. 2016. Pediatric psoriasis treated with apremilast. *JAAD Case Rep,* 2**,** 89-91.

SONG, P. & ZOU, M. H. 2014. Redox regulation of endothelial cell fate. *Cell Mol Life Sci,* 71**,** 3219-39.

SPIEGEL, S. & MILSTIEN, S. 2002. Sphingosine 1-phosphate, a key cell signaling molecule. *J Biol Chem,* 277**,** 25851-4.

STEWART, J. C., VILLASMIL, M. L. & FRAMPTON, M. W. 2007. Changes in fluorescence intensity of selected leukocyte surface markers following fixation. *Cytometry A,* 71**,** 379-85.

STRUB, G. M., MACEYKA, M., HAIT, N. C., MILSTIEN, S. & SPIEGEL, S. 2010. Extracellular and intracellular actions of sphingosine-1-phosphate. *Adv Exp Med Biol,* 688**,** 141-55.

SU, G., ATAKILIT, A., LI, J. T., WU, N., BHATTACHARYA, M., ZHU, J., SHIEH, J. E., LI, E., CHEN, R., SUN, S., SU, C. P. & SHEPPARD, D. 2012. Absence of integrin alphavbeta3 enhances vascular leak in mice by inhibiting endothelial cortical actin formation. *Am J Respir Crit Care Med,* 185**,** 58-66.

SUDLOW, G., BIRKETT, D. J. & WADE, D. N. 1975. The characterization of two specific drug binding sites on human serum albumin. *Mol Pharmacol,* 11**,** 824-32.

SYED, S. N., RAUE, R., WEIGERT, A., VON KNETHEN, A. & BRUNE, B. 2019. Macrophage S1PR1 Signaling Alters Angiogenesis and Lymphangiogenesis During Skin Inflammation. *Cells,* 8**,** 785.

TAKABE, K., KIM, R. H., ALLEGOOD, J. C., MITRA, P., RAMACHANDRAN, S., NAGAHASHI, M., HARIKUMAR, K. B., HAIT, N. C., MILSTIEN, S. & SPIEGEL, S. 2010. Estradiol induces export of sphingosine 1-phosphate from breast cancer cells via ABCC1 and ABCG2. *J Biol Chem,* 285**,** 10477-86.

TAKUWA, Y., DU, W., QI, X., OKAMOTO, Y., TAKUWA, N. & YOSHIOKA, K. 2010. Roles of sphingosine-1-phosphate signaling in angiogenesis. *World J Biol Chem,* 1**,** 298-306.

TAMAMA, K., TOMURA, H., SATO, K., MALCHINKHUU, E., DAMIRIN, A., KIMURA, T., KUWABARA, A., MURAKAMI, M. & OKAJIMA, F. 2005. High-density lipoprotein inhibits migration of vascular smooth muscle cells through its sphingosine 1-phosphate component. *Atherosclerosis,* 178**,** 19-23.

TANEW, A., RADAKOVIC-FIJAN, S., SCHEMPER, M. & HONIGSMANN, H. 1999. Narrowband UV-B phototherapy vs photochemotherapy in the treatment of chronic plaque-type psoriasis: a paired comparison study. *Arch Dermatol,* 135**,** 519-24.

THEILMEIER, G., SCHMIDT C FAU - HERRMANN, J., HERRMANN J FAU - KEUL, P., KEUL P FAU - SCHAFERS, M., SCHAFERS M FAU - HERRGOTT, I., HERRGOTT I FAU - MERSMANN, J., MERSMANN J FAU - LARMANN, J., LARMANN J FAU - HERMANN, S., HERMANN S FAU - STYPMANN, J., STYPMANN J FAU - SCHOBER, O., SCHOBER O FAU - HILDEBRAND, R., HILDEBRAND R FAU - SCHULZ, R., SCHULZ R FAU - HEUSCH, G., HEUSCH G FAU - HAUDE, M., HAUDE M FAU - VON WNUCK LIPINSKI, K., VON WNUCK LIPINSKI K FAU - HERZOG, C., HERZOG C FAU - SCHMITZ, M., SCHMITZ M FAU - ERBEL, R., ERBEL R FAU - CHUN, J., CHUN J FAU - LEVKAU, B. & LEVKAU, B. 2006. High-density lipoproteins and their constituent, sphingosine-1-phosphate, directly protect the heart against ischemia/reperfusion injury in vivo via the S1P3 lysophospholipid receptor.

TIRUPPATHI, C., MINSHALL, R. D., PARIA, B. C., VOGEL, S. M. & MALIK, A. B. 2002. Role of Ca2+ signaling in the regulation of endothelial permeability. *Vascul Pharmacol,* 39**,** 173-85.

TOLLEFSON, M. M., CROWSON, C. S., MCEVOY, M. T. & MARADIT KREMERS, H. 2010. Incidence of psoriasis in children: a population-based study. *J Am Acad Dermatol,* 62**,** 979-87.

TRPKOVIC, A., RESANOVIC, I., STANIMIROVIC, J., RADAK, D., MOUSA, S. A., CENIC-MILOSEVIC, D., JEVREMOVIC, D. & ISENOVIC, E. R. 2015. Oxidized low-density lipoprotein as a biomarker of cardiovascular diseases. *Critical Reviews in Clinical Laboratory Sciences,* 52**,** 70-85.

VAISAR, T., PENNATHUR, S., GREEN, P. S., GHARIB, S. A., HOOFNAGLE, A. N., CHEUNG, M. C., BYUN, J., VULETIC, S., KASSIM, S., SINGH, P., CHEA, H., KNOPP, R. H., BRUNZELL, J., GEARY, R., CHAIT, A., ZHAO, X. Q., ELKON, K., MARCOVINA, S., RIDKER, P., ORAM, J. F. & HEINECKE, J. W. 2007. Shotgun proteomics implicates protease inhibition and complement activation in the antiinflammatory properties of HDL. *J Clin Invest,* 117**,** 746-56.

VICENTE-MANZANARES, M., WEBB, D. J. & HORWITZ, A. R. 2005. Cell migration at a glance. *Journal of Cell Science,* 118**,** 4917.

VON ZYCHLINSKI, A. & KLEFFMANN, T. 2015. Dissecting the proteome of lipoproteins: New biomarkers for cardiovascular diseases? *Translational Proteomics,* 7**,** 30-39.

VON ZYCHLINSKI, A., KLEFFMANN, T., WILLIAMS, M. J. & MCCORMICK, S. P. 2011. Proteomics of Lipoprotein(a) identifies a protein complement associated with response to wounding. *J Proteomics,* 74**,** 2881-91.

WANG, J., BADEANLOU, L., BIELAWSKI, J., CIARALDI, T. P. & SAMAD, F. 2014. Sphingosine kinase 1 regulates adipose proinflammatory responses and insulin resistance. *Am J Physiol Endocrinol Metab,* 306**,** E756-68.

WANG, L., LEE, J. F., LIN, C. Y. & LEE, M. J. 2008. Rho GTPases mediated integrin alpha v beta 3 activation in sphingosine-1-phosphate stimulated chemotaxis of endothelial cells. *Histochem Cell Biol,* 129**,** 579-88.

WEINSTEIN, G. D., MCCULLOUGH, J. L. & ROSS, P. 1984. Cell proliferation in normal epidermis. *J Invest Dermatol,* 82**,** 623-8.

WEINSTEIN, G. D., MCCULLOUGH, J. L. & ROSS, P. A. 1985. Cell kinetic basis for pathophysiology of psoriasis. *J Invest Dermatol,* 85**,** 579-83.

WERRY, T. D., WILKINSON, G. F. & WILLARS, G. B. 2003. Mechanisms of cross-talk between G-protein-coupled receptors resulting in enhanced release of intracellular Ca2+. *Biochem J,* 374**,** 281-96.

WIELOSZ, E., MAJDAN, M., ZYCHOWSKA, I. & JELENIEWICZ, R. 2008. Coexistence of five autoimmune diseases: diagnostic and therapeutic difficulties. *Rheumatol Int,* 28**,** 919-23.

WOODCOCK, J. 2006. Sphingosine and ceramide signalling in apoptosis. *IUBMB Life,* 58**,** 462-6.

WORTHEN, L. M. & NOLLERT, M. U. 2000. Intracellular calcium response of endothelial cells exposed to flow in the presence of thrombin or histamine. *J Vasc Surg,* 32**,** 593-601.

WORTZEL, I. & SEGER, R. 2011. The ERK Cascade: Distinct Functions within Various Subcellular Organelles.

XIONG, Y., PIAO, W., BRINKMAN, C. C., LI, L., KULINSKI, J. M., OLIVERA, A., CARTIER, A., HLA, T., HIPPEN, K. L., BLAZAR, B. R., SCHWAB, S. R. & BROMBERG, J. S. 2019. CD4 T cell sphingosine 1-phosphate receptor (S1PR)1 and S1PR4 and endothelial S1PR2 regulate afferent lymphatic migration. *Sci Immunol,* 4**,** eaav1263.

YAMASAKI, K., NAKAGAWA, H., KUBO, Y., OOTAKI, K. & JAPANESE BRODALUMAB STUDY, G. 2017. Efficacy and safety of brodalumab in patients with generalized pustular psoriasis and psoriatic erythroderma: results from a 52-week, open-label study. *Br J Dermatol,* 176**,** 741-751.

YATOMI, Y., IGARASHI, Y., YANG, L., HISANO, N., QI, R., ASAZUMA, N., SATOH, K., OZAKI, Y. & KUME, S. 1997. Sphingosine 1-Phosphate, a Bioactive Sphingolipid Abundantly Stored in Platelets, Is a Normal Constituent of Human Plasma and Serum. *Journal of Biochemistry,* 121**,** 969-973.

YU, X. H., FU, Y. C., ZHANG, D. W., YIN, K. & TANG, C. K. 2013. Foam cells in atherosclerosis. *Clin Chim Acta,* 424**,** 245-52.

ZHANG, C. X., ADAMOS, C., OH, M. J., BARUAH, J., AYEE, M. A. A., MEHTA, D., WARY, K. K. & LEVITAN, I. 2017. oxLDL induces endothelial cell proliferation via Rho/ROCK/Akt/p27(kip1) signaling: opposite effects of oxLDL and cholesterol loading. *American Journal of Physiology-Cell Physiology,* 313**,** C340-C351.

ZHANG, H., DESAI, N. N., OLIVERA, A., SEKI, T., BROOKER, G. & SPIEGEL, S. 1991. Sphingosine-1-phosphate, a novel lipid, involved in cellular proliferation. *J Cell Biol,* 114**,** 155-67.

ZHANG, J., DUNK, C. E. & LYE, S. J. 2013. Sphingosine signalling regulates decidual NK cell angiogenic phenotype and trophoblast migration. *Hum Reprod,* 28**,** 3026-37.